THE UNIVERSITY of ADELAIDE

SAHMRI

Unravelling Resistance Mechanisms in Philadelphia Positive Leukemias: Targeted Treatment Strategies to Overcome Resistance

Govinda Poudel

Bachelor of Medical Science (Honours)

A thesis submitted in fulfilment of the Doctor of Philosophy Degree in Medicine

Department of Health and Medical Sciences

School of Medicine

University of Adelaide, Australia

June 2023

This page has been intentionally left blank.

Table of Contents

Abstract

The advent of Tyrosine Kinase Inhibitors (TKIs) has significantly improved the survival outcomes of Philadelphia-positive (Ph+) leukaemias, including Chronic Myeloid Leukaemia (CML) and Ph+ Acute Lymphoblastic Leukaemia (ALL). However, the development of TKI resistance remains a major challenge, particularly in cases where mutations other than in BCR::ABL1 are involved. Cancer-associated gene mutations, such as those in Protein tyrosine phosphatase non-receptor type-11 (PTPN11), are frequently found in patients with poor prognosis, but their role in mechanisms of resistance is poorly understood.

In this study, I investigated the role of two PTP domain PTPN11 mutations (p.A461T and p.P491H) in cell line models of Ph+ ALL. I modelled these mutations in multiple cell lines and demonstrated that they directly lead to TKI resistance. I also showed that Ph+ ALL cell lines with PTPN11 mutations were resistant to venetoclax, a BCL-2 inhibitor. I found that genetically knocking down PTPN11 could sensitize cells to both TKIs and venetoclax. Furthermore, I demonstrated a novel mechanism of TKI resistance involving re-activation of pBCR-Y177 part of BCR::ABL1 and overexpression of pERK1/2 and anti-apoptotic protein BCL-XL. This study is the first to show BCR::ABL1 dependent mechanisms of resistance driven by non-BCR::ABL1 mutations.

I investigated potential therapeutic options and demonstrated that targeting the anti-apoptotic proteins BCL-2 and MCL-1 could overcome resistance in Ph+ ALL cells with PTP domain PTPN11 mutations. Inhibition of MCL-1 in these cells could also be achieved by blocking BCR::ABL1 activation, which also overcame resistance when combined with

venetoclax. This discovery of a new precision medicine approach could be a promising treatment option for Ph+ ALL patients carrying PTP domain PTPN11 mutations.

I also investigated targeting MEK, an upstream molecule of ERK in MAPK pathway, with its inhibitor to overcome resistance, but its clinical translation may be limited due to its significant side effects. Before testing this combination treatment option for Ph+ ALL patients in clinical trials, future work should test this treatment option in mouse models.

In conclusion, this study not only provides a promising treatment option for Ph+ ALL patients carrying PTPN11 mutations, but also adds knowledge in understanding the function of the poorly understood SHP-2 protein and implications when mutations are acquired in the PTP domain. The knowledge from this study could also be used in understanding the mechanisms of poor response and resistance in Ph- leukaemias such as JMML, AML and MDS where PTPN11 mutations are highly prevalent, and patients have very limited treatment options.

Declaration of originality

I certify that this work contains no material which has been accepted for the award of any other degree or diploma in my name, in any university or other tertiary institution and, to the best of my knowledge and belief, contains no material previously published or written by another person, except where due reference has been made in the text. In addition, I certify that no part of this work will, in the future, be used in a submission in my name, for any other degree or diploma in any university or other tertiary institution without the prior approval of the University of Adelaide and where applicable, any partner institution responsible for the joint award of this degree.

The author acknowledges that copyright of published works contained within the thesis resides with the copyright holder(s) of those works.

I give permission for the digital version of my thesis to be made available on the web, via the University's digital research repository, the Library Search and also through web search engines, unless permission has been granted by the University to restrict access for a period of time.

I acknowledge the support I have received for my research through the provision of an Australian Government Research Training Program Scholarship.

Govinda Poudel

June 2023

Acknowledgments

First and foremost, I extend my heartfelt gratitude to Professor Tim Hughes for accepting me as his PhD student and providing me with the rare opportunity to learn and grow under his expert guidance. I feel immensely privileged to be one of his more than 18 PhD graduates. Professor Tim, you have been more than a supervisor to me - you have been a mentor and a role model. Your unwavering support and belief in my potential, even during the most challenging times, have inspired me to strive for excellence in everything I do. I admire your remarkable people skills and your dedication to making a positive impact through ground-breaking research. I pledge to do my utmost to make you proud as one of your PhD graduates.

I am also deeply grateful to my co-supervisor, Dr. Ilaria Pagani, for her invaluable guidance and unwavering support throughout my PhD journey. Ilaria, your unwavering belief in me, even during my lowest moments, has helped me to overcome obstacles and achieve milestones that I once thought was unattainable. Our shared passion for research and desire to make a positive impact have been the foundation of our achievements together. I am inspired by your drive and commitment to professional excellence, and I will always cherish the lessons you have taught me about hard work and perseverance.

I would also like to express my gratitude to Associate Professor David Yeung and Professor Deb White, my co-supervisors, for their valuable contributions to my PhD project. David, I truly appreciate your valuable time, especially considering your busy schedule. You have been incredibly generous in offering guidance and support whenever I have needed it.

I owe a debt of gratitude to the Leukaemia Research Group (LRG) lab, where I conducted my research. I would like to thank Verity Saunders, our LRG lab manager, for her tireless efforts in helping me with everything from training to sample cryopreservation. I am grateful to Dr. Yazad Irani, Dr. Liu Lu, Phuong Dang, Madeline Hughes, and Molly Tolland from the CML group for their support and collaboration on my research project. I would also like to thank Dr. Barbara McClure, Dr. Laura Eadie, Jacqui Rehn, and the rest of the ALL team for providing a wonderful work environment in the lab. I am indebted to A/Prof Dan Thomas's group, Dr. Devendra's group, and the Prostate Cancer group for their assistance and support with my research. I am especially grateful to Stephanie Arbon for her assistance with ordering reagents and to Randall Grose for his invaluable help with my Flow Core needs.

I am immensely grateful to my family and friends for their unwavering support throughout my PhD journey. My beautiful wife Namrata deserves special recognition for her unwavering support and selflessness. She has been my rock throughout the journey, always putting my needs before her own. Her encouragement and unwavering faith in me have been a constant source of inspiration. I am also grateful to my sister, brother-in-law, and close friends, who have been a pillar of support during difficult times, including the birth of our son 'Sakshat' in 2021.

Finally, I extend my appreciation to you, the reader of this thesis. I hope that my passion for research and the hard work I have put into this project come through in these pages.

Publications

Poudel, G.; Tolland, M.G.; Hughes, T.P.; Pagani, I.S. Mechanisms of Resistance and Implications for Treatment Strategies in Chronic Myeloid Leukaemia. *Cancers* **2022**, *14*, doi:10.3390/cancers14143300.

Pagani, I.S.; **Poudel, G.**; Wardill, H.R. A Gut Instinct on Leukaemia: A New Mechanistic Hypothesis for Microbiota-Immune Crosstalk in Disease Progression and Relapse. *Microorganisms* **2022**, *10*, doi:10.3390/microorganisms10040713.

Flietner, E., Yu, M., **Poudel, G.**, Veltri, A.J., Zhou, Y., Rajagopalan, A., Feng, Y., Lasho, T., Wen, Z., Sun, Y. and Patnaik, M.M., 2023. Molecular characterization stratifies VQ myeloma cells into two clusters with distinct risk signatures and drug responses. *Oncogene*, pp.1-12. (Not part of this thesis)

Conference Presentations

Dec 2022 64th American Society of Haematology, New Orleans, LA, USA

Poster Presentation

Poudel G, Yeung DT, White DL, Hughes TP, Pagani IS. PTPN11 Mutations Drive Tyrosine Kinase Inhibitor As Well As Venetoclax Resistance in Ph+ ALL Cells, but Are Sensitive to the Combination. Blood **2022**, 140(Supplement 1), 3128-3129. doi:10.1182/blood-2022-162194.

May 2022 New Directions in Leukaemia Research (NDLR), Brisbane, Australia

Poster Presentation

Poudel G, Yeung DT, White DL, Hughes TP, Pagani IS. Ph+ ALL cell line with PTPN11 mutations is resistant to all TKIs as well as venetoclax but sensitive to the combination

Sept 2021 15th Annual Florey Postgraduate Research Conference, Adelaide, Australia

Poster Presentation

Poudel G, Asari K, Yeung DT, White DL, Hughes TP, Pagani IS. Strategies to Overcome Resistance in Ph+ ALL with MAPK Pathway Mutations

Sept 2021 European Hematology Society Association (EHA) Virtual Congress

Poster Presentation

Poudel G, Yeung DT, White DL, Hughes TP, Pagani IS. Ph+ ALL Cell Line with PTPN11 Mutations Is Resistant to All TKIs As Well As Venetoclax but Sensitive to the Combination

May 2021 ASMR National Scientific Meeting, Adelaide, Australia

Oral Presentation

Poudel G, Yeung DT, White DL, Hughes TP, Pagani IS. MEK inhibitors as a targeted therapy approach to overcome resistance in Ph+ ALL cell line with PTPN11 mutations

May 2021 European School of Haematology (ESH) Translational Research E-Conference

Poster Presentation

Poudel G, Yeung DT, White DL, Hughes TP, Pagani IS. Ph+ ALL Cell Line with PTPN11 Mutations Is Resistant to All TKIs As Well As Venetoclax but Sensitive to the Combination

Nov 2020 ASMR National Scientific Meeting, Adelaide, Australia

Oral Presentation

Poudel G, Asari K, Yeung DT, White DL, Hughes TP, Pagani IS. Understanding the mechanisms of imatinib resistance in a Ph+ acute lymphoblastic leukaemia cell line

Scholarships and Awards

Adelaide Medical School/Biomedicine Research Travel Award, 2022

Travel grants to attend 64th American Society of Haematology, New Orleans, LA, USA

Australian Government Research Training Program Scholarships (RTPS)

Scholarship to support High Degree by research student for their educational and professional development.

Chapter 1: Introduction

The Philadelphia Chromosome

Chronic Myeloid Leukaemia (CML) and a subset of Acute Lymphoblastic Leukaemia (ALL) share a common pathogenic lesion: a chromosomal translocation that forms the Philadelphia (Ph) chromosome [1, 2]. The Ph chromosome results from the t(9;22)(q34;q11) balanced reciprocal translocation between chromosome 9 and 22 [3]. At the gene level this results in the fusion of the Breakpoint Cluster Region (*BCR*) with the Abelson1 proto-oncogene (*ABL1*), generating the *BCR::ABL1* fusion gene, which is sufficient to cause leukaemia [4]. BCR::ABL1 is a potent tyrosine kinase signalling protein that drives cell proliferation and reduces apoptosis [3, 4]. Depending on the position of the breakpoints, generally in intronic regions, different BCR::ABL1 protein isoforms are generated. The most common are the p210 and p190 **(Figure 1.1)**. In *ABL1*, the breakage occurs generally upstream of second exon in the intron 1, while in *BCR* breaks usually occur in one of three regions termed as: major (M-BCR, p210, with breaks in introns 13 and 14), minor (m-BCR, p190, with breaks in intron 1) and micro-BCR (μ-BCR, p230, with breaks downstream to exon 19) **(Figure 1.1)** [5, 6]. Genomics breaks in M-BCR and upstream to *ABL1* exon 2 generates the b2a2 (or e13a2) and b3a2 (or e14a2) transcripts. They give rise to a protein of 210 kDa termed p210, which is found in over 90% of CML patients. Moreover, breaks in m-BCR generates the e1a2 transcript, which gives rise to a 190 kDa protein. This protein is rare in CML but found in 90% of children and 50-70% of adult Ph+ ALL patients [6-8]. Finally, the e19a2 transcript produces a protein of 230 kDa (p230), which is associated with a rare once so called chronic neutrophilic leukaemia [9]. As *ABL1* breakpoint is always invariably constant and *BCR* breakpoint varies greatly among diseases, one can deduce that ABL1 part of BCR::ABL1 probably contains transformative potential and the BCR part may dictate the phenotypes. This notion is supported by the fact that ABL1 holds its transformative ability even when fused with

other fusion partners to form fusion proteins such as ETV6-ABL1, ZMIZ1-ABL1, and EML1-ABL1 in ALL [10].

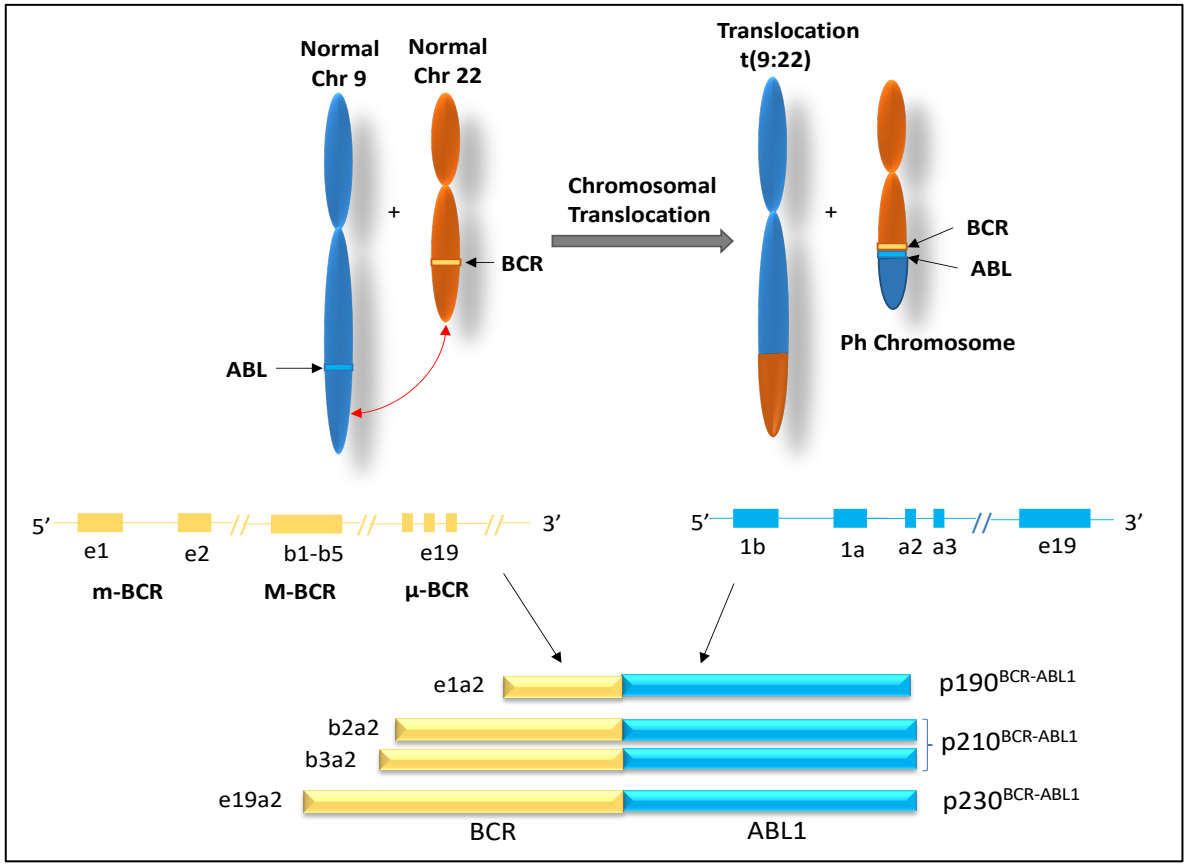

Figure 1.1: Formation of Philadelphia (Ph) chromosome. Translocation of chromosome 9 and 22 forms Ph chromosome with *BCR-ABL1* oncogene with either of three breakpoint regions in BCR resulting into $p190^{BCR::ABL1}$, $p210^{BCR::ABL1}$ and $p230^{BCR::ABL1}$ transcripts. Breakage patterns in ABL1 and BCR genes. In ABL1, breaks typically occur upstream of the second exon in intron 1. In contrast, BCR breaks can be categorized into three regions: major (M-BCR, p210, with breaks in introns 13 and 14), minor (m-BCR, p190, with breaks in intron 1), and micro-BCR (μ-BCR, p230, with breaks downstream of exon 19). These break patterns result in the generation of specific transcripts, such as b2a2 (or e13a2) and b3a2 (or e14a2), with implications for genomics. Image adapted from Avelino *et al.,* 2017 [11].

Tyrosine Kinase Inhibitor Therapy

CML and Ph+ ALL are both treated using Tyrosine Kinase Inhibitors (TKIs), which include first generation imatinib, second generation nilotinib, bosutinib, dasatinib, and third generation ponatinib. These TKIs work by inhibiting the kinase activity of BCR::ABL1 [12]. Asciminib, an allosteric inhibitor of BCR::ABL1, has been approved for the treatment of CML in patients who have been previously treated with multiple TKIs or who have the T315I mutation [13]. Despite the significant improvement in treatment outcomes with TKIs, resistance to these drugs remains a significant challenge. Current strategies to address TKI resistance primarily focus on enhancing the effectiveness and specificity of drugs targeting BCR::ABL1 [14]. However, this approach may be less effective for CML patients who develop resistance through mechanisms independent of BCR::ABL1. In a comprehensive review titled "Mechanism of Resistance and Implications for Treatment Strategies in Chronic Myeloid Leukaemia," attached herewith, we discuss the current challenges in the treatment of CML and Ph+ ALL and provide an overview of the key mechanisms underlying TKI resistance.

A- BCR::ABL1 dependent:

1. *ABL1 Kinase domain mutations*
2. *Myristoyl domain mutations*
3. *BCR::ABL1 overexpression*
4. *Altered expression of drug transporters*

B- BCR::ABL1 independent:

1. *Alternative Activation of MAPK Pathway*
2. *Alternative Activation of JAK/STAT Pathway*
3. *Alternative Activation of PI3K/AKT Pathway and Dysregulation of Autophagy*
4. *Activation of Wnt/β-Catenin Signalling*

5. *Protein Phosphatase 2A (PP2A) Level*
6. *Epigenetic Alterations*
7. *Inflammatory TNF-α and TGF-β Pathways*
8. *Sonic Hedgehog Pathway Activation*
9. *Dysregulation of Apoptotic Protein Expression*

We also investigate various treatment strategies that involve combining tyrosine kinase inhibitors (TKIs) with inhibitors targeting alternative growth pathways or anti-apoptotic pathways [14]. This approach aims to overcome resistance in cases where resistance is not driven by BCR-ABL1-dependent mechanisms, but rather by mutations that activate alternative survival or apoptotic pathways. By employing these combination strategies, we can tackle existing challenges in treatment and enhance the effectiveness of therapies for these diseases.

To illustrate, the combination of TKIs with agents that target alternative survival signalling may be necessary to achieve better treatment outcomes in patients with Philadelphia chromosome-positive (Ph+) leukemia [14]. Additionally, utilizing a combination approach could help eliminate leukemia stem cells, leading to longer periods of treatment-free remission in chronic myeloid leukemia (CML) and increased sensitivity to TKIs in non-responders [14]. Therefore, frontline administration of combination strategies that specifically target CML-leukemia stem cells could be considered, while CML patients who do not respond to TKIs without exhibiting kinase domain or myristoyl domain mutations should be screened for alternative resistance mechanisms [14]. Identifying such alternative mechanisms would enable the selection of an appropriate combination treatment approach. These combination approaches hold promise in addressing the current unmet treatment needs in CML by eliminating leukemia stem cells

and enhancing the response of TKI-resistant progenitor cells, ultimately improving treatment outcomes [14].

In conclusion, it is crucial to comprehend the mechanisms behind TKI resistance and develop effective combination treatment strategies to enhance the outcomes for patients with CML and Ph+ acute lymphoblastic leukemia (ALL).

Mechanism of Resistance and Implications for Treatment Strategies in Chronic Myeloid Leukaemia

Statement of Authorship

Title of Paper	Mechanisms of Resistance and Implications for Treatment Strategies in Chronic Myeloid Leukaemia
Publication Status	☑ Published ☐ Accepted for Publication ☐ Submitted for Publication ☐ Unpublished and Unsubmitted work written in manuscript style
Publication Details	Poudel, G.; Tolland, M.G.; Hughes, T.P.; Pagani, I.S. Mechanisms of Resistance and Implications for Treatment Strategies in Chronic Myeloid Leukaemia. Cancers 2022, 14, doi:10.3390/cancers14143300.

Principal Author

Name of Principal Author (Candidate)	Govinda Poudel
Contribution to the Paper	Conceptualization, original draft preparation and project administration
Overall percentage (%)	90%
Certification:	This paper reports on original research I conducted during the period of my Higher Degree by Research candidature and is not subject to any obligations or contractual agreements with a third party that would constrain its inclusion in this thesis. I am the primary author of this paper.
Signature	Date: 26/6/2023

Co-Author Contributions

By signing the Statement of Authorship, each author certifies that:

i. the candidate's stated contribution to the publication is accurate (as detailed above);

ii. permission is granted for the candidate in include the publication in the thesis; and

iii. the sum of all co-author contributions is equal to 100% less the candidate's stated contribution.

Name of Co-Author	Timothy P. Hughes
Contribution to the Paper	Supervised development of work, reviewed and edited the draft
Signature	Date: 26/6/2023

Text

Name of Co-Author	Ilaria S. Pagani
Contribution to the Paper	Supervised development of work, reviewed and edited the draft
Signature	Date: 28/06/2023 ~~26/6/2023~~

Please cut and paste additional co-au

Name of Co-Author: Molly G. Tolland

Contribution to the paper: Reviewed and edited the draft

Signature: Date: 26/6/2023

cancers

MDPI

Review

Mechanisms of Resistance and Implications for Treatment Strategies in Chronic Myeloid Leukaemia

Govinda Poudel [1,2,3], Molly G. Tolland [1,2], Timothy P. Hughes [1,2,3,4] and Ilaria S. Pagani [1,2,3,*]

[1] Cancer Program, Precision Medicine Theme, South Australian Health and Medical Research Institute (SAHMRI), Adelaide, SA 5000, Australia; govinda.poudel@sahmri.com (G.P.); molly.tolland@sahmri.com (M.G.T.); tim.hughes@sahmri.com (T.P.H.)
[2] School of Medicine, Faculty of Health and Medical Sciences, University of Adelaide, Adelaide, SA 5000, Australia
[3] Australasian Leukaemia and Lymphoma Group, Richmond, VIC 3121, Australia
[4] Department of Haematology and Bone Marrow Transplantation, Royal Adelaide Hospital and SA Pathology, Adelaide, SA 5000, Australia
* Correspondence: Ilaria.Pagani@sahmri.com

Simple Summary: Chronic myeloid leukaemia (CML) is a type of blood cancer that is currently well-managed with drugs that target cancer-causing proteins. However, a significant proportion of CML patients do not respond to those drug treatments or relapse when they stop those drugs because the cancer cells in those patients stop relying on that protein and instead develop a new way to survive. Therefore, new treatment strategies may be necessary for those patients. In this review, we discuss those additional survival pathways and outline combination treatment strategies to increase responses and clinical outcomes, improving the lives of CML patients.

Abstract: Tyrosine kinase inhibitors (TKIs) have revolutionised the management of chronic myeloid leukaemia (CML), with the disease now having a five-year survival rate over 80%. The primary focus in the treatment of CML has been on improving the specificity and potency of TKIs to inhibit the activation of the BCR::ABL1 kinase and/or overcoming resistance driven by mutations in the BCR::ABL1 oncogene. However, this approach may be limited in a significant proportion of patients who develop TKI resistance despite the effective inhibition of BCR::ABL1. These patients may require novel therapeutic strategies that target both BCR::ABL1-dependent and BCR::ABL1-independent mechanisms of resistance. The combination treatment strategies that target alternative survival signalling, which may contribute towards BCR::ABL1-independent resistance, could be a successful strategy for eradicating residual leukaemic cells and consequently increasing the response rate in CML patients.

Keywords: chronic myeloid leukaemia; tyrosine kinase inhibitors; therapy resistance; BCR::ABL1-independent mechanism of TKI resistance; combination treatments

Citation: Poudel, G.; Tolland, M.G.; Hughes, T.P.; Pagani, I.S. Mechanisms of Resistance and Implications for Treatment Strategies in Chronic Myeloid Leukaemia. *Cancers* **2022**, *14*, 3300. https://doi.org/10.3390/cancers14143300

Academic Editor: Mary Frances McMullin

Received: 31 May 2022
Accepted: 4 July 2022
Published: 6 July 2022

1. Introduction

Chronic myeloid leukaemia (CML) is a malignancy characterized by the clonal proliferation of white blood cells that are mostly originated from the myeloid lineage in the bone marrow [1]. CML arises from the t(9;22)(q34;q11) balanced reciprocal translocation between chromosome 9 and 22 that forms the Philadelphia chromosome [2,3]. The translocation event results in the fusion of the *Breakpoint Cluster Region* (*BCR*) gene with the *Abelson proto-oncogene 1* (*ABL1*) gene, generating the *BCR::ABL1* fusion gene [4]. The resulting chimeric protein, BCR::ABL1, is a potent tyrosine-kinase signalling protein that drives cell proliferation and reduces apoptosis, which causes leukaemia [4]. Depending on the position of the *BCR* breakpoint, different BCR::ABL1 protein isoforms are generated (Figure 1A) [5]. The e13a2/e14a2 alternative transcripts (or b2a2/b3a2), resulting from the juxtaposition

of *BCR* exon 13 or 14 with *ABL1* exon 2, produce a 210 kDa protein, which is found in over 90% of CML patients. The e1a2 transcript encodes a 190 kDa protein (p190), which is rare in CML but is relatively common in acute lymphoblastic leukaemia, occurring in around 70% of cases (Figure 1B) [5,6]. Approximately 95% of CML patients are diagnosed at the chronic phase, which is relatively indolent but can involve symptoms such as fatigue, abdominal pain, or weight loss. During this phase, the disease can be effectively managed with tyrosine kinase inhibitors (TKIs). If untreated, CML could progress to an accelerated phase (AP), which can last for up to a year, and eventually progress into the terminal blast phase of the disease, termed the blast crisis (BC). The blast crisis is characterized by the presence of excess blast cells in the blood or bone marrow [7]. Blast crisis results in dismal treatment outcomes, and it is often fatal even with intervention [7]. Patients in AP and BC are generally grouped together as advanced-phase CML patients [8].

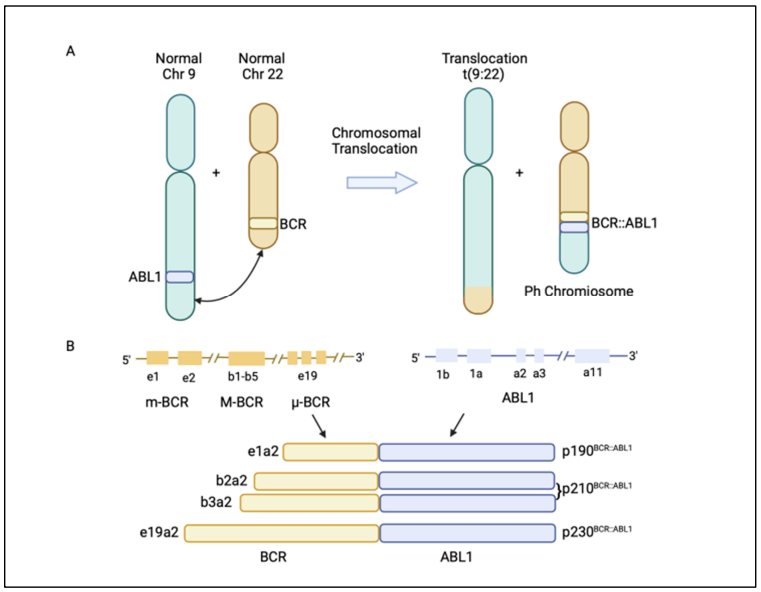

Figure 1. (**A**) Philadelphia (Ph) chromosome is formed from the translocation t(9;22)(q34;q11) of chromosome 9 and 22. The translocation event leads to the fusion of the *breakpoint cluster region* (*BCR*) gene with the *Abelson1 proto-oncogene 1* (*ABL1*) gene, resulting in a *BCR::ABL1* fusion gene. (**B**) Different *BCR::ABL1* fusion gene transcripts $p190^{BCR::ABL1}$, $p210^{BCR::ABL1}$, and $p230^{BCR::ABL1}$ are generated, depending on where the break occurs in the *BCR* gene [5]. Figure created in BioRender.com.

The *BCR::ABL1* fusion gene is translated into the BCR::ABL1 protein, which contains several domains from BCR and ABL1. The BCR region of this protein regulates its enzymatic activity and provides sites for its binding partners [9,10]. The coil–coil domain of the BCR N-terminal part is responsible for the oligomerization and constitutive activation of BCR::ABL1 activity (Figure 2C) [11]. The ABL1 component of the BCR::ABL1 protein contains an SRC-homology-2 (SH2) domain, an SH3 domain, and a kinase domain [4]. When not fused with BCR, ABL1 has a myristoylated N-terminal responsible for the autoinactivation of ABL1 kinase activity [4]. However, the myristoylated N-terminal is lost during the BCR::ABL1 fusion process [12]. The BCR:ABL1 kinase domain consists of key motifs responsible for its activity, including the phosphate binding loop (p-loop), the contact site (ATP/IM binding site), the catalytic domain, and activation loop (A-loop) (Figure 2C) [13]. BCR::ABL1 is active when ATP binds to the active site in the ABL1 ki-

nase domain and transfers its phosphate group to ABL1 substrate. However, tyrosine kinase inhibitors (TKIs) compete with ATP for binding to the active site, inhibiting the BCR::ABL1 activation and preventing leukaemia (Figure 2A) [14].

The treatment of CML with TKIs has been paradigm-shifting, increasing the survival from 20% to over 80% today [14]. There are five available approved TKIs, prescribed based on disease phase, individual risk assessment, response level, presence of BCR::ABL1 kinase domain mutations, and response to prior TKI therapy [15,16]. The current available TKIs include the first-generation TKI imatinib (Glivec, Novartis, Basel, Switzerland); second-generation TKIs dasatinib (Sprycel, Bristol-Myers Squibb, New York, USA), nilotinib (Tasigna, Novartis), and bosutinib (Bosulif, Pfizer, New York, USA); and third-generation ponatinib (Iclusig, Takeda/Incyte, Tokyo, Japan). Ponatinib is approved as a third-line treatment, when two or more TKIs are not effective, and for patients harbouring the T315I mutation in the BCR::ABL1 kinase domain. In October 2021, the Food and Drug Administration approved the new allosteric inhibitor of BCR::ABL1, asciminib (Scemblix, Novartis), for CML patients previously treated with two or more TKIs and for T315I mutations [17]. Asciminib binds to the myristoyl's site on BCR::ABL1 and allosterically inhibits its activation, including that of BCR::ABL1 with T315I mutation, with very high selectivity, preventing downstream signalling [18]. ABL1 can normally self-regulate its activity via its engagement with the myristoylated N-terminal; however, in patients with CML, this ability is lost when ABL1 is fused with BCR (Figure 2B) [12]. Therefore, the binding of asciminib to a myristoyl pocket facilitates the inhibition of BCR::ABL1 activity by restoring its allosteric inhibition ability (Figure 2B).

The response to TKIs is assessed by measuring the levels of *BCR::ABL1* transcript in the peripheral blood by quantitative real-time PCR (RT-qPCR) and based on the achievement of molecular milestones over time [20]. *BCR::ABL1*% is expressed and reported on a log scale, where 10%, 1%, 0.1%, 0.01%, 0.0032%, and 0.001% corresponds to 1, 2, 3, 4, 4.5, and 5 log reductions, respectively, below the standard baseline used in IRIS study [21]. Both 4-log (MR4) and 4.5-log (MR4.5) reductions are described as deep molecular responses [22]. Optimal molecular response corresponds to achieving specific milestones, which are the early molecular response of *BCR::ABL1* $\leq$ 10% at 3 months and the major molecular response (MMR) to *BCR::ABL1* $\leq$ 0.1% at 12 months. The main goal for CML patients is to achieve a durable remission, known as treatment-free remission, which first requires maintaining a deep molecular response (DMR) (*BCR::ABL1* $\leq$ 0.01% or undetectable; limit of detection of 0.001%) [23]. Patients who achieve a deep molecular response (MR4 or MR4.5) have a better outcome with low risk of disease progression or relapse [22].

Chronic-phase CML patients who achieve an optimal response to treatment can expect a comparable life expectancy to that of the general population. About 25% of patients can cease their TKI therapy and maintain treatment-free remission [24–27]. Despite this enormous success, several challenges remain. The failure to eradicate persistent CML cells leads to a relapse in about 50% of patients who cease therapy. These patients therefore need to restart therapy, which can cause considerable emotional stress. Additionally, about 20% of CML patients respond poorly to frontline therapy, with 5–10% progressing to blast crisis [28]. This is due to the development of resistance, which represents a "bottleneck to cure" [29]. While a lot of progress has been made in understanding the BCR::ABL1-dependent mechanisms of resistance that rely on BCR::ABL1 reactivation, the mechanisms of BCR::ABL1-independent resistance have remained largely elusive [30]. It is becoming increasingly clear that TKI resistance can be driven by mechanisms that do not depend on BCR::ABL1 activation [31]. These mechanisms need to be considered in the curative approach of CML. In this review, we discuss BCR::ABL1-dependent and BCR::ABL1-independent mechanisms of TKI resistance in CML, highlighting combination-treatment strategies for overcoming resistance in a situation where resistance is driven by a BCR::ABL1-independent mechanism. The combination strategies we explore here could address current treatment challenges and improve treatment outcomes in CML.

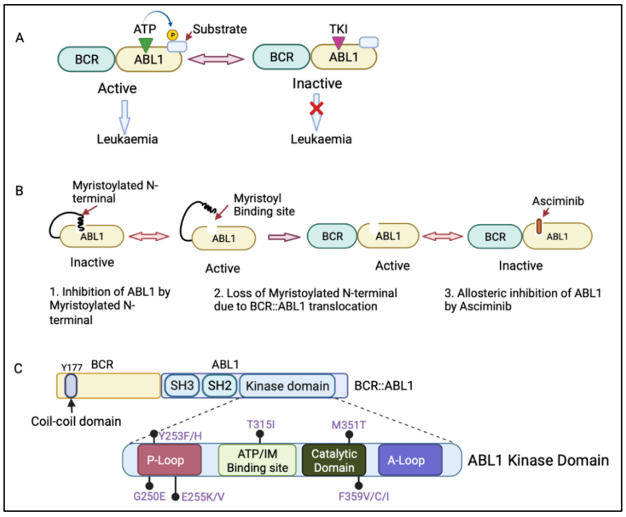

Figure 2. (**A**) Mechanism of action of adenosine triphosphate (ATP)-competitive tyrosine kinase inhibitors (TKIs). ATP binds to the ABL1 kinase domain, and the phosphate group is transferred to the ABL1 substrate, leading to BCR::ABL1 activation. The TKI competes with ATP for binding to the ABL1 kinase domain, inhibiting BCR::ABL1 activation and therefore preventing leukaemia progression. (**B**) Mechanism of action of asciminib, an allosteric inhibitor of BCR::ABL1. Asciminib binds to the myristoyl binding site, leading to BCR::ABL1 inactivation via allosteric inhibition of ABL1 kinase. (**C**) Schematic diagram of the BCR and ABL1 components of the BCR::ABL1 protein showing the N-terminal coil–coil domain (containing key tyrosine residue at 177 position, Y177) of BCR and an SRC-homology-2 (SH2) domain, an SH3 domain, and a kinase domain of ABL1. The ABL1 kinase domain shows the P-loop, ATP/imatinib binding site, catalytic domain, A-loop, and the most clinically relevant mutations affecting the kinase domain [19]. Figure created in BioRender.com.

2. BCR::ABL1-Dependent Mechanisms of Resistance

BCR::ABL1-dependent mechanisms are the most common and well-studied mechanisms of TKI resistance in CML that reactivate the kinase activity of BCR::ABL1 [32,33].

2.1. Kinase Domain Mutations

The most common and extensively studied mechanism of secondary resistance to imatinib is due to mutations in the *ABL1* kinase domain [34]. The *ABL1* kinase domain mutations account for approximately 40–60% of CML patients who experience haematological relapse on imatinib therapy [29]. The point mutations (more than 50 different mutations) in the ABL1 kinase domain, including the ATP-binding domain (P-loop), catalytic domain, the activation loop (A-loop), and in amino acids, in the imatinib binding site, are known to be responsible for clinical imatinib resistance (Figure 2C) [35]. The most clinically relevant mutations are G250E, Y253F/H, and E255K/V mutations in the P-loop, T315I in the imatinib binding site, and M351T and F359V/C/I in the catalytic domain (Table 1) [19]. Optimal drug binding requires structural adjustments in BCR::ABL1, which is prevented in P-loop mutants, while the kinase is stabilized in an active state in A-loop mutants [19]. The T315I mutation, also known as "the gatekeeper" mutation, is generated when threonine is replaced with isoleucine, preventing imatinib from forming a hydrogen bond with the protein [19].

The second-generation TKIs, nilotinib and dasatinib, have an increased potency and activity against most imatinib-resistant mutants but are not effective against a T315I mutation

(Table 1) [36]. Ponatinib is effective against most kinase domain mutations, including T315I, but there still remains some compound mutations, which are two or more mutations in the same allele (e.g., Y253H/T315I or E255V/T315I) that can confer resistance to ponatinib [37]. The new allosteric inhibitor asciminib was shown to be potent and effective against naive as well as mutated BCR::ABL1 proteins, including the T315I BCR::ABL1 mutation [16,38]. In 2019, Hughes et al. reported the results of the first large phase I study of asciminib as a second line of therapy for CML patients who failed or were intolerant to at least two previous TKIs [16]. Asciminib effectively induced complete haematological responses in 14/16 (88%) and major molecular responses in 4/17 (24%) CML patients with T315I mutations [16]. Similarly, Cortes et al. also reported favourable safety and acceptable clinical efficacy in CML patients with the T315I mutation, showing that around 50% of these patients achieve a major molecular response with asciminib treatment [39]. Moreover, Gutiérrez et al. reported that in CML patients who were heavily pretreated with three or more TKIs prior to asciminib treatment, 48% achieved a complete cytogenic response, and 33% achieved a major molecular response [40]. Pagani et al. reported the results of asciminib treatment in a CML patient with an atypical e19a2 *BCR::ABL1* transcript, who had previously developed a T315I kinase domain mutation. The patient had reached a deep molecular response and maintained it for 4.6 years when the study was published [38]. The first trial of asciminib as a front-line therapy is now currently ongoing and enrolling newly diagnosed CML patients (NCT03578367).

Table 1. Clinically important BCR::ABL1 kinase domain mutations and their sensitivity to different TKIs [30,41].

Kinase Domain Mutations	TKI Sensitivity
T315I, Y253F/H, E255K/V, Q252H, M244V, L248V, G250E, F317L, M351T, M355D, F359V, and H396R/P/A	Reduced sensitivity to imatinib
T315I, L248V, Y253H, E255K/V, and F359V/I/C	Reduced sensitivity to nilotinib
T315I/A, V299L, and F317L/V/I/C	Reduced sensitivity to dasatinib
T315I, E255V/K, V299L, G250E, E255K/V, and F317L/V/I/C	Reduced sensitivity to bosutinib
T315M/L	Reduced sensitivity to ponatinib

2.2. Myristoyl Domain Mutations

Despite the promising efficacy of asciminib, especially against the T315I mutation, some patients acquire mutations in the myristoyl-binding pocket [23]. They include the A337V, P465S, V468F, I502L, and C464W mutations, which have been shown to confer asciminib resistance while retaining sensitivity to ATP-competitive kinase inhibitors [42,43]. Combining asciminib (50 or 250 nM) lowered the IC50 of ponatinib by 1.9 to 18.5-fold for compound mutants involving the T315I mutation and by 3.1 to 6.3-fold for compound mutants not involving the T315I mutation [43]. Similarly, mutant clones with kinase domain and myristoyl-binding site mutations conferred resistance to asciminib or ponatinib, but resistance was largely overcome when the two treatments were combined [43]. This finding supports the exciting possibility of combining an approved TKI with asciminib for the treatment of patients displaying resistance.

2.3. BCR::ABL1 Overexpression

BCR::ABL1 overexpression due to Ph chromosome duplication, *BCR::ABL1* gene amplification, or altered transcription of *BCR::ABL1* gene can occur in some patients. However, the role of BCR::ABL's overexpression in the context of TKI resistance is not as well understood as the role of kinase domain mutations [44]. One hypothesis is that increased BCR::ABL1 levels may provide cells with sufficient kinase activity for acquiring kinase domain mutations to induce resistance in TKI-treated cells [33]. Therefore, higher BCR::ABL1 expression appears to provide a selective advantage for CML cells. This

increased expression is common in advanced-stage CML, where reduced TKI sensitivity and development of resistance is often observed [30].

2.4. Altered Expression of Drug Transporters

Another mechanism that potentially prevents complete inhibition of BCR::ABL1 by TKIs is an increase in drug efflux. Intracellular drug concentration is controlled by ATP-binding cassette (ABC) transporters such as P-glycoprotein (ABCB1) and a breast cancer-resistant protein (ABCG2) [45]. Different ABC family transporters were identified to be resistant to different TKIs. For instance, ABCB1 was implicated in imatinib and nilotinib resistance [46,47]; ABCC6 was implicated in nilotinib and dasatinib resistance; and ABCG2 was mainly associated with asciminib resistance [48]. Low activity of organic cation transporter-1 (OCT-1), a cellular influx pump, can reduce the intracellular drug availability, consequently promoting imatinib resistance [49]. However, OCT-1 does not appear to regulate the intracellular uptake of second- and third-generation TKIs [50,51]. The resistance induced by overexpression of a particular transporter could be treated by using a TKI that is not susceptible to that transporter or by adding an inhibitor of that transporter [52]. For instance, Agrawal et al. reported that imatinib-resistant CML patients had high levels of ABCB1 expression but still responded to second-line nilotinib treatment [53]. Similarly, Qiang et al. identified the overexpression of ABCG2 as a major mechanism of resistance in asciminib-resistant K562 cells and showed that an inhibitor of ABCG2, Ko143 (100 nM), was able to restore the effectiveness of asciminib against those cells [43].

3. BCR::ABL1-Independent Mechanisms of Resistance/Persistence

Approximately 50% of CML patients with poor responses/disease progression have kinase domain mutations, suggesting that the remaining patients display alternative mechanisms of resistance [54]. This could be due to mechanisms intrinsic to the leukaemic cells that alternatively activate or create de novo parallel bypass survival pathways [55]. Additionally, because TKIs target only differentiated and cycling cells [56], certain leukaemic cells could also "escape" the apoptosis induced by TKIs and become dormant [56]. In this section, we describe the principal BCR::ABL1-independent mechanisms of resistance, including the alternative activation of major BCR::ABL1-driven pathways and other pathways that support alternative survival mechanisms. We also focus on the development of targeted therapies against specific deregulated pathways.

3.1. Alternative Activation of MAPK Pathway

The mitogen-activated protein kinase (MAPK) pathway (also known as the RAF/RAS/MEK/ERK pathway or RAS pathway) is a major BCR::ABL1-downstream signalling pathway responsible for cell proliferation, cell survival, and prevention of apoptosis in BCR::ABL1-positive cells (Figure 3) [57]. TKIs can inhibit this pathway by blocking BCR::ABL1 and inducing apoptosis in CML cells. However, the activation of the RAS pathway driven by mechanisms independent of BCR::ABL1 signalling, such as mutations in intermediates of the RAS pathway, can lead to TKI resistance in CML [58,59]. Ma et al. demonstrated that the increased activation of the RAS pathway as a result of *protein kinase c* (*PKC*) overexpression led to BCR::ABL1-independent imatinib resistance in K562 cells, as well as in patient-derived CML leukaemic stem cells [58]. Likewise, Kuman et al. also reported that imatinib-resistant CML leukaemic stem cells in contact with stroma had increased ERK1/2 phosphorylation. The inhibition of ERK1/2 using U0126 (ERK1/2 inhibitor) led to imatinib-induced apoptosis in those cells [60].

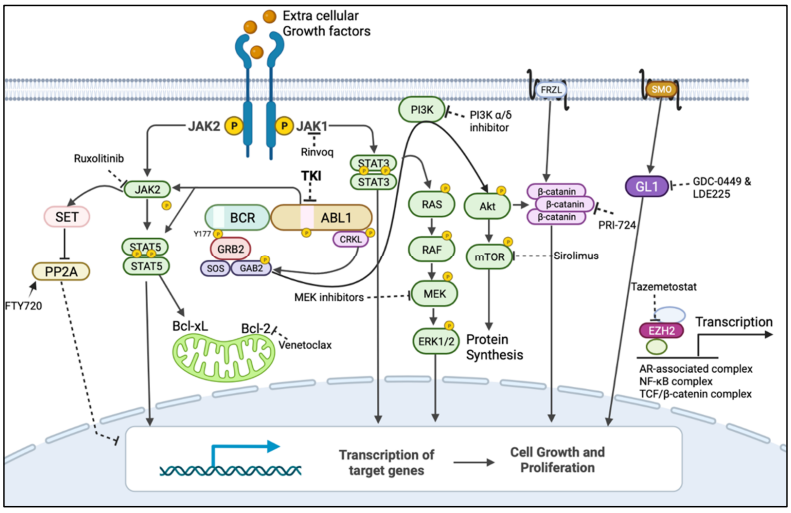

Figure 3. BCR::ABL1-dependent/independent pathways and drugs showing their targets for their BCR::ABL1-independent expression/activation to be used in combination with TKIs. Dark arrow indicates activation, dotted line indicates inhibition by inhibitor/s and encircled p indicates phosphorylation. The mitogen-activated protein kinase (MAPK) pathway (also known as rat sarcoma virus (RAS)/rapidly accelerated fibrosarcoma (RAF)/mitogen-activated kinase kinases (MEK)/extracellular signal-regulated kinase (ERK)), PhosphatidylInositol-3-Kinase (PI3K)/AKT/mammalian target of rapamycin (mTOR) and Janus Tyrosine Kinase (JAK), and signal transducer and activator of transcription (STAT) pathways are the major BCR::ABL1-downstream pathways responsible for BCR::ABL1-independent TKI resistance when re-activated by alternate routes. BCR::ABL1 can mediate the inhibition of the tumour-suppressor protein phosphatase 2A (PP2A) and activation of β-catenin to promote leukaemia, but this can also occur independently from BCR::ABL1. Leukaemic cells can also use JAK1/STAT3, Wnt signalling, the sonic hedgehog pathway, and the expression of the epigenetic modulator EZH2 to remain quiescent, which could contribute to resistance and relapse [30]. These pathways could be targeted by using inhibitors/activators that were developed for other diseases and could be repurposed for a combination treatment with TKIs to treat Ph+ leukaemias. Figure created in BioRender.com.

3.2. Alternative Activation of JAK/STAT Pathway

JAK/STAT signalling is another major BCR::ABL1-downstream signalling pathway that regulates proliferation, survival, and drug resistance in CML (Figure 3) [57,61]. JAK/STAT signalling is mediated by two important effectors, STAT3 and STAT5 [62]. Deininger et al. observed the activation of STAT3 via phosphorylation of Y705, leading to TKI resistance in CML CD34+ cells. A subsequent combination treatment with imatinib and a highly potent and specific STAT3 inhibitor, BP-5-087, reduced the survival of both TKI-resistant leukaemic stem and progenitor cells [63]. Kuepper et al. also observed similar results when BCR::ABL1 and JAK1 were co-inhibited. The JAK-specific inhibitors filgotinib and itacitinib were used to target JAK1 [64]. A significant increase in pSTAT3 Y705 was also identified by using single-cell mass cytometry in nilotinib-treated CML patients. This finding has possible prognostic potential [65]. Extrinsically activated JAK1/STAT3 signalling driven by external stimuli has also been shown to mediate stem cell persistence in CML [64]. Similarly, a high expression of STAT5 has also been shown to significantly reduce the sensitivity of CML cells to TKI-induced apoptosis in in vitro and in vivo studies [66].

3.3. Alternative Activation of PI3K/AKT Pathway and Dysregulation of Autophagy

The activation of the PI3K/AKT/mammalian target of rapamycin (mTOR) signalling pathway is another major BCR::ABL1-driven pathway that promotes cell growth and cell proliferation in CML cells (Figure 3) [67]. Burchert et al. showed AKT/mTOR pathway activation as a BCR::ABL1-independent compensatory pathway in imatinib-treated BCR::ABL1-positive LAMA cells [68]. BCR::ABL1-independent PI3K/AKT pathway activation and imatinib resistance was also observed in primary leukaemia cells and in imatinib-treated CML patients [68]. Moreover, Wagle et al. revealed imatinib and dasatinib dual-resistant K562 cells had sustained PI3K/AKT pathways with an elevated forkhead box O1 (FOXO1) level in the cytoplasm. However, the treatment with a class I PI3K inhibitor, GDC-0941 (pictilisib), led to the nuclear translocation of FOXO1 and induction of apoptosis in those cells [69]. Elevated FOXO1 levels were also observed in primary samples from relapsed CML patients who lacked kinase domain mutations [69]. Furthermore, Mitchell et al. showed an alternative activation of mTOR in BCR::ABL1-independent ponatinib-resistant CML cells and demonstrated that the inhibition of mTOR induce autophagy and that the inhibition of autophagy sensitizes those cells to ponatinib treatment [70].

Bellodi et al. demonstrated that BCR::ABL1 suppresses autophagy partly via the PI3K/AKT/mTOR pathway, leading to the downregulation of key autophagy genes *Beclin 1* and *Autophagy related 5* (*ATG5*) [71]. Autophagy is a conserved catabolic process responsible for protein degradation and the mediation of antigen presentation [72]. Autophagy is an important process for the maintenance of normal haematopoietic stem cells, and the dysregulation of autophagy is a common characteristic of leukaemic stem cells [72]. Several studies have described autophagy as a key process in drug resistance, where autophagy helps cells tolerate stress and prevents apoptosis induced by anti-cancer drugs [73]. Michell et al. demonstrated the genetic or pharmacological inhibition of mTOR, and therefore, autophagy primed BCR::ABL1-independent ponatinib-resistant CML cells to the mTOR inhibitor and induced apoptosis [70]. Moreover, Karvela et al. also showed that the knockdown of ATG7, an autophagy protein, sensitized CML progenitor cells to TKI-induced cell death [74]. The survival of normal cells remained unaffected, suggesting this strategy could be used as a novel way to target persistent leukaemic cells in CML [74].

3.4. Activation of Wnt/β-Catenin Signalling

The Wnt signalling pathway is necessary for the self-renewal of normal cells, but it has been implicated in cancer progression [55]. The activation of nuclear β-catenin and expression of its transcriptional targets leads to leukaemic progression, TKI resistance, and self-renewal in CML stem cells [55]. The expression of β-catenin is shown to be regulated by BCR::ABL1 via the PI3K/AKT pathway and to enhance the leukaemic progression in a CML murine model (Figure 3) [75]. BCR::ABL1 also led to a reduction in the protein expression of β-catenin antagonist Chibby1, which was more prominent in leukaemic stem cells compared with progenitor cells [76]. However, Eiring et al. demonstrated that leukaemic cells maintained their cytoplasmic β-catenin expression despite BCR::ABL1's inhibition by imatinib, suggesting that β-catenin expression was decoupled from BCR::ABL1 and contributed to intrinsic TKI resistance in CML cells [55]. In addition, Zhou et al. showed that the overexpression of β-catenin was present in blast crisis CML stem and progenitor cells and that the pharmacological and genetic inhibition of β-catenin impaired the self-renewal of stem and progenitor leukaemic cells [77].

3.5. Protein Phosphatase 2A (PP2A) Level

The tumour-suppressor protein phosphatase 2A (PP2A) gene encodes for a multimeric serine/threonine phosphatase and is involved in the regulation of transcription factor β-catenin, apoptosis, and the maintenance of G1/S cyclin levels during cell cycle progression [78,79]. BCR::ABL1 regulates PP2A and inhibits its phosphatase activity via the expression of an endogenous inhibitor, SET (Figure 3) [57,80]. Neviani et al. showed that the re-activation of PP2A was associated with growth arrest and apoptosis in BCR::ABL1-

positive cells [80]. Moreover, BCR::ABL1 protein expression was required for JAK2 activation, whereas kinase activity was not; in turn, this activated SET-dependent PP2A inhibition, leading to the expression of β-catenin and subsequent self-renewal and survival signalling in quiescent LSCs [80].

3.6. Epigenetic Alterations

Genetic alteration of epigenetic regulator genes such as Additional sex combs-like 1 (ASXL1), DNA (cytosine-5)-methyltransferase 3A (DNMT3A), runt-related transcription factor 1 (RUNX1), and Tet methylcytosine dioxygenase 2 (TET2) are frequently found in a CML blast crisis [81,82]. Somatic mutations in epigenetic regulator genes have been associated with poor TKI response and progression to the advanced stage of disease in CML patients when acquired during TKI therapy [83–85]. However, their causal relationship to TKI resistance, disease progression, and relapse is yet to be elucidated. Similarly, expression of the enhancer of zeste homolog 2 (EZH2), an epigenetic re-programmer, has been implicated in TKI resistance in CML. EZH2 is a histone methyltransferase and a catalytic subunit of polycomb repressive complex 2 (PRC2) [86]. In a CML mouse model, Scott et al. demonstrated that EZH2 was overexpressed in LSCs and that its dysregulation was responsible for TKI resistance and LSCs' protection [87]. The inactivation of EZH2 through CRISPR/Cas9-mediated gene editing led to the reduced initiation, maintenance, and survival of LSCs, irrespective of BCR::ABL1 mutations [86]. The dysregulation of PRC2 has also been demonstrated in CML stem cells, where the re-programming of EZH2 and H3K27me3 led to apoptosis prevention and LSC survival [87].

3.7. Inflammatory TNF-α and TGF-β Pathways

Single-cell transcriptomic analysis showed the enrichment of inflammation-related gene expressions such as inflammatory tumour-necrosis factor (TNF)-α and the transforming growth factor (TGF)-β genes in LSCs, compared with normal HSCs [88]. The increase in the pathway activity of TNF-α and TGF-β was associated with increased stem cell quiescence and thereby TKI resistance in poor responder CML patients (patients not achieving MMR) [88]. Giustacchini et al. tested the effect of TNF-α and TGF-β on normal HSCs and CML-LSCs in vitro and observed that TNF-α promoted quiescence in both normal HSCs and CML-LSCs, while TGF-β promoted higher cell division in CML-LSCs [88]. Targeting TNF-α and TGF-β activity could be effective in reducing stem cell quiescence and increasing the possibility of eliminating leukaemic stem cells.

3.8. Sonic Hedgehog Pathway Activation

The sonic hedgehog pathway is an evolutionarily conserved signalling pathway that plays a role in embryogenesis, cell proliferation, and growth [89]. It is a master regulator of the self-renewal of normal and leukaemic stem cells [90]. Cancer cells with aberrant hedgehog signalling undergo self-renewal, invasion, proliferation, and survival [89]. Hedgehog ligands act on cancer stem cells, both in a paracrine and an autocrine manner, leading to chemotherapy resistance, cancer cell survival, and relapse [91]. The binding of hedgehog ligands activates smoothened (SMO), which in turn activates the transcription factor GL1 [92]. GL1 modulates the transcription of several target genes in the nucleus, such as genes involved in cell cycle regulation and apoptosis, and promotes the MDM2-dependent degradation of p53 (Figure 3) [90]. Studies demonstrated that the treatment of CML-LSCs with the SMO inhibitor PF-04449913 promoted differentiation and increased their sensitivity to TKI [93,94]. Similarly, Anusha et al. showed that the sonic hedgehog pathway was activated in mutation-independent imatinib-resistant CML-LSCs and that treatment with the inhibitor of this pathway potentiated cells to imatinib treatment [95].

3.9. Dysregulation of Apoptotic Proteins' Expression

The intrinsic apoptotic pathway is regulated by the B-cell lymphoma-2 (Bcl-2) family proteins that maintain mitochondrial membrane integrity and regulate the apoptosis

cascade through processes such as apoptosome formation, cytochrome-c release, caspase activation, and cleavage of intracellular targets [96]. The Bcl-2 family proteins consists of pro-apoptotic (e.g., BIM and BAD) and pro-survival/anti-apoptotic (e.g., Bcl-2, Mcl-1, and Bcl-xL) proteins. The balance of pro- and anti-apoptotic proteins determines the activation of Bax and Bak. The activation of Bax and Bak leads to cytochrome-c release and the induction of apoptosis [96]. The dysregulation of anti-apoptotic proteins has been implicated in leukemogenesis, disease progression, and treatment resistance in myeloid leukaemia [96]. The overexpression of anti-apoptotic Bcl-2 protein and reduced expression of BIM have been shown to be involved in TKI resistance in CML [96]. BCR::ABL1 increases the expression of anti-apoptotic proteins such Bcl-2, Bcl-xL, and Mcl-1, which all play a role in preventing apoptosis in leukaemic cells [97]. The dysregulation of anti-apoptotic proteins has been observed in CML [97].

4. Targeted Therapies against BCR::ABL1-Independent Resistant Cells

Given the variety of BCR::ABL1-independent mechanisms of resistance, it is now important to focus the studies on the development of the most appropriate targeted therapy for a specific deregulated pathway. This will also involve the development of sensitive techniques for identifying specific biomarkers using phospho-flow and next-generation sequencing at diagnosis or at relapse [98]. Mutations in several genes have been identified in CML patients, such as *ASXL1*, *RUNX1*, *TET2*, *BCL6 Corepressor-Like 1* (*BCORL1*), *GATA-binding factor 2* (*GATA2*), and others [81]. Kim et al. showed a strong correlation between the mutations in *TP53*, *Lysine Methyltransferase 2D* (*KMT2D*), and *TET2* during TKI therapy and treatment failure in CML patients [82]. Additionally, *IKAROS Family Zinc Finger 1* (*IKZF1*) exon deletion has been reported to be associated with poorer outcomes in CML patients [81]. In an interesting study, Chan et al. discovered that mutations converging in one principal driver pathway were able to promote progression toward leukaemia [99]. Conversely, divergent signalling pathways represented a powerful barrier to transformations. Mutations in these divergent pathways prevented leukaemia instead of promoting it [99]. This finding is of principal relevance for the development of new targeted therapies against deregulated pathways in leukaemia. Chan et al. also demonstrated that targeting divergent pathways had a counterproductive effect on cancer progression. It is therefore vital to identify the driver pathway and target it [99]. This supports the possibility of developing drugs that could target different mediators of a driver pathway, increasing the possibility of finding the best precision medicine therapeutic approach.

In the context of BCR::ABL1-independent pathways, combination therapies that target both BCR::ABL1 and alternative survival pathways have the potential to eliminate leukaemic stem cells and sensitize progenitor cells, improving the treatment of CML. For instance, using a CML-mouse model, Shan et al. demonstrated that the inhibition of BCR::ABL1 with TKIs, combined with inhibition of the RAS pathway using trametinib, an FDA-approved MEK inhibitor, synergistically induced cell death in BCR::ABL1-independent MAPK pathway-driven imatinib-resistant CML stem cells [58]. Similarly, the JAK/STAT pathway has also been implicated in the survival of quiescent leukaemic stem cells, and the combination therapy of TKIs and ruxolitinib (JAK2 inhibitor) has been demonstrated to reduce their number in murine xenografts [100]. In a phase I clinical trial (NCT01702064), the combination therapy of nilotinib and ruxolitinib resulted in undetectable *BCR::ABL1* in 40% of CML patients after 6 months, as measured by RT-qPCR [101]. As a result, this combination treatment was recommended for further investigation in a phase II clinical trial [101]. Moreover, Yagi et al. reported that the specific activation of STAT3 in CML and the combined inhibition of JAK1 with tofacitinib and BCR::ABL1 with imatinib synergistically induced anti-tumour effects in CML cells [102]. Likewise, many PI3K/AKT/mTOR pathway inhibitors, including those which have received FDA approval, such as PI3K inhibitors (Idelalisib, Copanlisib, and Duvelisib) and mTOR inhibitors (Everolimus, Sirolimus, and Temsirolimus), have been studied as potential treatments against TKI-resistant CML, and active pre-clinical investigation is ongoing (Figure 3 and

Table 2) [67]. A clinical trial is underway for investigating the safety and efficacy of the co-treatment of imatinib and everolimus in CML (NCT00093639).

There are multiple clinical trials assessing the inhibitors of the WNT/β-catenin pathway in various haematological malignancies, including CML [32]. The results from phase I and II clinical trials are currently being evaluated for the safety and efficacy of PRI-724, an inhibitor of WNT/β-catenin pathway, in pancreatic cancer and leukaemia patients [32]. More recently, a combination treatment with dasatinib and okadaic acid (an inhibitor of PP2A) has also been shown to induce cell cycle arrest and apoptosis in the K562 cell line [103]. However, conflicting reports of the pro- and anti-survival role of PP2A warrants further investigation to understand the situations where such a dual role of PP2A exists [104]. Consistent with the previously reported tumour-suppressor role of PP2A, its activating drugs, such as FTY720 and OP449, have been shown to re-sensitize TKI-resistant LSCs to BCR::ABL1 inhibition by targeting the JAK2/PP2A/β-catenin pathway (Figure 3 and Table 2) [105]. Therefore, the combination of TKI and an FDA-approved PP2A activator FTY720 or OP449 has been actively investigated in preclinical studies [105].

Due to the ability of EZH2 to reprogram and prevent apoptosis in CML-leukaemic stem cells, the combination of TKI treatment and an FDA-approved inhibitor of EZH2, Tazemetostat, has also been actively investigated in pre-clinical trials [87]. Similarly, Stobo et al. demonstrated that the first-generation autophagy inhibitor hydroxychloroquine potentiated TKI-induced cell death in CML-leukaemic stem cells, but their recent clinical trial combining hydroxychloroquine with imatinib showed that clinically achievable doses of hydroxychloroquine were not sufficient to accomplish the efficient inhibition of autophagy [106]. Autophagy genes were found to be highly expressed in CML-patient-derived leukaemic stem cells compared with progenitor cells, and the genetic or pharmacological inhibition of autophagy with the second-generation autophagy inhibitor Lys05 resulted in decreased leukaemic cell viability and improved sensitivity to chemotherapy [107]. Therefore, the second-generation FDA-approved autophagy inhibitors Lys05 and PIK-III were combined with TKIs to investigate their effects in preclinical trials (Figure 3) [107].

There are ongoing clinical trials investigating the combination of TKIs and IFN-α to eliminate leukaemic stem cells, since IFN-α can augment immune responses while TKIs inhibit BCR::ABL1 to exert combined effects [108]. Palandri et al. revealed higher complete cytogenetic responses in the imatinib and IFN-α group compared with the imatinib-only group (60% vs. 42%, $p = 0.003$) at 6 months, with a more rapid response rate seen with the combination treatment [85]. However, there was no difference in the complete cytogenetic response rate at 48 months (88% vs. 88%). Another phase II study by the Nordic group showed higher major molecular response rates (82% vs. 54%) with an imatinib and IFN-α combination treatment compared with an imatinib-only treatment [109]. Another clinical trial investigating the combination of bosutinib with interferon is also underway, and results are yet to be published (NCT03831776) [110]. The combination therapy of TKIs and the hedgehog inhibitor trial was discontinued at a very early stage due to toxicity being observed [30]. If the drug could be further refined to minimize toxicity, there may be potential for using this combination treatment in CML.

Carter et al. first discovered that the anti-apoptotic protein Bcl-2 plays a key role in the survival of CML stem cells and progenitor cells, making it an attractive CML target [111]. The combined inhibition of Bcl-2 with venetoclax and TKI provided rationale for the potential curative treatment of CML (Figure 3 and Table 2) [111]. The phase II clinical trial (NCT02689440) combining TKI (dasatinib) and venetoclax in heavily pretreated blast-phase CML showed encouraging results, with a 75% overall response rate [112]. Another phase II clinical trial combining ponatinib, venetoclax, and decitabine in blast-phase CML is also underway, investigating the overall patient response rate (NCT04188405) [112].

Table 2. This table shows the BCR::ABL1-independent pathways and their inhibitors that could be used in combination with TKIs, and the stage of their current development for diseases listed that could be repurposed in the treatment of Ph+ leukaemias.

Target Pathway	Inhibitor/s	Stage of Development	Approved/Treated Disease	Ref.
RAS/RAF/MEK/ERK	• RAF inhibitor: Vemurafenib and Dabrafenib • MEK inhibitors: Trametinib and Cobimetinib (in combination with vemurafenib)	FDA approved FDA approved	BRAF(V600E) melanoma	[113]
JAK/STAT	1. JAK1 inhibitor: Rinvoq (upadacitinib) and Cibinqo (abrocitinib) 2. JAK2 inhibitor: Ruxolitinib 3. JAK1/2 inhibitor: Baricitinib	FDA approved FDA approved FDA approved	1. Myelofibrosis and ovarian cancer 2. Refractory moderate to severe atopic dermatitis 3. Rheumatoid arthritis	[114,115]
PI3K/AKT/mTOR	1. PI3K delta inhibitor: Idelalisib 2. PI3K alpha/delta inhibitor: Copanlisib 3. mTOR inhibitor: Sirolimus	FDA approved FDA approved FDA approved	1. Leukaemia and lymphoma 2. Relapsed follicular lymphoma 3. Lymphangioleiomyomatosis	[116,117]
Wnt/β-catenin	CBP/β-catenin antagonist: PRI-724	Phase 2 Clinical Trial (NCT01606579)	Acute myeloid leukaemia and chronic myeloid leukaemia	[118]
Tumour suppressor: PP2A	SET: FTY720 (Fingolimod)	FDA Approved	Multiple myeloma and mantle cell lymphoma	[119,120]
Epigenetic modulator: EZH2	Tazemetostat	FDA Approved	Advanced or metastatic epithelioid sarcoma	[121]
Immune system	IFN-α	FDA Approved	Hairy cell leukaemia, CML, follicular non-Hodgkin lymphoma, melanoma, and AIDS-related Kaposi's sarcoma	[34]
Hedgehog pathway	Vismodegib (GDC-0449) and Sonidegib (LDE225)	FDA Approved	Basal cell carcinoma and acute myeloid leukaemia	[122]
Intrinsic apoptotic pathway	Venetoclax	FDA Approved	Chronic lymphocytic leukaemia and acute myeloid leukaemia	[123]

5. Conclusions

Despite significant improvements in the treatment of CML with the clinical development of TKIs, some patients develop TKI resistance, some progress to blast crisis, and most remain dependent on TKI therapy for long-term disease control. The current strategies for addressing TKI resistance have mainly focused on improving the potency and specificity of the drugs that target BCR::ABL1 and/or on overcoming the resistance driven by mutations in the BCR::ABL1 oncogene. However, this approach may be less effective in many CML patients, who develop resistance despite the effective inhibition of BCR::ABL1 with TKIs, i.e., with BCR::ABL1-independent resistance mechanisms. Novel treatment strategies, such as combining TKIs with other agents that target alternative survival signalling, may be necessary to improve treatment outcomes in those patients. A combination-treatment approach could eradicate leukaemic stem cells to maximize treatment-free remission in CML and improve sensitivity to TKIs in non-responsive CML patients. Therefore, some combination strategies that target CML-leukaemic stem cells could be administered as a front-line treatment, while other CML patients who fail TKIs without evidence of any kinase domain/myristoyl domain mutations should be screened for alternative mechanisms of resistance, such as mutations, that can activate an alternative survival pathway to decide an appropriate combination-treatment approach. These combination approaches could

address the current unmet treatment needs in CML by eliminating leukaemic stem cells and sensitizing TKI-resistant progenitor cells, therefore improving treatment outcomes.

Author Contributions: Conceptualization, G.P., T.P.H. and I.S.P.; resources, T.P.H.; writing—original draft preparation, G.P.; writing—review and editing, G.P., M.G.T., T.P.H. and I.S.P.; supervision, T.P.H. and I.S.P.; project administration, G.P.; funding acquisition, T.P.H. All authors have read and agreed to the published version of the manuscript.

Funding: This research received no external funding.

Acknowledgments: Govinda Poudel received support through "Australian Government Research Training Program Scholarship". Ilaria S Pagani received support through the Cancer Council Beat Cancer Project Mid-Career Research Fellowship.

Conflicts of Interest: Authors do not have any disclosable conflicts of interest.

References

1. Bennett, J.H. Case of hypertrophy of the spleen and liver, in which death took place from suppuration of the blood. *Edinburgh Med. Sug. J.* **1845**, *64*, 413–423.
2. Nowell, P.C.; Hungerford, D.A. Chromosome studies on normal and leukemic human leukocytes. *J. Natl. Cancer Inst.* **1960**, *25*, 85–109. [PubMed]
3. Propp, S.; Lizzi, F.A. Brief Report: Philadelphia Chromosome in Acute Lymphocytic Leukemia. *Blood* **1970**, *36*, 353–360. [CrossRef] [PubMed]
4. Quintas-Cardama, A.; Cortes, J. Molecular biology of bcr-abl1-positive chronic myeloid leukemia. *Blood* **2009**, *113*, 1619–1630. [CrossRef] [PubMed]
5. Flis, S.; Chojnacki, T. Chronic myelogenous leukemia, a still unsolved problem: Pitfalls and new therapeutic possibilities. *Drug Des. Dev. Ther.* **2019**, *13*, 825–843. [CrossRef] [PubMed]
6. Deininger, M.W.; Goldman, J.M.; Melo, J.V. The molecular biology of chronic myeloid leukemia. *Blood* **2000**, *96*, 3343–3356. [CrossRef] [PubMed]
7. Saxena, K.; Jabbour, E.; Issa, G.; Sasaki, K.; Ravandi, F.; Maiti, A.; Daver, N.; Kadia, T.; DiNardo, C.D.; Konopleva, M.; et al. Impact of frontline treatment approach on outcomes of myeloid blast phase CML. *J. Hematol. Oncol.* **2021**, *14*, 94. [CrossRef]
8. Sessions, J. Chronic myeloid leukemia in 2007. *Am. J. Health-Syst. Pharm.* **2007**, *64*, S4–S9. [CrossRef]
9. McWhirter, J.R.; Wang, J.Y. An actin-binding function contributes to transformation by the Bcr-Abl oncoprotein of Philadelphia chromosome-positive human leukemias. *EMBO J.* **1993**, *12*, 1533–1546. [CrossRef]
10. Peiris, M.N.; Li, F.; Donoghue, D.J. BCR: A promiscuous fusion partner in hematopoietic disorders. *Oncotarget* **2019**, *10*, 2738–2754. [CrossRef]
11. Pendergast, A.M.; Quilliam, L.A.; Cripe, L.D.; Bassing, C.H.; Dai, Z.; Li, N.; Batzer, A.; Rabun, K.M.; Der, C.J.; Schlessinger, J. BCR-ABL-induced oncogenesis is mediated by direct interaction with the SH2 domain of the GRB-2 adaptor protein. *Cell* **1993**, *75*, 175–185. [CrossRef]
12. Hantschel, O.; Nagar, B.; Guettler, S.; Kretzschmar, J.; Dorey, K.; Kuriyan, J.; Superti-Furga, G. A myristoyl/phosphotyrosine switch regulates c-Abl. *Cell* **2003**, *112*, 845–857. [CrossRef]
13. Vinhas, R.; Lourenco, A.; Santos, S.; Lemos, M.; Ribeiro, P.; de Sousa, A.B.; Baptista, P.V.; Fernandes, A.R. A novel BCR-ABL1 mutation in a patient with Philadelphia chromosome-positive B-cell acute lymphoblastic leukemia. *Oncol. Targets Ther.* **2018**, *11*, 8589–8598. [CrossRef]
14. Shawver, L.K.; Slamon, D.; Ullrich, A. Smart drugs: Tyrosine kinase inhibitors in cancer therapy. *Cancer Cell* **2002**, *1*, 117–123. [CrossRef]
15. Radich, J.P.; Deininger, M.; Abboud, C.N.; Altman, J.K.; Berman, E.; Bhatia, R.; Bhatnagar, B.; Curtin, P.; DeAngelo, D.J.; Gotlib, J.; et al. Chronic Myeloid Leukemia, Version 1.2019, NCCN Clinical Practice Guidelines in Oncology. *J. Natl. Compr. Cancer Netw.* **2018**, *16*, 1108–1135. [CrossRef]
16. Hughes, T.P.; Mauro, M.J.; Cortes, J.E.; Minami, H.; Rea, D.; DeAngelo, D.J.; Breccia, M.; Goh, Y.-T.; Talpaz, M.; Hochhaus, A.; et al. Asciminib in Chronic Myeloid Leukemia after ABL Kinase Inhibitor Failure. *N. Engl. J. Med.* **2019**, *381*, 2315–2326. [CrossRef]
17. FDA. FDA Approves Asciminib for Philadelphia Chromosome-Positive Chronic Myeloid Leukemia. Available online: https://www.fda.gov/drugs/resources-information-approved-drugs/fda-approves-asciminib-philadelphia-chromosome-positive-chronic-myeloid-leukemia (accessed on 9 December 2021).
18. Wylie, A.A.; Schoepfer, J.; Jahnke, W.; Cowan-Jacob, S.W.; Loo, A.; Furet, P.; Marzinzik, A.L.; Pelle, X.; Donovan, J.; Zhu, W.; et al. The allosteric inhibitor ABL001 enables dual targeting of BCR-ABL1. *Nature* **2017**, *543*, 733–737. [CrossRef]
19. Soverini, S.; Mancini, M.; Bavaro, L.; Cavo, M.; Martinelli, G. Chronic myeloid leukemia: The paradigm of targeting oncogenic tyrosine kinase signaling and counteracting resistance for successful cancer therapy. *Mol. Cancer* **2018**, *17*, 49. [CrossRef]
20. Branford, S.; Fletcher, L.; Cross, N.C.; Muller, M.C.; Hochhaus, A.; Kim, D.W.; Radich, J.P.; Saglio, G.; Pane, F.; Kamel-Reid, S.; et al. Desirable performance characteristics for BCR-ABL measurement on an international reporting scale to allow consistent

interpretation of individual patient response and comparison of response rates between clinical trials. *Blood* **2008**, *112*, 3330–3338. [CrossRef]
21. Baccarani, M.; Deininger, M.W.; Rosti, G.; Hochhaus, A.; Soverini, S.; Apperley, J.F.; Cervantes, F.; Clark, R.E.; Cortes, J.E.; Guilhot, F.; et al. European LeukemiaNet recommendations for the management of chronic myeloid leukemia: 2013. *Blood* **2013**, *122*, 872–884. [CrossRef]
22. Breccia, M.; Molica, M.; Colafigli, G.; Massaro, F.; Quattrocchi, L.; Latagliata, R.; Mancini, M.; Diverio, D.; Guarini, A.; Alimena, G.; et al. Prognostic factors associated with a stable MR4.5 achievement in chronic myeloid leukemia patients treated with imatinib. *Oncotarget* **2018**, *9*, 7534–7540. [CrossRef]
23. Wang, R.; Cong, Y.; Li, C.; Zhang, C.; Lin, H. Predictive value of early molecular response for deep molecular response in chronic phase of chronic myeloid leukemia. *Medicine* **2019**, *98*, e15222. [CrossRef]
24. Hughes, T.; Boquimpani, C.; Takahashi, N.; Benyamini, N.; Clementino, N.; Shuvaev, V.; Ailawadhi, S.; Lipton, J.; Turkina, A.; Paz, R. Durable treatment-free remission after stopping second line nilotinib in patients with chronic myeloid leukemia in chronic phase: ENESTOP 96-wk update. *Haematologica* **2017**, *102*, 75.
25. Ross, D.M.; Pagani, I.S.; Shanmuganathan, N.; Kok, C.H.; Seymour, J.F.; Mills, A.K.; Filshie, R.J.; Arthur, C.K.; Dang, P.; Saunders, V.A.; et al. Long-term treatment-free remission of chronic myeloid leukemia with falling levels of residual leukemic cells. *Leukemia* **2018**, *32*, 2572–2579. [CrossRef]
26. Ross, D.M.; Hughes, T.P. Treatment-free remission in patients with chronic myeloid leukaemia. *Nat. Rev. Clin. Oncol.* **2020**, *17*, 493–503. [CrossRef]
27. Mahon, F.-X.; Réa, D.; Guilhot, J.; Guilhot, F.; Huguet, F.; Nicolini, F.; Legros, L.; Charbonnier, A.; Guerci, A.; Varet, B. Discontinuation of imatinib in patients with chronic myeloid leukaemia who have maintained complete molecular remission for at least 2 years: The prospective, multicentre Stop Imatinib (STIM) trial. *Lancet Oncol.* **2010**, *11*, 1029–1035. [CrossRef]
28. Bonifacio, M.; Stagno, F.; Scaffidi, L.; Krampera, M.; Di Raimondo, F. Management of Chronic Myeloid Leukemia in Advanced Phase. *Front. Oncol* **2019**, *9*, 1132. [CrossRef]
29. Soverini, S.; Bassan, R.; Lion, T. Treatment and monitoring of Philadelphia chromosome-positive leukemia patients: Recent advances and remaining challenges. *J. Hematol. Oncol.* **2019**, *12*, 39. [CrossRef]
30. Braun, T.P.; Eide, C.A.; Druker, B.J. Response and resistance to BCR-ABL1-targeted therapies. *Cancer Cell* **2020**, *37*, 530–542. [CrossRef]
31. Loscocco, F.; Visani, G.; Galimberti, S.; Curti, A.; Isidori, A. BCR-ABL Independent Mechanisms of Resistance in Chronic Myeloid Leukemia. *Front. Oncol.* **2019**, *9*, 939. [CrossRef]
32. Zhang, Y.; Wang, X. Targeting the Wnt/beta-catenin signaling pathway in cancer. *J. Hematol. Oncol.* **2020**, *13*, 165. [CrossRef] [PubMed]
33. Patel, A.B.; O'Hare, T.; Deininger, M.W. Mechanisms of Resistance to ABL Kinase Inhibition in Chronic Myeloid Leukemia and the Development of Next Generation ABL Kinase Inhibitors. *Hematol. Oncol. Clin. N. Am.* **2017**, *31*, 589–612. [CrossRef] [PubMed]
34. Borden, E.C. Interferons alpha and beta in cancer: Therapeutic opportunities from new insights. *Nat. Rev. Drug Discov.* **2019**, *18*, 219–234. [CrossRef] [PubMed]
35. Chandrasekhar, C.; Kumar, P.S.; Sarma, P. Novel mutations in the kinase domain of BCR-ABL gene causing imatinib resistance in chronic myeloid leukemia patients. *Sci. Rep.* **2019**, *9*, 2412. [CrossRef]
36. Redaelli, S.; Piazza, R.; Rostagno, R.; Magistroni, V.; Perini, P.; Marega, M.; Gambacorti-Passerini, C.; Boschelli, F. Activity of bosutinib, dasatinib, and nilotinib against 18 imatinib-resistant BCR/ABL mutants. *J. Clin. Oncol.* **2009**, *27*, 469–471. [CrossRef]
37. Zabriskie, M.S.; Eide, C.A.; Tantravahi, S.K.; Vellore, N.A.; Estrada, J.; Nicolini, F.E.; Khoury, H.J.; Larson, R.A.; Konopleva, M.; Cortes, J.E.; et al. BCR-ABL1 compound mutations combining key kinase domain positions confer clinical resistance to ponatinib in Ph chromosome-positive leukemia. *Cancer Cell* **2014**, *26*, 428–442. [CrossRef]
38. Pagani, I.S.; Dang, P.; Saunders, V.A.; Braley, J.; Thieleke, A.; Branford, S.; Hughes, T.P.; Ross, D.M. Clinical utility of genomic DNA Q-PCR for the monitoring of a patient with atypical e19a2 BCR-ABL1 transcripts in chronic myeloid leukemia. *Leuk. Lymphoma* **2020**, *61*, 2527–2529. [CrossRef]
39. Cortes, J.E.; Hughes, T.P.; Mauro, M.J.; Hochhaus, A.; Rea, D.; Goh, Y.T.; Janssen, J.; Steegmann, J.L.; Heinrich, M.C.; Talpaz, M.; et al. Asciminib, a First-in-Class STAMP Inhibitor, Provides Durable Molecular Response in Patients (pts) with Chronic Myeloid Leukemia (CML) Harboring the T315I Mutation: Primary Efficacy and Safety Results from a Phase 1 Trial. *Blood* **2020**, *136*, 47–50. [CrossRef]
40. Garcia-Gutierrez, V.; Luna, A.; Alonso-Dominguez, J.M.; Estrada, N.; Boque, C.; Xicoy, B.; Giraldo, P.; Angona, A.; Alvarez-Larran, A.; Sanchez-Guijo, F.; et al. Safety and efficacy of asciminib treatment in chronic myeloid leukemia patients in real-life clinical practice. *Blood Cancer J.* **2021**, *11*, 16. [CrossRef]
41. Soverini, S.; Abruzzese, E.; Bocchia, M.; Bonifacio, M.; Galimberti, S.; Gozzini, A.; Iurlo, A.; Luciano, L.; Pregno, P.; Rosti, G.; et al. Next-generation sequencing for BCR-ABL1 kinase domain mutation testing in patients with chronic myeloid leukemia: A position paper. *J. Hematol. Oncol.* **2019**, *12*, 131. [CrossRef]
42. Zhan, J.Y.; Ma, J.; Zheng, Q.C. Molecular dynamics investigation on the Asciminib resistance mechanism of I502L and V468F mutations in BCR-ABL. *J. Mol. Graph. Model.* **2019**, *89*, 242–249. [CrossRef]
43. Qiang, W.; Antelope, O.; Zabriskie, M.S.; Pomicter, A.D.; Vellore, N.A.; Szankasi, P.; Rea, D.; Cayuela, J.M.; Kelley, T.W.; Deininger, M.W.; et al. Mechanisms of resistance to the BCR-ABL1 allosteric inhibitor asciminib. *Leukemia* **2017**, *31*, 2844–2847. [CrossRef]

44. Yaghmaie, M.; Yeung, C.C. Molecular Mechanisms of Resistance to Tyrosine Kinase Inhibitors. *Curr. Hematol. Malig. Rep.* **2019**, *14*, 395–404. [CrossRef]
45. Choi, Y.H.; Yu, A.M. ABC transporters in multidrug resistance and pharmacokinetics, and strategies for drug development. *Curr. Pharm. Des.* **2014**, *20*, 793–807. [CrossRef]
46. Eadie, L.N.; Dang, P.; Saunders, V.A.; Yeung, D.T.; Osborn, M.P.; Grigg, A.P.; Hughes, T.P.; White, D.L. The clinical significance of ABCB1 overexpression in predicting outcome of CML patients undergoing first-line imatinib treatment. *Leukemia* **2017**, *31*, 75–82. [CrossRef]
47. Mahon, F.X.; Belloc, F.; Lagarde, V.; Chollet, C.; Moreau-Gaudry, F.; Reiffers, J.; Goldman, J.M.; Melo, J.V. MDR1 gene overexpression confers resistance to imatinib mesylate in leukemia cell line models. *Blood* **2003**, *101*, 2368–2373. [CrossRef]
48. Eadie, L.N.; Saunders, V.A.; Branford, S.; White, D.L.; Hughes, T.P. The new allosteric inhibitor asciminib is susceptible to resistance mediated by ABCB1 and ABCG2 overexpression in vitro. *Oncotarget* **2018**, *9*, 13423. [CrossRef]
49. White, D.L.; Saunders, V.A.; Dang, P.; Engler, J.; Venables, A.; Zrim, S.; Zannettino, A.; Lynch, K.; Manley, P.W.; Hughes, T. Most CML patients who have a suboptimal response to imatinib have low OCT-1 activity: Higher doses of imatinib may overcome the negative impact of low OCT-1 activity. *Blood* **2007**, *110*, 4064–4072. [CrossRef]
50. Hiwase, D.K.; Saunders, V.; Hewett, D.; Frede, A.; Zrim, S.; Dang, P.; Eadie, L.; To, L.B.; Melo, J.; Kumar, S.; et al. Dasatinib cellular uptake and efflux in chronic myeloid leukemia cells: Therapeutic implications. *Clin. Cancer Res.* **2008**, *14*, 3881–3888. [CrossRef]
51. Lu, L.; Saunders, V.; Leclercq, T.; Hughes, T.; White, D. Ponatinib is not transported by ABCB1, ABCG2 or OCT-1 in CML cells. *Leukemia* **2015**, *29*, 1792. [CrossRef]
52. Dohse, M.; Scharenberg, C.; Shukla, S.; Robey, R.W.; Volkmann, T.; Deeken, J.F.; Brendel, C.; Ambudkar, S.V.; Neubauer, A.; Bates, S.E. Comparison of ATP-binding cassette transporter interactions with the tyrosine kinase inhibitors imatinib, nilotinib, and dasatinib. *Drug Metab. Dispos.* **2010**, *38*, 1371–1380. [CrossRef] [PubMed]
53. Agrawal, M.; Hanfstein, B.; Erben, P.; Wolf, D.; Ernst, T.; Fabarius, A.; Saussele, S.; Purkayastha, D.; Woodman, R.C.; Hofmann, W.K.; et al. MDR1 expression predicts outcome of Ph+ chronic phase CML patients on second-line nilotinib therapy after imatinib failure. *Leukemia* **2014**, *28*, 1478–1485. [CrossRef] [PubMed]
54. Shanmuganathan, N.; Branford, S. The Hidden Pathogenesis of CML: Is BCR-ABL1 the First Event? *Curr. Hematol. Malig. Rep.* **2019**, *14*, 501–506. [CrossRef] [PubMed]
55. Eiring, A.M.; Khorashad, J.S.; Anderson, D.J.; Yu, F.; Redwine, H.M.; Mason, C.C.; Reynolds, K.R.; Clair, P.M.; Gantz, K.C.; Zhang, T.Y. β-Catenin is required for intrinsic but not extrinsic BCR-ABL1 kinase-independent resistance to tyrosine kinase inhibitors in chronic myeloid leukemia. *Leukemia* **2015**, *29*, 2328. [CrossRef]
56. Mojtahedi, H.; Yazdanpanah, N.; Rezaei, N. Chronic myeloid leukemia stem cells: Targeting therapeutic implications. *Stem Cell Res. Ther.* **2021**, *12*, 603. [CrossRef]
57. Amarante-Mendes, G.P.; Rana, A.; Datoguia, T.S.; Hamerschlak, N.; Brumatti, G. BCR-ABL1 Tyrosine kinase complex signaling transduction: Challenges to overcome resistance in chronic myeloid leukemia. *Pharmaceutics* **2022**, *14*, 215. [CrossRef]
58. Ma, L.; Shan, Y.; Bai, R.; Xue, L.; Eide, C.A.; Ou, J.; Zhu, L.J.; Hutchinson, L.; Cerny, J.; Khoury, H.J.; et al. A therapeutically targetable mechanism of BCR-ABL-independent imatinib resistance in chronic myeloid leukemia. *Sci. Transl. Med.* **2014**, *6*, 252ra121. [CrossRef]
59. Suzuki, M.; Abe, A.; Imagama, S.; Nomura, Y.; Tanizaki, R.; Minami, Y.; Hayakawa, F.; Ito, Y.; Katsumi, A.; Yamamoto, K. BCR-ABL-independent and RAS/MAPK pathway-dependent form of imatinib resistance in Ph-positive acute lymphoblastic leukemia cell line with activation of EphB4. *Eur. J. Haematol.* **2010**, *84*, 229–238. [CrossRef]
60. Kumar, A.; Bhattacharyya, J.; Jaganathan, B.G. Adhesion to stromal cells mediates imatinib resistance in chronic myeloid leukemia through ERK and BMP signaling pathways. *Sci. Rep.* **2017**, *7*, 9535. [CrossRef]
61. Bousoik, E.; Montazeri Aliabadi, H. "Do We Know Jack" About JAK? A Closer Look at JAK/STAT Signaling Pathway. *Front. Oncol.* **2018**, *8*, 287. [CrossRef]
62. Brachet-Botineau, M.; Polomski, M.; Neubauer, H.A.; Juen, L.; Hedou, D.; Viaud-Massuard, M.C.; Prie, G.; Gouilleux, F. Pharmacological Inhibition of Oncogenic STAT3 and STAT5 Signaling in Hematopoietic Cancers. *Cancers* **2020**, *12*, 240. [CrossRef]
63. Eiring, A.; Kraft, I.; Page, B.; O'hare, T.; Gunning, P.; Deininger, M. STAT3 as a mediator of BCR-ABL1-independent resistance in chronic myeloid leukemia. *Leuk. Suppl.* **2014**, *3*, S5. [CrossRef]
64. Kuepper, M.K.; Butow, M.; Herrmann, O.; Ziemons, J.; Chatain, N.; Maurer, A.; Kirschner, M.; Maie, T.; Costa, I.G.; Eschweiler, J.; et al. Stem cell persistence in CML is mediated by extrinsically activated JAK1-STAT3 signaling. *Leukemia* **2019**, *33*, 1964–1977. [CrossRef]
65. Gullaksen, S.E.; Skavland, J.; Gavasso, S.; Tosevski, V.; Warzocha, K.; Dumrese, C.; Ferrant, A.; Gedde-Dahl, T.; Hellmann, A.; Janssen, J.; et al. Single cell immune profiling by mass cytometry of newly diagnosed chronic phase chronic myeloid leukemia treated with nilotinib. *Haematologica* **2017**, *102*, 1361–1367. [CrossRef]
66. Warsch, W.; Kollmann, K.; Eckelhart, E.; Fajmann, S.; Cerny-Reiterer, S.; Holbl, A.; Gleixner, K.V.; Dworzak, M.; Mayerhofer, M.; Hoermann, G.; et al. High STAT5 levels mediate imatinib resistance and indicate disease progression in chronic myeloid leukemia. *Blood* **2011**, *117*, 3409–3420. [CrossRef]
67. Singh, P.; Kumar, V.; Gupta, S.K.; Kumari, G.; Verma, M. Combating TKI resistance in CML by inhibiting the PI3K/Akt/mTOR pathway in combination with TKIs: A review. *Med. Oncol.* **2021**, *38*, 10. [CrossRef]

68. Burchert, A.; Wang, Y.; Cai, D.; Von Bubnoff, N.; Paschka, P.; Müller-Brüsselbach, S.; Ottmann, O.; Duyster, J.; Hochhaus, A.; Neubauer, A. Compensatory PI3-kinase/Akt/mTor activation regulates imatinib resistance development. *Leukemia* **2005**, *19*, 1774. [CrossRef]
69. Wagle, M.; Eiring, A.M.; Wongchenko, M.; Lu, S.; Guan, Y.; Wang, Y.; Lackner, M.; Amler, L.; Hampton, G.; Deininger, M.W.; et al. A role for FOXO1 in BCR-ABL1-independent tyrosine kinase inhibitor resistance in chronic myeloid leukemia. *Leukemia* **2016**, *30*, 1493–1501. [CrossRef]
70. Mitchell, R.; Hopcroft, L.E.M.; Baquero, P.; Allan, E.K.; Hewit, K.; James, D.; Hamilton, G.; Mukhopadhyay, A.; O'Prey, J.; Hair, A.; et al. Targeting BCR-ABL-Independent TKI Resistance in Chronic Myeloid Leukemia by mTOR and Autophagy Inhibition. *J. Natl. Cancer Inst.* **2018**, *110*, 467–478. [CrossRef]
71. Bellodi, C.; Lidonnici, M.R.; Hamilton, A.; Helgason, G.V.; Soliera, A.R.; Ronchetti, M.; Galavotti, S.; Young, K.W.; Selmi, T.; Yacobi, R. Targeting autophagy potentiates tyrosine kinase inhibitor–induced cell death in Philadelphia chromosome–positive cells, including primary CML stem cells. *J. Clin. Investig.* **2013**, *123*, 3634. [CrossRef]
72. Nazio, F.; Bordi, M.; Cianfanelli, V.; Locatelli, F.; Cecconi, F. Autophagy and cancer stem cells: Molecular mechanisms and therapeutic applications. *Cell Death Differ.* **2019**, *26*, 690–702. [CrossRef] [PubMed]
73. Rothe, K.; Porter, V.; Jiang, X. Current Outlook on Autophagy in Human Leukemia: Foe in Cancer Stem Cells and Drug Resistance, Friend in New Therapeutic Interventions. *Int. J. Mol. Sci.* **2019**, *20*, 461. [CrossRef] [PubMed]
74. Karvela, M.; Baquero, P.; Kuntz, E.M.; Mukhopadhyay, A.; Mitchell, R.; Allan, E.K.; Chan, E.; Kranc, K.R.; Calabretta, B.; Salomoni, P.; et al. ATG7 regulates energy metabolism, differentiation and survival of Philadelphia-chromosome-positive cells. *Autophagy* **2016**, *12*, 936–948. [CrossRef] [PubMed]
75. Arrigoni, E.; Del Re, M.; Galimberti, S.; Restante, G.; Rofi, E.; Crucitta, S.; Barate, C.; Petrini, M.; Danesi, R.; Di Paolo, A. Concise Review: Chronic Myeloid Leukemia: Stem Cell Niche and Response to Pharmacologic Treatment. *Stem Cells Transl. Med.* **2018**, *7*, 305–314. [CrossRef]
76. Leo, E.; Mancini, M.; Aluigi, M.; Luatti, S.; Castagnetti, F.; Testoni, N.; Soverini, S.; Santucci, M.A.; Martinelli, G. BCR-ABL1-associated reduction of beta catenin antagonist Chibby1 in chronic myeloid leukemia. *PLoS ONE* **2013**, *8*, e81425. [CrossRef]
77. Zhou, H.; Mak, P.Y.; Mu, H.; Mak, D.H.; Zeng, Z.; Cortes, J.; Liu, Q.; Andreeff, M.; Carter, B.Z. Combined inhibition of beta-catenin and Bcr-Abl synergistically targets tyrosine kinase inhibitor-resistant blast crisis chronic myeloid leukemia blasts and progenitors in vitro and in vivo. *Leukemia* **2017**, *31*, 2065–2074. [CrossRef]
78. Ciccone, M.; Calin, G.A.; Perrotti, D. From the Biology of PP2A to the PADs for Therapy of Hematologic Malignancies. *Front. Oncol.* **2015**, *5*, 21. [CrossRef]
79. Zhan, T.; Rindtorff, N.; Boutros, M. Wnt signaling in cancer. *Oncogene* **2017**, *36*, 1461–1473. [CrossRef]
80. Neviani, P.; Harb, J.G.; Oaks, J.J.; Santhanam, R.; Walker, C.J.; Ellis, J.J.; Ferenchak, G.; Dorrance, A.M.; Paisie, C.A.; Eiring, A.M. PP2A-activating drugs selectively eradicate TKI-resistant chronic myeloid leukemic stem cells. *J. Clin. Investig.* **2013**, *123*, 4144–4157. [CrossRef]
81. Branford, S.; Kim, D.D.H.; Apperley, J.F.; Eide, C.A.; Mustjoki, S.; Ong, S.T.; Nteliopoulos, G.; Ernst, T.; Chuah, C.; Gambacorti-Passerini, C.; et al. Laying the foundation for genomically-based risk assessment in chronic myeloid leukemia. *Leukemia* **2019**, *33*, 1835–1850. [CrossRef]
82. Kim, T.; Tyndel, M.S.; Kim, H.J.; Ahn, J.S.; Choi, S.H.; Park, H.J.; Kim, Y.K.; Kim, S.Y.; Lipton, J.H.; Zhang, Z.; et al. Spectrum of somatic mutation dynamics in chronic myeloid leukemia following tyrosine kinase inhibitor therapy. *Blood* **2017**, *129*, 38–47. [CrossRef]
83. Mitani, K.; Nagata, Y.; Sasaki, K.; Yoshida, K.; Chiba, K.; Tanaka, H.; Shiraishi, Y.; Miyano, S.; Makishima, H.; Nakamura, Y.; et al. Somatic mosaicism in chronic myeloid leukemia in remission. *Blood* **2016**, *128*, 2863–2866. [CrossRef]
84. Togasaki, E.; Takeda, J.; Yoshida, K.; Shiozawa, Y.; Takeuchi, M.; Oshima, M.; Saraya, A.; Iwama, A.; Yokote, K.; Sakaida, E.; et al. Frequent somatic mutations in epigenetic regulators in newly diagnosed chronic myeloid leukemia. *Blood Cancer J.* **2017**, *7*, e559. [CrossRef]
85. Palandri, F.; Castagnetti, F.; Iacobucci, I.; Martinelli, G.; Amabile, M.; Gugliotta, G.; Poerio, A.; Testoni, N.; Breccia, M.; Bocchia, M.; et al. The response to imatinib and interferon-alpha is more rapid than the response to imatinib alone: A retrospective analysis of 495 Philadelphia-positive chronic myeloid leukemia patients in early chronic phase. *Haematologica* **2010**, *95*, 1415–1419. [CrossRef]
86. Xie, H.; Peng, C.; Huang, J.; Li, B.E.; Kim, W.; Smith, E.C.; Fujiwara, Y.; Qi, J.; Cheloni, G.; Das, P.P.; et al. Chronic Myelogenous Leukemia- Initiating Cells Require Polycomb Group Protein EZH2. *Cancer Discov.* **2016**, *6*, 1237–1247. [CrossRef]
87. Scott, M.T.; Korfi, K.; Saffrey, P.; Hopcroft, L.E.M.; Kinstrie, R.; Pellicano, F.; Guenther, C.; Gallipoli, P.; Cruz, M.; Dunn, K.; et al. Epigenetic Reprogramming Sensitizes CML Stem Cells to Combined EZH2 and Tyrosine Kinase Inhibition. *Cancer Discov.* **2016**, *6*, 1248. [CrossRef]
88. Giustacchini, A.; Thongjuea, S.; Barkas, N.; Woll, P.S.; Povinelli, B.J.; Booth, C.A.G.; Sopp, P.; Norfo, R.; Rodriguez-Meira, A.; Ashley, N.; et al. Single-cell transcriptomics uncovers distinct molecular signatures of stem cells in chronic myeloid leukemia. *Nat. Med.* **2017**, *23*, 692–702. [CrossRef]
89. Niyaz, M.; Khan, M.S.; Mudassar, S. Hedgehog Signaling: An Achilles' Heel in Cancer. *Transl. Oncol.* **2019**, *12*, 1334–1344. [CrossRef]

90. Dierks, C.; Beigi, R.; Guo, G.-R.; Zirlik, K.; Stegert, M.R.; Manley, P.; Trussell, C.; Schmitt-Graeff, A.; Landwerlin, K.; Veelken, H. Expansion of Bcr-Abl-positive leukemic stem cells is dependent on Hedgehog pathway activation. *Cancer Cell* **2008**, *14*, 238–249. [CrossRef]
91. Cochrane, C.R.; Szczepny, A.; Watkins, D.N.; Cain, J.E. Hedgehog Signaling in the Maintenance of Cancer Stem Cells. *Cancers* **2015**, *7*, 1554–1585. [CrossRef]
92. Rimkus, T.K.; Carpenter, R.L.; Qasem, S.; Chan, M.; Lo, H.W. Targeting the Sonic Hedgehog Signaling Pathway: Review of Smoothened and GLI Inhibitors. *Cancers* **2016**, *8*, 22. [CrossRef]
93. Sadarangani, A.; Pineda, G.; Lennon, K.M.; Chun, H.J.; Shih, A.; Schairer, A.E.; Court, A.C.; Goff, D.J.; Prashad, S.L.; Geron, I.; et al. GLI2 inhibition abrogates human leukemia stem cell dormancy. *J. Transl. Med.* **2015**, *13*, 98. [CrossRef] [PubMed]
94. Zhao, C.; Chen, A.; Jamieson, C.H.; Fereshteh, M.; Abrahamsson, A.; Blum, J.; Kwon, H.Y.; Kim, J.; Chute, J.P.; Rizzieri, D. Hedgehog signalling is essential for maintenance of cancer stem cells in myeloid leukaemia. *Nature* **2009**, *458*, 776–779. [CrossRef] [PubMed]
95. Anusha; Dalal, H.; Subramanian, S.; Snijesh, V.P.; Gowda, D.A.; Krishnamurthy, H.; Damodar, S.; Vyas, N. Exovesicular-Shh confers Imatinib resistance by upregulating Bcl2 expression in chronic myeloid leukemia with variant chromosomes. *Cell Death Dis.* **2021**, *12*, 259. [CrossRef] [PubMed]
96. Parry, N.; Wheadon, H.; Copland, M. The application of BH3 mimetics in myeloid leukemias. *Cell Death Dis.* **2021**, *12*, 222. [CrossRef]
97. Zhang, J.; Liu, X.; Yin, C.; Zong, S. hnRNPK/Beclin1 signaling regulates autophagy to promote imatinib resistance in Philadelphia chromosome-positive acute lymphoblastic leukemia cells. *Exp. Hematol.* **2022**, *108*, 46–54. [CrossRef]
98. Medina, A.; Puig, N.; Flores-Montero, J.; Jimenez, C.; Sarasquete, M.E.; Garcia-Alvarez, M.; Prieto-Conde, I.; Chillon, C.; Alcoceba, M.; Gutierrez, N.C.; et al. Comparison of next-generation sequencing (NGS) and next-generation flow (NGF) for minimal residual disease (MRD) assessment in multiple myeloma. *Blood Cancer J.* **2020**, *10*, 108. [CrossRef]
99. Chan, L.N.; Murakami, M.A.; Robinson, M.E.; Caeser, R.; Sadras, T.; Lee, J.; Cosgun, K.N.; Kume, K.; Khairnar, V.; Xiao, G.; et al. Signalling input from divergent pathways subverts B cell transformation. *Nature* **2020**, *583*, 845–851. [CrossRef]
100. Gallipoli, P.; Cook, A.; Rhodes, S.; Hopcroft, L.; Wheadon, H.; Whetton, A.D.; Jorgensen, H.G.; Bhatia, R.; Holyoake, T.L. JAK2/STAT5 inhibition by nilotinib with ruxolitinib contributes to the elimination of CML CD34+ cells in vitro and in vivo. *Blood* **2014**, *124*, 1492–1501. [CrossRef]
101. Sweet, K.; Hazlehurst, L.; Sahakian, E.; Powers, J.; Nodzon, L.; Kayali, F.; Hyland, K.; Nelson, A.; Pinilla-Ibarz, J. A phase I clinical trial of ruxolitinib in combination with nilotinib in chronic myeloid leukemia patients with molecular evidence of disease. *Leuk. Res.* **2018**, *74*, 89–96. [CrossRef]
102. Yagi, K.; Shimada, A.; Sendo, T. Pharmacological inhibition of JAK3 enhances the antitumor activity of imatinib in human chronic myeloid leukemia. *Eur. J. Pharmacol.* **2018**, *825*, 28–33. [CrossRef]
103. Ozel, B.; Kipcak, S.; Biray Avci, C.; Gunduz, C.; Saydam, G.; Aktan, C.; Selvi Gunel, N. Combination of dasatinib and okadaic acid induces apoptosis and cell cycle arrest by targeting protein phosphatase PP2A in chronic myeloid leukemia cells. *Med. Oncol.* **2022**, *39*, 46. [CrossRef]
104. Perrotti, D.; Agarwal, A.; Lucas, C.M.; Narla, G.; Neviani, P.; Odero, M.D.; Ruvolo, P.P.; Verrills, N.M. Comment on "PP2A inhibition sensitizes cancer stem cells to ABL tyrosine kinase inhibitors in BCR-ABL human leukemia". *Sci. Transl. Med.* **2019**, *11*, eaau0416. [CrossRef]
105. Mazhar, S.; Taylor, S.E.; Sangodkar, J.; Narla, G. Targeting PP2A in cancer: Combination therapies. *Biochim. Biophys. Acta Mol. Cell Res.* **2019**, *1866*, 51–63. [CrossRef]
106. Horne, G.A.; Stobo, J.; Kelly, C.; Mukhopadhyay, A.; Latif, A.L.; Dixon-Hughes, J.; McMahon, L.; Cony-Makhoul, P.; Byrne, J.; Smith, G.; et al. A randomised phase II trial of hydroxychloroquine and imatinib versus imatinib alone for patients with chronic myeloid leukaemia in major cytogenetic response with residual disease. *Leukemia* **2020**, *34*, 1775–1786. [CrossRef]
107. Baquero, P.; Dawson, A.; Mukhopadhyay, A.; Kuntz, E.M.; Mitchell, R.; Olivares, O.; Ianniciello, A.; Scott, M.T.; Dunn, K.; Nicastri, M.C. Targeting quiescent leukemic stem cells using second generation autophagy inhibitors. *Leukemia* **2019**, *33*, 981–994.
108. Mu, H.; Zhu, X.; Jia, H.; Zhou, L.; Liu, H. Combination Therapies in Chronic Myeloid Leukemia for Potential Treatment-Free Remission: Focus on Leukemia Stem Cells and Immune Modulation. *Front. Oncol.* **2021**, *11*, 643382. [CrossRef]
109. Simonsson, B.; Gedde-Dahl, T.; Markevarn, B.; Remes, K.; Stentoft, J.; Almqvist, A.; Bjoreman, M.; Flogegard, M.; Koskenvesa, P.; Lindblom, A.; et al. Combination of pegylated IFN-alpha2b with imatinib increases molecular response rates in patients with low- or intermediate-risk chronic myeloid leukemia. *Blood* **2011**, *118*, 3228–3235. [CrossRef]
110. Gisslinger, H.; Zagrijtschuk, O.; Buxhofer-Ausch, V.; Thaler, J.; Schloegl, E.; Gastl, G.A.; Wolf, D.; Kralovics, R.; Gisslinger, B.; Strecker, K.; et al. Ropeginterferon alfa-2b, a novel IFN.Nalpha-2b, induces high response rates with low toxicity in patients with polycythemia vera. *Blood* **2015**, *126*, 1762–1769. [CrossRef]
111. Carter, B.Z.; Mak, P.Y.; Mu, H.; Zhou, H.; Mak, D.H.; Schober, W.; Leverson, J.D.; Zhang, B.; Bhatia, R.; Huang, X. Combined targeting of BCL-2 and BCR-ABL tyrosine kinase eradicates chronic myeloid leukemia stem cells. *Sci. Transl. Med.* **2016**, *8*, ra117–ra355. [CrossRef]
112. Maiti, A.; Franquiz, M.J.; Ravandi, F.; Cortes, J.E.; Jabbour, E.J.; Sasaki, K.; Marx, K.; Daver, N.G.; Kadia, T.M.; Konopleva, M.Y.; et al. Venetoclax and BCR-ABL Tyrosine Kinase Inhibitor Combinations: Outcome in Patients with Philadelphia Chromosome-Positive Advanced Myeloid Leukemias. *Acta Haematol.* **2020**, *143*, 567–573. [CrossRef]

113. Samatar, A.A.; Poulikakos, P.I. Targeting RAS-ERK signalling in cancer: Promises and challenges. *Nat. Rev. Drug Discov.* **2014**, *13*, 928–942. [CrossRef]
114. Han, E.S.; Wen, W.; Dellinger, T.H.; Wu, J.; Lu, S.A.; Jove, R.; Yim, J.H. Ruxolitinib synergistically enhances the anti-tumor activity of paclitaxel in human ovarian cancer. *Oncotarget* **2018**, *9*, 24304–24319. [CrossRef]
115. Mogul, A.; Corsi, K.; McAuliffe, L. Baricitinib: The Second FDA-Approved JAK Inhibitor for the Treatment of Rheumatoid Arthritis. *Ann. Pharmacother.* **2019**, *53*, 947–953. [CrossRef]
116. Song, M.; Bode, A.M.; Dong, Z.; Lee, M.-H. AKT as a therapeutic target for cancer. *Cancer Res.* **2019**, *79*, 1019–1031. [CrossRef]
117. Blagosklonny, M.V. Rapamycin for longevity: Opinion article. *Aging* **2019**, *11*, 8048–8067. [CrossRef]
118. Jung, Y.S.; Park, J.I. Wnt signaling in cancer: Therapeutic targeting of Wnt signaling beyond beta-catenin and the destruction complex. *Exp. Mol. Med.* **2020**, *52*, 183–191. [CrossRef]
119. Tinsley, S.L.; Allen-Petersen, B.L. PP2A and cancer epigenetics: A therapeutic opportunity waiting to happen. *NAR Cancer* **2022**, *4*, zcac002. [CrossRef] [PubMed]
120. O'Connor, C.M.; Perl, A.; Leonard, D.; Sangodkar, J.; Narla, G. Therapeutic targeting of PP2A. *Int. J. Biochem. Cell Biol.* **2018**, *96*, 182–193. [CrossRef] [PubMed]
121. Li, C.; Wang, Y.; Gong, Y.; Zhang, T.; Huang, J.; Tan, Z.; Xue, L. Finding an easy way to harmonize: A review of advances in clinical research and combination strategies of EZH2 inhibitors. *Clin. Epigenet.* **2021**, *13*, 62. [CrossRef]
122. Jamieson, C.; Martinelli, G.; Papayannidis, C.; Cortes, J.E. Hedgehog Pathway Inhibitors: A New Therapeutic Class for the Treatment of Acute Myeloid Leukemia. *Blood Cancer Discov.* **2020**, *1*, 134–145. [CrossRef] [PubMed]
123. Lasica, M.; Anderson, M.A. Review of Venetoclax.x in CLL, AML and Multiple Myeloma. *J. Pers. Med.* **2021**, *11*, 463. [CrossRef] [PubMed]

Philadelphia positive Acute Lymphoblastic Leukaemia

ALL is a type of cancer characterized by overproduction of immature progenitors of B cell or T cell origin that invade the bone marrow [15]. ALL is the most common paediatric cancer and the leading cause of non-traumatic death in children in developed countries [16]. The incidence of ALL is higher in children aged 1-4 years, than in adult. However, the overall survival reaches 90% in children, versus only 30-40% in adults older than 40 years [16]. Ph+ ALL is also characterized by the presence of the *BCR::ABL1* fusion gene, which is rare in children, but it is the most frequent cytogenetic abnormality found in adult patients with ALL [17]. Ph+ ALL accounts for about 50% of patients older than the age of 60 years [18-20]. Ph+ ALL is associated with aggressive disease and historically dismal outcome [21, 22]. Despite shift in classification of ALL from age, white blood count and chemotherapy response to more precise genetic aberrations with more specific treatment options, the backbone of therapy remains multi-agent chemotherapy [15, 23]. The initial approach for treating acute lymphoblastic leukemia (ALL) typically involves four stages: achieving remission, intensifying therapy, maintaining long-term health, and targeting the prevention of central nervous system relapse [15]. To combat ALL, patients are administered various drug combinations, which may include glucocorticoids, vincristine (a type of vinca alkaloid), doxorubicin (an anthracycline), cytarabine and methotrexate (antimetabolites), cyclophosphamide (an alkylating agent), and L-asparaginase [23]. Elderly patients carry a poor prognosis because they are often unable to tolerate such high chemotherapeutic regimen [23]. Ph+ ALL patients have greatly benefited from the addition of TKIs into chemotherapy regimens [24]. In Ph+ ALL, the addition of TKIs to the intensive chemotherapy regimen for younger patients and non-intensive chemotherapy regimen for older patients, has resulted in improved remission and long-term survival rates to about 40-50% [25]. Frontline induction chemotherapy

induces rates of complete remission up to 90%, but about 40-50% of adult patients relapse, with survival rates of only 10% with second salvage [26]. Despite significant advancement in the treatment of ALL, the disease recurs in about 15-20% of paediatric and in 40-75% of adult patients [27]. The acquisition of additional mutations including the T315I in the kinase domain of *BCR::ABL1*, may lead to resistance/relapse in Ph+ ALL associated with high mortality rate [12]. Most Ph+ ALL relapse due to the acquisition of kinase domain mutations in *ABL1* gene. However, many patients relapse/develop resistance to TKIs due to mechanisms which are still poorly understood likely independent of BCR::ABL1 such as acquisition of cancer associated (non-*BCR::ABL1*) gene mutations [28, 29].

Genomic mechanisms influencing outcome in Ph+ Leukaemias

Mutations in non-*BCR::ABL1* cancer-related genes, such as Additional Sex Combs-Like 1 (ASXL1), IKAROS Family Zinc Finger 1 (IKZF1), Runt-Related Transcription factor 1 (RUNX1), Protein phosphatase non-receptor type 11 (PTPN11), and many more are frequently found in poor responder CML patients **(Figure 1.2)** [30, 31]. In Ph+ ALL patients, genetic instability occurs similar to that of blast crisis-CML patients which fosters the acquisition of further mutations that may reduce the effectiveness of TKIs [32]. In Ph+ ALL, IKZF1 mono or biallelic deletion, ASXL1, RUNX1, Tumour Protein P53 (TP53), cyclin-dependent kinase inhibitor 2A/B (CDKN2A/B), Paired Box 5(PAX5), B-Cell Translocation Gene 1 (BTG1), and PTPN11 mutations have been associated with poor prognosis [33, 34]. Highly sensitive mutation screening technologies, such as Next-Generation sequencing, could be used to screen for potential mutations that may influence TKI sensitivity and disease prognosis in Ph+ ALL [35, 36]. By studying the

significance of these mutations in TKI sensitivity, novel treatment strategies could be employed to improve outcomes in Ph+ ALL. For example, mutations in PTPN11 cause leukemia and are responsible for therapy resistance in leukemia, including CML and ALL patients [34]. Therefore, investigating PTPN11 mutations could also help identify mechanisms of TKI resistance in Ph+ ALL.

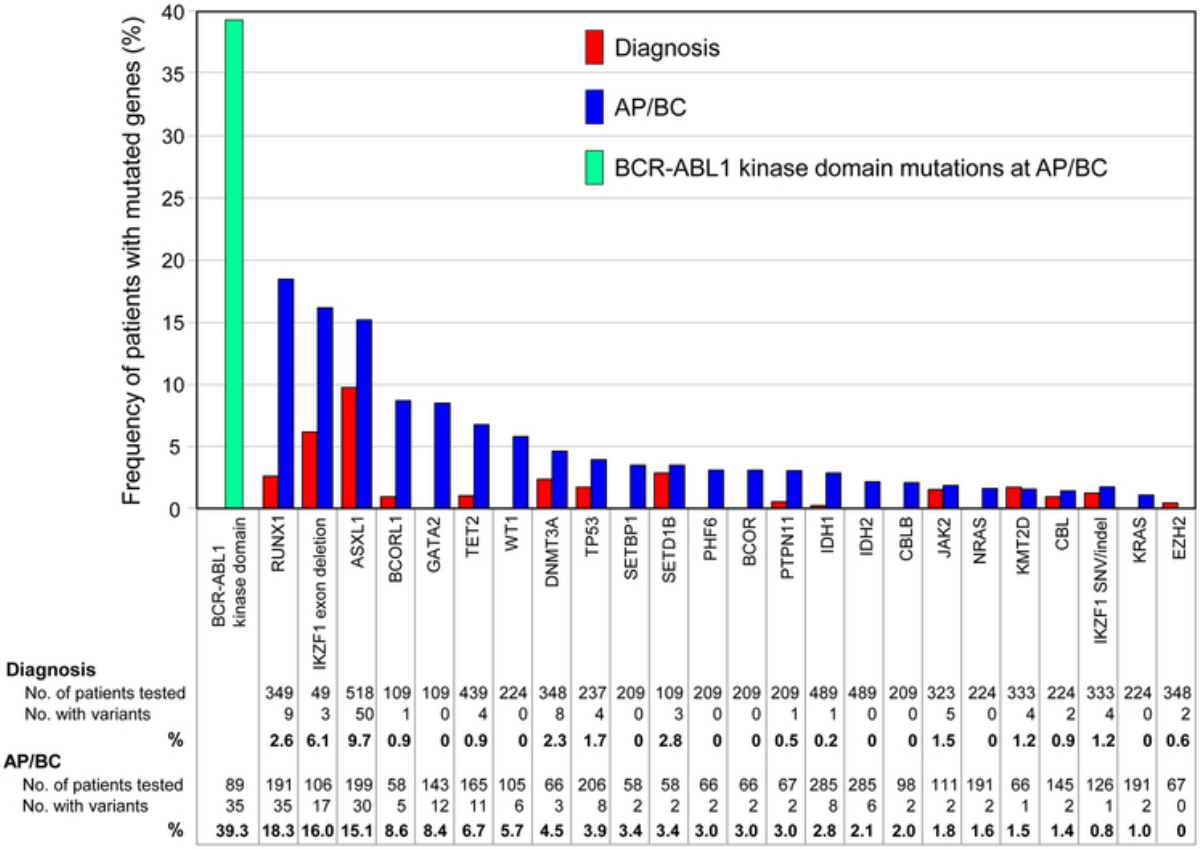

	BCR-ABL1 kinase domain	RUNX1	IKZF1 exon deletion	ASXL1	BCORL1	GATA2	TET2	WT1	DNMT3A	TP53	SETBP1	SETD1B	PHF6	BCOR	PTPN11	IDH1	IDH2	CBLB	JAK2	NRAS	KMT2D	CBL	IKZF1 SNV/indel	KRAS	EZH2
Diagnosis																									
No. of patients tested		349	49	518	109	109	439	224	348	237	209	109	209	209	209	489	489	209	323	224	333	224	333	224	348
No. with variants		9	3	50	1	0	4	0	8	4	0	3	0	0	1	1	0	0	5	0	4	2	4	0	2
%		**2.6**	**6.1**	**9.7**	**0.9**	**0**	**0.9**	**0**	**2.3**	**1.7**	**0**	**2.8**	**0**	**0**	**0.5**	**0.2**	**0**	**0**	**1.5**	**0**	**1.2**	**0.9**	**1.2**	**0**	**0.6**
AP/BC																									
No. of patients tested	89	191	106	199	58	143	165	105	66	206	58	58	66	66	67	285	285	98	111	191	66	145	126	191	67
No. with variants	35	35	17	30	5	12	11	6	3	8	2	2	2	2	2	8	6	2	2	2	1	2	1	2	0
%	**39.3**	**18.3**	**16.0**	**15.1**	**8.6**	**8.4**	**6.7**	**5.7**	**4.5**	**3.9**	**3.4**	**3.4**	**3.0**	**3.0**	**3.0**	**2.8**	**2.1**	**2.0**	**1.8**	**1.6**	**1.5**	**1.4**	**0.8**	**1.0**	**0**

Figure 1.2: Graph illustrating the frequency of mutated cancer genes in patients with chronic myeloid leukemia (CML) at the time of diagnosis. Red bars indicate the frequency of observed gene mutations during the initial diagnosis, while blue bars represent mutations observed in the accelerated phase (AP) or blast crisis (BC) of the disease. This figure, adapted from a study by [37] with permission, offers crucial insights into the genetic changes linked to disease progression in CML patients.

In CML, PTPN11 mutations have been found in approximately 5-10% of patients with advanced-stage disease and have been associated with poor response to imatinib therapy, the first line TKI used for treating CML [38-40]. PTPN11 mutations can activate the RAS/MAPK pathway, promoting cell survival and inhibiting apoptosis, thereby conferring resistance to imatinib [41, 42].

In Ph+ ALL, PTPN11 mutations have been reported in about 4% paediatric and 5% adult Ph+ ALL patients [43-45]. PTPN11 mutations in Ph+ ALL have been associated with poor prognosis and resistance to not only TKIs, but also to chemotherapeutic agents commonly used in the treatment of ALL [46]. Similar to CML, PTPN11 mutations in Ph+ ALL can activate the RAS/MAPK pathway and promote cell survival [43].

Non-*BCR::ABL1* mutational mechanisms of resistance continue to pose treatment challenge also in Ph+ ALL [28]. Recent studies have explored the potential of targeting PTPN11 mutations in the treatment of CML and Ph+ ALL. One study found that a SHP2 inhibitor, which targets the SHP-2 protein encoded by the PTPN11 gene, was able to overcome imatinib resistance in CML cells with PTPN11 mutations [47]. Another study showed that a combination of a MEK inhibitor and a BCL-2 inhibitor could overcome resistance in Ph+ ALL cells with PTPN11 mutations [48].

Src homology 2 (SH2) domain-containing protein tyrosine phosphatase-2 (SHP-2)

PTPN11 gene encodes for Src homology 2 (SH2) domain-containing protein tyrosine phosphatase-2 (SHP-2). SHP-2 is a cytosolic protein ubiquitously expressed in various tissues and cell types [49]. PTPN11 is located on chromosome 12q24 [50] and SHP-2 is an oncogenic tyrosine phosphatase associated with many important signalling cascades

including RAS/MAPK, JAK/STAT, PI3K/AKT, PD-1/PD-L1, mTOR and Hippo pathways [51-53]. SHP-2 is required for full and sustained activation of RAS/MAPK pathway [54]. SHP-2 is involved in several cellular processes including survival, proliferation, differentiation and migration [55]. SHP-2 is critical for the survival of the receptor tyrosine kinase (RTK) driven cancers, and it is also a central node in intrinsic and acquired resistance to targeted cancer therapy [56, 57]. SHP-2 is required for BCR::ABL1 induced myeloid (CML) and lymphoid (Ph+ ALL) neoplasia [58].

Structure and function of SHP-2 protein

SHP-2, an allosteric enzyme that acts as an intramolecular switch, transitioning between its N-terminus SH2 (N-SH2) and protein tyrosine phosphatase (PTP) domains [58]. SHP-2 is a protein containing 527 amino acids which is highly homologous and has similar structure to the hematopoietic cell specific phosphatase, SHP-1 [59-61]. While both SHP-1 and SHP-2 act downstream of receptor tyrosine kinase to propagate signalling cascades, their functions are specific to their phosphatase domains [62, 63]. At the N-terminus, SHP-2 has two tandem SH2 domains (N-SH2 and C-SH2) and one protein tyrosine phosphatase (PTP) domain at the C-terminus (**Figure 1.3**). PTP domain has phosphate binding site, the cysteine residue at 459 position, which is responsible for the catalytic activity of SHP-2 [64]. In its basal state, the N-SH2 domain of SHP-2 is connected to the PTP domain through flexible polypeptide linkers, which results in auto-inhibition of SHP-2 by obstructing the catalytic site. Binding of SHP-2 to phosphorylated tyrosine residues in the target protein is mediated via N-SH2 domain which leads to the confirmational change that exposes catalytic site to the substrates (**Figure 1.3**) [61, 65-67]. C-SH2 domain provides binding energy and facilitate confirmational change during the activation process [61, 68]. SHP-2 also has two tyrosine phosphorylation sites (Tyr542

and Tyr580) at the c-terminus which are reported of being involved in the recruitment of SHP-2 to the receptor [61, 69-73].

Upon extracellular stimulation, SHP2 can undergo phosphorylation at specific sites in its C-terminal tail, such as Tyr542 and Tyr580. In its inactive state, SHP-2 adopts a self-inhibited conformation, where the interaction between its N-SH2 domain and PTP domain limits its catalytic activity **(Figure 1.3)** [74]. However, the binding of growth factors or cytokines disrupts this self-inhibition, leading to the activation of SHP-2 **(Figure 1.3)** [74]**.** Therefore, maintaining the self-inhibited state could serve as a potential strategy to inhibit SHP-2 activity, offering a novel approach for the design of SHP2 inhibitors.

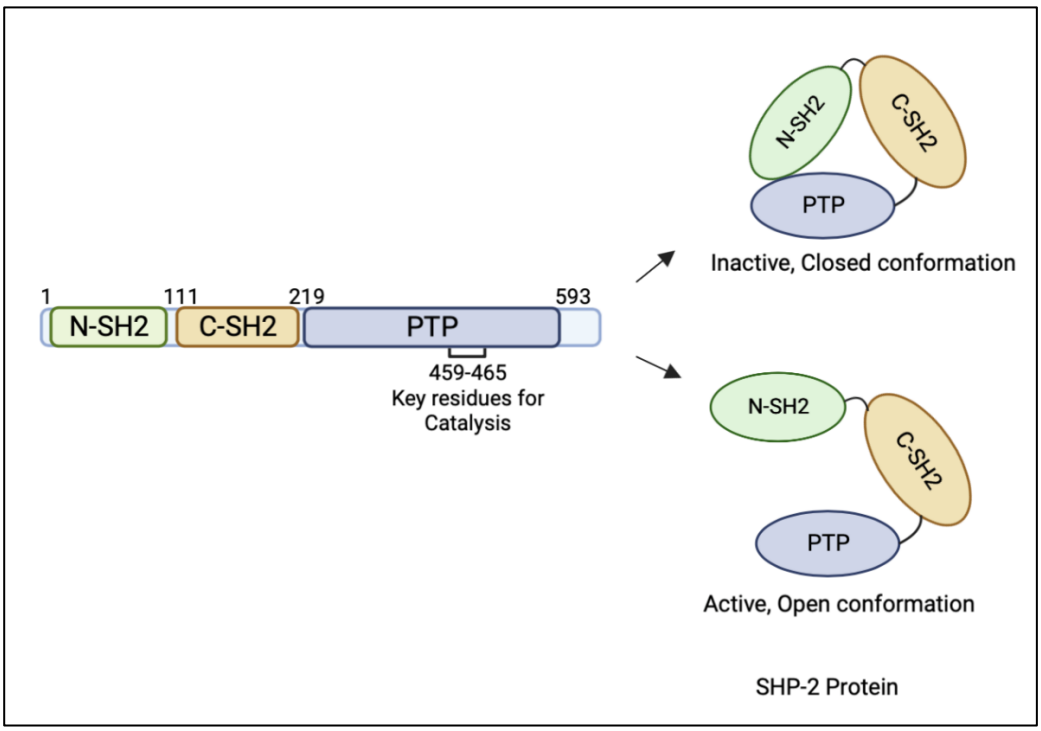

Figure 1.3: The schematic representation of the SHP-2 protein, highlighting its structural domains. The SHP-2 protein is composed of two consecutive SH2 domains, designated as N-SH2 and C-SH2, along with a PTP domain. The N-SH2 domain and the PTP domain are linked by flexible polypeptide connectors, resulting in a closed

conformation of the SHP-2 protein. Activation of the protein induces a conformational change, transitioning it to an open state. Within the PTP domain, residues 459 to 465 play a pivotal role in catalysis, serving as essential components for the enzymatic activity of SHP-2. These residues are critical for the proper functioning of the catalytic site within the PTP domain. Figure created using BioRender.com.

SHP-2 has been implicated in numerous signalling pathways including those that are initiated by the growth factors such as Epidermal growth factor, Platelet-Derived Growth Factor, and Insulin-like growth factor 1; insulin, interferons and cytokines such as IL-3, Erythropoietin (EPO), and Granulocyte-macrophage colony-stimulating factor [75, 76]. SHP-2, a protein, is engaged with receptor tyrosine kinases either directly or indirectly. This engagement occurs through the involvement of docking proteins such as insulin receptor substrate-1 (IRS-1) and GRB2-associated binding protein 1 or 2 (GAB1/2) [55, 77, 78]. SHP-2 plays a role in a signalling cascade that includes GRB2 and Son of Sevenless (SOS) [77, 79-82]. Within this cascade, SOS facilitates the activation of the MAPK pathway by promoting the conversion of GDP bound to RAS to GTP [56, 83-85]. Therefore, SHP-2 is critical for activation of MAPK pathway downstream of growth factor receptors [86]. Activation of SHP-2 activates numerous downstream pathways including RAS/ERK1/2, PI3K/AKT, JAK/STAT, FLT3, and NF- κB; overexpression of anti-apoptotic proteins MCL-1, BCL-2 and BCL-XL and PD-1 mediated immune invasion [87-90].

In Philadelphia positive cells, BCR::ABL1 induced transformation requires Grb2 which is recruited by phosphorylated Y177, an autophosphorylation site of BCR::ABL1, which in turn recruits SHP-2 and Gab2 [91]. Gab2 is a critical mediator of PI3K/AKT and RAS/RAF/MEK/ERK pathways in BCR::ABL1 positive cells [92]. Furthermore, Gu *et al.*

also showed that SHP-2 is required for RAS/RAF/MEK/ERK pathway activation as it dephosphorylates inhibitors of this pathway in BCR::ABL1 positive cells. Gu *et al.* used genetic loss of function approach and bone marrow transplantation model to demonstrate that BCR::ABL1 mediated myeloid and lymphoid neoplasia needed SHP-2 for the initiation and maintenance of CML and induction of Ph+ ALL cells [58]. This highlights the important of intact SHP-2 in BCR::ABL1 positive cells and possible implications when *PTPN11* gene is mutated.

PTPN11 gene mutations can result in gain or loss of function of the encoded protein SHP2 [93]. Gain-of-function mutations enhance SHP-2 activity, leading to aberrant signalling and contributing to diseases like cancer [94]. Loss-of-function mutations reduce SHP2 activity, disrupting signalling and causing developmental disorders like Noonan and LEOPARD syndromes [94]. The effects of PTPN11 mutations depend on their specific location and nature, as well as the cellular context [95]. These mutations provide insights into the importance of SHP-2 in cellular signalling pathways and highlight its role in various diseases, making it a potential therapeutic target for intervention [95].

PTPN11 mutations in genetic disorders

Germline mutations in *PTPN11* genes lead to developmental disorders such as Noonan (autosomal dominant) and LEOPARD (rare, autosomal dominant) syndromes characterized by growth defects, craniofacial abnormalities, cardiac malformations, and mental retardation in some cases [96] [97, 98]. Infants with Noonan syndrome (NS) with PTPN11 mutations also have the increased risk of developing leukaemias [99, 100].

More than 50% of patients with Noonan syndrome carry PTPN11 mutations, frequently in the N-SH2 domain and the PTP domain contact site, leading to gain-of-function effects and increased SHP-2 activity [97]. In contrast, mutations in PTPN11 causing LEOPARD syndrome are commonly found in the PTP domain and result in catalytic defects [101]. Notably, Y279C, A461T, and G464A mutations are frequently observed in LEOPARD syndrome, while D61G, D61Y, E76D, and E76K are the most frequent mutations in Noonan syndrome **(Figure 1.4)** [97, 102-104].

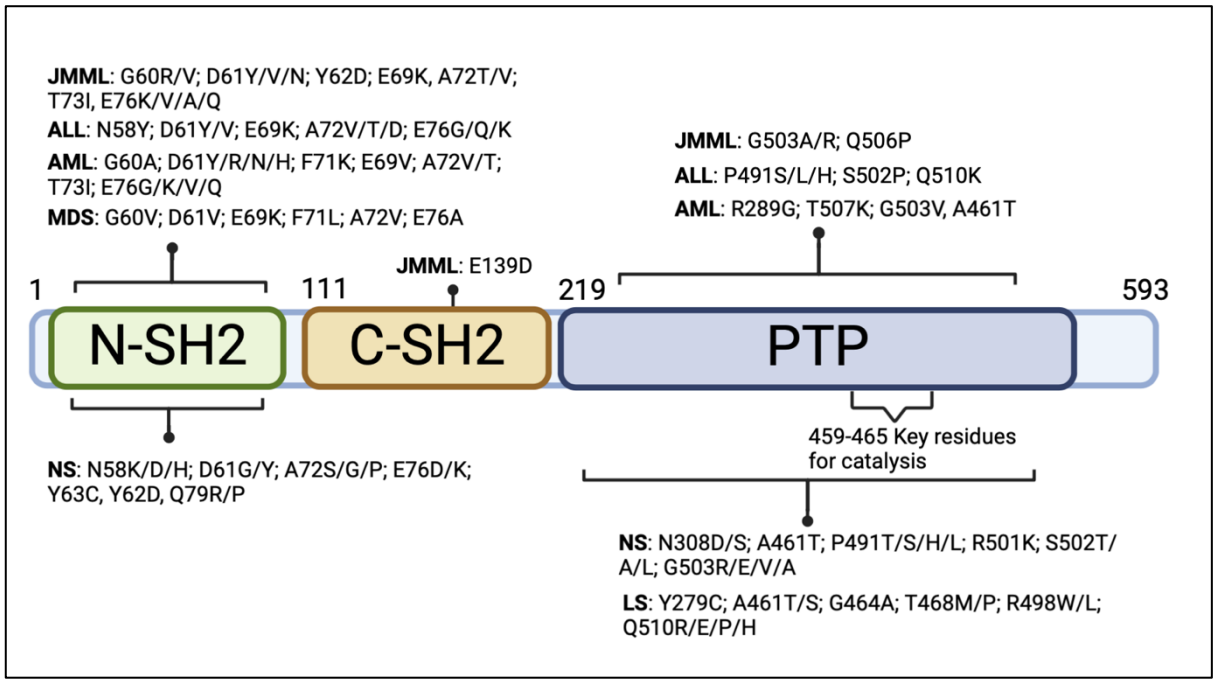

Figure 1.4: PTPN11 mutations in genetic disorders and haematological malignancies. This schematic illustrates the three domains of the SHP-2 protein: the N-terminus SH2 (N-SH2), C-terminus SH2 (C-SH2), and the Phosphotyrosine Phosphatase (PTP) domain, which includes key catalytic residues from 459 to 465. The figure also highlights common mutations found in various disorders, including Juvenile Myelomonocytic Leukemia (JMML), Acute Lymphoid Leukemia (ALL), Acute Myeloid Leukemia (AML), Myelodysplastic Syndromes (MDS), Noonan Syndrome (NS), and

LEOPARD Syndrome (LS), indicating their respective locations within different domains of the SHP-2 protein. Figure created using BioRender.com.

PTPN11 mutations in haematological malignancies

Somatic mutations in the PTPN11 gene can be classified into gain of function and loss of function mutations, each contributing to different aspects of disease development and progression [105]. Gain of function mutations in PTPN11 are observed in various hematological malignancies, including Juvenile Myelomonocytic Leukemia (JMML), Myelodysplastic Syndromes (MDS), Acute Lymphoblastic Leukemia (ALL), and Acute Myeloid Leukemia (AML), where they contribute to both disease occurrence and therapy resistance [106-110]. Patients with PTPN11 mutations, particularly those over 60 years of age and with secondary AML, tend to have poor overall survival and rapid disease progression [111, 112]. The co-occurrence of PTPN11 mutations with other genetic abnormalities, such as MLL-AF10 translocation, further exacerbates disease severity [113, 114]. Moreover, PTPN11 gain of function mutations are associated with resistance to anti-apoptotic protein inhibitors and tyrosine kinase inhibitors (TKIs) in chronic myeloid leukemia (CML) [31, 115]. Targeted treatment approaches are needed to address the high-risk subtype of myeloid malignancies associated with PTPN11 mutations [111]. On the other hand, loss of function mutations in PTPN11 are less common and have been observed in specific residues within the protein structure, affecting its phosphatase activity [116]. For example, mutations at cysteine 459 completely abolish the enzymatic activity of SHP-2, acting as dominant negatives against the wild-type protein [86].

Activating mutations, such as D61V/G/Y and E76K, are frequently found in hematological malignancies and show increased phosphatase activity [70, 117, 118]. Mutations in the

N-SH2 domains and PTP domain, including T73I, Y63C, Q79R, N308D, and S502T, also exhibit enhanced phosphatase activity [68, 117, 122]. Notably, the E76K mutation has been reported of being able to significantly activate the RAS/RAF/MEK/ERK pathway, promoting IL-3 independent growth and survival [53, 119, 120]. Similarly, Y279C and T468M mutations contribute to the activation of the RAS/RAF/MEK/ERK pathway [124]. These findings underscore the pivotal role of PTPN11 mutations in cancer development and progression.

The SHP-2 protein consists of N-SH2, PTP, and C-SH2 domains, with the N-SH2 domain connected to the PTP domain by flexible polypeptide linkers, leading to auto-inhibition of SHP-2 through blocking the catalytic site [121]. Binding of SHP-2 to phosphorylated tyrosine residues in target proteins is mediated via the N-SH2 domain, inducing a conformational change that exposes the catalytic site to substrates [61, 65-67]. The PTP domain of SHP-2 contains a phosphate binding site, with a critical cysteine residue at position 459 responsible for the catalytic activity of SHP-2 [64]. Residues 459-465, including p.A461T, are key residues for catalysis [116].

The p.P491H mutation does not contribute to either N-SH2/PTP interaction or the catalytic function of SHP-2 [122]. Interestingly, mutations in the p.P491 position are frequently found in JMML and ALL patients [123-125]. Previous studies have suggested that PTPN11 mutations at the p.P491 position may occur as a late event in ALL patients, providing a proliferative advantage in a leukemia subclone [123-125].

The p.A461T mutation is common in Noonan Syndrome and has been shown to reduce the phosphatase activity of SHP-2 by 930-fold compared to the wild type. This mutation

alters the active site pocket and destabilizes the first transition state of the substrate during the catalysis process [126]. X-ray crystallography has also demonstrated that SHP-2 protein with the p.A461T mutation adopts the autoinhibited closed conformation, similar to that of the wild type [126]. However, the effects of the combination of p.A461T and p.P491H mutations have not been previously investigated.

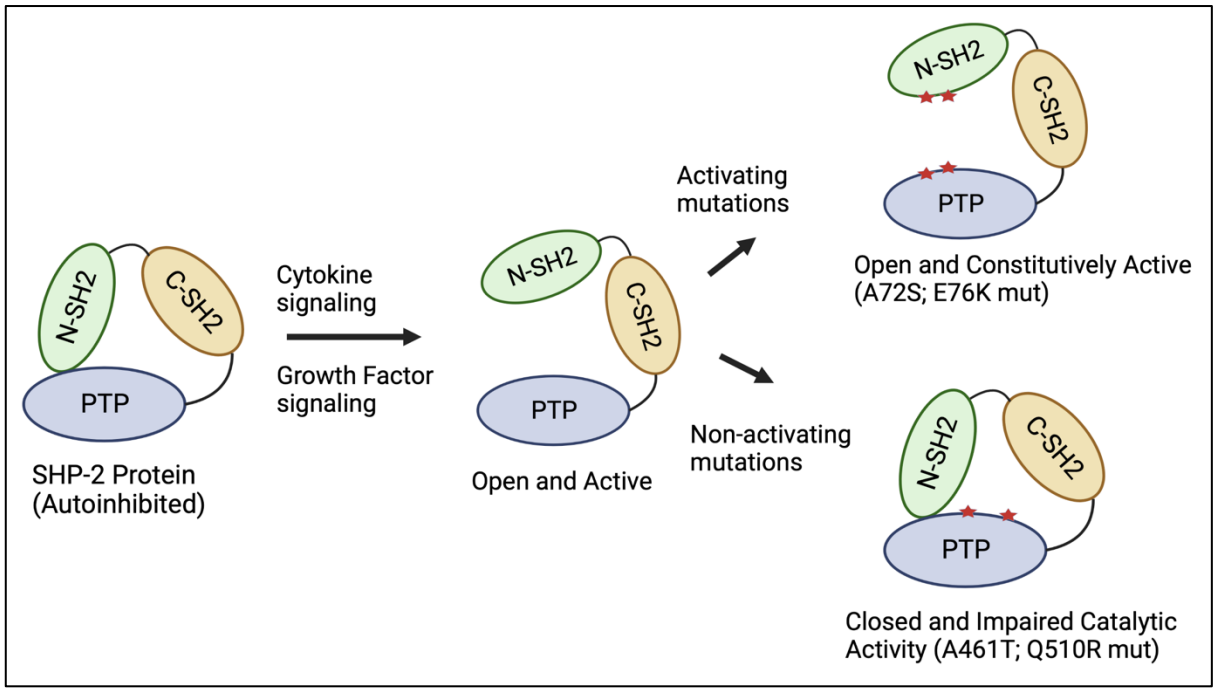

Figure 1.5: Schematic diagram of SHP-2 protein and different conformations. This figure illustrates various conformational states of the SHP-2 protein. First, it adopts a native autoinhibited conformation, followed by an open and active state in response to cytokine or growth factor signalling. Additionally, activating mutations at the contact site between N-SH2 and the PTP domain, such as A72S or E76K, lead to an open and constitutively active conformation. Conversely, mutations in the PTP domain, like A461T or Q510R, induce a closed conformation with impaired catalytic activity. This representation provides insights into the dynamic behaviour of SHP-2 in response to different regulatory cues and genetic alterations. Figure created using BioRender.com.

Treatment strategies for leukaemia with *PTPN11* mutations

PTPN11 mutations are present in approximately 7% of patients with ALL [53, 127]. Currently, there are no targeted treatment options available for PTPN11 mutations in the clinic, although efforts have been made to directly target the SHP-2 protein and other intermediate molecules of the RAS pathway signalling, with limited benefits for patients.

SHP-2 inhibitor

The SHP-2 protein is challenging to target due to its structural similarity with other phosphatases, particularly SHP-1, which has almost identical catalytic sites except for four proximal regions [53, 70]. SHP-1 is a classical tumour suppressor encoded by the PTPN6 gene [128]. It has been shown to be involved in the regulation of SHP-2 and imatinib resistance in CML cell lines [129]. First-generation SHP-2 inhibitors are non-allosteric and bind to the PTP catalytic pocket [51]. However, the first-generation inhibitors were not specific to SHP-2 and led to severe side effects, as they had low cell permeability and were unable to sufficiently inhibit SHP-2 activity [52]. Furthermore, activating mutations in PTPN11 further reduce the ability of SHP-2 specific inhibitors to bind to SHP-2, leading to an increase in phosphatase activity [130]. Therefore, developing more specific and effective inhibitors that can overcome these challenges is crucial for the development of targeted therapies for PTPN11-mutated cancers.

Recent research has shown that the first generation non-allosteric SHP-2 inhibitors were not effective due to their low specificity and severe side effects [131]. As a result, second generation allosteric SHP-2 inhibitors have been developed to address these issues. These allosteric inhibitors have been found to be more efficient and have four distinct binding sites on SHP-2 [132]. One such inhibitor is SHP099, which is a selective, potent,

and orally available allosteric inhibitor of SHP-2 that was developed by NOVARTIS researchers [56]. Unlike first-generation inhibitors, SHP099 binds to SHP-2 at a tunnel-like pocket between N-SH2, C-SH2, and PTP domains, and does not bind to SHP-1. SHP099 prevents receptor tyrosine kinase-driven cell proliferation by inhibiting the RAS/ERK pathway [133]. In preclinical studies, treatment of MV4-11 AML cells with SHP099 led to reduced cell proliferation with a marked reduction in pERK1/2, BCL-XL, and cleaved PARP [134]. However, it is important to note that SHP099 is prone to resistance due to activating mutations such as D61 and A72 positions in PTPN11, and it inhibits the activity of PTPN11 E69K and E76K mutants only at higher concentrations [134, 135]. Further studies are needed to fully understand the potential of allosteric inhibitors of SHP-2 in the treatment of PTPN11-mutant malignancies.

II-B08, a salicylic acid-based SHP-2 specific inhibitor, inhibited RAS/ERK and PI3K/AKT pathway and led to reduction in GM-CSF mediated bone marrow cells growth with PTPN11 D61Y and E76K mutations [136]. II-B08 exhibited limited efficacy or unintended consequences in fibroblast cells, as reported in reference [71]. Researchers are currently investigating the potential of various allosteric SHP-2 inhibitors, including JAB-3068, RMC4630, TN0155, and JAB3312, for their therapeutic effectiveness in treating cancer. TN0155 is developed by Novartis which blocks SHP-2 in its inactive confirmation [51]. TN0155 has been tested against PTPN11 mutations in this study as the PTPN11 mutations identified contributes to closed, inactive confirmation.

PROTAC Inhibitor of SHP-2

Proteolysis-targeting chimera (PROTAC) inhibitors are novel class of SHP-2 inhibitors, known as SHP-2 degraders, which use the degradation mechanism of the ubiquitin

proteasome system to break down SHP-2 [137]. SHP-2-D26, a degrader, has shown to be 30 times more effective at reducing cell proliferation and pERK levels than SHP099 [138]. However, these inhibitors are still in the early stages of clinical development, and it may take some time before they can be used in the clinic [139].

MEK inhibitors

The MAPK pathway plays a critical role in regulating various cellular processes such as proliferation, differentiation, survival, and motility [140]. Mutations in genes encoding activators of this pathway, such as receptor tyrosine kinase, PTPN11, NF1, RAS, or RAF, can lead to constitutive activation of the pathway and promote oncogenesis [141]. SHP-2 is a positive regulator of the MAPK pathway, acting between receptor tyrosine kinase and RAS [142, 143]. Inhibitors of the RAS/RAF/MEK/ERK signalling pathway, such as MEK inhibitors, have the potential to be used as treatment options for leukemia driven by activating mutations in the PTPN11 gene [144]. Trametinib (GSK1120212), an allosteric non-ATP competitive inhibitor of MEK1 and MEK2, was the first MEK inhibitor approved by the FDA in 2013 for the treatment of melanoma with BRAF V600E or V600K mutations [145]. A study by Farnault *et al.* showed that Trametinib induced a good response in histiocytosis with an activating PTPN11 mutation [146]. The second MEK inhibitor approved by the FDA was cobimetinib (GDC-0973, XL518) for melanoma with BRAF V600E mutation, which also showed efficacy against KRAS-mutated cell lines in xenograft models [147, 148]. There are many MEK inhibitors under clinical or pre-clinical development that have been reviewed elsewhere [149]. In a study conducted by Esposit in 2019, it was demonstrated that the presence of clonal mutations in RAS and PTPN11 genes was linked to the development of resistance to chemotherapy in acute lymphoblastic leukemia (ALL) [150]. Moreover, the study revealed that the

administration of MEK inhibitors enhanced the effectiveness of prednisolone in the treatment of ALL, by increasing its sensitivity [150]. Mirdametinib (PD0325901) is a MEK inhibitor that is currently in Phase II clinical trial for the treatment of symptomatic inoperable neurofibromatosis type-1 (NF1)-associated plexiform neurofibromas (PNs) [151]. In addition, this inhibitor is being tested in this thesis against imatinib-resistant Ph+ ALL cells with sustained pERK1/2 expression. Although MEK inhibitors show potential in treating leukemias caused by PTPN11 mutations, their use may be restricted due to their high off-target effects [152].

Summary

Although there is evidence suggesting that PTPN11 is associated with TKI resistance and poor prognosis in Ph+ leukemia, a direct causal relationship between PTPN11 and TKI resistance has not yet been firmly established. This study aims to address this gap by utilizing multiple cell line models. The study also investigates potential treatment options targeting the RAS/ERK pathway, including SHP-2 and MEK inhibitors, as well as exploring strategies targeting anti-apoptotic proteins to overcome TKI resistance in Ph+ ALL cells with PTPN11 mutations.

Project Rationale, Hypothesis and Aims

Philadelphia positive Acute Lymphoblastic Leukemia (Ph+ ALL) ALL is an aggressive subtype of ALL driven by the BCR::ABL1 fusion oncoprotein [153, 154]. While progress has been made in understanding the biology of Ph+ ALL, there is a need for improved treatment options [23]. Adding Tyrosine Kinase Inhibitors (TKIs) to the chemotherapy regimen has improved remission rates, with imatinib combination showing a 70%

disease-free survival rate at 5 years [154]. However, overall survival remains below 50% [155]. BCR::ABL1 kinase domain mutations, are predominant driver of TKI resistance. However, in approximately 30% of Ph+ ALL patients the mechanisms of TKI resistance are not well known [28].

The role of non-*BCR::ABL1* somatic mutations in TKI sensitivity needs further investigation. These mutations are frequently acquired in Ph+ leukemic cells and associated with poor outcomes. Understanding their impact on TKI response can optimize treatment approaches.

Phosphotyrosine phosphatase non-receptor type-11 (*PTPN11*) mutations, frequently observed in haematological malignancies, have been implicated in the development of resistance to TKIs and venetoclax, an inhibitor of the anti-apoptotic protein BCL-2, in Ph+ ALL. Venetoclax is currently being studied in clinical trials for its efficacy in treating Ph+ ALL. By examining the impact of PTPN11 mutations on the sensitivity of TKIs and venetoclax, as well as identifying disrupted pathways, it becomes possible to guide the creation of novel targeted therapies that effectively counter resistance mechanisms.
The aims of this thesis are to:

1. Investigate BCR::ABL1-dependent resistance mechanisms in TKI-resistant Ph+ ALL cells, including BCR::ABL1 activation, kinase domain mutations, drug transporter expression, and BCR::ABL1 mRNA expression.

2. Model PTPN11 mutations in BaF3 cells and BaF3 cells expressing BCR::ABL1 p190. Additionally, genetically inhibit PTPN11 in resistant SUP-B15 cells to determine if this re-sensitizes them to imatinib treatment.

3. Utilize a precision medicine approach to explore the RAS/ERK pathways influenced by PTPN11 mutations, aiming to identify potential targets within these pathways and beyond. This investigation aims to overcome resistance and develop effective strategies.

References:

1. Nowell, P.C. and D.A. Hungerford, *Chromosome studies on normal and leukemic human leukocytes.* Journal of the National Cancer Institute, 1960. **25**(1): p. 85-109.
2. Propp, S. and F.A. Lizzi, *Brief Report: Philadelphia Chromosome in Acute Lymphocytic Leukemia.* Blood, 1970. **36**(3): p. 353-360.
3. Kang, Z.-J., et al., *The Philadelphia chromosome in leukemogenesis.* Chinese journal of cancer, 2016. **35**: p. 48-48.
4. Quintás-Cardama, A. and J. Cortes, *Molecular biology of bcr-abl1–positive chronic myeloid leukemia.* Blood, The Journal of the American Society of Hematology, 2009. **113**(8): p. 1619-1630.
5. Goldman, J.M. *Chronic myeloid leukemia: a historical perspective*. in *Seminars in hematology*. 2010. Elsevier.
6. Flis, S. and T. Chojnacki, *Chronic myelogenous leukemia, a still unsolved problem: pitfalls and new therapeutic possibilities.* Drug design, development and therapy, 2019. **13**: p. 825.
7. Deininger, M.W., J.M. Goldman, and J.V. Melo, *The molecular biology of chronic myeloid leukemia.* Blood, 2000. **96**(10): p. 3343-3356.
8. Arana-Trejo, R.M., et al., *Frequency of p190 and p210 BCR-ABL Fusions Genes in Acute Lymphoblastic Leukemia in a Long Group of Adults and Childhood.* Blood, 2016. **128**(22): p. 5273.
9. Quackenbush, R.C., et al., *Analysis of the biologic properties of p230 Bcr-Abl reveals unique and overlapping properties with the oncogenic p185 and p210 Bcr-Abl tyrosine kinases.* Blood, 2000. **95**(9): p. 2913-2921.
10. De Braekeleer, E., et al., *ABL1 fusion genes in hematological malignancies: a review.* Eur J Haematol, 2011. **86**(5): p. 361-71.
11. Avelino, K.Y.P.S., et al., *Smart applications of bionanosensors for BCR/ABL fusion gene detection in leukemia.* Journal of King Saud University - Science, 2017. **29**(4): p. 413-423.
12. Braun, T.P., C.A. Eide, and B.J. Druker, *Response and Resistance to BCR-ABL1-Targeted Therapies.* Cancer Cell, 2020. **37**(4): p. 530-542.
13. Mauro, M.J., et al., *Asciminib monotherapy in patients with CML-CP without BCR::ABL1 T315I mutations treated with at least two prior TKIs: 4-year phase 1 safety and efficacy results.* Leukemia, 2023. **37**(5): p. 1048-1059.
14. Poudel, G., et al., *Mechanisms of Resistance and Implications for Treatment Strategies in Chronic Myeloid Leukaemia.* Cancers (Basel), 2022. **14**(14).
15. Terwilliger, T. and M. Abdul-Hay, *Acute lymphoblastic leukemia: a comprehensive review and 2017 update.* Blood Cancer J, 2017. **7**(6): p. e577.
16. Malczewska, M., et al. *Recent Advances in Treatment Options for Childhood Acute Lymphoblastic Leukemia*. Cancers, 2022. **14**, DOI: 10.3390/cancers14082021.
17. Shi, T., et al., *Adult Ph-positive acute lymphoblastic leukemia-current concepts in cytogenetic abnormalities and outcomes.* Am J Cancer Res, 2020. **10**(8): p. 2309-2318.
18. Zhang, W., P. Kuang, and T. Liu, *Role of BCR-ABL1 isoforms on the prognosis of Philadelphia chromosome positive acute lymphoblastic leukemia in the tyrosine kinase inhibitor era: A meta-analysis.* PLoS One, 2020. **15**(12): p. e0243657.
19. Ribeiro, R.C., et al., *Clinical and biologic hallmarks of the Philadelphia chromosome in childhood acute lymphoblastic leukemia.* 1987.

20. Moorman, A.V., et al., *A population-based cytogenetic study of adults with acute lymphoblastic leukemia.* Blood, The Journal of the American Society of Hematology, 2010. **115**(2): p. 206-214.
21. Yilmaz, M., et al., *Philadelphia chromosome-positive acute lymphoblastic leukemia in adults: current treatments and future perspectives.* Clin Adv Hematol Oncol, 2018. **16**(3): p. 216-223.
22. Wang, H., et al., *Venetoclax-ponatinib for T315I/compound-mutated Ph+ acute lymphoblastic leukemia.* Blood Cancer Journal, 2022. **12**(1): p. 20.
23. Samra, B., et al., *Evolving therapy of adult acute lymphoblastic leukemia: state-of-the-art treatment and future directions.* Journal of Hematology & Oncology, 2020. **13**(1): p. 70.
24. Ravandi, F., *Current management of Philadelphia chromosome positive ALL and the role of stem cell transplantation.* Hematology 2014, the American Society of Hematology Education Program Book, 2017. **2017**(1): p. 22-27.
25. Ribera, J.-M. and S. Chiaretti, *Modern Management Options for Ph+ ALL.* Cancers, 2022. **14**(19): p. 4554.
26. Greenbaum, U., et al., *Chimeric Antigen Receptor T-Cells in B-Acute Lymphoblastic Leukemia: State of the Art and Future Directions.* Front Oncol, 2020. **10**: p. 1594.
27. Lejman, M., et al., *Targeted Therapy in the Treatment of Pediatric Acute Lymphoblastic Leukemia-Therapy and Toxicity Mechanisms.* Int J Mol Sci, 2021. **22**(18).
28. Mian, A.A., et al., *Oncogene-independent resistance in Philadelphia chromosome - positive (Ph(+)) acute lymphoblastic leukemia (ALL) is mediated by activation of AKT/mTOR pathway.* Neoplasia, 2021. **23**(9): p. 1016-1027.
29. Hochhaus, A., et al., *Long-term outcomes of imatinib treatment for chronic myeloid leukemia.* New England Journal of Medicine, 2017. **376**(10): p. 917-927.
30. Branford, S., et al., *Integrative genomic analysis reveals cancer-associated mutations at diagnosis of CML in patients with high-risk disease.* Blood, 2018. **132**(9): p. 948-961.
31. Branford, S., et al., *Laying the foundation for genomically-based risk assessment in chronic myeloid leukemia.* Leukemia, 2019. **33**(8): p. 1835-1850.
32. Soverini, S., R. Bassan, and T. Lion, *Treatment and monitoring of Philadelphia chromosome-positive leukemia patients: recent advances and remaining challenges.* Journal of Hematology & Oncology, 2019. **12**(1): p. 39.
33. Branford, S., et al., *Laying the foundation for genomically-based risk assessment in chronic myeloid leukemia.* Leukemia, 2019. **33**(8): p. 1835-1850.
34. Komorowski, L., et al., *Philadelphia Chromosome-Positive Leukemia in the Lymphoid Lineage—Similarities and Differences with the Myeloid Lineage and Specific Vulnerabilities.* International Journal of Molecular Sciences, 2020. **21**(16): p. 5776.
35. Parker, W.T., et al., *Sensitive detection of BCR-ABL1 mutations in patients with chronic myeloid leukemia after imatinib resistance is predictive of outcome during subsequent therapy.* J Clin Oncol, 2011. **29**(32): p. 4250-4259.
36. Kizilors, A., et al., *Impact of finding of low level kinase domain mutations using ultra deep next generation sequencing in patients with chronic phase CML.* Blood, 2015. **126**(23): p. 347.
37. Branford, S., et al., *Laying the foundation for genomically-based risk assessment in chronic myeloid leukemia.* Leukemia, 2019. **33**(8): p. 1835-1850.

38. Rosti, G., et al., *Tyrosine kinase inhibitors in chronic myeloid leukaemia: which, when, for whom?* Nature reviews clinical oncology, 2017. **14**(3): p. 141-154.
39. Swoboda, D.M., et al., *PTPN11 mutations are associated with poor outcomes across myeloid malignancies.* Leukemia, 2021. **35**(1): p. 286-288.
40. Bidikian, A., et al., *Prognostic impact of ASXL1 mutations in chronic phase chronic myeloid leukemia.* Blood Cancer Journal, 2022. **12**(10): p. 144.
41. Nishioka, C., Ikezoe, T., Yang, J., Yokoyama, A., *The novel SHP-2 inhibitor K-756 enhances imatinib-induced apoptosis in chronic myeloid leukemia (CML) cells harboring T315I BCR-ABL mutation.* Oncotarget, 2018. **9**(8): p. 8136–8145.
42. Fattah, M., et al., *PTPN11 Mutations in the Ras-MAPK Signaling Pathway Affect Human White Matter Microstructure.* Cereb Cortex, 2021. **31**(3): p. 1489-1499.
43. Sulong, S., et al., *A comprehensive analysis of the CDKN2A gene in childhood acute lymphoblastic leukemia reveals genomic deletion, copy number neutral loss of heterozygosity, and association with specific cytogenetic subgroups.* Blood, The Journal of the American Society of Hematology, 2009. **113**(1): p. 100-107.
44. Loh, M.L., et al., *Tyrosine kinome sequencing of pediatric acute lymphoblastic leukemia: a report from the Children's Oncology Group TARGET Project.* Blood, 2013. **121**(3): p. 485-8.
45. Chiaretti, S.B., Federica; Bassan, Renato; Vitale, Antonella; Elia, Loredana; Piciocchi, Alfonso; Fabbiano, Francesco; Salutari, Priscilla; Cimino, Giuseppe; Rossi, Davide; Gaidano, Gianluca; Guarini, Anna, *Mutation status of genes beyond Philadelphia-chromosome oncoproteins in adult acute lymphoblastic leukemia.* Leukemia research, 2016. **48**: p. 52-60.
46. Cortes, J.E., Kantarjian, H., *Resistance to BCR-ABL inhibition: mechanisms and management.* Blood, 2011. **117**(20): p. 7140-7150.
47. Wu X, Z.Z., Li W, Fu X, Su J, *SHP2 inhibitor, SHP099, as a novel candidate agent for the treatment of imatinib-resistant K562 cells.* Medical science monitor basic research, 2018. **24**: p. 77-84.
48. Niu, X., Wang, H., Li, W., Huang, Y., & Wu, X., *Targeting SHP2 overcomes dasatinib resistance in Philadelphia chromosome-positive acute lymphoblastic leukemia.* Investigational New Drugs, 2020. **38**(3): p. 623-634.
49. Zheng, H., S. Alter, and C.-K. Qu, *SHP-2 tyrosine phosphatase in human diseases.* International Journal of Clinical and Experimental Medicine, 2009. **2**(1): p. 17.
50. Pandey, R., M. Saxena, and R. Kapur, *Role of SHP2 in hematopoiesis and leukemogenesis.* Current opinion in hematology, 2017. **24**(4): p. 307.
51. Liu, Y., et al., *Targeting SHP2 as a therapeutic strategy for inflammatory diseases.* European Journal of Medicinal Chemistry, 2021. **214**: p. 113264.
52. Song, Z., et al., *Tyrosine phosphatase SHP2 inhibitors in tumor-targeted therapies.* Acta Pharmaceutica Sinica B, 2021. **11**(1): p. 13-29.
53. Yuan, X., et al., *Recent advances of SHP2 inhibitors in cancer therapy: current development and clinical application.* Journal of medicinal chemistry, 2020. **63**(20): p. 11368-11396.
54. Saxton, T.M., et al., *Abnormal mesoderm patterning in mouse embryos mutant for the SH2 tyrosine phosphatase Shp-2.* The EMBO journal, 1997. **16**(9): p. 2352-2364.
55. Tajan, M., et al., *SHP2 sails from physiology to pathology.* European journal of medical genetics, 2015. **58**(10): p. 509-525.
56. Chen, Y.-N.P., et al., *Allosteric inhibition of SHP2 phosphatase inhibits cancers driven by receptor tyrosine kinases.* Nature, 2016. **535**(7610): p. 148-152.

57. Prahallad, A., et al., *PTPN11 is a central node in intrinsic and acquired resistance to targeted cancer drugs.* Cell reports, 2015. **12**(12): p. 1978-1985.
58. Gu, S., et al., *SHP2 is required for BCR-ABL1-induced hematologic neoplasia.* Leukemia, 2018. **32**(1): p. 203-213.
59. Adachi, M., et al., *Mammalian SH2-containing protein tyrosine phosphatases.* Cell, 1996. **85**(1): p. 15.
60. Yi, T., J.L. Cleveland, and J.N. Ihle, *Identification of novel protein tyrosine phosphatases of hematopoietic cells by polymerase chain reaction amplification.* 1991.
61. Hof, P., et al., *Crystal structure of the tyrosine phosphatase SHP-2.* Cell, 1998. **92**(4): p. 441-450.
62. Tang, T.L., et al., *The SH2-containing protein-tyrosine phosphatase SH-PTP2 is required upstream of MAP kinase for early Xenopus development.* Cell, 1995. **80**(3): p. 473-483.
63. O'Reilly, A.M. and B.G. Neel, *Structural determinants of SHP-2 function and specificity in Xenopus mesoderm induction.* Molecular and cellular biology, 1998. **18**(1): p. 161-177.
64. Yu, B., et al., *Targeting protein tyrosine phosphatase SHP2 for the treatment of PTPN11-associated malignancies.* Molecular cancer therapeutics, 2013. **12**(9): p. 1738-1748.
65. Eck, M.J., et al., *Spatial constraints on the recognition of phosphoproteins by the tandem SH2 domains of the phosphatase SH-PTP2.* Nature, 1996. **379**(6562): p. 277-280.
66. Koch, C.A., et al., *SH2 and SH3 domains: elements that control interactions of cytoplasmic signaling proteins.* Science, 1991. **252**(5006): p. 668-674.
67. Shen, D., et al., *Therapeutic potential of targeting SHP2 in human developmental disorders and cancers.* European Journal of Medicinal Chemistry, 2020. **190**: p. 112117.
68. Nian, Q., et al., *A small molecule inhibitor targeting SHP2 mutations for the lung carcinoma.* Chinese Chemical Letters, 2021. **32**(5): p. 1645-1652.
69. Liu, Q., et al., *Targeting SHP2 as a promising strategy for cancer immunotherapy.* Pharmacological research, 2020. **152**: p. 104595.
70. Vainonen, J.P., M. Momeny, and J. Westermarck, *Druggable cancer phosphatases.* Science Translational Medicine, 2021. **13**(588): p. eabe2967.
71. Mali, R.S., et al., *Role of SHP2 phosphatase in KIT-induced transformation: identification of SHP2 as a druggable target in diseases involving oncogenic KIT.* Blood, The Journal of the American Society of Hematology, 2012. **120**(13): p. 2669-2678.
72. Fragale, A., et al., *Noonan syndrome–associated SHP2/PTPN11 mutants cause EGF-dependent prolonged GAB1 binding and sustained ERK2/MAPK1 activation.* Human mutation, 2004. **23**(3): p. 267-277.
73. Vogel, W. and A. Ullrich, *Multiple in vivo phosphorylated tyrosine phosphatase SHP-2 engages binding to Grb2 via tyrosine 584.* Cell Growth and Differentiation-Publication American Association for Cancer Research, 1996. **7**(12): p. 1589-1598.
74. Song, Y., et al., *A multifunctional cross-validation high-throughput screening protocol enabling the discovery of new SHP2 inhibitors.* Acta Pharm Sin B, 2021. **11**(3): p. 750-762.
75. Neel, B.G. and N.K. Tonks, *Protein tyrosine phosphatases in signal transduction.* Current opinion in cell biology, 1997. **9**(2): p. 193-204.

76. Huyer, G. and D.R. Alexander, *Immune signalling: SHP-2 docks at multiple ports.* Current biology, 1999. **9**(4): p. R129-R132.
77. Schaeper, U., et al., *Coupling of Gab1 to c-Met, Grb2, and Shp2 mediates biological responses.* The Journal of cell biology, 2000. **149**(7): p. 1419-1432.
78. Schaeper, U., et al., *Distinct requirements for Gab1 in Met and EGF receptor signaling in vivo.* Proceedings of the National Academy of Sciences, 2007. **104**(39): p. 15376-15381.
79. Wöhrle, F.U., R.J. Daly, and T. Brummer, *Function, regulation and pathological roles of the Gab/DOS docking proteins.* Cell Communication and Signaling, 2009. **7**(1): p. 1-28.
80. Bennett, A.M., et al., *Protein-tyrosine-phosphatase SHPTP2 couples platelet-derived growth factor receptor beta to Ras.* Proceedings of the National Academy of Sciences, 1994. **91**(15): p. 7335-7339.
81. Li, W., et al., *A new function for a phosphotyrosine phosphatase: linking GRB2-Sos to a receptor tyrosine kinase.* Molecular and cellular biology, 1994. **14**(1): p. 509-517.
82. Araki, T., H. Nawa, and B.G. Neel, *Tyrosyl phosphorylation of Shp2 is required for normal ERK activation in response to some, but not all, growth factors.* Journal of Biological Chemistry, 2003. **278**(43): p. 41677-41684.
83. Nichols, R.J., et al., *RAS nucleotide cycling underlies the SHP2 phosphatase dependence of mutant BRAF-, NF1-and RAS-driven cancers.* Nature cell biology, 2018. **20**(9): p. 1064-1073.
84. Deb, T.B., et al., *A common requirement for the catalytic activity and both SH2 domains of SHP-2 in mitogen-activated protein (MAP) kinase activation by the ErbB family of receptors: A specific role for SHP-2 in MAP, but not c-Jun amino-terminal kinase activation.* Journal of Biological Chemistry, 1998. **273**(27): p. 16643-16646.
85. Maroun, C.R., et al., *The tyrosine phosphatase SHP-2 is required for sustained activation of extracellular signal-regulated kinase and epithelial morphogenesis downstream from the met receptor tyrosine kinase.* Molecular and cellular biology, 2000. **20**(22): p. 8513-8525.
86. Qu, C.K., *The SHP-2 tyrosine phosphatase: signaling mechanisms and biological functions.* Cell research, 2000. **10**(4): p. 279-288.
87. Alfayez, M., et al., *The Clinical impact of PTPN11 mutations in adults with acute myeloid leukemia.* Leukemia, 2021. **35**(3): p. 691-700.
88. Nabinger, S.C., et al., *The protein tyrosine phosphatase, Shp2, positively contributes to FLT3-ITD-induced hematopoietic progenitor hyperproliferation and malignant disease in vivo.* Leukemia, 2013. **27**(2): p. 398-408.
89. Hui, E., et al., *T cell costimulatory receptor CD28 is a primary target for PD-1–mediated inhibition.* Science, 2017. **355**(6332): p. 1428-1433.
90. Yang, Z., et al., *Activating PTPN11 mutants promote hematopoietic progenitor cell-cycle progression and survival.* Experimental hematology, 2008. **36**(10): p. 1285-1296.
91. Sattler, M., et al., *Critical role for Gab2 in transformation by BCR/ABL.* Cancer cell, 2002. **1**(5): p. 479-492.
92. Sattler, M. and J.D. Griffin, *Mechanisms of transformation by the BCR/ABL oncogene.* International journal of hematology, 2001. **73**(3): p. 278-291.
93. Guo, W. and Q. Xu, *Phosphatase-independent functions of SHP2 and its regulation by small molecule compounds.* Journal of Pharmacological Sciences, 2020. **144**(3): p. 139-146.

94. Dong, L., et al., *Activating Mutation of SHP2 Establishes a Tumorigenic Phonotype Through Cell-Autonomous and Non-Cell-Autonomous Mechanisms.* Front Cell Dev Biol, 2021. **9**: p. 630712.
95. Pandey, R., M. Saxena, and R. Kapur, *Role of SHP2 in hematopoiesis and leukemogenesis.* Curr Opin Hematol, 2017. **24**(4): p. 307-313.
96. Zhu, L., et al., *Drug repositioning for Noonan and LEOPARD syndromes by integrating transcriptomics with a structure-based approach.* Frontiers in Pharmacology, 2020. **11**: p. 927.
97. Tartaglia, M., et al., *Mutations in PTPN11, encoding the protein tyrosine phosphatase SHP-2, cause Noonan syndrome.* Nature genetics, 2001. **29**(4): p. 465-468.
98. Serra-Nédélec, A.D.R., et al., *Noonan syndrome-causing SHP2 mutants inhibit insulin-like growth factor 1 release via growth hormone-induced ERK hyperactivation, which contributes to short stature.* Proceedings of the National Academy of Sciences, 2012. **109**(11): p. 4257-4262.
99. Jongmans, M.C., et al., *Cancer risk in patients with Noonan syndrome carrying a PTPN11 mutation.* European Journal of Human Genetics, 2011. **19**(8): p. 870-874.
100. Grossmann, K.S., et al., *The tyrosine phosphatase Shp2 in development and cancer.* Advances in cancer research, 2010. **106**: p. 53-89.
101. Digilio, M.C., et al., *Grouping of multiple-lentigines/LEOPARD and Noonan syndromes on the PTPN11 gene.* The American Journal of Human Genetics, 2002. **71**(2): p. 389-394.
102. Kontaridis, M.I., et al., *PTPN11 (Shp2) mutations in LEOPARD syndrome have dominant negative, not activating, effects.* Journal of Biological Chemistry, 2006. **281**(10): p. 6785-6792.
103. Yoshida, R., et al., *Two novel and one recurrent PTPN11 mutations in LEOPARD syndrome.* American journal of medical genetics Part A, 2004. **130**(4): p. 432-434.
104. Dong, L., et al., *Activating mutation of SHP2 establishes a tumorigenic phonotype through cell-autonomous and non-cell-autonomous mechanisms.* Frontiers in Cell and Developmental Biology, 2021: p. 3.
105. Hu, Z., et al., *A tyrosine phosphatase SHP2 gain-of-function mutation enhances malignancy of breast carcinoma.* Oncotarget, 2015. **7**(5).
106. Tartaglia, M., et al., *Somatic mutations in PTPN11 in juvenile myelomonocytic leukemia, myelodysplastic syndromes and acute myeloid leukemia.* Nature genetics, 2003. **34**(2): p. 148-150.
107. Loh, M., et al., *PTPN11 mutations in pediatric patients with acute myeloid leukemia: results from the Children's Cancer Group.* Leukemia, 2004. **18**(11): p. 1831-1834.
108. Kratz, C.P., et al., *The mutational spectrum of PTPN11 in juvenile myelomonocytic leukemia and Noonan syndrome/myeloproliferative disease.* Blood, 2005. **106**(6): p. 2183-2185.
109. Steelman, L.S., et al., *Roles of the Ras/Raf/MEK/ERK pathway in leukemia therapy.* Leukemia, 2011. **25**(7): p. 1080-1094.
110. Kanumuri, R., et al., *Targeting SHP2 phosphatase in hematological malignancies.* Expert Opinion on Therapeutic Targets, 2022. **26**(4): p. 319-332.
111. Tsai, C.-H., et al., *Genetic alterations and their clinical implications in older patients with acute myeloid leukemia.* Leukemia, 2016. **30**(7): p. 1485-1492.
112. Makishima, H., et al., *Dynamics of clonal evolution in myelodysplastic syndromes.* Nature genetics, 2017. **49**(2): p. 204-212.
113. Fu, J.F., et al., *Cooperation of MLL/AF10 (OM-LZ) with PTPN11 activating mutation induced monocytic leukemia with a shorter latency in a mouse bone marrow*

transplantation model. International Journal of Cancer, 2017. **140**(5): p. 1159-1172.
114. Chen, L., et al., *Mutated Ptpn11 alters leukemic stem cell frequency and reduces the sensitivity of acute myeloid leukemia cells to Mcl1 inhibition.* Leukemia, 2015. **29**(6): p. 1290-1300.
115. Dudka, W., et al., *Targeting Integrated Stress Response by ISRIB combined with imatinib attenuates STAT5 signaling and eradicates therapy-resistant Chronic Myeloid Leukemia cells.* bioRxiv, 2021: p. 2021.05.05.442756.
116. Athota, J.P., et al., *Molecular and clinical studies in 107 Noonan syndrome affected individuals with PTPN11 mutations.* BMC Medical Genetics, 2020. **21**(1): p. 50.
117. Araki, T., et al., *Mouse model of Noonan syndrome reveals cell type–and gene dosage–dependent effects of Ptpn11 mutation.* Nature medicine, 2004. **10**(8): p. 849-857.
118. Chan, G., et al., *Leukemogenic Ptpn11 causes fatal myeloproliferative disorder via cell-autonomous effects on multiple stages of hematopoiesis.* Blood, The Journal of the American Society of Hematology, 2009. **113**(18): p. 4414-4424.
119. Liu, M., et al., *Strategies to overcome drug resistance using SHP2 inhibitors.* Acta Pharmaceutica Sinica B, 2021.
120. Schubbert, S., et al., *Functional analysis of leukemia-associated PTPN11 mutations in primary hematopoietic cells.* Blood, 2005. **106**(1): p. 311-317.
121. Song, Y., et al., *Crystallographic landscape of SHP2 provides molecular insights for SHP2 targeted drug discovery.* Medicinal Research Reviews, 2022. **42**(5): p. 1781-1821.
122. Tartaglia, M., et al., *Diversity and Functional Consequences of Germline and Somatic PTPN11 Mutations in Human Disease.* The American Journal of Human Genetics, 2006. **78**(2): p. 279-290.
123. Tartaglia, M., et al., *Diversity and functional consequences of germline and somatic PTPN11 mutations in human disease.* Am J Hum Genet, 2006. **78**(2): p. 279-90.
124. Tartaglia, M., et al., *Genetic evidence for lineage-related and differentiation stage–related contribution of somatic PTPN11 mutations to leukemogenesis in childhood acute leukemia.* Blood, 2004. **104**(2): p. 307-313.
125. Tartaglia, M., et al., *Somatic PTPN11 mutations in childhood acute myeloid leukaemia.* British journal of haematology, 2005. **129**(3): p. 333-339.
126. Yu, Z.-H., et al., *Molecular basis of gain-of-function LEOPARD syndrome-associated SHP2 mutations.* Biochemistry, 2014. **53**(25): p. 4136-4151.
127. Tartaglia, M., et al., *Erratum: Somatic mutations in PTPN11 in juvenile myelomonocytic leukemia, myelodysplastic syndromes and acute myeloid leykemia.* Nature Genetics, 2003. **34**(4): p. 464-464.
128. Abram, C.L. and C.A. Lowell, *Shp1 function in myeloid cells.* Journal of Leukocyte Biology, 2017. **102**(3): p. 657-675.
129. Esposito, N., et al., *SHP-1 expression accounts for resistance to imatinib treatment in Philadelphia chromosome–positive cells derived from patients with chronic myeloid leukemia.* Blood, 2011. **118**(13): p. 3634-3644.
130. Kerr, D.L., F. Haderk, and T.G. Bivona, *Allosteric SHP2 inhibitors in cancer: Targeting the intersection of RAS, resistance, and the immune microenvironment.* Current Opinion in Chemical Biology, 2021. **62**: p. 1-12.
131. Song, Z., et al., *Tyrosine phosphatase SHP2 inhibitors in tumor-targeted therapies.* Acta Pharm Sin B, 2021. **11**(1): p. 13-29.

132. He, R., et al., *Small molecule tools for functional interrogation of protein tyrosine phosphatases.* The FEBS journal, 2013. **280**(2): p. 731-750.
133. Chen, M.-J., et al., *PAK1 confers chemoresistance and poor outcome in non-small cell lung cancer via β-catenin-mediated stemness.* Scientific reports, 2016. **6**(1): p. 1-10.
134. Sun, X., et al., *Selective inhibition of leukemia-associated SHP2E69K mutant by the allosteric SHP2 inhibitor SHP099.* Leukemia, 2018. **32**(5): p. 1246-1249.
135. LaRochelle, J.R., et al., *Structural reorganization of SHP2 by oncogenic mutations and implications for oncoprotein resistance to allosteric inhibition.* Nature communications, 2018. **9**(1): p. 1-10.
136. Mali, R.S., R. Chan, and R. Kapur, *Targeting SHP2 phosphatase in myeloproliferative neoplasms.* Oncotarget, 2012. **3**(10): p. 1049.
137. Li, Q., et al., *Proteolysis-targeting chimeras in biotherapeutics: Current trends and future applications.* European Journal of Medicinal Chemistry, 2023: p. 115447.
138. Wang, M., et al., *Discovery of SHP2-D26 as a first, potent, and effective PROTAC degrader of SHP2 protein.* Journal of medicinal chemistry, 2020. **63**(14): p. 7510-7528.
139. Yu, D., et al., *Proteolysis-targeting chimera molecules targeting SHP2.* Future Medicinal Chemistry, 2022. **14**(8): p. 587-600.
140. Chang, L. and M. Karin, *Mammalian MAP kinase signalling cascades.* Nature, 2001. **410**(6824): p. 37-40.
141. Fedele, C., et al., *SHP2 Inhibition Prevents Adaptive Resistance to MEK Inhibitors in Multiple Cancer Models.* Cancer discovery, 2018. **8**(10): p. 1237-1249.
142. Ran, H., et al., *Sticking it to cancer with molecular glue for SHP2.* Cancer cell, 2016. **30**(2): p. 194-196.
143. Neel, B.G. and N.K. Tonks, *Protein tyrosine phosphatases in cancer*. 2016: Springer.
144. Leonard, J.T., et al., *Functional and genetic screening of acute myeloid leukemia associated with mediastinal germ cell tumor identifies MEK inhibitor as an active clinical agent.* Journal of hematology & oncology, 2016. **9**(1): p. 1-6.
145. Gilmartin, A.G., et al., *GSK1120212 (JTP-74057) is an inhibitor of MEK activity and activation with favorable pharmacokinetic properties for sustained in vivo pathway inhibition.* Clinical cancer research, 2011. **17**(5): p. 989-1000.
146. Farnault, L., et al., *Response to trametinib of histiocytosis with an activating PTPN11 mutation.* Leukemia & Lymphoma, 2020. **61**(1): p. 194-197.
147. Rice, K.D., et al., *Novel carboxamide-based allosteric MEK inhibitors: discovery and optimization efforts toward XL518 (GDC-0973).* ACS medicinal chemistry letters, 2012. **3**(5): p. 416-421.
148. Choo, E.F., et al., *PK-PD modeling of combination efficacy effect from administration of the MEK inhibitor GDC-0973 and PI3K inhibitor GDC-0941 in A2058 xenografts.* Cancer chemotherapy and pharmacology, 2013. **71**(1): p. 133-143.
149. Cheng, Y. and H. Tian, *Current Development Status of MEK Inhibitors.* Molecules (Basel, Switzerland), 2017. **22**(10): p. 1551.
150. Esposito, M.T., *The Impact of PI3-kinase/RAS Pathway Cooperating Mutations in the Evolution of KMT2A-rearranged Leukemia.* HemaSphere, 2019. **3**(3).
151. Weiss, B.D., et al., *NF106: a neurofibromatosis clinical trials consortium phase II trial of the MEK inhibitor mirdametinib (PD-0325901) in adolescents and adults with NF1-related plexiform neurofibromas.* Journal of Clinical Oncology, 2021. **39**(7): p. 797.
152. Wauson, E.M., et al., *Off-Target Effects of MEK Inhibitors.* Biochemistry, 2013. **52**(31): p. 5164-5166.

153. Yokota, T. and Y. Kanakura, *Genetic abnormalities associated with acute lymphoblastic leukemia.* Cancer Science, 2016. **107**(6): p. 721-725.
154. Saleh, K., A. Fernandez, and F. Pasquier *Treatment of Philadelphia Chromosome-Positive Acute Lymphoblastic Leukemia in Adults*. Cancers, 2022. **14**, DOI: 10.3390/cancers14071805.
155. Fielding, A.K., *Curing Ph+ ALL: assessing the relative contributions of chemotherapy, TKIs, and allogeneic stem cell transplant.* Hematology Am Soc Hematol Educ Program, 2019. **2019**(1): p. 24-29.

Chapter 2: Materials and Methods

2.1. Common reagents used in experiments

Table 2.1 Common reagents used in experiments

Category	Reagent	Supplier	Catalogue Number
General Chemicals	*DC*™ Protein Assay Kit	Bio-Rad	#5000112
	Dulbecco's phosphate-buffered saline (DPBS) (10X), no calcium, no magnesium	Gibco	#14200-075
	Ethanol	Merck Millipore	#6-10107-2511
	Glycerol	Univar	#242 – 500 mL
	Hydrochloric acid (HCl, 32%)	ACI LABSCAN	#RP1104-P2.5L
	Isopropanol	Chem-Supply	#PA013-2.5LP
	Methanol	Chem-Supply	#MA004-2.5L-P
	Tris (hydroxymethyl) aminomethane	Sigma-Aldrich	#252859 – 500 g
	β-mercaptoethanol	Aldrich	M6250 – 100 mL
	Sodium chloride	Univar	#465 – 2.5 kg
Cell Culture Reagents	Fetal bovine serum (FBS)	Sigma/SAFC	#12003C
	Dimethyl sulfoxide	Sigma-Aldrich	#1.02952.2500
	Dulbecco's Modified Eagle's Medium (DMEM)-Low Glucose	Sigma-Aldrich	#D6046
	Iscove's Modified Dulbecco's Medium (IMDM)	Sigma-Aldrich	#I3390

	Roswell Park Memorial Institute (RPMI) 1640 Medium- No Glutamine	Gibco	#21870-076
	L-glutamine 200 mM	Sigma-Aldrich	#G7513
	Lymphoprep	Axis Shield. Oslo Norway	#1114547
	Newborn Calf Serum (NCS)	Sigma-Aldrich	#13023C
	Penicillin/Streptomycin	Sigma-Aldrich	#P4333-100 mL
	Trypan blue 0.4%	Sigma-Aldrich	#T8154-100 mL
Flow Cytometry Assay	16% Paraformaldehyde, EM grade	Electron Microscopy Sciences	#15710
	Fixable Viability Stain 780	BD Bioscience	#565388
	Annexin-V-PE	BD Bioscience	#556421
	Calcium Chloride	Sigma-Aldrich	#C1016 – 500 g
	Hanks' Balanced Salt solution (HBSS)	Sigma-Aldrich	#H9394
	HEPES solution, 1 M, pH 7.0-7.6	Sigma-Aldrich	#H0887
	Mcl-1 inhibitor S63845	Medchem Express	# HY-100741
	Trametinib (GSK1120212)	Selleck Chemicals	# S2673

	Bcl-xL Inhibitor (**A-1155463)**	Selleck Chemicals	#S7800
	Venetoclax (ABT-199)	Selleck Chemicals	#S8048
	MEK Inhibitor (PD0325901)	Stem Cell Technologies	#72182
	Navitoclax (ABT-263)	Selleck Chemicals	#S1001
SDS-PAGE / Western Blotting	4–15% CriterionTM TGXTM Precast Midi Protein Gel, 18 well, 30 µl	Bio-Rad	#5671084
	Bovine Serum Albumin (BSA)	Sigma-Aldrich	A9418
	Precision Plus Protein^{TM} Kaleidoscope	Bio-Rad	#161-0375
	cOmplete^{TM} Mini EDTA-Free Protease Inhibitor Cocktail Tablets	Roche	#04693159001
	Leupeptin Protease Inhibitor	Sigma-Aldrich	#L0649-5 mg
	Sodium fluoride	Sigma-Aldrich	#S7920
	Sodium (ortho) Vanadate (Na_3VO_4)	Sigma-Aldrich	#S6508
	β-Glycerol Phosphate	Sigma-Aldrich	#G9422

	Sodium Pyrophosphate	Sigma-Aldrich	#P8010-500 mg
	Aprotinin Protease Inhibitor	Sigma-Aldrich	#9087-70-1
	PMSF	Sigma-Aldrich	#P7628-250 g
	Glycerol	Sigma-Aldrich	#G5516-1L
	Ponceau S	Sigma-Aldrich	#P3504-10 g
	SDS (Sodium Dodecyl Sulphate)	Sigma-Aldrich	#L4509
	Trans-Blot Turbo 5 x Transfer Buffer	Bio-Rad	#10026938
	Trans-Blot® TurboTM RTA Midi LF PVDF Transfer Kit	Bio-Rad	#1704275
	Li-Core (Millennium) Intercept (Odyssey) Blocking Buffer (PBS)	Millennium Science	# 927-70003
	Tween-20	Sigma-Aldrich	#P2287 – 500 mL
	Western blot recycling stripping buffer (10x)	Alpha Diagnostic International	#90101
	100bp DNA Ladder	New England Biolabs	#N3231s
	1kb DNA ladder	New England Biolabs	#N3232S

	Sample Buffer, LaemmLi 2× Concentrate	Sigma-Aldrich	#S3401-10VL
	Gel Loading Dye, Purple (6X)	New England Biolabs	# B7024S
	Agarose	Sigma-Aldrich	#A6013-500 g
Genomics	AmpliTaq Gold DNA Polymerase	Thermo Fisher Scientific	#N8080241
	Chloroform	Merck Millipore	#100776B
	Deoxynucleotide Set, 100 mM	Sigma-Aldrich	#DNTP100-1KT
	DNA hydration solution	Qiagen	#158914
	EDTA Disodium Salt	Univar	#AJA180-100 g
	ExoSAP-IT	TheroFisher Scientific	# 78201.1.ML
	Gel Loading Dye, Purple (6x), no SDS	New England Biolabs	#B7025S
	GelRed^{TM} Nucleic Acid Stain	Biotium	#41002
	Glycogen for molecular biology	Roche	#10 901 393 001
	Nuclease-free water (NF-H_2O)	Qiagen	#129117
	Paraformaldehyde powder, 95%	Fluka	#76240
	Phusion High-fidelity DNA Polymerase	New England Biolabs	M0530L
	Proteinase K	Roche	#03115887001

	Superscript II Reverse Transcriptase	Invitrogen	#1904427
	RNAse A	Qiagen	#205313
	RT2 SYBR® Green qPCR Mastermix	Qiagen	#19101
	TRIzol® reagent	Life Technologies	#330503
	Ultrapure^{TM} Buffer Saturated Phenol	Invitrogen	#15515-039
	UltraPure^{TM} Phenol: Chloroform:Isoamyl alcohol (25:24:1, v/v)	Invitrogen	#15593-031
	Ampicillin	Sigma-Aldrich	#A5354
	DNA Polymerase I, Large (Klenow) Fragment	New England Biolabs	#M0210S
	Kanamycin Sulfate	Gibco	#15160-054
	Polybrene®	Santa Cruz Biotechnology	#sc-134220
Molecular Cloning	Select Agar^{TM}	Invitrogen	#30391-023
	Bacterial Peptone	Oxoid	#LP0037
	Yeast Extract	Sigma-Aldrich	#Y1625-250 g
	SOC Medium	ThermoFisher Scientific	# 15544034

	Shrimp Alkaline Phosphatase (rSAP)	New England Biolabs	#M0371S
	One Shot MAX Efficiency DH5α-T1 Competent Cells	Life Tech	#12297-016
	T4 DNA Ligase	New England Biolabs	#M0202
	EcoRI-HF	New England BioLabs	#R3101
	NotI-HF	New England Biolabs	#R3189L
	BigDye Xterminator Purification Kit	ThermoFisher Scientific	#4376486
	Phusion High-Fidelity DNA Polymerase	New England Biolabs	#M0530L
	Q5 High-Fidelity DNA Polymerase	New England Biolabs	#M0491S
	T4 DNA Polymerase	New England Biolabs	#M0203S
	BigDye™ Terminator v3.1 Cycle Sequencing Kit	ThermoFisher Scientific	#4337455
	Q5 Site-Directed Mutagenesis Kit	New England Biolabs	#E0554S
	Lipofectamine™ 2000 Transfection Reagent	Thermo Fisher scientific	#11668027

	SH-PTP2 shRNA (h) Lentiviral Particles	Santa Cruz	#sc-36488-V
	copGFP Control Lentiviral Particles	Santa Cruz	#sc-108084
	Control shRNA Lentiviral Particles-A	Santa Cruz	#sc-108080
	Puromycin dihydrochloride (CAS 58-58-2)	Santa Cruz	#sc-108071
	Opti-MEM I + Glutamax	Gibco	#51985-034
	pLVX-EF1α-IRES-ZsGreen1 Expression Vector	Gift from Daniel Thomas	
	psPAX2 Plasmid	Adgene	#12260
	pMD2.G Plasmid	A Gift from Daniel Thomas	

Table 2.2 – List of Western blotting antibodies

Target	**Antibody**	**Molecular Weight (kDa) of Target Protein**	**Species and Conc. Used**	**Supplier**	**Catalogue Number**
BCR::ABL1 Signalling	CRKL (c-20)	39	Rabbit (1:2000)	Santa Cruz	#sc-319

	Phospho-Bcr (Tyr177)	160 (Bcr), 190 (BCR::ABL1) & 210 (BCR::ABL1)	Rabbit (1:1000)	Cell Signalling	#3901
	c-Abl Monoclonal Antibody (ZC015)	135 (c-Abl), 190 (BCR::ABL1) & 210 (BCR::ABL1)	Mouse (1:2000)	Thermo Fisher Scientific	#41-2900
	phospho-Abl (Tyr245) (7E35)	190 (BCR::ABL1) & 210 (BCR::ABL1)	Rabbit (1:1000)	Cell Signalling	#2868
SHP1/SHP-2 Signalling	SHP-2 Antibody	72	Rabbit (1:1000)	Cell Signalling	#3752
	SHP-1 (C14H6)	68	Rabbit (1:1000)	Cell Signalling	#3759
MAPK Signalling	Phospho-p44/42 MAPK (Erk1/2) (Thr202/Tyr204)	44 and 42	Rabbit (1:1000)	Cell Signalling	#9101
	p44/42 MAPK (Erk1/2) (L34F12)	44 and 42	Mouse (1:2000)	Cell Signalling	#4696

mTOR signalling	mTOR (L27D4)	289	Mouse (1:2000)	Cell Signalling	#4517
	Phospho-mTOR (Ser2448)	289	Rabbit (1:1000)	Cell Signalling	#2971
JAK/STAT Signalling	Phospho-Stat5 (Y694)	90	Rabbit (1:1000)	Cell Signalling	#9359
	Stat5	90	Rabbit (1:1000)	Cell Signalling	#9363
Apoptotic Signalling	PARP/ Cleaved PARP	116 and 89	Rabbit (1:1000)	Cell Signalling	#9542
	Bcl-xL (54H6)	30	Rabbit (1:1000)	Cell Signalling	#2764
	Bcl-2 (D17C4)	26	Rabbit (1:1000)	Cell Signalling	#3498
	Bim (C34C5)	23, 15 and 12	Rabbit (1:1000)	Cell Signalling	#2933
	Mcl-1	40	Rabbit (1:1000)	Cell Signalling	#4572
Loading Control	β-actin (13E5)	45	Rabbit (1:2000)	Cell Signalling	#4970
	GAPDH (14C10)	37	Rabbit (1:2000)	Cell Signalling	#2118
	β-Tubulin (9F3)	50	Rabbit (1:2000)	Cell Signalling	#2128

Secondary Antibodies	Donkey-anti-rabbit-IRDye®-680LT	NA	Donkey (1:10000)	Li-COR	#926-68023
	Donkey-anti-rabbit-IRDye®-800CW	NA	Donkey (1:10000)	Li-COR	#925-32213
	Donkey-anti-mouse-IRDye® 800CW	NA	Donkey (1:10000)	Li-COR	#925-68022
	Donkey-anti-mouse-IRDye®-680LT	NA	Donkey (1:10000)	Li-COR	#926-32212

Table 2.3 – List of phospho-flow antibodies

Antibody	**Clone and conc. used**	**Isotype**	**Catalogue no.**	**Supplier**
PE anti-human CD338 (ABCG2) Antibody	5D3 (1:20)	IgG2b, κ	#332007	BD Phosflow
PE mouse anti-Stat5 (pY694)	47/Stat5(pY694) (1:5)	IgG1, κ	# 612567	BD Phosflow
PE Mouse anti-Akt (pS473)	M89-61 (1:20)	IgG1, κ	#561671	BD Phosflow

PE Mouse Anti-ERK1/2 (pT202/pY204)	20A (1:5)	IgG1, κ	# 612566	BD Phosflow
PE Mouse IgG1 κ Isotype Control	MOPC-21 (1:50)	IgG1, κ	#555749	BD Pharmingen
Isoptype Reagent IgG2b κ Isotype Control	- (1:20)	IgG2b, κ	#X0951	Dako Denmark

2.2. Cell Culture Media & Solutions

Cell culture media were stored at 4°C and preheated to 37°C (unless otherwise stated) in a water bath prior to use.

SUP-B15 Ph+ ALL cell culture media

Iscove′s Modified Dulbecco′s Medium (IMDM)

4 mM *L*-glutamine

50 units/mL Penicillin

50 µg/mL Streptomycin

20% FBS

0.05 mM b-mercaptoethanol

BaF3 parental wildtype cell culture media

RPMI-1640 medium

2 mM *L*-glutamine

50 units/mL Penicillin

50 µg/mL Streptomycin

10% Foetal bovine serum (FBS)

5% WEHI-3B complete media (source of IL-3)

BaF3 *BCR::ABL1* p190 (IL-3 independent) cell culture media

RPMI-1640 medium

2 mM *L*-glutamine

50 units/mL Penicillin

50 µg/mL Streptomycin

10% FBS

HEK-293T cell culture media

Dulbecco's Modified Eagle's Medium (DMEM)

2 mM *L*-glutamine

50 units/mL Penicillin

50 µg/mL Streptomycin

10% FBS

WEHI-3B cell culture media

RPMI-1640 medium

2 mM *L*-glutamine

50 units/mL Penicillin

50 µg/mL Streptomycin

10% FBS

CRKL IC50 and other western blot media

90% Cell culture media

10% Newborn calf serum (NCS)

Cryopreservation media

70% Cell culture media

20% FBS

10% Dimethyl sulfoxide (DMSO)

2.3. Inhibitors

2.3.1. Imatinib (STI-571)

MW: 589.71

Imatinib mesylate (Novartis, Australia) was dissolved in sterile Milli-Q® water at a concentration of 10 mM. The solution was then filtered through a sterile filter and kept at a temperature of -80°C for storage. Prior to use in an experiment, the imatinib mesylate solution was diluted in sterile Milli-Q® water using serial dilutions.

2.3.2. Dasatinib (BMS-354825)

MW: 488.01

Dasatinib (Bristol-Myers Squibb, USA) was dissolved in DMSO to 10 mM and stored at 4°C. Serial dilutions were made in sterile DMSO before using in an experiment.

2.3.3. Nilotinib (AMN107)

MW: 529.5

Nilotinib (Novartis, Australia) stock solutions was prepared at 10 mM in DMSO and stored at -20°C. Serial dilutions were made in sterile DMSO before using in an experiment.

2.3.4. Ponatinib (AP24534)

MW: 532.56

Ponatinib (ARIAD Pharmaceuticals, USA) stock solutions was prepared at 10 mM in DMSO and stored at -20°C. Serial dilutions were made in sterile DMSO before using in an experiment.

2.3.5. Asciminib (ABL001)

Asciminib (Novartis, Australia) stock solutions was prepared at 10 mM in DMSO and stored at -20°C. Serial dilutions were made in sterile DMSO before using in an experiment.

2.3.6. Venetoclax (ABT-199)

MW: 868.44

Venetoclax (Selleck Chemicals, Houston TX, USA) was dissolved to 10 mM in DMSO and stored at -20°C. Serial dilutions were made in sterile DMSO before using in an experiment.

2.3.7. Mcl-1 inhibitor (S63845)

MW: 829.26

S63845 (Medchem Express, USA) was dissolved to 10 mM in DMSO and stored at- 20°C. Serial dilutions were made in sterile DMSO before using in an experiment.

2.3.8. Bcl-xL Inhibitor (A-1155463)

MW: 669.79

A-1155463 (Selleck Chemicals, Houston TX, USA) was dissolved to 10 mM in DMSO and stored at -20°C. Serial dilutions were made in sterile DMSO before using in an experiment.

2.3.9. Trametinib (GSK1120212)

MW: 615.39

Trametinib (Selleck Chemicals, Houston TX, USA) was dissolved to 10 mM in DMSO and stored at -20°C. Serial dilutions were made in sterile DMSO before using in an experiment.

2.3.10. MEK Inhibitor (PD0325901)

MW: 482.19

PD0325901 (Stem Cell Technologies, Australia) was dissolved to 10 mM in DMSO and stored at -20°C. Serial dilutions were made in sterile DMSO before using in an experiment.

2.3.11. Navitoclax (ABT-263)

MW: 974.61

Navitoclax (Selleck Chemicals, Houston TX, USA) was dissolved to 10 mM in DMSO and stored at -20°C. Serial dilutions were made in sterile DMSO before using in an experiment.

2.3.12. Batoprotafib (TNO155)

MW: 421.95

Batoprotafib (Selleck Chemicals, Houston TX, USA) was dissolved to 10 mM in DMSO and stored at -20°C. Serial dilutions were made in sterile DMSO before using in an experiment.

2.4. Buffers & Solutions used in Protein Assays

2.4.1. 1x Phosphate-buffered saline (1x PBS)

10 x PBS stock (Gibco #14200-075) was diluted 1:10 in sterile Milli-Q® ultra-purified water.

Solution was prepared, autoclaved for sterilization when needed and stored at 4^{O}C or at RT as required.

2.4.2. 1x Tris-buffered saline (1x TBS)

20 mM Tris-HCL (pH 7.5)

150 mM NaCl

RO water

Solution was prepared and stored at room temperature (RT).

2.4.3. 1x Tris-buffered saline + 0.1% Tween-20 (1x TBST)

20 mM Tris-HCL (pH 7.5)

150 mM NaCl

0.1% Tween20

RO water

Solution was prepared and stored at room temperature (RT).

2.4.4. 1x SDS-PAGE gel running buffer

25 mM Tris

192 mM Glycine

0.1% SDS

RO water

Solution was prepared and stored at RT.

2.4.5. NP-40 Lysis Buffer Reagents

10 mM Tris-HCL pH 7.4

137 mM NaCl

10% Glycerol

1% NP-40 (Igepal™)

Stock for 10 mL NP-40 buffer with above listed reagents was prepared and stored at 4^{o}C. The below listed reagents were freshly added each time before using it for creating cell lysates.

10 mM β-glycerol phosphate

2 mM Sodium Vanadate

2 mM Sodium Fluoride

2 mM PMSF

10 mM Sodium Pyrophosphate

1 µg/mL Leupeptin

5 µg/mL Aprotinin

1x Complete, mini EDTA-free protease inhibitors Cocktail tablet (Roche)

2.4.6. Ponceau S staining solution

0.5% w/v Ponceau S

5% acetic acid

Milli-Q® dH2O

Solution was prepared and stored at RT.

2.5. Buffers & Solutions for Flow Cytometry Analysis

2.5.1. 1x Binding buffer for 'Annexin-V / Fixable Viability Stain 780' assay

Hanks Balance Salt Solution

10 mM HEPES

5 mM $CaCl_2$

Solution was freshly prepared and kept on ice.

2.5.2. 1x Binding buffer for phospho-flow assay

1x PBS

1% BSA

Solution was freshly prepared and kept on ice.

2.5.3. Methanol permeabilization solution for phospho-flow assay

80% analytical grade methanol

20% Milli-Q® dH_2O

Solution was stored at -20°C and used ice-cold for each application.

2.5.4. Flow cytometry fixative (FACS fix)

1x PBS

1% Formaldehyde

111 mM D-glucose

0.02% sodium-azide

Solution was prepared at RT and stored at 4°C.

2.6. Molecular Biology Reagents

2.6.1. dNTP set (N=A, T, C, G)

25 mM: 40 µL of each dNTP

5 mM: 1:5 dilution of 25 mM stock in 80 µL DEPC water

Solution was prepared and stored at -20°C.

2.6.2. LB Broth

10 g Luria broth base

To 400 mL with Milli-Q® water

Solution was sterilised (autoclaved) and stored at RT. A suitable antibiotic was added to the LB broth prior to setting up a bacterial culture as a selection reagent.

2.6.3. LB Agar

10 g Luria broth base

6 g Select Agar™

To 400 mL with Milli-Q® water

The Agar solution underwent sterilization through autoclaving and was subsequently stored at room temperature (RT). The solidified LB agar stock was heated in a microwave oven until the agar had completely melted. It was then cooled to 37°C before the antibiotics (100 µg/µL ampicillin or 50 µg/µL kanamycin) were added. Following the addition of antibiotics, the LB agar solution was promptly and aseptically transferred into sterile petri dishes, where it was allowed to solidify at room temperature (RT). The LB agar plates were carefully sealed using Parafilm M® (Bermis Inc., USA) and stored at 4°C.

2.6.4. 1x Tris-acetate EDTA (1x TAE) buffer

40 mM Tris (pH 7.6)

20 mM acetic acid

1 mM EDTA

Milli-Q® water

Stored at RT.

2.6.5. Agarose (1%) gel for DNA electrophoresis

1% agarose powder

0.01% GelRed™ nucleic acid stain

1x TAE buffer

Solution was freshly made prior to gel-electrophoresis.

2.7. General Cell Culture Techniques

2.7.1. Subculturing of cell lines

To analyse cell viability and density, Trypan blue exclusion (1:1 dilution) was employed. A haemocytometer (Marienfeld Superior GMBH & Co. KG, Germany) was utilized for this purpose. The assessment of percentage viability and density was conducted using an Olympus CX41 microscope (Olympus Corporation, USA) with a 10x objective. Cell sub-culturing took place in a biosafety class II cabinet (Esco Global, Singapore). The process involved transferring cells into T25, T75, or T150 culture flasks (Corning Inc., USA). The recommended cell densities for sub-culturing were determined based on the desired final

volume (Table 2.5). The sub-culturing was carried out with warm media at 37°C, as described in section 2.2 of the 'Cell Culture Media & Solutions' reference.

Table 2.4 – Cell culture seeding densities

Cell line	**Cell type**	**Species**	**Recommended Live Cell Seeding Density**
SUP-B15 Ph+ ALL	B lymphoblasts	Human	$5x10^5$ /mL
BaF3 Parental	Pro-B Cell	Mouse	$1x10^5$ /mL
BaF3 IL-3 Independent (BaF3 BCR::ABL1 p190)	Pro-B Cell	Mouse	$5x10^4$ /mL
HEK-293T	Embryonic Kidney Cells	Human	$1x10^4$ /cm^2

2.7.2. Cryopreservation of cell lines

The cell lines were preserved for future use by cryopreservation. To achieve this, approximately 1 x 10^7 cells per sample were centrifuged at 1400 rpm for 5 minutes at room temperature (RT) in a 50 mL centrifuge tube. After discarding the supernatant, the pelleted cells were suspended in 1 mL of cryoprotectant freezing solution, which was added slowly with gentle agitation (refer to **'2.2 Cryopreservation solution'**).

Immediately, the cell suspension was transferred into 1.5 mL Cryo-vials (ThermoFisher Scientific, USA) and placed in a pre-chilled Mr. Frosty freezing container (ThermoFisher Scientific, USA). The container was then cooled overnight at a rate of -1°C per minute in a

-80°C ultracool freezer. Following that, the ampoules were transferred to long-term storage in liquid nitrogen (-196°C) and retrieved as needed.

2.7.3. Cell washout protocol for TKI resistant cells

Cells resistant to TKI (tyrosine kinase inhibitor) were cultured with TKI and then collected by centrifugation at 1,400 rpm for 5 minutes in a 50 mL centrifuge tube. The liquid portion was subsequently discarded, and the cells were suspended again in preheated (37°C) media that did not contain TKI. This process was repeated twice to ensure complete removal of the drug.

For thorough elimination of the TKI, the TKI-resistant cells were placed in a humidified incubator at 37°C, without the presence of TKI, and incubated overnight. This approach aimed to minimize the impact of different TKIs, as their effective washout times might vary. The next day, approximately 12 hours later, the cells were centrifuged at 1,400 rpm for 5 minutes in a 50 mL centrifuge tube, and once again resuspended in preheated (37°C) media without TKI, ready to be used in the experiment.

It's worth highlighting that the SUP-B15 cells, which have developed resistance to imatinib, require a constant presence of 5 μM imatinib in their growth medium to support long-term proliferation. Interestingly, during the initial 84 hours following the removal of imatinib (comprising a 12-hour washout period followed by a subsequent 72-hour assay period), no discernible impact on their viability was observed.

2.8. Annexin-V-PE/ Fixable Viability Stain 780 Assay

2.8.1. Drug treatment of cells for Annexin-V-PE/Fixable Viability Stain 780 cell-death assay

The analysis of cell viability and density was performed using Trypan blue exclusion. Afterwards, the cell density was adjusted to a final concentration of 5 x 10^4 cells/mL for BaF3 cells or 5 x 10^5 cells/mL for SUP-B15 cells. Various concentrations of TKI stocks were freshly prepared through serial dilutions using appropriate solvents. For TKIs that required DMSO as a solvent, the stocks were prepared in a way that ensured the final concentration of DMSO did not exceed 0.1% in the cell culture. Depending on the specific experimental design, cells were exposed to different concentrations of TKI (in 1 mL media) in technical duplicates within a 24-well plate. Subsequently, the cell culture plates were incubated at 37°C in a humidified chamber with 5% CO_2 for a period of 72 hours before cell harvesting for subsequent analysis of cell death.

2.8.2. Annexin-V-PE/ Fixable Viability Stain 780 staining protocol

After a 72-hour drug exposure, the cell culture was mixed by pipetting up and down. Then, 250 µL of the cell culture was transferred to a 96-well U-bottom plate. The cells were pelleted, and the media was removed by centrifugation at 1400 rpm for 5 minutes at room temperature (RT). Subsequently, the cells were washed with 200 µL of 1x PBS, and the PBS was removed by centrifugation at 1400 rpm for 5 minutes. The washed cells were then incubated in 20 µL of Fixable Viability Stain 780 (diluted 1:1000 with 1x PBS) for 10 minutes at RT in the dark. After incubation, the Fixable Viability Stain 780 was washed with 200 µL of 1x PBS, and the PBS was removed by centrifugation at 1400 rpm for 5 minutes. The cells were further incubated in 20 µL of Annexin-V-PE stain (diluted 1:50 with 1x binding buffer) for 20 minutes on ice, in the dark. Finally, 1x binding buffer (HBSS + 1% HEPES + 5 mM $CaCl_2$) was added to each well.

To establish reference parameters for forward and side-scatter measurements, control samples were employed. These samples comprised unstained cells, cells stained solely with Fixable Viability Stain 780, and cells stained exclusively with Annexin-V-PE Stain. In addition, baseline fluorescence intensity gates were established by utilizing the fluorescence characteristics of Fixable Viability Stain 780 (maximum excitation at 759 nm and maximum emission at 780 nm) and Annexin-V-PE (maximum excitation at 496 nm and maximum emission at 578 nm). The dual-stained samples were acquired using the FACS Canto II-Flow Cytometer with applied compensation, and the data was exported as FCS files. Batch analysis of the data was performed using FlowJo® software (FlowJo, LLC, USA).

2.9. Phospho-flow Assay

2.9.1. Drug treatment of cells for Phospho-flow assay

After overnight incubation of TKI-resistant cells in TKI-free media (as described in section '2.7.3 - Cell Washout protocol for TKI-resistant cells'), the cells were adjusted to a final concentration of 1 x 10^6 cells/mL using viability/density analysis through Trypan blue exclusion. Subsequently, the cells were resuspended in warm IMDM/1%BSA media and allowed to rest in a 37°C humidified incubator (5% CO_2) for 1 hour before the addition of drugs. Freshly prepared TKI stocks at different concentrations were obtained through serial dilutions using appropriate solvents. The cells were treated with TKIs, specifically 5 μM imatinib, in 6 mL of IMDM/1%BSA for 4 hours at 37°C in a humidified incubator (5% CO_2).

2.9.2. Preparation of TKI treated cells for Phospho-flow assay

The cells treated with the drug were fixed with 100 µL of 16% paraformaldehyde (PFA) per mL of cell suspension and incubated at 37°C in a humidified incubator (5% CO_2). Afterward, the cells were centrifuged at 1400 rpm for 5 minutes and washed with 1x PBS at room temperature. The pellet was then resuspended in ice-cold 80% methanol, added dropwise while gently vortexing the sample at 600 rpm to facilitate cell permeabilization. The cells were stored at -20°C overnight, and antibody staining was conducted the following day.

The fixed and permeabilized cells were pelleted and resuspended in (50 µL) 1x phospho-flow buffer (1x PBS + 1% BSA). Antibodies were prepared in the phospho-flow buffer as outlined in Table 2.7. The respective antibodies (50 µL) were added to the corresponding samples and incubated for 1 hour at room temperature in the dark. Subsequently, the cells were washed with 1 mL of 1x PBS, pelleted, and resuspended in 150 µL of ice-cold 1x PBS before analysis on the FACS Canto II-Flow Cytometer.

Table 2.5- Quantity of Antibodies for Phospho-flow Staining

Antibody	**Clone**	**Company**	**Cat #**	**Vol./ test**	**Iso-type**
IgG1-PE isotype control		BD Pharmingen	555749	2ul	
pY694 STAT5-PE	47	BD Phosflow	612567	20ul	IgG1
pT202/pY204 ERK1/2-PE	20A	BD Phosflow	612566	20ul	IgG1
pS473 Akt-PE		BD Phosflow	561671	5ul	IgG1

2.9.3. Phospho-flow assay for ABCG2 transporter protein

The naïve and imatinib (5 μM) resistant SUP-B15 cells were adjusted to a final concentration of 1 x 10^6 cells/mL using viability/density analysis by Trypan blue exclusion. The cells were washed three times with 1 x PBS, pelleted, and resuspended in 1 x phospho-flow buffer (1x PBS+1% BSA). Antibodies against ABCG2 and isotype control IgG2b were prepared in phospho-flow buffer according to the table 2.8 below. The antibodies were added (50 μL) to the respective samples and incubated for 1 hour at RT in the dark. Cells were then washed with 1 mL of 1 x PBS, pelleted, and resuspended in 150 μL of ice-cold 1 x PBS before analysing on FACS Canto II- Flow Cytometer.

Table 2.6 Quantity of Antibodies for Phospho-flow Staining

Antibody	Clone	Company	Cat#	Vol./100 μL	Isotype
IgG2b-PE isotype control	-	Dako Denmark	X0951	5 μL of 100 μg/mL stock	IgG2b, κ
PE anti-human CD338 (ABCG2) Antibody	5D3	BD Phosflow	#332007	5 μL of 100 μg/mL stock	IgG2b, κ

2.10. Gel Electrophoresis of Cellular Proteins

2.10.1. Drug treatment of cells

After allowing TKI resistant cells to incubate overnight in a TKI-free medium, the viability and density of the cells were assessed using Trypan blue exclusion, following the '2.7.3 Cell Washout protocol for TKI resistant cells'. The cell density was subsequently adjusted to achieve a final concentration of 1.2 x 10^5 cells/mL for BaF3 cells or 1.5 x 10^5 cells/mL

for SUP-B15 cells. To prepare the treatment drug stocks, various concentrations were freshly made through serial dilutions using appropriate solvents. In the case of drugs that required DMSO as a solvent, the stocks were prepared to ensure that the final concentration of DMSO did not exceed 0.1% in the cell culture. The cells were then exposed to the drugs in 15 mL tubes for a duration of 4 hours at 37°C in a humidified incubator with a 5% CO_2 atmosphere.

2.10.2. Preparation of protein lysates

TKI resistance cells were incubated in TKI-free media overnight as required depending on the downstream experiment. The cells were washed in iced-cold 1 x PBS, pelleted by centrifuging at 6800 rpm for 5 min at 4 ^{o}C then 6 x 10^5 BaF3 cells or 7.5 x 10^5 SUP-B15 cells were resuspended in 30 µL freshly made ice-cold NP40 lysis buffer (Refer to '**2.4.5. NP-40 Lysis Buffer Reagents'**). The lysates were then incubated on ice for 10 minutes and centrifuged at 13000 rpm for 10 minutes to remove cell debris. Five microlitres of supernatant was kept aside for protein quantitation assay. The rest of the supernatant was mixed with 4 x Laemmli's loading buffer (final 1 x) before denaturing at 100 ^{o}C for 5 minutes then stored at -20^{o}C.

2.10.3. Protein quantitation assay

Protein concentration of each lysate was estimated by using Bio-Rad DC assay kit using manufacturer's recommended procedure. Briefly, 1:3 dilutions of each lysate (5 µL) were made in water (15 µL). Protein standards were prepared by using serial dilutions (0, 0.2, 0.4, 0.8, 1.2, 1.6 and 2 µg/µL) of 2 µg/µL BSA as per the standard curve chart below.

Standard Curve Chart

Std curve (µg/µL)	**0**	**0.2**	**0.4**	**0.8**	**1.2**	**1.6**	**2.0**
H_2O (µL)	12	10.8	9.6	7.2	4.8	2.4	0
2 µg/µL BSA (µL)	0	1.2	2.4	4.8	7.2	9.6	12

The measurements and examples (5 µL each) were divided equally into a 96-well plate for duplication. To create Reagent A', Reagent S was combined with Reagent A at a ratio of 20 µL per mL. Each well received 25 µL of Reagent A' and 200 µL of Reagent B, followed by gentle mixing. The samples were then incubated in darkness at room temperature for 15 minutes, and their absorbance was measured at a wavelength of 595 nm using the PerkinElmer 2030 multilabel Reader.

To establish a standard curve, the optical density readings (y) were plotted against the concentration of BSA (x) in µg/µL. The curve was generated using the formula (y = mx + c), where m represents the gradient obtained from the formula, and c is a constant term. The aim was to achieve an R2 value as close to 1 as possible. Based on this standard curve, the protein concentration in the samples was estimated using the formula.

2.10.4. SDS-PAGE protein electrophoresis

Following the Bio-Rad Criterion precast gel system instructions, 4-15% Criterion™ TGX stain-free gel was set up in the Criterion gel tank with sufficient 1x SDS-PAGE Running Buffer. The first lane of the gel received a 5-µl volume of Bio-Rad® Kaleidoscope protein ladder. For the remaining lanes, the lysates containing 40 µg of protein each were thawed on ice, heated to 100°C for 3 minutes, pulse centrifuged, and then pipetted into their respective wells. An electrical current of 100V was applied for 20 minutes to initially

stack the proteins. The voltage was then increased to 200V and allowed to run until the green marker (37 kDa) was approximately 1.5 cm from the end. This separation process was carried out for IC50 assays, taking around 60-65 minutes, and for non-IC50 Western, taking approximately 30-35 minutes. This setup allowed for the separation of CRKL and p-CRKL proteins.

2.10.5. Western blotting of proteins

The resolved proteins were transferred onto a midi LF-PVDF membrane from the Bio-Rad RTA TransBlot Turbo Transfer kit using SDS-PAGE electrophoresis. The transfer assembly was prepared according to the instructions of the Bio-Rad TransBlot™ Turbo® System. The PVDF membrane was pre-wetted in 100% methanol and then soaked in 1x TransBlot Turbo Transfer Buffer in a Bio-Rad tray. Two transfer pads from the RTA kit were also soaked in 1x TransBlot Turbo Transfer Buffer in a separate Bio-Rad tray. The gel, PVDF membrane, and transfer pads were assembled by placing one soaked pad on the cassette, followed by the PVDF membrane, and then another soaked pad on top, creating a complete sandwich. The gel was removed from the criterion gel cassette and placed onto the PVDF membrane. The assembly was transferred using the Trans-Blot® Turbo™ semi-dry western apparatus with the settings: 1.3 A / 25 V for 7 minutes. The efficacy of protein transfer was assessed by Ponceau S staining. Depending on the size of the proteins of interest, the membrane was cut into separate fragments to allow simultaneous incubation with multiple antibody solutions. The membrane was dried for 1 hour, re-wetted in 100% methanol, and then incubated in Li-Cor (Millennium) Intercept-Odyssey Blocking Buffer (OBB) on a rocking platform (Ratek Instruments Pty Ltd., Australia) with gentle agitation for 1 hour at room temperature. Subsequently, the membranes were incubated overnight at 4°C with gentle shaking in primary antibody

solutions prepared in OBB buffer, following the manufacturer's recommended concentration (refer to **Table 2.2 - List of Western blotting antibodies**). The membranes were washed four times with 1x TBST for 5 minutes each. Respective secondary antibodies were added to the membranes and incubated for 2 hours at room temperature with shaking. The blots were then washed three times with 1x TBST and three times with 1x TBS before being analysed on the Odyssey® DLx Imaging System. The anti-pAbl (Y245) antibody was detected by using a goat-anti-rabbit-IgG-HRP-conjugated secondary antibody and scanning on the ChemiDoc imaging system (Bio-Rad, California, USA).

2.10.6. PVDF membranes stripping for re-probing other proteins

The recycling stripping buffer for Western blot (10x concentration) was mixed with Milli-Q water at a 1:10 dilution. The PVDF membranes were then immersed in the diluted stripping buffer and gently agitated for 15 minutes at room temperature. This process was repeated as necessary until the desired level of stripping was attained. The blots were washed with 1 x PBS then blocked by incubating in RT OBB blocking buffer for 30 minutes. The membranes were re-proved with new antibodies by incubating in new antibody solutions at 4^{o}C overnight. The membrane was processed and analysed as described in **2.10.5. Western blotting of proteins**.

2.10.7. Densitometry analysis of proteins

The data collected from Odyssey® DLx Imaging System were analysed in Image Studio Lite (Millennium Science). Each band was analysed for the intensity of their fluorescence and the corresponding background signals were subtracted for net signal. The intensities

of housekeeping proteins such as GAPDH, β-actin or β-tubulin were used to normalize any other proteins of interest. The phosphorylated proteins were further normalized to their total counterparts. The difference in protein expression or phosphorylation were presented in a graph either as the percentage of the negative control or as their normalized intensity measured.

2.11 BCR::ABL1 Analysis

2.11.1 IC50 Assay using CRKL as the surrogate for BCR::ABL1 Kinase activity

The data form western blot was analysed by using Image Studio Lite software. The gel was run long enough to allow enough separation between CRKL and pCRKL (size between 37-39 kDa) to detect both bands with CRKL antibody. Densitometry analysis of upper band pCRKL and lower band CRKL were used to calculate the percentage of pCRKL compared to total CRKL (pCRKL+ CRKL). A curve was generated by using the percentage of pCRKL in response to increasing concentration of TKIs, which is then normalized against the maximum and minimum test concentrations to calculate the TKI concentration required to reduce pCRKL by 50%, which is defined as IC50. IC50 value for TKI also represents the concentration required to inhibit BCR::ABL11 activation by 50%.

2.11.2 *BCR::ABL1* RQ-PCR

2.11.2.1 cDNA synthesis

The RNA was extracted from SUP-B15 cell pellets lysed in Trizol via the standard chloroform/isopropanol RNA extraction method (Refer to **2.13.1 RNA Extraction**). cDNA was synthesized from SUP-B15 cell-lines harbouring the p190 (e1a2) via the

SuperScript II RT-PCR method. Briefly, 1000 ng of RNA samples were added to 1 µL of Hexamer primers (250 ng/µL) and incubated at 70°C for 10 min followed by briefly chilling at 4°C. The samples were then mixed with 9 µL of Master mix for SuperScript II RT-PCR (Refer to **Table 2.7**) then incubated in thermocycler at 25°C for 10 min, 42°C for 50 min and 70°C for 10 minutes.

Table 2.7 Master mix for SuperScript II RT-PCR

Reagents	**Volume (µL)**
5 x First strand buffer	4
0.1 m DTT	2
5 mM dNTPs	2
Superscript	1

Controls: High and Low copy number controls were prepared simultaneously with the cDNA synthesis of samples of interest by using pDNAs of known concentrations (Refer to **2.11.2.2 Preparation of p190 working plasmid standards)**.

2.11.2.2 Preparation of p190 working plasmid standards

Plasmid standards (p190) were obtained from Haley Altamura, Leukaemia Research Unit, Molecular Pathology, SA Pathology, Frome Rd Adelaide. A dilution series of the plasmid was prepared using standard diluent (brought to room temperature).

The original Plasmid standards (p190) was diluted 1 in 100.

1. 10 µL plasmid + 990 µL standard diluent =10^8

2. 200 µL of 1. + 1800 µL standard diluent =10^7

3. 200 µL of 2. + 1800 µL standard diluent =10^6

4. 200 µL of 3. + 1800 µL of standard diluent = 10^5

5. 200 µL of 4. + 1800 µL of standard diluent = 10^4

6. 200 µL of 5. + 1800 µL of standard diluent = 10^3

7. 200 µL of 6. + 1800 µL of standard diluent = 10^2

8. 200 µL of 7. + 1800 µL of standard diluent = 10

Each 2 mL standard was dispensed into 200 µl aliquots for storage of a stock solution. A 200 µl aliquot was further dispensed into 20 µl aliquots for routine use. All standard aliquots were stored at -80ºC.

2.11.2.3 Preparation of BCR working standards

Using 7 x 10^7 aliquots, tubes were mixed and pooled to final volume of 420 µL and the dilutions were prepared as follows:

Add 400 µL of 10^7 standard to 3600 µL of standard diluent = 10^6 standard

Add 400 µL of 10^6 standard to 3600 µL of standard diluent = 10^5 standard

Add 400 µL of 10^5 standard to 3600 µL of standard diluent = 10^4 standard

Add 400 µL of 10^4 standard to 3600 µL of standard diluent = 10^3 standard

2.11.2.4 Primers and Probes for QR-PCR of BCR::ABL11 mRNA

The following primers and probes were used for QR-PCR of BCR::ABL11 mRNA

Primers:

BCR_F B8 5’ CCT TCG ACG TCA ATA ACA AGG AT 3’

BCR_R B9 5’ CCT GCG ATG GCG TTC AC 3’

p190 Forward: 5’ CGA GGG CGC CTT CCA T 3’

p190 Reverse: 5’ CTG AGG CTC AAA GTC AGA TGC TAC T 3’

Probes:

p190 = 5'-(6-Fam)-ACG CAG GAA CCC TTC AGC GGC (Tamra)-3'

BCR = 5'-6FAM-TCC ATC TCG CTC ATC ATC ACC GAC A 3'

2.11.2.5 Experimental procedure of RQ-PCR

The QR-PCR reaction conditions for each transcript were run in the same 96 well reaction. The BCR control gene was run for every cDNA sample. Each sample and control were amplified in duplicate, each PCR was performed three times for n=3. The master mix was prepared as follows based on template set-up prepared in Microsoft excel spreadsheet.

Table 2.8 Reagents for RQ-PCR master mix

Reagents	Final Concentration
DEPC or NF H_2O	to 22.5 µL
Universal Master Mix (4°C)	1x 12.5 µL
Forward Primer	0.4 µM
Reverse Primer	0.4 µM
TaqMan Probe	0.25 µM

The 96 well plate containing sample solution was run and read on QuantStudio 7 (ThermoFisher Scientific) using experimental properties as Fast 96 well, Standard Curve (relative), TaqMan Reagents and Standard for standard master mix. The samples, controls and standards were run on thermal cycler conditions 50°C for 2 minutes, 95°C for 10 minutes 43 cycles of 95°C for 15 seconds and 56°C for 1 minute. The data was analysed and exported into Excel and BCR::ABL1% Q-PCR was calculated in Excel.

2.11.3 Kinase Domain Mutations Analysis

The long PCR primers designed to isolate the BCR::ABL1 allele Long_p190_BCR_F: CTCGCAACAGTCCTTCGACA and Long_p190_ABL1_R: CCTGCAGCAAGGTACTCACA were used as previously described [1]. The master mix for PCR reaction was prepared as follows.

Table 2.9 Reagents for master mix for long PCR

Component	Volume for 1 Sample (μL)	Final Concentration
25mM dNTP	0.375	0.75mM
MB grade H_2O	5.16	-
Forward Primer* (50uM)	0.075	0.3μM
Reverse Primer* (50uM)	0.075	0.3μM
10xBuffer 3**	1.25	1x
25mM $MgCl_2$	0.375	3.5mM
MB grade H_2O	4 or 3.5 μl	-
Expand Enzyme Mix	0.188	2.5U

The samples were then run on the thermal cycler under following conditions.

94°C 2min

94°C 10sec, 60°C 30sec, 68°C 2min: 10 cycles

94°C 10sec, 60°C 30sec, 68°C 2min – increase by 20sec every cycle: 30 cycles

68°C 7min

12°C ∞

The PCR products (3.5 µL each) were run on 1 % agarose gel to visualize the size and amount of DNA. The PCR products were purified by using ExoSAP-IT protocol.

2.11.3.1 PCR product purification using ExoSAP-IT

Ratio of 5 µL of a post PCR product with 2 µL of ExoSAP-IT were mixed for a combined 7 µL reaction volume. The samples were run on thermocycler with the following steps.

37°C for 15 minutes to degrade remaining primers and nucleotides.

80°C for 15 minutes to inactivate ExoSAP-IT.

Hold at 4°C.

The PCR product was diluted 1:10 before using it in sequencing reaction.

2.11.3.2 Sanger Sequencing reaction

The purified PCR products were sequenced by using BigDye Terminator v3.1 Cycle Sequencing Kit (ThermoFisher Scientific) following manufacturer's instructions. Briefly, clean PCR DNA samples were mixed with BigDye XTerminator reaction mix as follows.

Table 2.10 Master mix for BigDye XTerminator Sequencing reaction

Reagents	Volume (µL) for 1 sample
H2O	13.175
Bid Dye Seq Buffer	3.5
Sequencing Primers	0.325
Big Dye Terminator reaction mix	1

Following sequencing primers were used for sequencing ABL1 kinase domain of BCR::ABL1.

E4 F: 5' GCCGAGTTGGTTCATCATCATTCAAC 3'

E5 F: 5' AGAAGCTGCAGTCATGAAAGAGATCA 3'

E6 F: 5' GGTGCTGCTGTACATGGCC 3'

E10 R: 5' AGGCACGTCAGTGGTGTCTCT 3'

E11 R: 5' CAATGGAGACACGGCAGGCT 3'

Separate master mixes were prepared for each sequencing primers. Two micro litres (20-40 ng) of PCR DNA sample were added to the master mix and run-on thermocycler under following conditions at ramp up rate of 1°C/second.

96°C	1 min	
96°C	10 sec	25 Cycles
50°C	5 sec	
60°C	4 min	
4°C	Infinite hold	

The samples were then purified by sequencing reactions with BigDye XTerminator before using them on capillary electrophoresis.

2.11.3.3 Purification of sequencing reactions with BigDye XTerminator

BigDye XTerminator beads (20 µL each) were used in purification process by vortexing them for 8-10 seconds before mixing with the SAM solution (90 µL). The SAM/BigDye XTerminator bead working solution (110 µL) was added to each sequencing samples then

vortexed at 1800 rpm for 30 minutes. The beads were pelleted by centrifuging the solution at 1000 x g for 2 minutes. The samples were then analysed on SeqStudio Genetic Analyzer (ThermoFisher Scientific). The data were further visualized and aligned with a reference ABL1 sequences on Benchling (Biology Software).

2.12 Real-Time PCR of Drug Transporters

Master mixes were prepared for individual gene using following reagents.

Table 2.11 Master mix for RT-PCR reaction

Reagent	**x 1 (µL)**	**x 48 + 5% (µL)**
SYBR Green	5	252
Primer Forward (10 µM)	0.8	40.3
Primer Reverse (10 µM)	0.8	40.3
Water	1.4	70.8
Total:	8	403.6

The following primers were used for RT-PCR reaction for ABCB1, ABCG2 and GUSB (Gene control).

ABCB1 F: 5’ AGA CAT GAC CAG GTA TGC CTA T 3’

ABCB1 R: 5’ AGC CTA TCT CCT GTC GCA TTA 3’

ABCG2 F: 5’ CAC CTT ATT GGC CTC AGG AA 3’

ABCG2 R: 5’ CCT GCT TGG AAG GCT CTA TG 3’

GUSB F: 5’ CTG AAC AGT CAC CGA CGA GA 3’

GUSB R: 5’ GAA CGC TGC ACT TTT TGG TT 3’

According to the PCR set-up sheet prepared in excel spreadsheet, 2 µL of unknown/cell line control (VBL100 and K562 were used for ABCB1 and ABCG2 respectively) cDNA samples and NF water for no template control were added to 8 µL of master mix. RQ-PCR was performed on the Bio-Rad® CFX Connect™ real-time PCR detection system under following conditions.

Cycle	**Cycle point**
Hold 1 @ 50℃, 2 min	
Hold 2 @ 95℃, 15 min	
Cycling (40 repeats)	Step 1 @ 95°C, hold 15 secs
	Step 2 @ 60°C, hold 26 secs
	Step 3 @ 72°C, hold 10 secs, Capture data

The data was examined using the Bio-Rad® CFX Manager™ software and then exported to Microsoft Excel. To determine the fold change of genes between sensitive and resistant samples, I employed the comparative Ct (2-ΔΔCt) method. Graphs were created, and statistical analysis was performed using GraphPad Prism.

2.13 Transcriptomic Sequencing (mRNA-seq)

2.13.1 RNA Extraction

For RNA extraction, 5 x 10^6 cells were pelleted by centrifugation at 1400 rpm for 5 minutes and washed with ice cold 1 x PBS then collected in 2 mL microcentrifuge tube. The cells were re-suspended in 1 mL TRIzol® solution, allowing it to make homogeneous solution by 5 minutes incubation at RT and stored in -80°C. Samples were thawed on ice before adding 200 µl of chloroform then tubes were vigorously shaken until homogenous

solution was achieved. These steps were done in a fume hood. The specimens were placed at room temperature (RT) for a duration of 2-3 minutes, after which they were subjected to centrifugation at a force of 1200 times the acceleration due to gravity (x g) for 15 minutes at a temperature of 4 degrees Celsius. The upper liquid phase, containing the desired substance, was carefully extracted without disturbing any intervening layers and transferred to pre-labelled 1.7 mL microcentrifuge tubes. To these tubes, 500 µL of isopropanol (analytical grade, 100%) and 1 µg of glycogen (molecular grade) were introduced. The tubes were vigorously shaken and then left at RT for 10 minutes. Subsequently, the samples were centrifuged at a force of 12,000 x g for 10 minutes at 4^{o}C. The resulting supernatants were discarded, and the solid residues (pellets) were rinsed with 1 mL of freshly prepared 75% ethanol. Once again, the samples were subjected to centrifugation, this time at a force of 7,500 x g for 5 minutes at 4^{o}C. After removing supernatant, pellets were briefly centrifuged to remove excess ethanol. The pellets were air dried before adding 30-50 µl NF-water and incubating at 55^{o}C for 10 min to rehydrate the RNA. The samples were immediately transferred on to ice and analysed for quality and quantity by Nanodrop™ 8000 spectrophotometer. The samples were used for cDNA synthesis/mRNA-seq or stored at -80°C for long-term storage.

2.13.2 RNA preparation for mRNA-seq

To conduct RNA-seq analysis, three sets of RNA were extracted from SUP-B15 parental and imatinib resistant cells. Each RNA sample was prepared at a concentration of 10 ng/µL in a 50 µL volume. The concentration of each sample was determined using the Qubit® RNA high-sensitivity assay kit (ThermoFisher Scientific, USA). However, the initial RNA concentrations were too high to be directly used with the Qubit® system. Therefore, each sample was diluted by a factor of 1:30 in HF-water, and then further diluted by a

factor of 1:200 in the Qubit® working solution. After briefly vortexing the diluted samples, they were incubated for 2 minutes at room temperature and subsequently analysed using the Qubit® 2.0 Fluorometer (ThermoFisher Scientific, USA). The RNA samples were sent to South Australian Genomic Centre (SAGC) at 10 ng/μL in 50 μL volume for further quality check, library preparation and RNA sequencing. Mutational analysis of sequencing results was courtesy of Jacqueline Rehn. The differential expression, hierarchical clustering, heatmap and volcano plots, pathway and network analysis were performed by SAGC's Standardised Analysis Pipelines.

2.13.3 RNAseq Analysis of SUP-B15 cells

RNA (500 ng) was prepared in 50 μl H2O for parental and imatinib-resistant SUP-B15 cells in biological triplicates. The conversion of total RNA to strand-specific Illumina-compatible sequencing libraries was performed using the Nugen Universal Plus Total RNA-Seq library kit from Tecan (Mannedorf, Switzerland), following the manufacturer's instructions (MO1485 v4). The final libraries underwent 12 cycles of PCR amplification. Sequencing of the library pool was carried out on the Illumina Nextseq 500 platform using a high output kit, generating 2x75 bp paired end reads.

To align the raw reads to the GRCh37 human reference genome, STAR-aligner v2.7.3a was employed in two-pass mode [2]. Raw gene counts were obtained from the resulting BAM files using featureCounts [3]. Variant calling was performed with GATK HaplotypeCaller v4.0.1.2, following the GATK best practice for RNA-seq variant discovery. The called variants were then annotated using Annovar [4]. For sequence variant calling, a minimum of 5 reads supporting the alternate allele and a variant allele frequency of > 0.1 were

required. Prioritized variants either had previous reports in COSMIC or had a population frequency < 0.1 (Exome Aggregation Consortium - Non-Finnish European).

Gene fusions were identified using a combination of SOAPfuse v1.26 [5], JAFFA v1.09 [6], and fusionCatcher (fusioncatcher.py 0.99.7c beta) [7]. Only fusions detected by multiple callers were considered as likely candidates. Gene fusions and sequence variants reported in the manuscript were detected in at least 2 biological replicates.

2.14 ShRNA Knockdown of *PTPN11* in SUP-B15 cells

shRNA lentiviral particles: control shRNA and SH-PTP2 shRNA (human) were purchased from Santa Cruz Biotechnology Inc. (Dallas, USA). Gene Silencers generally consist of pools of three to five target-specific 19-25 nucleotide sequences in length. Lentiviral transduction was performed in SUP-B15 cells following manufacturer's instructions. Briefly, 50 µl viral supernatant was added to 1x10^5 cells in 200 µL media with polybrene (8 µg/ml) in 24 wells plate. The plate was spun at 1800 RPM for 2 hours at 37°C and 500 µL fresh media was added to the reaction after the spin then incubated overnight. After 3 passages, the cells were examined under microscope for GFP positive cells. Stable shRNA expressing (GFP+) cells were selected via puromycin dihydrochloride selection (3 µg/ml). Western blot was used to confirm knockdown of *PTPN11* by measuring SHP-2 protein level.

2.15 Generation of BaF3 and BaF3 *BCR::ABL1* p190 cells with *PTPN11* mutations

2.15.1 PCR Amplification of wild type and mutated *PTPN11* genes

The wild type and mutated PTPN11 genes were PCR amplified from cDNA generated from mRNAs extracted from parental and resistant (to 5 µM imatinib) SUP-B15 cell line by

using forward primer PTPN11_PCR_F: 5' GAGGGCGGGAGGAACATGACATC 3' and reverse primer PTPN11_PCR_R: 5' GGGAGAGGGTGAAAGTCCACATC 3'.

Master mix was prepared without cDNA templates by using following reagents and kept on ice throughout the procedure.

Table 2.12 Reagents for PCR master mix

Component	**20 µL Reaction**	**3 X Samples (µL)**	**Final Concentration**
Nuclease-free water	11.8	35.4	
5 x Phusion HF or GC Buffer	4	12	1x
10 mM dNTPs	0.4	1.2	200 µM
10 µM PTPN11 PCR_F primer	1	3	0.5 µM
10 µM PTPN11 PCR_R primer	1	3	0.5 µM
DMSO	0.6	1.8	3%
Phusion HF DNA Polymerase	0.2	0.6	1 unit/ 50 µL PCR

About 250 ng of cDNA was added to the master mix in DNA/RNA free hood and transfer into thermocycler with the following conditions.

STEP	**TEMPERATURE**	**TIME**
Initial Denaturation	98°C	30 Seconds
35 Cycles	98°C	10 seconds
	68°C	30 Seconds
	72°C	1 Minutes

Final Extension	72°C	10 Minutes
Hold	4°C	Infinite

The PCR products were enzymatically cleaned by using ExoSAP-IT™ PCR Product Cleanup Reagent (ThermoFisher Scientific) to remove excess primers and unincorporated nucleotides (refer to **2.11.3.1 PCR product purification using ExoSAP-IT)**. The cleaned PCR products were analysed for purity by gel electrophoresis prior to using them in sequencing reaction.

2.15.2 Gel Electrophoresis of PCR product for purity check

One percentage agarose gel was prepared by using 1:100 gm/mL of agarose and 1 x TAE buffer respectively (Refer to **2.6.5. Agarose (1%) gel for DNA electrophoresis**). The agarose and TAE buffer mixture was microwaved until agarose is fully dissolved. GelRed™ nucleic acid stain was added to the dissolved gel before pouring into a gel holder with an appropriate comb and allowing it to set for 20 minutes. The gel was transferred into a tank and covered with 1 x TAE buffer. The gel was positioned in a way to make sure DNA runs from negative to positive terminal. The DNA samples (5 µL) were mixed with 6 x purple loading buffer (1.5 µL) before loading into the gel. Appropriate DNA ladder was used to estimate the size of each DNA fragment separated by electrophoresis according to their size. The gel was run at 100 V for 60 minutes and analysed by Molecular Imager® Gel Doc™ XR System (Bio-Rad).

2.15.3 Gel Purification of PCR product

The remaining PCR products were electrophoresed, and gel purified by using The QIAquick Gel Extraction Kit (QIAGEN, Germany) following manufacturer's recommendations. Briefly, gel was analysed under low UV settings and the correct size band was exercised by using a clean sharp scalpel. The gel fragment was dissolved in 3

volumes of Buffer QG to 1 volume of gel (i.e., 300 µL of Buffer QG for 100 mg of gel) by incubating at 50°C for 10 minutes or until the gel was fully dissolved. One gel volume of isopropanol was added and mixed to the sample. The sample was then added to a QIAquick spin column with 2 mL collection tube and centrifuged at 17,900 x g for 1 minute. The flow through was discarded and 500 µL of Buffer QG was added to QIAquick spin column and centrifuged at 17,900 x g for 1 minute. Flow through was discarded and 750 µL of Buffer PE (Ethanol added) to QIAquick spin column letting the column stand for 5 minutes before centrifuging at 17,900 x g for 1 minute and removing the flowthrough. The QIAquick spin column was transferred into a 1.5 mL microcentrifuge tube and the DNA was eluted by adding 30-50 µL Buffer EB (10 mM Tris·Cl, pH 8.5) centrifuging 17,900 x g for 2 minutes after allowing Buffer EB to stand in QIAquick spin column for 3-5 minutes. The purified DNA was further assessed for purity by gel electrophoresis (**2.15.2 Gel Electrophoresis of PCR product for purity check**).

2.15.4 Sanger Sequencing of Purified PCR products

The following primers were used to sequence PCR amplified wild type and mutated PTPN11 cDNA (refer to **2.11.3.2 Sanger Sequencing reaction)**.

1. PTP11 _PCR_F: 5' GAGGGCGGGAGGAACATGACATC 3'
2. PTPN11_E3_Seq_F: 5' GGAGCTGTCACCCACATCAAGA 3’
3. PTPN11_E4_Seq_R: 5' GTCCATGAAACCACCTTTCAGAGG 3’
4. PTPN11_E4_Seq_F: 5' GTACGAGAGAGCCAGAGCCAC 3’
5. PTPN11_E5_Seq_F: 5' CAGTACTACAACTCAAGCAGCCCC 3’
6. PPTN11_E8_Seq_F: 5' CCAGGGTTGTCCTACACGATGGTG 3’
7. PTPN11_E11_F: 5' GGCAATACCACTTTCGGACCTGGC 3’

8. PTPN11_E13_R: 5' GCTCTTCTTCAATCCTGCGCTGTAGTG 3’
9. PTP11 _PCR_R: 5' GGGAGAGGGTGAAAGTCCACATC 3’

2.15.5 Insertion of PCR products into pCR-Blunt II-TOPO vector

The purified wild type and mutated PTPN11 PCR products were inserted into pCR-Blunt II-TOPO (pTOPO) vector by using 4 µL of purified DNA, 1 µL of pTOPO vector and 1 mL of salt solution (Refer to **Figure 2.1**). A negative empty vector control was also used by replacing PCR product with water. The samples were incubated at 4°C overnight.

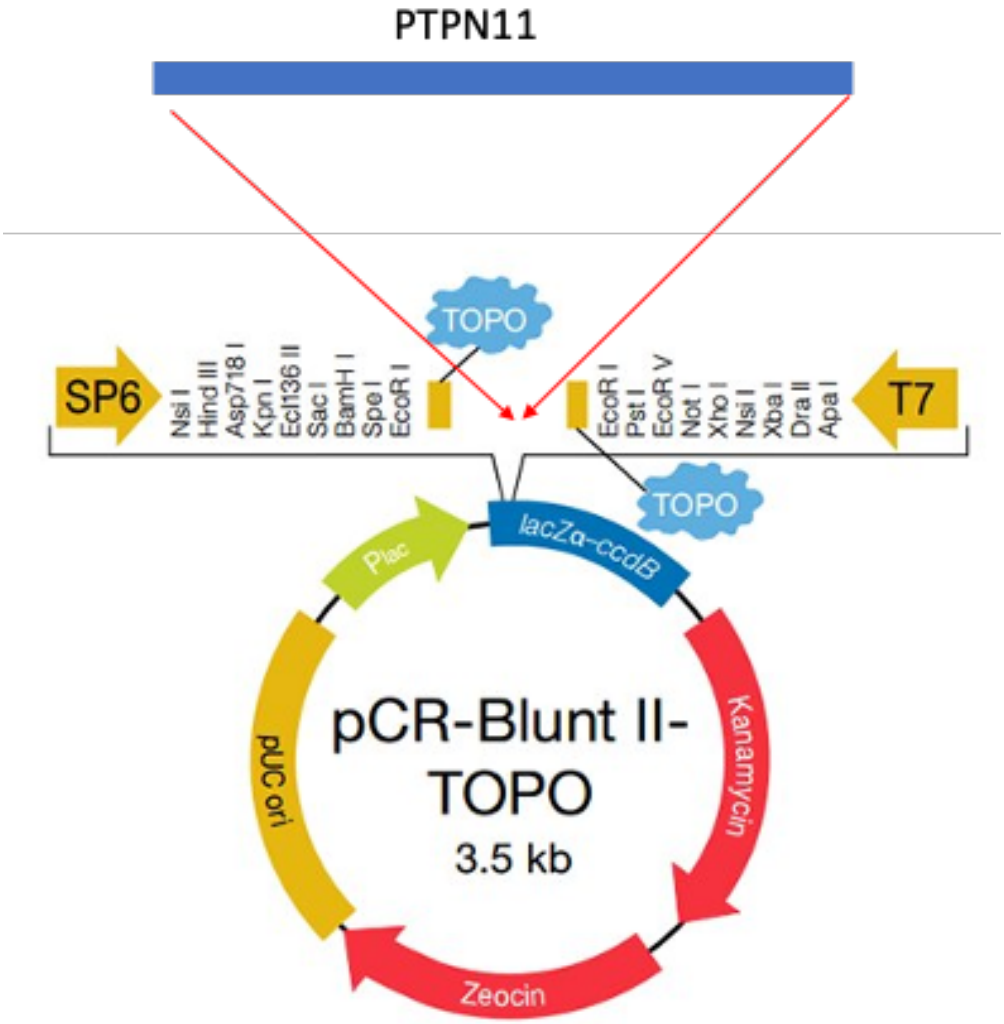

Figure 2.1 The pCR-Blunt II-TOPO (pTOPO) vector for blunt end PTPN11 PCR product ligation.

2.15.6 Transformation of pCR-Blunt II-TOPO (pTOPO) vector into 5DHα *E. coli*

The pTOPO vector containing *PTPN11* genes and empty vector control were transformed into NEB® 5-alpha Competent *E. coli* (High Efficiency) containing kanamycin antibiotic selection. This was done by adding 5-10 µL of pTOPO ligation reaction mix with 50 µL of 5DHα *E. coli* then incubating on ice for 30 minutes, applying heat shock at 42°C for 2 minutes, incubating on ice for another 5 minutes before adding 450 µL of RT SOC media (ThermoFisher Scientific). The culture was incubated shaking at 37°C for 1 hour and centrifuged at 400 x g for 5 minutes. The *E. coli* was resuspended into 50 µL SOC media and spread into warm kanamycin agar plates at 37°C overnight. Next day number of colonies were counted on each plate and 6-10 colonies were screened for insertion using miniprep kits (QIAGEN, Germany). The selected colonies were further grown in 2 mL LB Broth containing 10 mg/mL kanamycin overnight shaking at 37°C overnight. The plasmid DNA was extracted from each colony by using miniprep protocol.

2.15.7 Miniprep protocol for plasmid DNA extraction and screening from *E. coli*

The plasmid DNA from selected colonies were extracted and purified by using QIAprep® Spin Miniprep Kit (QIAGEN, Germany) following manufacturer's instructions. Briefly, 1.5 mL bacterial overnight culture was pelleted by centrifugation at 6800 x g for 3 minutes at RT and resuspended in 250 µL of Buffer P1 (50 µg/mL RNase added). The bacterial suspension was lysed by adding 250 µL Buffer P2 (Lysis Buffer) and inverting the tube 4-6 times. The lysate was neutralized by adding 350 µL Buffer N3 and mixing by inversion 4-6 times. The sample was then centrifuged at 17900 x g for 10 minutes. The supernatant

was transferred into the QIAprep 2.0 spin column by adding 800 µL each time, centrifuging at 17900 x g for 30 seconds and discarding flowthrough until all finished. The QIAprep 2.0 spin column was washed with 500 µL of Buffer PB then with 750 µL of Buffer PE. The QIAprep 2.0 spin column was centrifuged 17900 x g for 1 minute to remove washing buffers then transferred into a clean 1.7 mL microcentrifuge tube. To elude plasmid DNA, 30-50 µL of Buffer EB (10 mM TrisCl, pH 8.5) was added to the QIAprep 2.0 spin column. After allowing QIAprep 2.0 spin column to stand for 3-5 minutes in Buffer EB, pDNA was eluted by centrifuging at 17900 x g for 2 minutes.

Restriction digestion reaction was performed on extracted pDNA by incubating 7.5 µL of MQ water, 1 µL of cutsmart buffer (10 x), 0.5 µL restriction enzyme (EcoRI) and 1 µL pDNA at 37°C for 2 hours.

The restriction digestion products were analysed by gel electrophoresis (Refer to **2.15.2 Gel Electrophoresis of PCR product for purity check**) to screen for the presence of insert into pTOPO vector. Once the presence of right size insert was confirmed, the insert in the pDNA was then sequenced by using M13 forward (M13 F: 5' GTAAAACGACGGCCAG 3') and reverse (M13 R: 5' CAGGAAACAGCTATGAC 3') primers for further confirmation of the insert (Refer to **2.11.3.2 Sanger Sequencing reaction**) and using the primers listed above for *PTPN11* gene (Refer to **2.15.4 Sanger Sequencing of Purified PCR products**) for confirming the right sequences. Streak plates were created by spreading selected bacteria colony (containing right insert) onto a kanamycin agar plate following the aseptic techniques to allow selection of a single colony after incubating at 37°C overnight.

2.15.8 Miraprep protocol for plasmid DNA extraction from *E. coli*

Single *E. coli* bacteria colony from streak plate containing pDNA with correct insert was further expanded and pDNA was extracted by using previously described Miraprep protocol [8]. Briefly, 50 mL bacterial culture was incubated in kanamycin selection media shaking at 37°C overnight. The next day the culture was centrifuged at 4000 x g at 4°C for 10 minutes. The supernatant was discarded, and the pellet was resuspended into 2 mL Buffer P1 (50 µg/mL RNase added). The bacterial suspension was lysed by adding 2 mL Buffer P2 (Lysis Buffer) and inverting the tube 4-6 times. The lysate was neutralized by adding 2 mL Buffer N3 and mixing by inversion 4-6 times. The bacterial lysates were transferred into 4 x 1.7 mL centrifuge tubes by pouring then centrifuged at 17900 x g for 10 minutes. The supernatants were pooled into a 15 mL tube and mixed with same volume (~5 mL) of 96% ethanol. The solution was mixed thoroughly for 5 seconds then transferred into 5 x QIAprep 2.0 spin column by adding 700 µL in three sequential aliquots by centrifuging at 17900 x g for 30 seconds and discarding flowthrough until all finished. The QIAprep 2.0 spin column was washed with 500 µL of Buffer PB then with 750 µL of Buffer PE. The QIAprep 2.0 spin column was centrifuged 17900 x g for 1 minute to remove washing buffers then transferred into a clean 1.7 mL microcentrifuge tube. To elude plasmid DNA, 50 µL of Buffer EB (10 mM TrisCl, pH 8.5) was added to each QIAprep 2.0 spin column. After allowing QIAprep 2.0 spin column to stand for 3-5 minutes in Buffer EB, pDNA was eluted by centrifuging at 17900 x g for 2 minutes. The eluted pDNA from all 5 columns was pooled into one tube and DNA concentration was measured by NanoDrop™ 2000/2000c Spectrophotometer (ThermoFisher Scientific). The product was further confirmed by sanger sequencing before using it in downstream experiments.

2.15.9 Site Directed mutagenesis of *PTPN11* mutations

The Q5® High-Fidelity DNA Polymerase protocol (New England Biolabs) was used to generate site specific mutations on double stranded plasmid DNA. The pTOPO vector containing PTPN11 wild type insert was used to generate p.A461T (G1381A) and p.P491H (C1472A) mutations using the following primers designed from NEBaseChanger™ tool (New England Biolabs).

PTPN11 _A461T_F: GCACTGCAGTACTGGAATTGGCCGG

PTPN11 _A461T_R: ACCACGACCGGCCCTGCA

PTPN11 _P491H_F: ATTGACGTTCACAAAACCATC

PTPN11 _P491H_R: ATCGCAGTCAACACCTTTC

The master mix for PCR amplification of mutagenesis product was prepared by using following reagents.

Table 2.13 Master mix reagents for site directed mutagenesis reaction

Component	**25 µL Reaction**	**Final Concentration**
5X Q5 Reaction Buffer	5 µL	1X
10 mM dNTPs	0.5 µL	200 µM
10 µM Forward Primer	1.25 µL	0.5 µM
10 µM Reverse Primer	1.25 µL	0.5 µM
Q5 High-Fidelity DNA Polymerase	0.25 µL	0.02 U/µL
5X Q5 High GC Enhancer (optional)	(5 µL)	(1X)
Nuclease-Free Water	to 25 µL	

Plasmid DNA (pTOPO) containing wild type *PTPN11* gene was added to each reaction and the reaction was proceeded on thermocycler under the following conditions.

TEP	**TEMP**	**TIME**
Initial Denaturation	98°C	30 seconds
25–35 Cycles	98°C *50–72°C 72°C	5–10 seconds 10–30 seconds 20–30 seconds/kb
Final Extension	72°C	2 minutes
Hold	4°C	

The amplified site directed mutagenesis product was gel purified (Refer to **2.15.3 Gel Purification of PCR product**). The purified DNA product was then treated with the following KLD reagents and incubated at RT for 5 minutes.

Table 2.14 Reagents for KLD treatment reaction

Reagents	**VOLUME (µL)**
PCR Product	1
2X KLD Reaction Buffer	5
10X KLD Enzyme Mix	1
Nuclease-free Water	3

Following KLD treatment the pDNA was transformed into chemically competent *E. Coli* (Refer to **2.15.6 Transformation of pCR-Blunt II-TOPO (pTOPO) vector into 5DHα *E. coli***) and screened colonies for right product following procedure described in **2.15.7**

Miniprep protocol for plasmid DNA extraction and screening from *E. coli* and **2.15.8 Miraprep protocol for plasmid DNA extraction from *E. coli.***

2.15.10. Long-term storage of transformed bacterial cells

Once bacterial culture was confirmed of having plasmid DNA with desired correct insert, 250 µL of confluent cell culture was mixed with 250 µL of 80% glycerol for final volume of 500 µL in to 2 mL screw-capped vials and stored at -80°C.

2.15.11. Molecular cloning of *PTPN11* gene

PTPN11 gene in pTOPO construct needed to be sub-cloned into a mammalian compatible lentiviral vector to allow efficient expression of this gene in mammalian cells. The wild type and mutated PTPN11 cDNAs were sub-cloned into pLVX-EF1α-IRES-ZsGreen1, a mammalian expressing lentiviral vector courtesy of Associate Professor Daniel Thomas. Wild type PTPN11 and PTPN11 cDNA insert with p.A461T, p.P491H and both (p.A461T and p.P491H) mutations were removed from pTOPO by EcoRI restriction digestion enzyme and ligated into pLVX-EF1α-IRES-ZsGreen1 recipient vector, which was also digested with EcoRI restriction enzyme to create steaky ends. The ligation reaction was performed by using T4 DNA ligase (New England Biolabs). The orientation of insert into pLVX-EF1α-IRES-ZsGreen1 was confirmed by using IRES reverse primer (5' ACACCGGCCTTATTCCAAG 3').

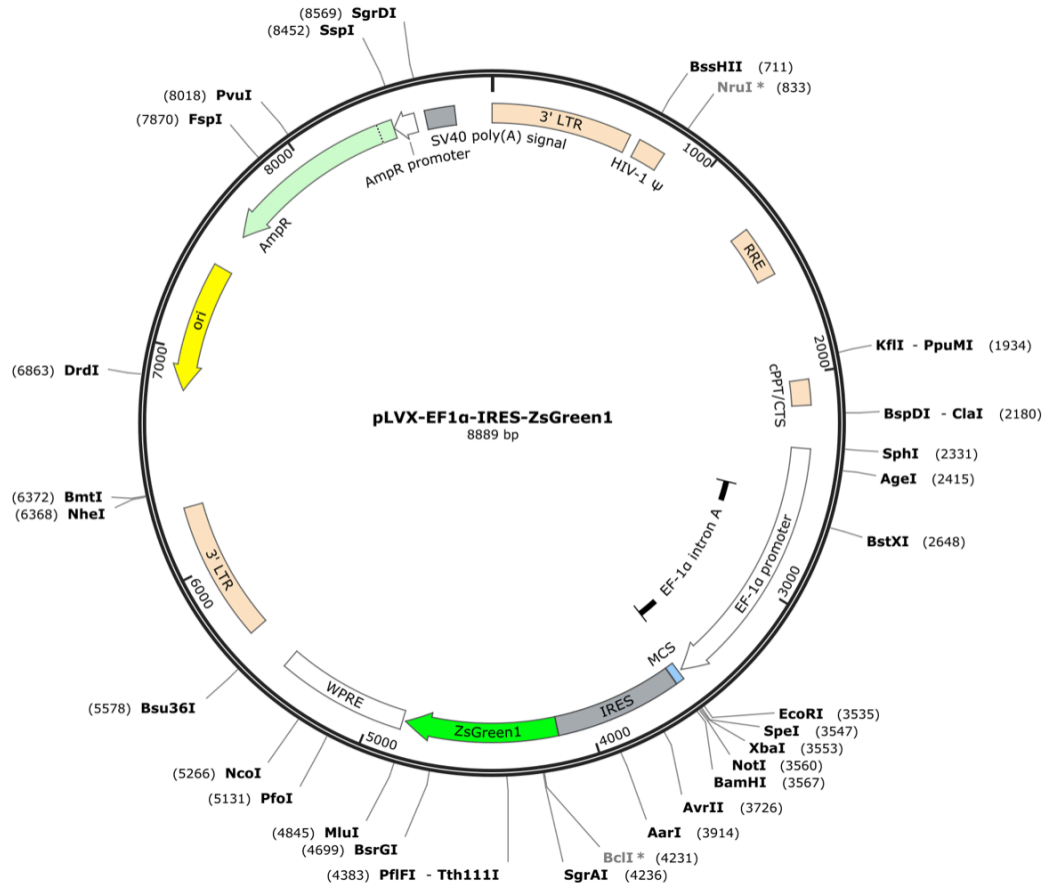

Figure 2.2 pLVX-EF1α-IRES-ZsGreen1 Mammalian expression (Recipient) vector

The restriction digestion reaction was done for both recipient pLVX-EF1α-IRES-ZsGreen1 vector and donor pTOPO vector with PTPN11 inserts using following reagents.

15 µL H2O

2 µL pDNA (>2 µg)

2 µL cutsmart buffer

1 µL EcoRI-HF enzyme (Restriction enzyme)

The solution was incubated at 37°C for 1 hour. The recipient vector pLVX-EF1α-IRES-ZsGreen1 was dephosphorylated at its 5' end by adding Shrimp Alkaline Phosphatase (rSAP) into restriction digest reaction at 30 minutes time and allowing it to proceed for

30 minutes. The rSAP enzyme was heat inactivated by incubating at 65°C for 5 minutes at the completion of restriction digestion reaction. The EcoRI restriction digest products pLVX-EF1α-IRES-ZsGreen1 vector and PTPN11 inserts were gel purified (Refer to **2.15.3 Gel Purification of PCR product**) and quantitated by using NanoDrop™ 2000/2000c Spectrophotometer.

The PTPN11 cDNA with p.E76K mutation was purchased from Integrated DNA Technologies Pte. Ltd. (Coralville, USA) as a gBlocks Gene Fragments 1751-2000 bp. The DNA fragment was directly ligated into pLVX-EF1α-IRES-ZsGreen1 vector by using restriction enzyme and T4 DNA ligase. The ligation reaction between recipient vector pLVX-EF1α-IRES-ZsGreen1 and PTPN11 inserts was carried out using reagents listed in Table 2.17. NEBioCalcularor (NEB Biolegends) tool was used to calculate molar ratios of vector and insert.

Table 2.15 Reagents for DNA ligation reaction

COMPONENT	***20 µL REACTION***
*T4 DNA Ligase Buffer (10*X)*	*2 µL*
*Vector DNA (*8.89 *kb) (p*LVX*)*	*50 ng*
*Insert DNA (*1.86 *kb)*	*30.5 ng*
Nuclease-free water	*to 20 µL*
T4 DNA Ligase	*1 µL*

The reaction was gently mixed by pipetting up and down then incubated at 16°C overnight. The next day T4 Ligase was heat inactivated by incubating reaction at 65°C for 10 minutes. The ligation product was chilled on ice and 5 µL of ligation product was transformed into 50 µL competent *E. coli* cells (Refer to **2.15.6 Transformation of pCR-**

Blunt II-TOPO (pTOPO) vector into 5DHα E. coli). The colonies were counted and screened for right product, sequenced for right orientation and the presence of desired mutations as described above (Refer to **2.15.7 Miniprep protocol for plasmid DNA extraction and screening from *E. coli*).** The pLVX-EF1α-IRES-ZsGreen1 vector containing right PTPN11 constructs was expanded in *E. coli*, extracted from *E. coli,* gel and sequence verified before using them for generating lentiviral particles.

2.15.12. Generation of lentiviral particles via transfection of HEK-293T cells

Human embryonic kidney 293 (HEK-293T) cells were seeded into a T25 flask at a density of 8 x 10^5 cells. The cells were allowed to rest overnight in a humidified incubator at 37°C overnight. The next day, media was changed when HEK293T cells were about 80% confluent. The pLVX-EF1α-IRES-ZsGreen1 vector containing PTPN11 gene constructs were co-transfected along with its packaging vector psPAX2 (Adgene, USA) and envelope vector pMD2.G (courtesy of Aso/Prof Daniel Thomas) in the presence of Lipofectamine™ 2000 (Thermo Fisher Scientific, USA). This was done by preparing DNA solution by mixing 500 µL OPTI-MEM (Gibco, USA) and 4.5 µg of expression vector (pLVX), pLVX + PTPN11 WT, pLVX + PTPN11 A461T Mut, pLVX + PTPN11 P491H Mut and pLVX + PTPN11 A461T + P491H Mut along with 3 µg of psPAX2 packaging vector and 1.5 µg of pMD2.G envelope vector. Lipofectamine solution was prepared separately by adding 500 µL OPTI-MEM and 20 µL of Lipofectamine™ 2000 per sample. The DNA solution and the lipofectamine solution were incubated at RT for 5 minutes before mixing and further incubated at RT for 30 minutes. The mixture was added dropwise to HEK293T cells and incubated in humidified incubator at 37°C (5% CO_2) overnight. Next day (after 12-16

hours), the HEK293T media was replaced with 5 mL target cell media and incubated in humidified incubator at 37°C for 48 hours. On the subsequent day, the viral supernatant was acquired by recovering the culture medium of transfected HEK293T cells. To accomplish this, a 10 mL syringe (Terumo® Medical Corporation, USA) was employed to collect the medium, which was subsequently filtered through a sterile filter with a pore size of 0.45 μM.

2.15.13. Lentiviral transduction of BaF3 and BaF3 *BCR::ABL1* p190 cells

In a Biosafety class II cabinet, viral supernatant (2.5 mL) and fresh media (2.5 mL) was added to BaF3 or BaF3 *BCR::ABL1* p190 cells using 1 x 10^6 cells per well in 6-well plate. Final concentration of 4 μg/mL of polybrene was added to each well and the plate was centrifuged with brake off for 2 hours at 1800 rpm at 37°C. The culture dish was placed in a temperature-controlled incubator with humidity at 37°C and 5% CO_2 for an extended period. Following three rounds of cell division, the cells expressing GFP (a marker indicating successful gene transfer) were isolated using the BD FACSAriaTM Fusion flow cytometer, while the cells lacking GFP were removed from the analysis.

2.15.14. Confirmation of successful transduction and expression of SHP-2 protein in BaF3 and BaF3 *BCR::ABL1* p190 cells

Transduced BaF3 and BaF3 *BCR::ABL1* p190 cells were analysed for the presence of PTPN11 gene constructs in gDNA by PCR amplification of PTPN11 gene and sequencing for correct sequences. The expression of SHP-2 (protein encoded by PTPN11 gene) was confirmed by western blot analysis.

2.15.15 DNA Extraction by Phenol-chloroform

To perform the extraction of genomic DNA, a total of 5 x 10^6 cells were gathered by centrifugation at 1400 rpm for 5 minutes. Following this, the cells were washed using 1 x PBS and then collected in 1.7 mL microcentrifuge tubes. The resulting pellet was stored at -80°C and later thawed on ice. Subsequently, the pellet was resuspended in 480 µL of DNA lysis buffer. For each tube, 12.5 µL of 20% SDS and 10 µL of Proteinase K (Roche Molecular Systems, Inc.) were added. The samples were then incubated overnight at 37°C.

On the following day, 5 µL of RNase A (Qiagen, Hilden, Germany) was added to each tube. The tubes were inverted around 50 times and further incubated at 37°C for 10 minutes. Ten microliters of 5 M NaCl and 1 µL of glycogen carrier (Roche Molecular Systems, Inc.) were subsequently included in each tube. With caution taken in a fume hood, 500 µL of buffer-saturated phenol was added, and the tubes were vigorously shaken until achieving a uniform milky solution. The samples were then centrifuged at 16,000 x g for 5 minutes. Carefully, the aqueous upper layer was collected without disturbing the interface between the aqueous and organic layers, and it was dispensed into new 1.7 mL tubes labeled accordingly.

Next, 500 µL of Phenol:Chloroform:Isoamyl alcohol (PCI; 25:24:1, v/v) was added to the tubes. The tubes were vigorously shaken and then subjected to centrifugation at 16,000 x g for 3 minutes. Once again, the aqueous upper layer was carefully collected and transferred into new 1.5 mL microcentrifuge tubes. To precipitate the DNA, 1 mL of ice-cold 80% ethanol was added. The tubes were then centrifuged at 20,000 x g for 10 minutes, and the supernatant was discarded. The DNA pellet was washed with 800 µL of

70% ethanol and briefly air-dried. Finally, the pellet was resuspended in 200 µL of DNA hydration solution (Qiagen, Hilden, Germany).

2.16 Statistical Analysis

GraphPad Prism 9 (GraphPad Software Inc., San Diego, USA) was used to generate figures and perform statistics. Graphs illustrate the average value, accompanied by error bars that indicate the variability measured as standard deviation (SD). Normality tests were performed on each data set using the D'Agostino & Pearson omnibus normality test. Statistical analysis was performed using a 2-tailed Student's *t*-test, One-way ANOVA, Two-way ANNOVA or Mann-Whitney test where appropriate and differences were statistically significant when the probability value (*p*-value) was less than 0.05. The synergism of combination treatment with two inhibitors were analysed by CalcuSyn software (Biosoft, United Kingdom) and combination index (CI) was reported as CI score, less than one being significantly synergistic combination.

References:

1. Minieri, V., et al., *Targeting STAT5 or STAT5-Regulated Pathways Suppresses Leukemogenesis of Ph+ Acute Lymphoblastic Leukemia.* Cancer research, 2018. **78**(20): p. 5793-5807.
2. Dobin, A., et al., *STAR: ultrafast universal RNA-seq aligner.* Bioinformatics, 2012. **29**(1): p. 15-21.
3. Liao, Y., G.K. Smyth, and W. Shi, *featureCounts: an efficient general purpose program for assigning sequence reads to genomic features.* Bioinformatics, 2014. **30**(7): p. 923-30.
4. Wang, K., M. Li, and H. Hakonarson, *ANNOVAR: functional annotation of genetic variants from high-throughput sequencing data.* Nucleic Acids Res, 2010. **38**(16): p. e164.
5. Jia, W., et al., *SOAPfuse: an algorithm for identifying fusion transcripts from paired-end RNA-Seq data.* Genome Biol, 2013. **14**(2): p. R12.
6. Davidson, N.M., I.J. Majewski, and A. Oshlack, *JAFFA: High sensitivity transcriptome-focused fusion gene detection.* Genome Med, 2015. **7**(1): p. 43.
7. Nicorici, D., et al., *FusionCatcher–a tool for finding somatic fusion genes in paired-end RNA-sequencing data.* biorxiv, 2014: p. 011650.
8. Pronobis, M.I., N. Deuitch, and M. Peifer, *The Miraprep: A protocol that uses a Miniprep kit and provides Maxiprep yields.* PLoS One, 2016. **11**(8): p. e0160509.

CHAPTER 3: Phospho-BCR-Y177 of BCR::ABL1 mediates phospho-ERK1/2 activation and TKI resistance

Chapter 3 summary

Over the last decade, there has been remarkable progress in understanding the disease pathology and treatment options for Ph+ Acute Lymphoblastic Leukaemia (Ph+ ALL) [1]. Tyrosine Kinase Inhibitors (TKIs) are added to the chemotherapy regimen in Ph+ ALL, which has significantly improved remission and survival rates. Combination of imatinib into conventional chemotherapy improved disease free survival rate to 70% in Ph+ ALL patients at 5 years [2]. However, 5 year overall survival does not exceed 50%, therefore novel treatment options are urgently needed [3]. While BCR::ABL1 kinase domain mutations are the predominant driver of TKI resistance, in approximately 30% of Ph+ ALL patients the mechanisms of TKI resistance are not well known [4].

In this chapter, I investigated the mechanisms of non-BCR::ABL1 kinase domain mutational resistance in a model of Ph+ ALL imatinib resistant cell line (SUP-B15 IR). The SUP-B15 IR cell line was generated by another student in my supervisor's laboratory by incremental dose escalation of imatinib to 5 μM using a well-established long-term dose escalation protocol. These cells had a novel BCR::ABL1 dependent mechanism of resistance with re-activation of pBCR::ABL1 (Y177) leading to sustained pERK1/2 and higher anti-apoptotic protein MCL-1 expression. Interestingly, TKI target of BCR::ABL1 protein, pBCR::ABL1(Y245) and its downstream signalling molecules pCRKL and pSTAT5 were inhibited with 5 μM imatinib. However, these cells had BCR::ABL1 independent overexpression of anti-apoptotic protein BCL-XL, a possible BCR::ABL1 independent survival mechanism.

Introduction

Ph+ ALL patients have immensely benefited from incorporation of TKIs into chemotherapy, but still face the challenges of TKI resistance [5, 6]. TKIs such as imatinib included into a chemotherapy backbone have resulted in increased remission rates and improved survival in Ph+ ALL patients [7]. However, resistance to imatinib is frequently observed in those patients [7, 8]. Second generation TKIs nilotinib and dasatinib and third generation TKI ponatinib have been developed to address resistance and intolerance [9]. As a result, complete response is achieved in over 90% of newly diagnosed Ph+ ALL patients when TKI is incorporated into chemotherapy [10-12]. However, relapse is frequent after initial response impairing overall the survival rate [13]. Imatinib resulted in only 43% 5-year disease free survival and overall survival when combined with intensive chemotherapy [14]. Dasatinib improved both 3 year event-free survival and overall survival to 55% and 69%, respectively [15] when combined with intensive chemotherapy. Ponatinib when combined with intensive chemotherapy improved 5-year overall survival to 72% in Ph+ ALL patients [16].

Despite the development of second and third generation TKIs, several mechanisms of TKI resistance including ABL1 kinase domain mutations are identified. Nevertheless, for many Ph+ ALL patients who relapse, their mechanisms of resistance are largely elusive [17]. Continuous exposure to TKI selects for resistant clones with resistance attributed to either BCR::ABL1 point mutations or a non-BCR::ABL1 mutational mechanism that pose a clinical challenge [18]. Ph+ ALL patients without BCR::ABL1 mutations unresponsive to multiple TKI treatment have very limited treatment options [4]. For instance, major molecular response was achieved in only 27% of poor responder patients treated with ponatinib in the PACE trial, a phase 2, uncontrolled, open-label trial of oral

ponatinib in patients with chronic myeloid leukemia (CML) and Ph+ ALL who were resistant or intolerant to nilotinib and dasatinib [19]. Results from the PACE trial highlight the treatment challenges faced by Ph+ leukaemia patients treated with even later generation TKIs. This further suggest that novel treatment approaches are urgently needed for relapsed Ph+ ALL patients [19].

TKI resistance can occur via mechanisms that enable reactivation of kinase activity of BCR::ABL1, such as kinase domain mutations, overexpression of *BCR::ABL1* or dysregulation of drug transporters that reduce intracellular concentrations of TKIs [20]. These mechanisms are BCR::ABL1 dependent while other mechanisms that do not rely on re-activation of BCR::ABL1 such as activation of alternative survival/anti-apoptotic pathways or mutations in cancer associated genes are BCR::ABL1 independent mechanisms [20]. Constitutively active BCR::ABL1 and its downstream signalling such Rat Sarcoma (RAS)-Extracellular Signal-Regulated Kinase (ERK), Janus Kinase (JAK)-Signal Transducer and Activator of Transcription (STAT), Phosphatidylinositol 3-Kinase (PI3K)-Protein Kinase B (PKB, also known as AKT) are responsible for development and progression of leukaemia [20, 21]. BCR::ABL1 activation and downstream signalling is mediated by several phosphorylation sites including two important tyrosine sites, one on ABL1 at 245 (pABL1 Y245) and another on BCR at 177 (pBCR Y177) [22, 23]. While pBCR::ABL1(Y245) is responsible for kinase activity (activity marker) of BCR::ABL1, pBCR::ABL1(Y177) acts as a docking site for adaptor protein growth factor receptor protein 2 (GRB2) responsible for activation of RAS/ERK and PI3K/AKT pathways [23-26]. TKIs competes with ATP binding to the ABL1 active site and results in inhibition of pBCR::ABL1 (Y245) which inhibits pBCR::ABL1 (Y177). Together, inhibition of those two phosphorylation sites acts as a marker for inhibition of BCR::ABL1 activity and

downstream signalling. The RAS/ERK pathway is one of the most commonly mutated/dysregulated pathways associated with therapy resistance and poor prognosis in multiple cancer types [27]. The RAS/ERK pathway have been previously shown to drive BCR::ABL1 independent imatinib resistance in Ph+ ALL cell line [28]. Unrestricted RAS/ERK signalling upregulates the anti-apoptotic molecules myeloid cell leukaemia-1 (MCL-1) [29, 30].

The mitochondrial apoptosis pathway is regulated by BCL-2 family proteins by modifying the integrity of outer mitochondrial membrane [31]. When death signals are triggered in the cells, the pro-apoptotic (BH3-only) proteins such as BIM, BID and PUMA dissociates from anti-apoptotic proteins such as BCL-2, BCL-XL and MCL-1 [31]. The free BH3-only proteins activate death effectors BAK and BAX which then oligomerize and form pores in the outer mitochondrial membrane. Permeabilization of mitochondrial membrane releases cytochrome c into the cytosol which activates the caspase cascade that commits cells to apoptosis [31]. Overexpression of anti-apoptotic proteins can sequester pro-apoptotic BH3-only proteins released from a death signal allowing cells to resist apoptosis [32]. Multiple studies have shown that overexpression of one or more anti-apoptotic protein can lead to TKI resistance in Ph+ leukaemia [30, 33-35].

In this chapter, I investigated non-BCR::ABL1 mutations driven resistance in a cell line model of Ph+ ALL and employed a targeted treatment strategy to overcome resistance. A novel mechanism of BCR::ABL1 dependent resistance was identified in imatinib resistant SUP-B15 IR cells with re-activation of pBCR::ABL1(Y177) of BCR::ABL1 protein leading to pERK1/2 and anti-apoptotic protein MCL-1 expression. There was an effective inhibition of pBCR::ABL1(Y245), the target of TKIs and its downstream signalling. In

addition to the BCR::ABL1 dependent mechanisms of resistance, imatinib resistant cells also had BCR::ABL1 independent overexpression of anti-apoptotic protein BCL-XL, a possible BCR::ABL1 independent mechanism of survival. Inhibition of the RAS/ERK pathway was tested as a targeted treatment option using MEK inhibitor which showed greater sensitivity in resistant cells than parental control.

Results

Imatinib resistant SUP-B15 cells were resistant to all ATP-competitive TKIs and to the allosteric ABL1 inhibitor asciminib

Imatinib resistant (to 5 μM) SUP-B15 (SUP-B15 IR) cells, which require imatinib for their long-term growth, were exposed to increasing concentrations of imatinib, nilotinib, dasatinib, ponatinib and asciminib for 72 hours and the concentration of drug required to induce apoptosis in 50% of cells (Lethal Dose, LD50) was calculated. As expected, SUP-B15 IR cells had higher LD50 for imatinib treatment compared to the parental cell line (>20 μM vs 6.3±0.71 μM respectively) (**Figure 3.1A**). Interestingly, SUP-B15 IR cells had higher LD50s for second generation TKIs: nilotinib and dasatinib treatment compared to parental cells (0.28±0.07 μM vs 0.04±0.01 μM dasatinib, p=0.0046, and >5 μM vs 2.6±0.33 μM nilotinib respectively) (**Figure 3.1B and C**). Similarly, LD50 was higher for third generation TKI: ponatinib and asciminib treatment compared to parental cells (>2.5 μM and 0.45±0.25 μM ponatinib, and >20 μM and 11.3±4.5 μM asciminib respectively) (**Figure 3.1D and E**). In all TKI treatments and concentrations assessed, SUP-B15 IR cells displayed significant resistance ($p \leq 0.05$) when compared to the parental control **(Figure 3.1A-E)**. The exception to this trend was observed only with dasatinib treatment at 1 μM. Notably, SUP-B15 IR cells necessitate the presence of 5 μM imatinib in their medium for optimal long-term growth. However, their viability did not exhibit significant change after

72 hours in the presence of 5 µM imatinib compared to the TKI-free control (p=0.327) **(Figure 3.1A)**. This contrasts with the observed response in similarly generated and previously characterized imatinib-dependent K562 cells **(see Appendix 1)**, where the removal of imatinib led to a substantial impact (increase, p= 0.0002) on viability during this 72-hour period.

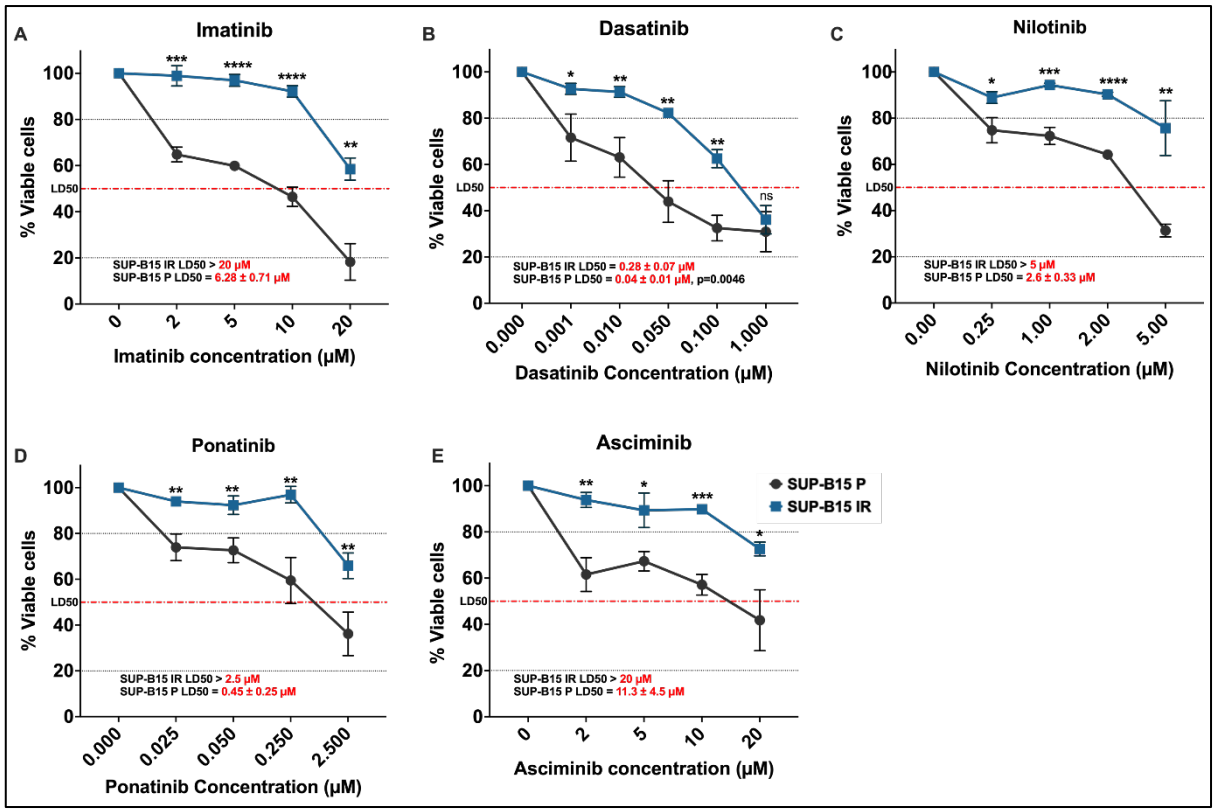

Figure 3.1: **Imatinib resistant (to 5 µM) SUP-B15 cells were resistant to second and third generation TKIs as well as to asciminib.** (A-E) SUP-B15 P and IR cells were subjected to increasing concentrations of imatinib, nilotinib, dasatinib, ponatinib, and asciminib over a 72-hour period. SUP-B15 IR cells underwent overnight washout procedure as described in '2.7.3. Cell washout protocol for TKI resistant cells of Chapter 2: Methods and Materials'. Viability was assessed using Annexin-V-PE and Fixable Viability Stain 780, measured via flow cytometry. The Y-axis represents the percentage of viable cells, determined by normalizing Annexin-V-PE low and Fixable Viability Stain low values to untreated/DMSO-only controls. LD50, the concentration inducing

apoptosis in 50% of cells, was calculated with GraphPad Prism 9 using nonlinear fitting of inhibitor response curves. For TKIs unable to achieve 50% cell death at the maximum concentration used, LD50 is denoted as greater than the maximum concentration. Data is derived from three independent experiments (n=3). Statistical significance was determined using unpaired t-tests. Ns, *, **, ***, and **** represent p-values of >0.05, ≤0.05, ≤0.01, ≤0.001 and ≤0.0001, respectively. Error bars indicate standard deviation (SD).

Reduced sensitivity to more potent higher generation TKIs warranted investigation into effectiveness of those TKIs to inhibit pBCR::ABL1 by using widely used pCRKL IC50 assay [36]. IC50 represents a TKI concentration required to inhibit 50% of pCRKL (IC50), a surrogate for pBCR::ABL1 kinase activity. The key readout of this assay is BCR::ABL1 kinase inhibition achieved after a 2-hour incubation. A significant increase in IC50 values indicates on-target BCR::ABL1 dependent resistance [36]. SUP-B15 IR cells showed higher IC50 for imatinib (2.1±0.06 μM vs 0.93±0.06 μM for parental, p<0.0001) (**Figure 3.2A-C**). SUP-B15 IR cells were further assessed for resistance to nilotinib, dasatinib and ponatinib, and again demonstrated higher IC50s compared to the parental cell line (198.3 ±7.64 nM vs. 117.6±29.26 nM nilotinib, p=0.009; 10±1.34 nM vs 6.6±0.53 nM dasatinib, p=0.0156; 8.4±1.22 nM vs 6.3±0.74 nM ponatinib, p=0.0449, for resistant and parental respectively) (**Figure 3.2C and Appendix 2**). Asciminib alone did not exhibit an inhibitory effect on pCRKL in both CML and Ph+ ALL cells within a 2-hour timeframe (data not shown); consequently, IC50 assays were not conducted with asciminib in SUP-B15 cells. This suggests that asciminib may not sufficiently inhibit BCR::ABL1 kinase activity to directly impact pCRKL within this short time frame. Asciminib functions as an allosteric inhibitor of BCR::ABL1, and as pCRKL is not its direct target, the effects on

pCRKL were likely not immediately evident within the 2-hour window. The moderately higher IC50s observed with all TKIs tested suggest that resistant SUP-B15 cells have BCR::ABL1-dependent mechanisms of resistance, but this alone does not fully explain the extent of resistance (LD50s) observed in response to those TKIs [37].

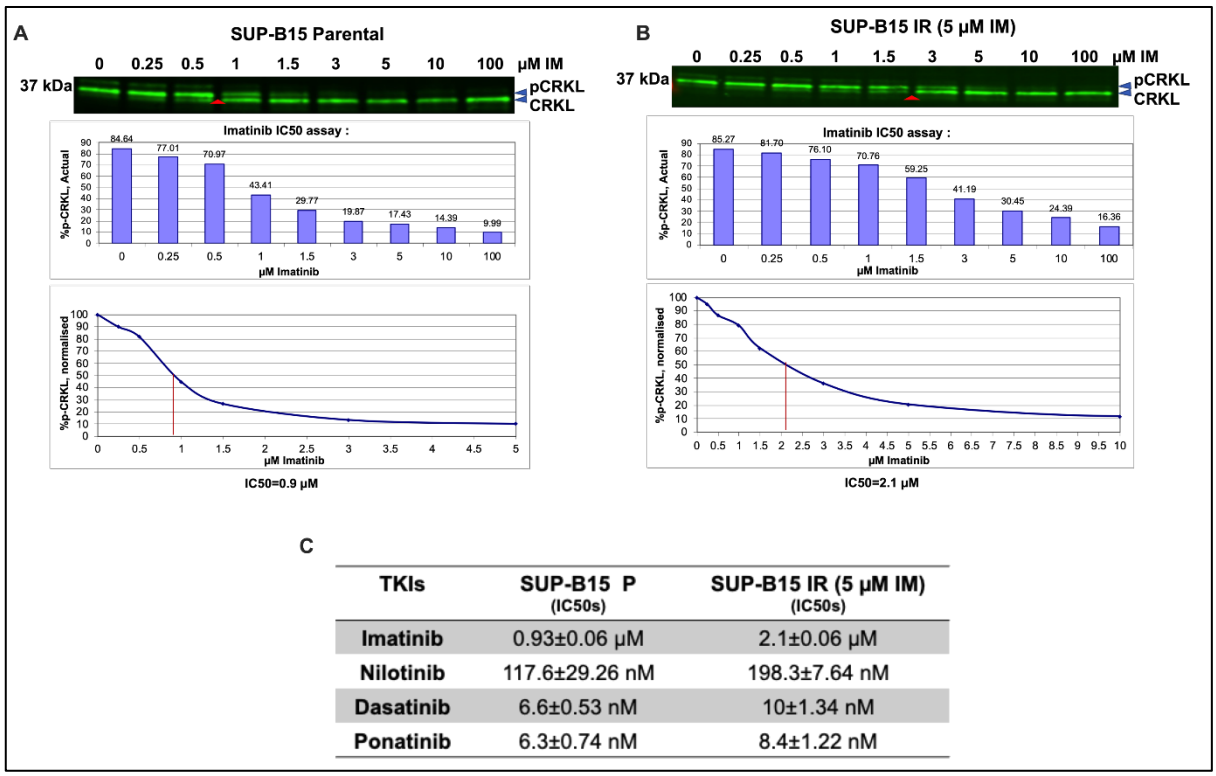

C

TKIs	SUP-B15 P (IC50s)	SUP-B15 IR (5 µM IM) (IC50s)
Imatinib	0.93±0.06 µM	2.1±0.06 µM
Nilotinib	117.6±29.26 nM	198.3±7.64 nM
Dasatinib	6.6±0.53 nM	10±1.34 nM
Ponatinib	6.3±0.74 nM	8.4±1.22 nM

Figure 3.2: SUP-B15 IR cells have higher imatinib pCRKL IC50 compared to SUP-B15 P cells. (A and B) SUP-B15 P and IR cells were exposed to increasing concentrations of imatinib (0 to 100 µM) for 2 hours at 37°C/5% CO_2. SUP-B15 IR cells underwent overnight washout procedure as described in '2.7.3. Cell washout protocol for TKI resistant cells of Chapter 2: Methods and Materials'. Densitometry analysis of pCRKL and CRKL was performed using Image Studio Lite. The concentration of imatinib required to inhibit pCRKL by 50% in 2 hours (IC50) was calculated, and graphs were generated in Microsoft Excel. The Western blots shown represent data from three independent experiments (n=3), with the red triangle indicating the approximate IC50 concentration. (C) A summary table of IC50 values for SUP-B15 cells treated with imatinib, nilotinib,

dasatinib, and ponatinib. Data represents mean IC50 values from three independent experiments. Statistical significance was determined using unpaired t-tests. *, **, and *** represent p-values of ≤0.05, ≤0.01, and ≤0.001 respectively.

ABL1 kinase domain mutations and drug transporters are not likely major driver of resistance in SUP-B15 IR cells

Common mechanisms that lead to BCR::ABL1 dependent TKI resistance are kinase domain mutations, overexpression of *BCR::ABL1* and dysregulation of drug transporters [37]. In order to investigate the mechanisms of resistance, I screened the ABL1 kinase domain by using long PCR coupled with Sanger sequencing as described in **2.11.3 Kinase Domain Mutations Analysis** of Materials and Methods chapter [38]. I found no evidence of any relevant ABL1 kinase domain mutations in SUP-B15 IR cells (**Figure 3.3**).

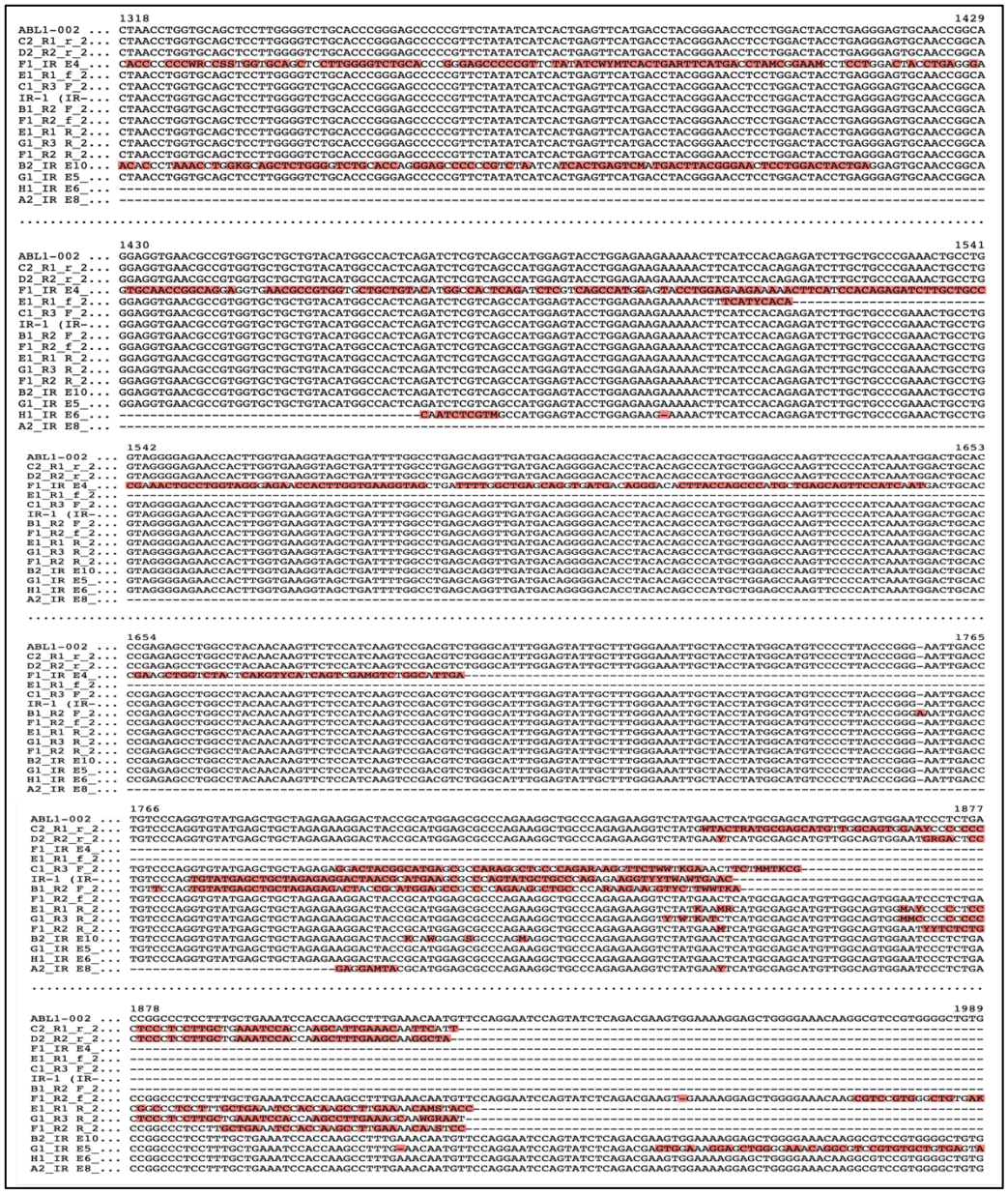

Figure 3.3: SUP-B15 IR cells do not have ABL1 kinase domain mutations. Sanger sequencing of the ABL1 kinase domain of BCR::ABL1 in SUP-B15 IR cells was conducted using a long PCR protocol described in '**2.11.3 Kinase Domain Mutations Analysis** of Chapter 2: Materials and Methods'. The ABL1 kinase domain was PCR-amplified with a forward primer located on BCR exon 1 (p190 FW: 5'-CTCGCAACAGTCCTTCGACA-3') and a reverse primer located on ABL1 exon 10 (REV: 5'-CCTGCAGCAAGGTACTCACA-3'). Gel-purified PCR products were sequenced bidirectionally using the following primers: FRD: 5'-GCCGAGTTGGTTCATCATCATTCAAC-3', 5'-GGTGCTGCTGTACATGGCC-3' and REV: 5'-

CAATGGAGACACGGCAGGCT-3', 5'-AGGCACGTCAGTGGTGTCTCT-3'. ABL1-002 serves as the reference sequence, and the sequences aligned below ABL1-002 represent the number of Sanger sequencing reads for SUP-B15 IR cells.

In the absence of kinase domain mutations, higher IC50s could be explained by increased levels of TKI efflux transporters leading to reduced intracellular concentrations of TKIs [37]. Intracellular drug concentration is controlled by ATP-binding cassette (ABC) transporters including P-glycoprotein (ABCB1) and breast cancer resistance protein (ABCG2) [39]. Overexpression of ABC family transporters ABCB1, ABCC6 and ABCG2 have been implicated in imatinib/nilotinib, nilotinib/dasatinib and asciminib resistance respectively [40-42]. Downregulation of organic cation transporter-1 (OCT-1) have been implicated in imatinib resistance in Ph+ leukemias [43]. In imatinib culture, SUP-B15 IR cells had decreased levels of *ABCB1* ($p<0.0001$) and *ABCG6* ($p=0.0084$) expression but had one-fold increase of *ABCG2* ($p=0.0185$), and 4-fold increase of *OCT-1* ($p=0.0426$) expression (**Figure 3.4A-D**). Assessment of ABCG2 protein expression via phospho-flow analysis (refer to **Appendix 3**) revealed no significant difference between parental and resistant SUP-B15 cells ($p=0.171$).

Drug resistance often stems from the activity of drug transporters, which can sometimes be overcome by employing various tyrosine kinase inhibitors (TKIs) that utilize distinct cellular transport mechanisms [36, 44]. However, the observation of pan-resistance to all tested TKIs in SUP-B15 IR cells suggests that drug transporters may not play a major role in TKI resistance in these cells.

It's important to acknowledge certain limitations in my analysis of drug transporters: this study does not comprehensively investigate all potential transporters, nor does it explore whether these transporters undergo changes in response to other TKI treatments or in the absence of TKIs.

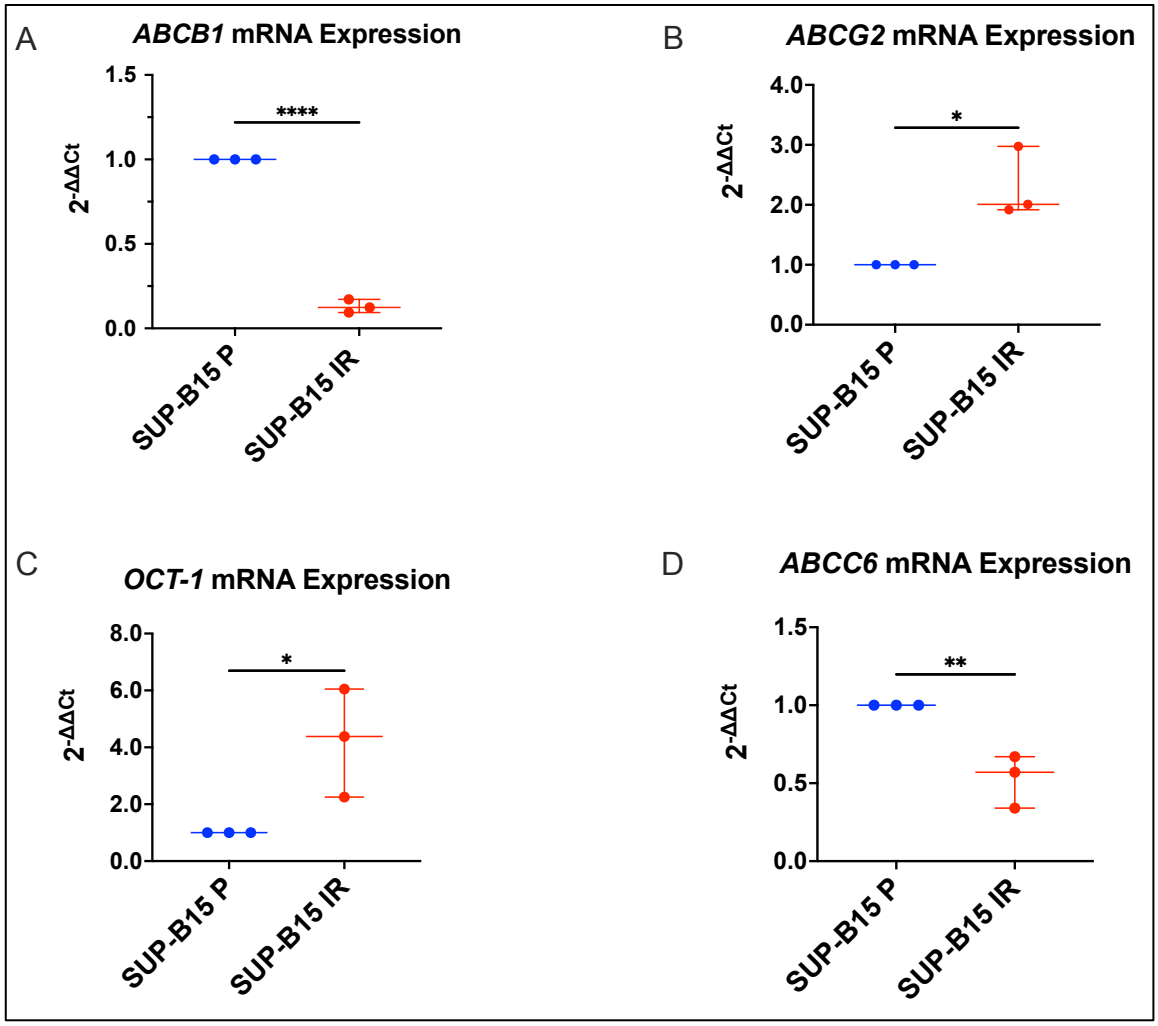

Figure 3.4: SUP-B15 IR cells have higher *ABCG2* and *OCT-1* and lower *ABCB1* and *ABCC6* mRNA expression. (A-D) Real-time PCR analysis of mRNA expression levels for *ABCB1*, *ABCG2*, *OCT-1*, and *ABCC6* in SUP-B15 P and SUP-B15 IR cells cultured in continuous 5 µM IM. Expression levels for each transporter were normalized to the housekeeping gene *GUSB*. Expression levels are presented as $2^{-\Delta\Delta Ct}$ (Fold Change) and represent a minimum of three independent samples (n=3). Statistical analysis was conducted using an unpaired t-test. Error bars indicate the 95% confidence interval

based on three independent experiments. Ns (non-significant), *, *, and *** denote p-values of >0.05, ≤0.05, ≤0.01, and ≤0.001, respectively.

SUP-B15 IR cells had similar *BCR::ABL1* mRNA expression with higher pBCR::ABL1 (Y177) in imatinib culture

BCR::ABL1 amplification is a well-characterized mechanism of imatinib resistance in in-vitro studies, though its clinical relevance may be limited [45, 46]. To investigate this, I initially examined BCR::ABL1 expression (please refer to **2.11.2 *BCR::ABL1* RQ-PCR** of Chapter 2: Materials and Methods for more details on protocol) in SUP-B15 IR cells cultured continuously in imatinib, as they require 5 μM imatinib for optimal growth. Subsequently, I conducted overnight washout experiments to remove imatinib and restore kinase activity.

In continuous imatinib culture conditions, a comparison of basal levels of BCR::ABL1 mRNA expression between SUP-B15 IR cells and the parental control revealed no significant difference (p=0.1667), as depicted in **Figure 3.5A**. However, at the protein level, there was a noteworthy approximately two-fold increase in total BCR::ABL1 (p=0.0028), as illustrated in **Figure 3.5B and C**. This observed increase in BCR::ABL1 protein abundance, despite the absence of a significant change in BCR::ABL1 transcripts, suggests a potential mechanism involving enhanced BCR::ABL1 protein stability in the presence of imatinib, rather than simple overexpression.

BCR::ABL1 protein undergoes phosphorylation at specific tyrosine residues, where pABL1-Y245 contributes to BCR::ABL1 kinase activity, while p-BCR-Y177 plays a pivotal role in modulating BCR::ABL1 activity by acting as a docking site for the Grb2 adaptor

protein, thereby linking to the RAS/ERK pathway [47]. Intriguingly, when examining SUP-B15 IR cells cultured continuously in the presence of 5 μM imatinib, Western blot analysis revealed an approximately two-fold reduction in pBCR::ABL1(Y177) (normalized to total BCR::ABL1) ($p<0.0001$) **(Figure 3.5B and D)**. However, it's noteworthy that the absolute levels of pBCR::ABL1(Y177) were higher ($p=0.0011$) in SUP-B15 IR cells when compared to parental cells treated with 5 μM imatinib for 4 hours **(Figure 3.5B and E)**. In contrast, pBCR::ABL1(Y245) phosphorylation was completely inhibited ($p=0.0016$) with 5 μM imatinib in both SUP-B15 IR and parental cells **(Figure 3.5B and F)**.

In the washout experiment, where imatinib was removed from the culture through overnight incubation, a substantial three-fold increase in pBCR::ABL1(Y245) ($p<0.0001$) was observed in SUP-B15 IR cells compared to the parental control **(Figure 3.5B and F).** These findings collectively suggest that there was insufficient inhibition of pBCR(Y177) in SUP-B15 IR cells when treated with 5 μM imatinib, despite effective inhibition of BCR::ABL1 kinase activity, as measured by pBCR::ABL1(Y245).

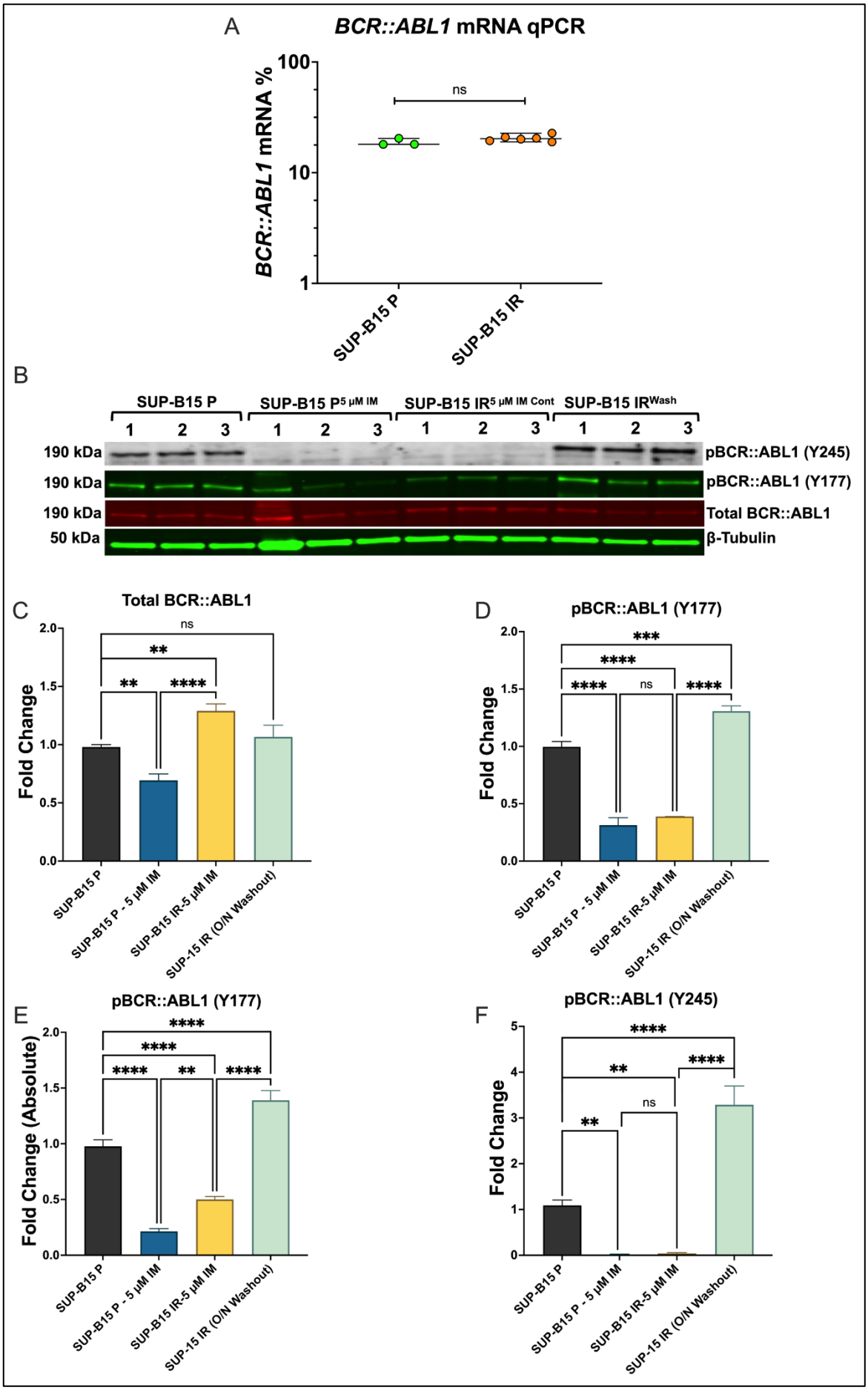
A
BCR::ABL1 mRNA qPCR
BCR::ABL1 mRNA %
100
10
1
ns
SUP-B15 P
SUP-B15 IR
B
SUP-B15 P
SUP-B15 P5 µM IM
SUP-B15 IR5 µM IM Cont
SUP-B15 IRWash
1 2 3 1 2 3 1 2 3 1 2 3
190 kDa
pBCR::ABL1 (Y245)
190 kDa
pBCR::ABL1 (Y177)
190 kDa
Total BCR::ABL1
50 kDa
β-Tubulin
C
Total BCR::ABL1
Fold Change
ns
**
**
****
SUP-B15 P
SUP-B15 P - 5 µM IM
SUP-B15 IR-5 µM IM
SUP-15 IR (O/N Washout)
D
pBCR::ABL1 (Y177)
Fold Change
***
****
****
ns
****
SUP-B15 P
SUP-B15 P - 5 µM IM
SUP-B15 IR-5 µM IM
SUP-15 IR (O/N Washout)
E
pBCR::ABL1 (Y177)
Fold Change (Absolute)
****
****
****
**
****
SUP-B15 P
SUP-B15 P - 5 µM IM
SUP-B15 IR-5 µM IM
SUP-15 IR (O/N Washout)
F
pBCR::ABL1 (Y245)
Fold Change
****
**
****
**
ns
SUP-B15 P
SUP-B15 P - 5 µM IM
SUP-B15 IR-5 µM IM
SUP-15 IR (O/N Washout)

Figure 3.5: Imatinib (5 μM) effectively inhibits pBCR::ABL1 (Y245) but not pBCR::ABL1 (Y177). (A) Quantitative PCR (RQ-PCR) was conducted to measure BCR::ABL1 mRNA expression in SUP-B15 P and SUP-B15 IR cells cultured in 5 μM imatinib. The analysis utilized cDNA synthesized from SUP-B15 cell-lines harboring the BCR::ABL1 p190 (e1a2) transcript, as previously described [48]. Total mRNA was extracted and converted to cDNA from both SUP-B15 P and SUP-B15 IR cells. The BCR control gene was included in every cDNA sample. Each sample and control were amplified in duplicate, and PCR was performed three times (n=3) for each. Statistical analysis was conducted using the Mann-Whitney test. The quantitative PCR assay follows a quality control protocol, incorporating high and low positive controls, to ensure consistent assay performance and reliability. Each assay's acceptability is determined by monitoring the BCR-ABL/BCR% mean and standard deviation of quality control samples (QC). The results are evaluated using Westgard Quality Control rules, with automatic acceptance or rejection of the assay based on predetermined limits and rules. The assay is rejected if the control value falls outside three standard deviations from the mean value. (B-F) Western blot analysis was conducted to evaluate the phosphorylation status of pBCR::ABL1(Y245), pBCR::ABL1(Y177), and total BCR::ABL1 in various cellular conditions. These conditions include SUP-B15 P cells without treatment, SUP-B15 P cells treated with 5 μM imatinib for 4 hours (SUP-B15 $P^{5\mu M\ IM}$), SUP-B15 IR cells cultured continuously in 5 μM imatinib (SUP-B15 $IR^{5\mu M\ IMCont}$), and SUP-B15 IR cells following the removal of imatinib to restore BCR::ABL1 tyrosine kinase activity (SUP-B15 IR^{wash}). SUP-B15 IR cells underwent overnight washout procedure as described in '2.7.3. Cell washout protocol for TKI resistant cells of Chapter 2: Methods and Materials'. Graphs depict fold changes relative to the untreated parental control, normalized to both housekeeping protein (beta -tubulin) and total BCR::ABL1. The fold change in absolute

pBCR::ABL1(Y177) phosphorylation is normalized to a housekeeping protein (beta-tubulin) but not to total BCR::ABL1 protein. Statistical analysis was carried out using One-Way ANOVA, and error bars represent the standard deviation (SD) based on three independent experiments (n=3). Significance levels are represented as 'Ns' (non-significant), '*', '**', '***', and '****' for p-values of >0.05, ≤0.05, ≤0.01, ≤0.001, and ≤0.0001, respectively.

Previous studies have shown potent transient inhibition of BCR::ABL1 kinase activity is sufficient to induce irreversible apoptosis in BCR::ABL1 positive cells [49-51]. To investigate the effectiveness of imatinib to transiently inhibit pBCR::ABL1 and downstream signalling, I performed overnight imatinib washout (equilibration in imatinib-free medium) and treated the cells with 5 μM imatinib for 4 hours. Upon overnight imatinib washout, there was no difference in total BCR::ABL1 expression ($p=0.478$), but there was 2-fold ($p<0.0001$) increase of pBCR::ABL1 in SUP-B15 IR cells (**Figure 3.6A and C**). Notably, downstream pathway proteins were also increased pSTAT5 (2.5-fold, $p<0.0001$) and pERK1/2 (4-fold, $p<0.0001$) (**Figure 3.6A, E-F and H**). However, 4 hours imatinib (5 μM) treatment effectively inhibited BCR::ABL1 kinase activity (pBCR::ABL1, $p<0.0001$ and p-CRKL, $p<0.0001$) as well as downstream pSTAT5 ($p<0.0001$) and pERK1/2 ($p<0.0001$) without any increase in total BCR::ABL1 expression ($p=0.478$) in SUP-B15 IR cells (**Figure 3.6A-H**). Interestingly, there was no increase in p-AKT (MFI 694 vs 1020 for parental control) in SUP-B15 IR cells after overnight imatinib washout and 5 μM imatinib treatment had minimal effect on p-AKT (MFI 694 vs 616 after 5 μM imatinib treatment) (**Figure 3.6H**). The effect of imatinib treatment was also moderate in parental controls (MFI 1020 vs 864 for 5 μM imatinib treatment) (**Figure 3.6H**). These results support the argument that 5 μM imatinib was effective in inhibiting

BCR::ABL1 kinase activity and downstream signalling in 4 hours, but the SUP-B15 IR cells remained viable possibly due to additional BCR::ABL1 independent mechanisms of survival [51].

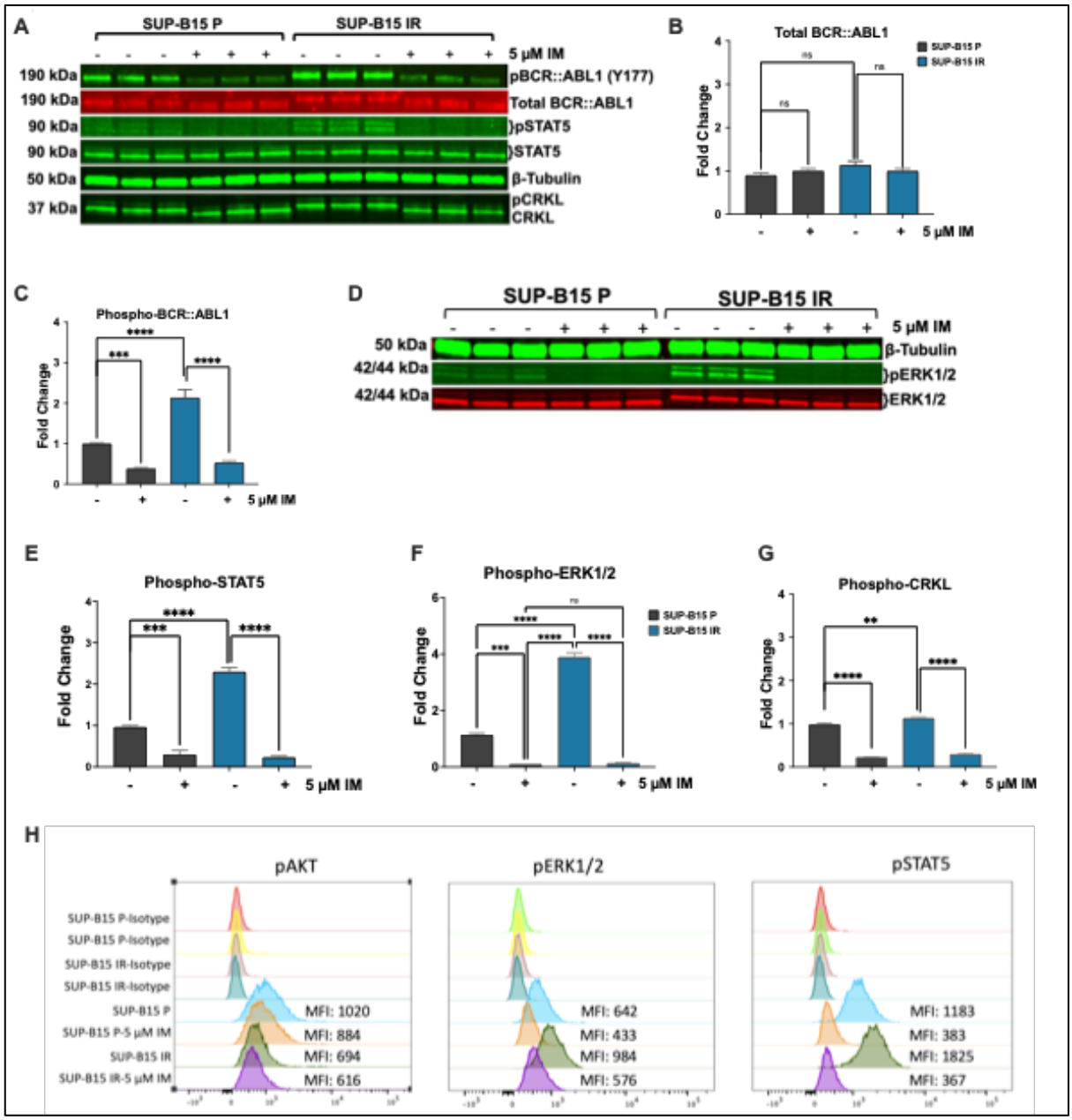

Figure 3.6: Imatinib resistant SUP-B15 cells also showed BCR::ABL1 independent mechanisms of resistance. (A-G) Western Blot and Densitometry Analysis: Imatinib-resistant SUP-B15 IR cells underwent overnight washout procedure as described in '2.7.3. Cell washout protocol for TKI resistant cells of Chapter 2: Methods and Materials',

followed by treatment with 5 μM imatinib for 4 hours. Western blot analysis was performed to assess the protein levels of total BCR::ABL1, pBCR::ABL1 (Y177), pSTAT5, p-CRKL, and pERK1/2. Each lane represents a sample from an independent experiment. Data presented are from three independent experiments (n=3). Statistical analysis was conducted using One-way ANOVA. Error bars represent the standard deviation (SD) derived from three independent experiments. (K) Phospho-Flow Analysis: Phospho-Flow analysis was conducted to evaluate the phosphorylation status of p-AKT, pERK1/2, and pSTAT5 in SUP-B15 cells, both with and without 5 μM imatinib treatment after overnight washout of imatinib from SUP-B15 IR cells. The graph represents data from three independent experiments (n=3). Two separate isotype controls for SUP-B15 P and IR cells were included for 5 μM imatinib-treated and untreated samples. MFI = Mean Fluorescent Intensity measurements. Significance levels are represented as 'Ns' (non-significant), '*', '**', '***', and '****' for p-values of >0.05, ≤0.05, ≤0.01, ≤0.001, and ≤0.0001, respectively.

ERK kinase was likely activated in SUP-B15 IR by pBCR::ABL Y177

Since, pBCR (Y177) plays an essential role in the activation of RAS/ERK and PI3K/AKT signalling [52], I investigated these pathways in continuous imatinib culture. While there was a decrease (MFI 1062 vs 805) in p-AKT in SUP-B15 IR cells in imatinib culture as measured by Phospho-flow (**Figure 3.7D**), the pERK1/2 was not affected (p=0.217) (**Figure 3.7A and E**). There was also reduction in pCRKL(p=0.0007) and pSTAT5 (p=0.0076) (**Figure 3.7A, F and G**), which is consistent with the inhibition of pBCR::ABL1 (Y245) [53]. These results confirmed the inhibition of pBCR::ABL1 (Y245) by 5 μM imatinib, but this dose of imatinib is unable to effectively inhibit pBCR::ABL1 (Y177)

which may have partially contributed to sustained pERK1/2 expression and survival of SUP-B15 IR cells in continuous imatinib culture.

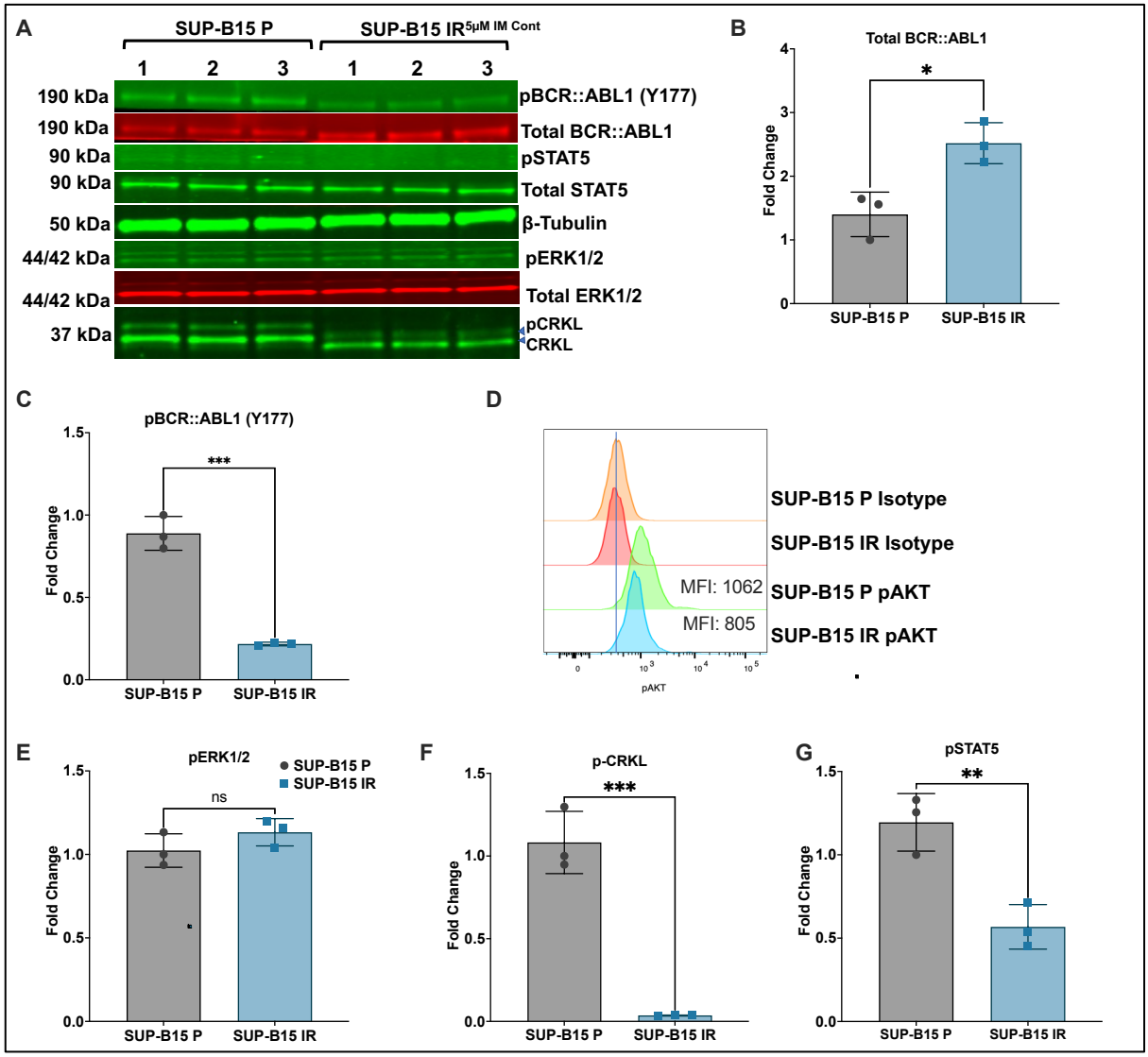

Figure 3.7: SUP-B15 IR cells had similar *BCR::ABL1* mRNA expression with sustained pERK1/2 in imatinib culture. (A-C, E-G) Western blot and densitometry analysis of total BCR::ABL1, pBCR::ABL1 (Y177), pSTAT5, pERK1/2, and pCRKL of SUP-B15 IR cells when in continuous 5 μM imatinib culture (SUP-B15 IR$^{5\mu M\ IM\ Cont.}$) compared to parental control. Numbers 1-3 represents three independent experiments. Statistical analysis was performed by using unpaired t-test. Error bars represent standard deviation (SD) of three independent experiments. (D) Phospho-flow analysis of p-AKT in SUP-B15

IR cells when in imatinib culture compared to parental control. Phospho-flow figure represents three independent samples. MFI = Mean Fluorescent Intensity measurements.

SUP-B15 IR cells also have activation of anti-apoptotic pathway

The most compelling hypothesis for cell survival upon oncogenic pathway inhibition is the activation of anti-apoptotic pathways [54]. To test this hypothesis, I investigated the three major anti-apoptotic proteins MCL-1, BCL-XL and BCL-2 for expression in resistant cells with and without imatinib treatment. Consistent with the hypothesis that SUP-B15 IR cells have BCR::ABL1 independent survival pathway, SUP-B15 IR cells had higher BCL-XL expression with ($p=0.0007$) or without ($p=0007$) imatinib treatment compared to parental control (**Figure 3.8A and B**). There was no difference in BCL-XL expression between ($p=0.487$) imatinib treated and untreated SUP-B15 IR cells (**Figure 3.8A and B**) suggesting BCL-XL expression was independent of BCR::ABL1 activation. Anti-apoptotic protein MCL-1, however, was increased with overnight imatinib washout ($p<0.0001$) (**Figure 3.8A and C**). Though there was significant reduction in MCL-1 expression ($p<0.0001$) with 5 μM imatinib treatment in SUP-B15 IR cells, the expression level was still higher ($p=0.0017$) compared to imatinib (5 μM imatinib for 4 hours) treated parental control (**Figure 3.8A and C**). There was no difference ($p=0.97$) in expression of BCL-2 between parental and resistant cells (**Figure 3.8A and D**).

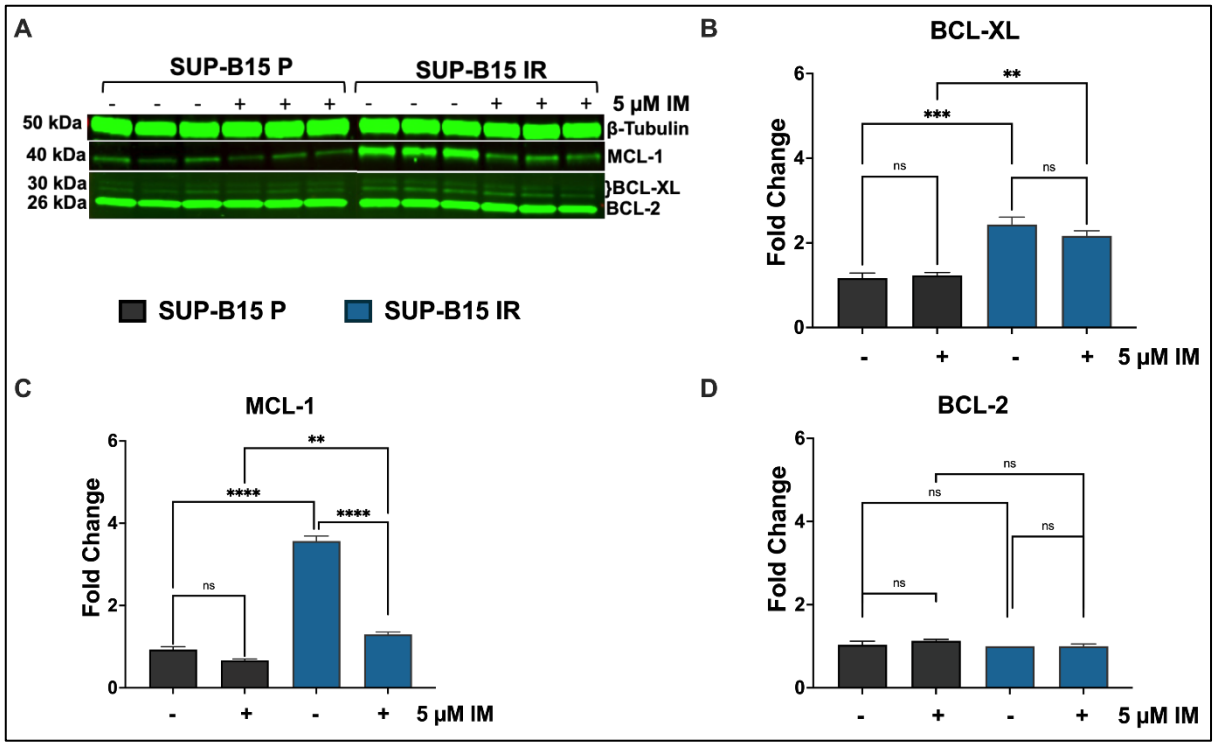

Figure 3.8: SUP-B15 IR cells also have activation of anti-apoptotic pathway. (A-D) Western blot and densitometry analysis of anti-apoptotic proteins MCL-1, BCL-XL and BCL-2 of SUP-B15 IR cells when imatinib was washed out overnight in TKI-free media then treated with 5 μM imatinib for 4 hours. Each lane represents a sample from an independent experiment. Data presented are from three independent experiments (n=3). Statistical analysis was performed by using One way ANOVA. Error bars represent standard deviation (SD) of three independent experiments. Significance levels are represented as 'Ns' (non-significant), '*', '**', '***', and '****' for p-values of >0.05, ≤0.05, ≤0.01, ≤0.001, and ≤0.0001, respectively.

SUP-B15 IR cells showed greater sensitivity to MEK inhibition with increase in BIM_{EL}/MCL-1 ratio

A significant increase in pERK1/2 in SUP-B15 IR cells after imatinib removal (**Figure 3.7F and G**) as well as sustained pERK1/2 activation in continuous imatinib culture (**Figure**

3.6A and F) corroborate possible involvement of pERK1/2 in the mechanism of resistance. Therefore, RAS/MEK/ERK axis presents an attractive therapeutic target in multi TKIs resistant SUP-B15 cells. To test this hypothesis, I treated SUP-B15 cells with MEK inhibitor (Mirdametinib or PD0325901). PD0325901 is a selective and non-ATP-competitive MEK inhibitor, which has completed phase II clinical trials for the treatment of patients with neurofibromatosis type 1 [55, 56]. Interestingly, PD0325901 treatment induced greater cell death in SUP-B15 IR cells compared to parental cells (LD50 58.2±33.67 nM vs 819.7±426.25, p=0.036 for parentals) (**Figure 3.9A**). Western blot analysis confirmed treatment of SUP-B15 IR cells with PD0325901 led to dose-dependent reduction of pERK1/2 in both SUP-B15 IR and parental cells without affecting pBCR::ABL1 level (**Figure 3.9B-D**). The treatment with PD0325901 not only reduced oncogenic RAS/ERK1/2 pathway, but also led to reduction of anti-apoptotic protein MCL-1 expression (**Figure 3.9B and F**) and dose dependent increase in BIM_{EL}, a pro-apoptotic protein, without affecting BCL-2 and BCL-XL protein expression **(Figure 3.9B, G and H)**. Despite BCL-XL expression not changing with PD0325901 treatment, there was a dose dependent increase in BIM and MCL-1 (pro and anti-apoptotic) protein ratio (**Figure 3.9B, F-H**). The change in dynamic of anti- and pro apoptotic proteins was consistent with the cell death observed in SUP-B15 IR cells.

It's important to note that during these experiments, I removed imatinib, a critical factor for the sustained growth of SUP-B15 IR cells. The absence of imatinib may have increased the susceptibility of SUP-B15 IR cells to MEK treatment when compared to parental cells, rendering them more responsive to the MEK inhibitor.

Furthermore, when I co-treated these cells with the MEK inhibitor and imatinib (2 μM), I observed only minimal effects on cell viability, with an LD50 exceeding 500 nM, the highest concentration of PD0325901 tested (please refer to **Appendix 4** for details). This observation may be attributed to the effectiveness of 5 μM imatinib in inhibiting the BCR::ABL1/pERK1/2 pathway when SUP-B15 IR cells underwent an overnight washout, effectively re-introducing imatinib, as demonstrated in **Figure 3.6A and 3.6D**. This principle may hold true for the 2 μM imatinib treatment as well. Consequently, the MEK inhibitor found itself without a viable target (pERK1/2) to exert its influence on cell viability. I propose that cell viability was likely sustained through the expression of anti-apoptotic proteins, as evidenced in **Figure 3.4.**

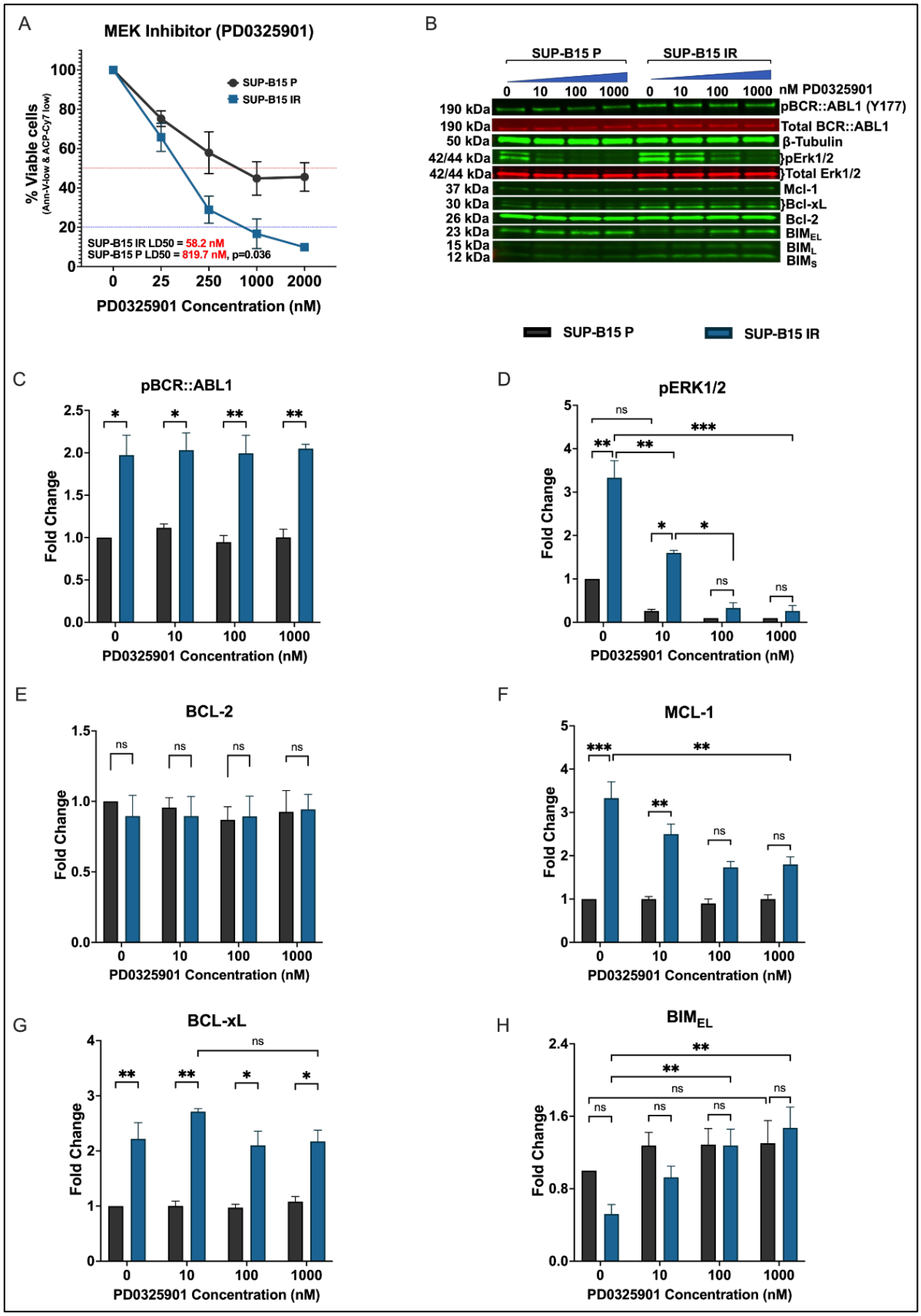

Figure 3.9: SUP-B15 IR cells showed greater sensitivity to MEK inhibition than parental cells (A) Cell Death Assay: SUP-B15 cells were exposed to increasing

concentrations of the MEK inhibitor PD0325901 for 72 hours. SUP-B15 IR cells underwent overnight washout as described in '2.7.3. Cell washout protocol for TKI resistant cells of Chapter 2: Methods and Materials'. Viability was assessed using Annexin-V-PE and Fixable Viability Stain 780, measured via flow cytometry. The Y-axis represents the percentage of viable cells, as indicated by Annexin-V-PE low and Fixable Viability Stain low values. The concentration of PD0325901 required to induce apoptosis in 50% of cells (Lethal dose, LD50) was calculated using GraphPad Prism 9. (B-H) Western blot analysis was performed to assess the protein levels of BCR::ABL1, pBCR::ABL1, ERK1/2, MCL-1, BCL-XL, BCL-2, and BIM in response to PD0325901. Densitometry analysis was conducted to quantify protein expression. Data presented are derived from three independent experiments (n=3). Statistical analysis was carried out using Two-Way ANOVA. Error bars represent the standard deviation (SD) based on three independent experiments. Significance levels are represented as 'Ns' (non-significant), *, **, ***, **** for p-values of >0.05, ≤0.05, ≤0.01, ≤0.001, and ≤0.0001, respectively.

Discussion

Despite significant advances in treating Ph+ leukemias with Tyrosine Kinase Inhibitors (TKIs), the emergence of TKI resistance remains a formidable challenge [37]. Current strategies to combat TKI resistance have predominantly focused on enhancing the potency and specificity of these inhibitors, with a particular emphasis on countering resistance stemming from mutations within the BCR::ABL1 gene [37]. However, a substantial body of evidence indicates that a notable fraction of Ph+ leukemia patients develop TKI resistance without harbouring kinase domain mutations in BCR::ABL1 [37, 57-59]. The underlying mechanisms responsible for such resistance remain poorly

understood but investigating them is imperative to identify targeted treatment approaches.

In this study, I investigate non-BCR::ABL1 mutational mechanisms of TKI resistance using a cell line model of Ph+ Acute Lymphoblastic Leukemia (ALL), employing imatinib-resistant (resistant to 5 μM IM) SUP-B15 (IR) cells. These IR cells were generated through a gradual dose-escalation approach with imatinib, as previously documented [60]. study sheds light on the dual mechanisms of TKI resistance in Ph+ ALL, encompassing both BCR::ABL1-dependent and -independent pathways, even in the absence of ABL1 kinase domain mutations. Additionally, my findings reveal sustained expression of pERK1/2 and BCR::ABL1-independent anti-apoptotic BCL-XL protein during imatinib treatment. Furthermore, I propose that targeting the RAS/ERK pathway with a MEK inhibitor could represent a promising strategy to surmount resistance in these cells. These discoveries hold significant clinical implications, as non-BCR::ABL1 mutation-driven resistance mechanisms remain enigmatic, and patients with multi-TKI-resistant or -intolerant Ph+ ALL often face limited treatment options.

Additionally, my study demonstrates that SUP-B15 IR cells exhibit resistance to higher-generation TKIs, including nilotinib, dasatinib, ponatinib, as well as the allosteric inhibitor of BCR::ABL1, asciminib. While these results support the existence of BCR:ABL1-independent resistance mechanisms [19], I confirm the presence of on-target BCR::ABL1-dependent resistance in these cells through pCRKL IC50 assays. SUP-B15 IR cells exhibited higher IC50 values for imatinib, as well as second and third generation TKIs. Importantly, these results challenge the conventional BCR::ABL1-dependent resistance mechanisms, such as ABL1 kinase domain mutations (including the "gate-

keeper" mutation T315I) [61], BCR::ABL1 overexpression, or dysregulation of drug transporters, which are often overcome by switching to higher-generation TKIs like ponatinib [62, 63]. Notably, my Sanger sequencing and RT-qPCR results did not support the involvement of ABL1 kinase domain mutations and ABC family drug transporter dysregulation as major contributors to the resistance mechanisms in these cells. Thus, my findings suggest that multi-TKI-resistant SUP-B15 cells possess a BCR::ABL1-dependent resistance mechanism that has not been extensively documented before. Moreover, this study has explored drug transporters that are commonly associated with TKI resistance. To deepen our comprehension of their involvement in the mechanisms of TKI resistance, a more extensive analysis of these drug transporters under various conditions, including treatment with different TKIs or in the absence of TKIs, holds the potential to provide valuable insights.

The BCR::ABL1 chimeric protein plays a pivotal role in this study, with two critical phosphorylation sites: one at tyrosine residue 245 on ABL1 (pBCR::ABL1-Y245), responsible for BCR::ABL1 protein kinase activity and the phosphorylation of CRKL and STAT5; and another at tyrosine residue 177 on BCR (pBCR::ABL1-Y177), responsible for initiating and transducing RAS/ERK and PI3K/AKT pathways [23-26, 47]. While TKIs effectively inhibit pBCR::ABL1 (Y245) and downstream molecules, indicating inhibition of ABL1 kinase activity, they only partially inhibit pBCR::ABL1 (Y177), suggesting a novel mechanism of BCR::ABL1 activation. I hypothesize that PTPN11 mutations, as detailed in Chapter 4, may contribute to the reactivation of pBCR::ABL1 (Y177) in the presence of imatinib. The sustained downstream pERK1/2 expression further supports the involvement of pBCR::ABL1 (Y177) in activating pERK1/2, as previous research has shown that blocking pBCR::ABL1 (Y177) impairs the RAS/ERK pathway, inhibits cell

growth, and induces apoptosis in CML cell lines [25]. However, an additional mechanism, possibly involving PTPN11 mutations, may contribute to boosting pERK1/2 expression to parental levels when pBCR::ABL1 (Y177) is reduced by imatinib. Notably, my results demonstrate moderate effects on p-AKT expression in SUP-B15 IR cells with transient or long-term imatinib (5 μM) treatment, excluding the involvement of the PI3K/AKT pathway in the resistance mechanisms. RAS/MEK/ERK pathway activation, independent of BCR::ABL1 activation, has been shown to be critical for the survival of imatinib-resistant CML stem cells [59, 64].

The low-level BCR::ABL1-dependent mechanism of resistance in SUP-B15 IR cells, as measured by pCRKL IC50, was not sufficient to account for the extent of resistance observed (as evidenced by the LD50 difference). Therefore, it is hypothesized that SUP-B15 IR cells likely employ additional resistance mechanisms. Previous studies have demonstrated that potent, transient inhibition of pBCR::ABL1 is enough to irreversibly induce apoptosis in cells [49, 50]. I observed that SUP-B15 IR cells equilibrated in TKI-free media overnight, which removed intracellular imatinib and restored BCR::ABL1 kinase activity. Transient imatinib (5 μM) treatment effectively inhibited the phosphorylation of BCR::ABL1 and all downstream signalling molecules without affecting the viability of SUP-B15 IR cells. It is likely that the activation of anti-apoptotic pathways contributes to the survival of transient pBCR::ABL1 inhibition in Ph+ cells [51]. Elevated expression of anti-apoptotic proteins BCL-XL and MCL-1 in SUP-B15 IR cells compared to parental controls, with or without imatinib treatment, suggests that BCL-XL and MCL-1 expression provides additional support to the low-level BCR::ABL1-dependent resistance mechanisms in SUP-B15 IR cells.

The significant involvement of the RAS/ERK pathway in the observed resistance mechanisms in SUP-B15 IR cells underscores the potential of this pathway as a promising target for overcoming resistance. MEK, acting as an intermediate molecule between RAS and ERK, can be effectively targeted, with Mirdametinib (PD0325901), an allosteric MEK inhibitor, representing a valuable tool for this purpose [55, 65]. argeting MEK holds great therapeutic potential in various cancer types, as MAPK pathways are implicated in numerous malignancies, leading to the FDA's approval of several MEK inhibitors [66]. For example, Trametinib, the first FDA-approved MEK inhibitor for melanoma treatment, demonstrated remarkable anti-leukemic effects in ALL cells driven by RAS mutations, enhancing prednisolone sensitivity. This supports the rationale for integrating MEK inhibitors into chemotherapy regimens [67]. Consistent with this hypothesis, SUP-B15 IR cells exhibited increased sensitivity to MEK inhibition compared to their parental counterparts. The MEK inhibitor not only effectively suppressed pERK1/2 activity in SUP-B15 IR cells but also tipped the balance in favor of apoptosis by increasing the BIM/MCL-1 ratio.

In Ph+ ALL, trametinib and dasatinib were successfully combined with chemotherapy in paediatric patients [68]. In precursor B-ALL, MEK inhibition sensitizes leukemic cells to dexamethasone [69]. However, it's important to note that not all patients or cancer types respond equally to MEK inhibitors, and the development of adaptive drug resistance is common with long-term treatment [66]. Moreover, MEK inhibitors are associated with significant side effects, such as rash, diarrhea, peripheral edema, fatigue, and dermatitis acneiform, which can be more pronounced compared to some other targeted therapies [70]. Therefore, in Chapter 5, I delve further into targeted treatment strategies by using

inhibitors of anti-apoptotic proteins BCL-XL and MCL-1 alone or in combination with TKIs to overcome resistance in SUP-B15 IR cells.

However, it's crucial to acknowledge certain limitations in the above findings. SUP-B15 IR cells rely on imatinib for their long-term optimal growth, and during MEK inhibitor treatment, imatinib was withdrawn from the culture medium. The increased susceptibility of SUP-B15 IR cells to MEK inhibition could potentially be attributed to the absence of imatinib, as evidenced by the negligible impact of MEK inhibitor treatment on cell viability when combined with imatinib. Therefore, while these results are promising, the context of imatinib dependency must be considered when interpreting the findings.

In the context of addressing TKI resistance in Ph+ leukaemias, it's crucial to recognize the limitations of this study. In the experiments involving SUP-B15 IR cells and the subsequent washout procedure, I encountered a notable limitation. Comparisons were made between SUP-B15 parental cells without imatinib and SUP-B15 IR cells following washout, as well as between SUP-B15 parental cells treated with 5 μM imatinib and SUP-B15 IR cells in continuous 5 μM imatinib culture. While these comparisons may not be ideal due to the inherent differences in treatment conditions, they were necessary because SUP-B15 parental cells could not be cultured continuously in 5 μM imatinib. Nonetheless, these cells serve as the best available control for studying SUP-B15 IR cells and provide valuable insights into the mechanisms of imatinib resistance.

In conclusion, this study has unveiled a novel BCR::ABL1-dependent resistance mechanism mediated via pBCR::ABL1 (Y177) within the BCR::ABL1 protein, resulting in sustained pERK1/2 activation. Additionally, the presence of supplementary BCR::ABL1-

independent resistance mechanisms, likely driven by the activation of anti-apoptotic pathways, has been confirmed. Furthermore, this study has demonstrated the feasibility of using MEK inhibitors to combat resistance in RAS/ERK-activated cells. However, it's essential to recognize that MEK inhibitors come with notable side effects. Therefore, there is an urgent need for the development of innovative treatment strategies to target non-BCR::ABL1 mutational resistance in Ph+ ALL.

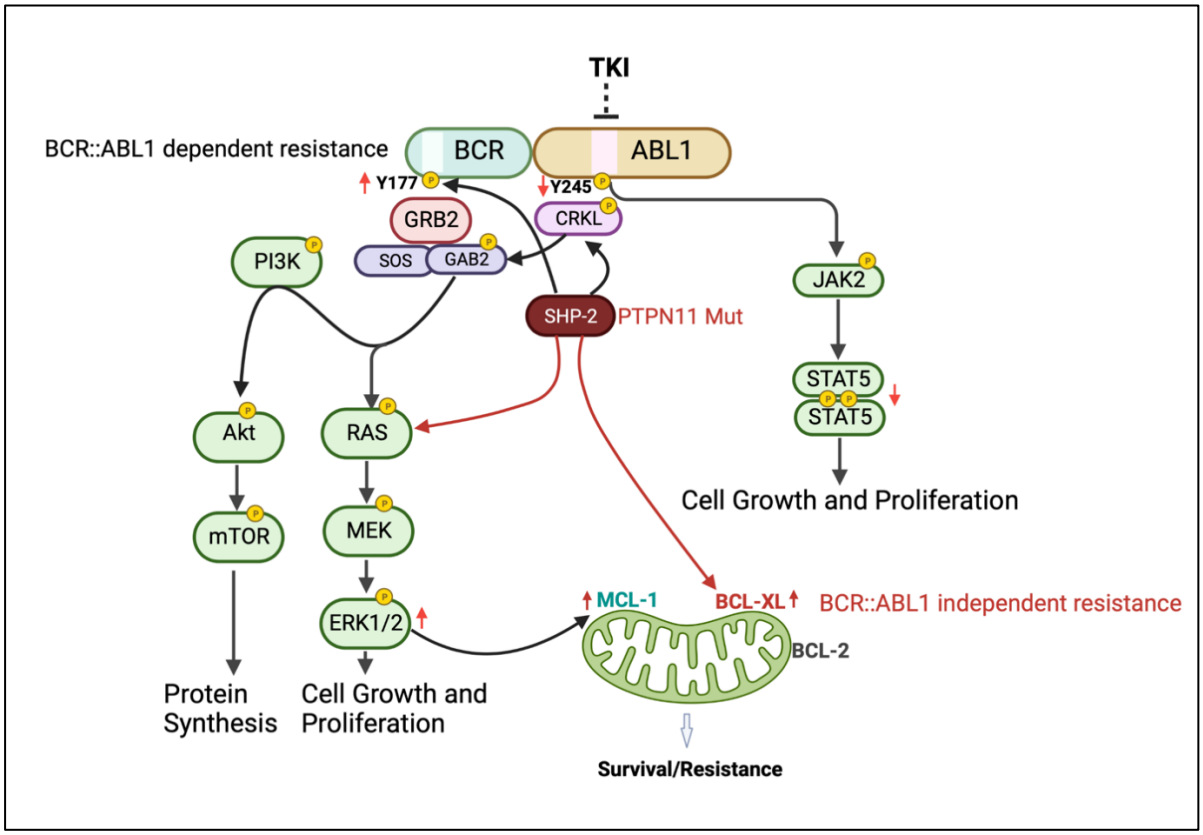

Chapter 3 Summary Figure: This schematic illustrates the dual mechanisms of resistance observed in imatinib-resistant SUP-B15 cells. The figure employs various arrow colours to distinguish between BCR::ABL1-dependent (black arrows) and BCR::ABL1-independent (dark red arrows) signalling pathways. Small bright red arrows indicate either an increase (pointing up) or decrease (pointing down) in the activation/expression of proteins. In the presence of TKI (imatinib), imatinib-resistant

SUP-B15 cells exhibit a BCR::ABL1-dependent mechanism of resistance characterized by the reactivation of pBCR::ABL1(Y177). This reactivation leads to the activation of pERK1/2, which is further enhanced by mutated SHP-2. Additionally, MCL-1 is overexpressed in the presence of TKI. Conversely, TKI treatment inhibits pBCR::ABL1(Y245), resulting in the inhibition of pCRKL and pSTAT5. Notably, pAKT levels remain relatively stable when comparing resistant and sensitive cells. Furthermore, resistant cells also employ a BCR::ABL1-independent survival mechanism mediated via PTPN11 mutations (as described in the next chapter). These mutations lead to the overexpression of the anti-apoptotic protein BCL-XL. The figure was created using BioRender.com.

References:

1. Samra, B., et al., *Evolving therapy of adult acute lymphoblastic leukemia: state-of-the-art treatment and future directions.* Journal of Hematology & Oncology, 2020. **13**(1): p. 70.
2. Saleh, K., A. Fernandez, and F. Pasquier *Treatment of Philadelphia Chromosome-Positive Acute Lymphoblastic Leukemia in Adults*. Cancers, 2022. **14**, DOI: 10.3390/cancers14071805.
3. Fielding, A.K., *Curing Ph+ ALL: assessing the relative contributions of chemotherapy, TKIs, and allogeneic stem cell transplant.* Hematology Am Soc Hematol Educ Program, 2019. **2019**(1): p. 24-29.
4. Mian, A.A., et al., *Oncogene-independent resistance in Philadelphia chromosome - positive (Ph(+)) acute lymphoblastic leukemia (ALL) is mediated by activation of AKT/mTOR pathway.* Neoplasia, 2021. **23**(9): p. 1016-1027.
5. Yilmaz, M., et al., *Philadelphia chromosome-positive acute lymphoblastic leukemia in adults: current treatments and future perspectives.* Clin Adv Hematol Oncol, 2018. **16**(3): p. 216-223.
6. Wang, H., et al., *Venetoclax-ponatinib for T315I/compound-mutated Ph+ acute lymphoblastic leukemia.* Blood Cancer Journal, 2022. **12**(1): p. 20.
7. Druker, B.J., et al., *Effects of a selective inhibitor of the Abl tyrosine kinase on the growth of Bcr–Abl positive cells.* Nature medicine, 1996. **2**(5): p. 561-566.
8. Ottmann, O., et al., *Phase II study of nilotinib in patients with relapsed or refractory Philadelphia chromosome—positive acute lymphoblastic leukemia.* Leukemia, 2013. **27**(6): p. 1411-1413.
9. Hantschel, O., F. Grebien, and G. Superti-Furga, *The growing arsenal of ATP-competitive and allosteric inhibitors of BCR–ABL.* Cancer research, 2012. **72**(19): p. 4890-4895.
10. Jabbour, E., et al., *Combination of hyper-CVAD with ponatinib as first-line therapy for patients with Philadelphia chromosome-positive acute lymphoblastic leukaemia: a single-centre, phase 2 study.* The Lancet Oncology, 2015. **16**(15): p. 1547-1555.
11. Jabbour, E., et al., *Combination of hyper-CVAD with ponatinib as first-line therapy for patients with Philadelphia chromosome-positive acute lymphoblastic leukaemia: long-term follow-up of a single-centre, phase 2 study.* The Lancet Haematology, 2018. **5**(12): p. e618-e627.
12. Morita, K., et al., *Outcome of patients with chronic myeloid leukemia in lymphoid blastic phase and Philadelphia chromosome–positive acute lymphoblastic leukemia treated with hyper-CVAD and dasatinib.* Cancer, 2021. **127**(15): p. 2641-2647.
13. DeAngelo, D.J., E. Jabbour, and A. Advani, *Recent advances in managing acute lymphoblastic leukemia.* American Society of Clinical Oncology Educational Book, 2020. **40**: p. 330-342.
14. Daver, N., et al., *Final report of a phase II study of imatinib mesylate with hyper-CVAD for the front-line treatment of adult patients with Philadelphia chromosome-positive acute lymphoblastic leukemia.* Haematologica, 2015. **100**(5): p. 653.
15. Ravandi, F., et al., *US intergroup study of chemotherapy plus dasatinib and allogeneic stem cell transplant in Philadelphia chromosome positive ALL.* Blood advances, 2016. **1**(3): p. 250-259.
16. Sasaki, K., et al., *Prognostic factors for progression in patients with Philadelphia chromosome-positive acute lymphoblastic leukemia in complete molecular response*

within 3 months of therapy with tyrosine kinase inhibitors. Cancer, 2021. **127**(15): p. 2648-2656.
17. O'hare, T., et al., *Pushing the limits of targeted therapy in chronic myeloid leukaemia.* Nature Reviews Cancer, 2012. **12**(8): p. 513-526.
18. Hochhaus, A., et al., *Long-term outcomes of imatinib treatment for chronic myeloid leukemia.* New England Journal of Medicine, 2017. **376**(10): p. 917-927.
19. Cortes, J.E., et al., *A phase 2 trial of ponatinib in Philadelphia chromosome–positive leukemias.* New England Journal of Medicine, 2013. **369**(19): p. 1783-1796.
20. Poudel, G., et al., *Mechanisms of Resistance and Implications for Treatment Strategies in Chronic Myeloid Leukaemia.* Cancers (Basel), 2022. **14**(14).
21. Amarante-Mendes, G.P., et al., *BCR-ABL1 Tyrosine Kinase Complex Signaling Transduction: Challenges to Overcome Resistance in Chronic Myeloid Leukemia.* Pharmaceutics, 2022. **14**(1).
22. Hantschel, O. and G. Superti-Furga, *Regulation of the c-Abl and Bcr–Abl tyrosine kinases.* Nature reviews Molecular cell biology, 2004. **5**(1): p. 33-44.
23. Reckel, S., et al., *Differential signaling networks of Bcr-Abl p210 and p190 kinases in leukemia cells defined by functional proteomics.* Leukemia, 2017. **31**(7): p. 1502-1512.
24. Pendergast, A.M., et al., *BCR-ABL-induced oncogenesis is mediated by direct interaction with the SH2 domain of the GRB-2 adaptor protein.* Cell, 1993. **75**(1): p. 175-185.
25. Li, Q., et al., *Blockade of Y177 and Nuclear Translocation of Bcr-Abl Inhibits Proliferation and Promotes Apoptosis in Chronic Myeloid Leukemia Cells.* Int J Mol Sci, 2017. **18**(3).
26. Chu, S., T. McDonald, and R. Bhatia, *Role of BCR-ABL-Y177-mediated p27kip1 phosphorylation and cytoplasmic localization in enhanced proliferation of chronic myeloid leukemia progenitors.* Leukemia, 2010. **24**(4): p. 779-87.
27. Conroy, M., et al., *Emerging RAS-directed therapies for cancer.* Cancer Drug Resistance, 2021. **4**(3): p. 543-558.
28. Suzuki, M., et al., *BCR-ABL-independent and RAS/MAPK pathway-dependent form of imatinib resistance in Ph-positive acute lymphoblastic leukemia cell line with activation of EphB4.* European Journal of Haematology, 2010. **84**(3): p. 229-238.
29. Li, Q., et al., *Sphingosine kinase-1 mediates BCR/ABL-induced upregulation of Mcl-1 in chronic myeloid leukemia cells.* Oncogene, 2007. **26**(57): p. 7904.
30. Aichberger, K.J., et al., *Identification of mcl-1 as a BCR/ABL-dependent target in chronic myeloid leukemia (CML): evidence for cooperative antileukemic effects of imatinib and mcl-1 antisense oligonucleotides.* Blood, 2005. **105**(8): p. 3303-3311.
31. Zhang, Q., et al., *Activation of RAS/MAPK pathway confers MCL-1 mediated acquired resistance to BCL-2 inhibitor venetoclax in acute myeloid leukemia.* Signal Transduction and Targeted Therapy, 2022. **7**(1): p. 51.
32. Pistritto, G., et al., *Apoptosis as anticancer mechanism: function and dysfunction of its modulators and targeted therapeutic strategies.* Aging (Albany NY), 2016. **8**(4): p. 603-19.
33. Parry, N., H. Wheadon, and M. Copland, *The application of BH3 mimetics in myeloid leukemias.* Cell death & disease, 2021. **12**(2): p. 222.
34. Zhang, J., et al., *hnRNPK/Beclin1 signaling regulates autophagy to promote imatinib resistance in Philadelphia chromosome-positive acute lymphoblastic leukemia cells.* Experimental Hematology, 2022. **108**: p. 46-54.

35. Amarante-Mendes, G.P., et al., *Bcr-Abl exerts its antiapoptotic effect against diverse apoptotic stimuli through blockage of mitochondrial release of cytochrome C and activation of caspase-3.* Blood, The Journal of the American Society of Hematology, 1998. **91**(5): p. 1700-1705.
36. Eadie, L.N., T.P. Hughes, and D.L. White, *ABCB1 Overexpression Is a Key Initiator of Resistance to Tyrosine Kinase Inhibitors in CML Cell Lines.* PLoS One, 2016. **11**(8): p. e0161470.
37. Poudel, G., et al., *Mechanisms of Resistance and Implications for Treatment Strategies in Chronic Myeloid Leukaemia.* Cancers, 2022. **14**(14): p. 3300.
38. Hoemberger, M., W. Pitsawong, and D. Kern, *Cumulative mechanism of several major imatinib-resistant mutations in Abl kinase.* Proceedings of the National Academy of Sciences, 2020. **117**(32): p. 19221-19227.
39. Hee Choi, Y. and A.-M. Yu, *ABC transporters in multidrug resistance and pharmacokinetics, and strategies for drug development.* Current pharmaceutical design, 2014. **20**(5): p. 793-807.
40. Eadie, L.N., et al., *The new allosteric inhibitor asciminib is susceptible to resistance mediated by ABCB1 and ABCG2 overexpression in vitro.* Oncotarget, 2018. **9**(17): p. 13423-13437.
41. Dulucq, S., et al., *Multidrug resistance gene (MDR1) polymorphisms are associated with major molecular responses to standard-dose imatinib in chronic myeloid leukemia.* Blood, The Journal of the American Society of Hematology, 2008. **112**(5): p. 2024-2027.
42. Eadie, L., et al., *The clinical significance of ABCB1 overexpression in predicting outcome of CML patients undergoing first-line imatinib treatment.* Leukemia, 2017. **31**(1): p. 75-82.
43. Patel, S., K. Shah, and R. Rawal, *Role of organic cation transporter-1 (OCT-1) in drug resistance condition of ph+ chronic myeloid leukemia (CML).* Cancer Research, 2019. **79**(13_Supplement): p. 2106-2106.
44. Agrawal, M., et al., *MDR1 expression predicts outcome of Ph+ chronic phase CML patients on second-line nilotinib therapy after imatinib failure.* Leukemia, 2014. **28**(7): p. 1478-1485.
45. Scappini, B., et al., *Changes associated with the development of resistance to imatinib (STI571) in two leukemia cell lines expressing p210 Bcr/Abl protein.* Cancer: Interdisciplinary International Journal of the American Cancer Society, 2004. **100**(7): p. 1459-1471.
46. Patel, A.B., T. O'Hare, and M.W. Deininger, *Mechanisms of Resistance to ABL Kinase Inhibition in Chronic Myeloid Leukemia and the Development of Next Generation ABL Kinase Inhibitors.* Hematol Oncol Clin North Am, 2017. **31**(4): p. 589-612.
47. Ma, G., et al., *Bcr phosphorylated on tyrosine 177 binds Grb2.* Oncogene, 1997. **14**(19): p. 2367-2372.
48. Moore, F.R., C.B. Rempfer, and R.D. Press, *Quantitative BCR-ABL1 RQ-PCR Fusion Transcript Monitoring in Chronic Myelogenous Leukemia*, in *Hematological Malignancies*, M. Czader, Editor. 2013, Humana Press: Totowa, NJ. p. 1-23.
49. Shah, N.P., et al., *Transient Potent BCR-ABL Inhibition Is Sufficient to Commit Chronic Myeloid Leukemia Cells Irreversibly to Apoptosis.* Cancer Cell, 2008. **14**(6): p. 485-493.
50. Simara, P., et al., *Apoptosis in chronic myeloid leukemia cells transiently treated with imatinib or dasatinib is caused by residual BCR–ABL kinase inhibition.* American Journal of Hematology, 2013. **88**(5): p. 385-393.

51. Schafranek, L., et al., *Sustained inhibition of STAT5, but not JAK2, is essential for TKI-induced cell death in chronic myeloid leukemia.* Leukemia, 2015. **29**(1): p. 76-85.
52. Chu, S., et al., *BCR-Tyrosine 177 Plays an Essential Role in Ras and Akt Activation and in Human Hematopoietic Progenitor Transformation in Chronic Myelogenous Leukemia.* Cancer Research, 2007. **67**(14): p. 7045-7053.
53. Bhat, A., et al., *Interactions of CBL with BCR-ABL and CRKL in BCR-ABL-transformed myeloid cells.* J Biol Chem, 1997. **272**(26): p. 16170-5.
54. Neophytou, C.M., et al. *Apoptosis Deregulation and the Development of Cancer Multi-Drug Resistance*. Cancers, 2021. **13**, DOI: 10.3390/cancers13174363.
55. Cheng, Y. and H. Tian, *Current Development Status of MEK Inhibitors.* Molecules, 2017. **22**(10).
56. Weiss, B.D., et al., *NF106: A Neurofibromatosis Clinical Trials Consortium Phase II Trial of the MEK Inhibitor Mirdametinib (PD-0325901) in Adolescents and Adults With NF1-Related Plexiform Neurofibromas.* J Clin Oncol, 2021. **39**(7): p. 797-806.
57. Soverini, S., et al., *Philadelphia-positive acute lymphoblastic leukemia patients already harbor BCR-ABL kinase domain mutations at low levels at the time of diagnosis.* Haematologica, 2011. **96**(4): p. 552-7.
58. Mian, A.A., et al., *Oncogene-independent resistance in Philadelphia chromosome - positive (Ph+) acute lymphoblastic leukemia (ALL) is mediated by activation of AKT/mTOR pathway.* Neoplasia, 2021. **23**(9): p. 1016-1027.
59. Ma, L., et al., *A therapeutically targetable mechanism of BCR-ABL–independent imatinib resistance in chronic myeloid leukemia.* Science translational medicine, 2014. **6**(252): p. 252ra121-252ra121.
60. Tang, C., et al., *Tyrosine kinase inhibitor resistance in chronic myeloid leukemia cell lines: investigating resistance pathways.* Leukemia & lymphoma, 2011. **52**(11): p. 2139-2147.
61. O'Hare, T., et al., *AP24534, a pan-BCR-ABL inhibitor for chronic myeloid leukemia, potently inhibits the T315I mutant and overcomes mutation-based resistance.* Cancer cell, 2009. **16**(5): p. 401-412.
62. Kujawski, L. and M. Talpaz, *Strategies for overcoming imatinib resistance in chronic myeloid leukemia.* Leukemia & Lymphoma, 2007. **48**(12): p. 2310-2322.
63. Lu, L., et al., *Modelling ponatinib resistance in tyrosine kinase inhibitor-naïve and dasatinib resistant BCR-ABL1+ cell lines.* Oncotarget, 2018. **9**(78): p. 34735-34747.
64. Asmussen, J., et al., *MEK-dependent negative feedback underlies BCR–ABL-mediated oncogene addiction.* Cancer discovery, 2014. **4**(2): p. 200-215.
65. Degirmenci, U., M. Wang, and J. Hu, *Targeting Aberrant RAS/RAF/MEK/ERK Signaling for Cancer Therapy.* Cells, 2020. **9**(1).
66. Wang, C., et al., *Research progress of MEK1/2 inhibitors and degraders in the treatment of cancer.* Eur J Med Chem, 2021. **218**: p. 113386.
67. Zhang, W., et al., *The Dual MEK/FLT3 Inhibitor E6201 Exerts Cytotoxic Activity against Acute Myeloid Leukemia Cells Harboring Resistance-Conferring FLT3 MutationsTargeting MEK/FLT3 via E6201 Overcomes TKI Resistance in AML.* Cancer research, 2016. **76**(6): p. 1528-1537.
68. Wang, J., et al., *Successful use of trametinib and dasatinib combined with chemotherapy in the treatment of Ph-positive B-cell acute lymphoblastic leukemia: A case report.* Medicine (Baltimore), 2021. **100**(25): p. e26440.
69. Polak, A., et al., *MEK Inhibition Sensitizes Precursor B-Cell Acute Lymphoblastic Leukemia (B-ALL) Cells to Dexamethasone through Modulation of mTOR Activity and Stimulation of Autophagy.* PLOS ONE, 2016. **11**(5): p. e0155893.

70. Kun, E., et al., *MEK inhibitor resistance mechanisms and recent developments in combination trials.* Cancer treatment reviews, 2021. **92**: p. 102137.

APPENDIX 1

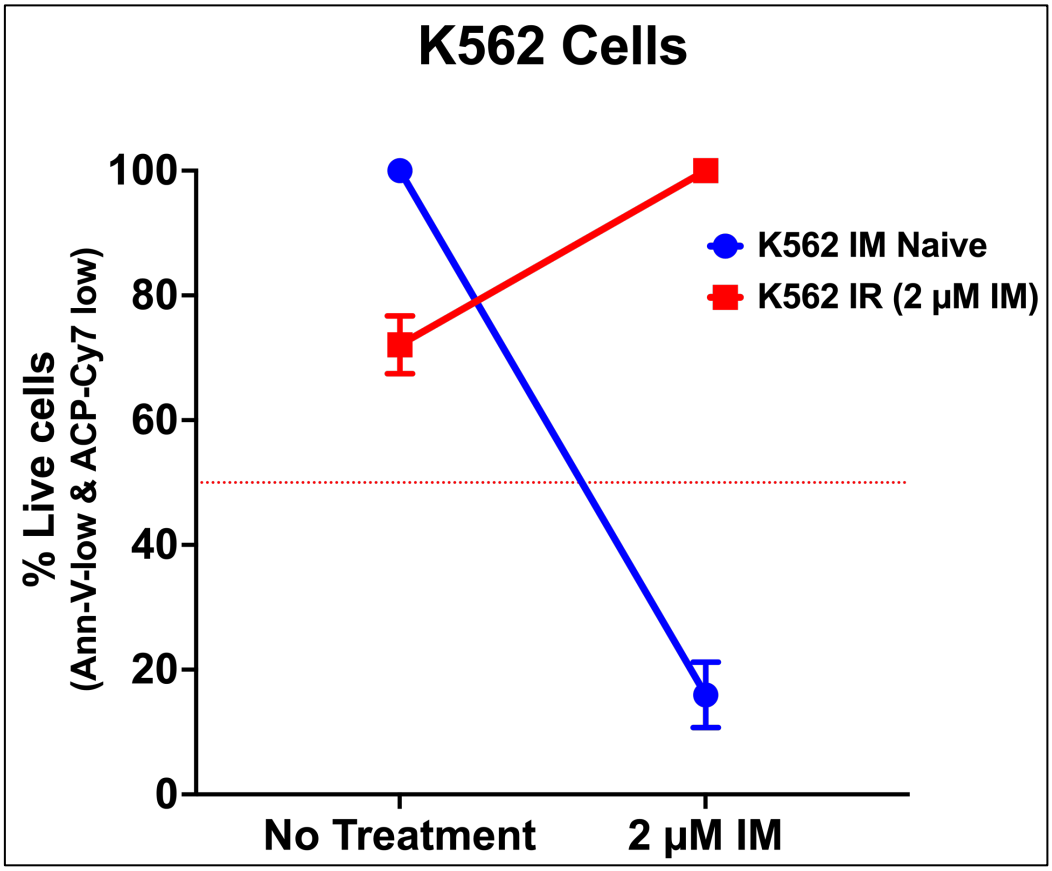

Viability of Imatinib-Resistant (2 µM) K562 Cells in Response to Imatinib Withdrawal and Imatinib Treatment. Imatinib-resistant K562 cells were generated using a dose escalation protocol, similar to SUP-B15 IR cells, resulting in the development of stable cells at 2 µM imatinib. In this experiment, imatinib resistant K562 cells were incubated in TKI free media overnight and both K562 naïve and imatinib-resistant cells were subjected to treatment with 2 µM imatinib for a duration of 72 hours. Viability was assessed using flow cytometry by measuring Annexin-V-PE and Fixable Viability Stain 780. The Y-axis represents the percentage of viable cells, which is indicated by Annexin-V-PE low and Fixable Viability Stain low values. The graph displays data collected from at least three independent experiments (n=3). The primary mechanism of resistance observed in the imatinib-resistant K562 cells is characterized by BCR::ABL1 overexpression.

APPENDIX 2

N=1

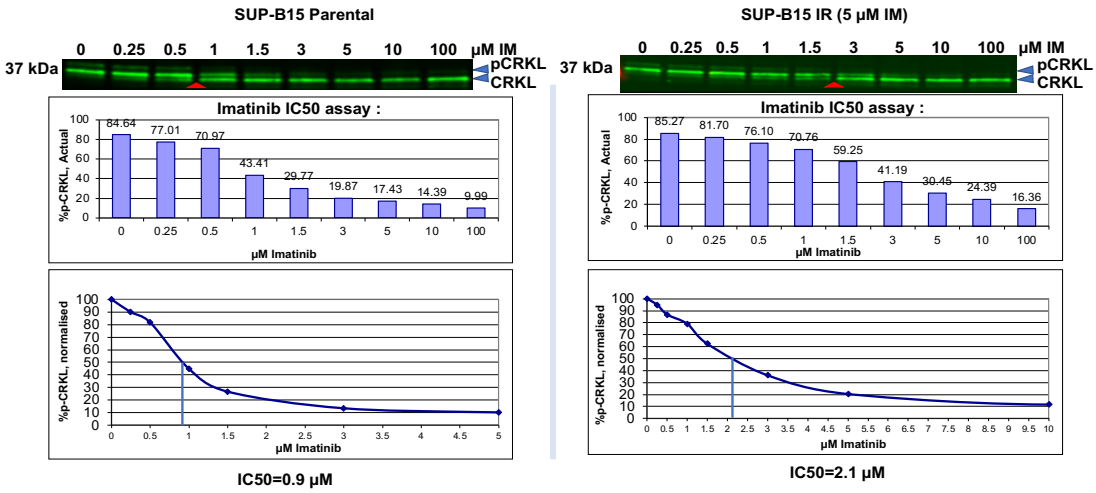

IC50=0.9 µM

IC50=2.1 µM

N=2

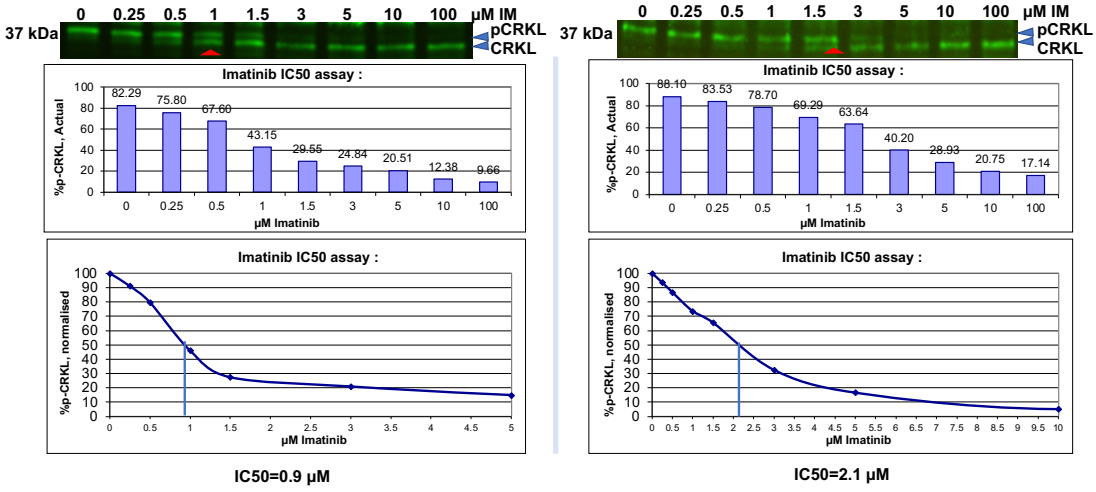

IC50=0.9 µM

IC50=2.1 µM

N=3

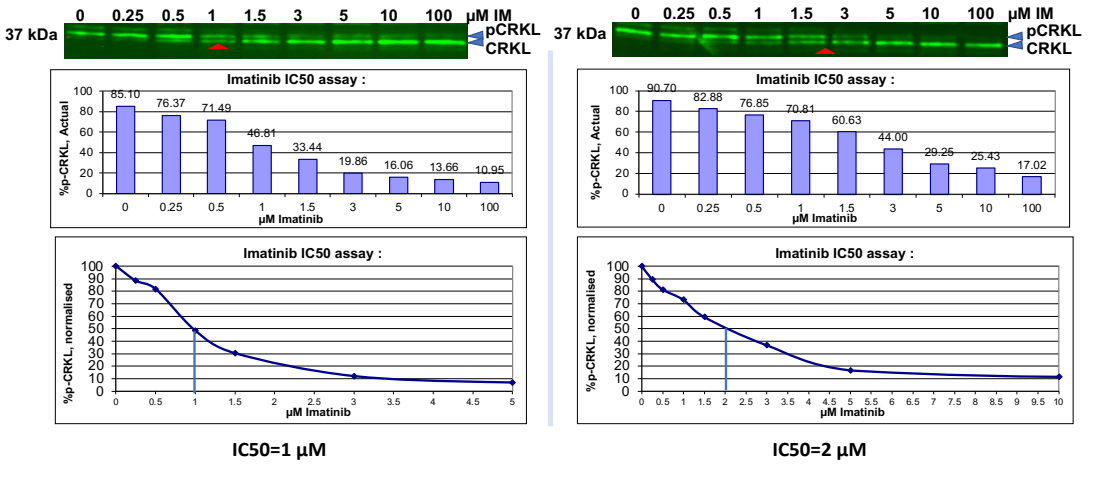

IC50=1 µM

IC50=2 µM

1. SUP-B15 IR cells have higher imatinib pCRKL IC50 compared to SUP-B15 P cells.

To investigate the differential sensitivity to imatinib, Western immunoblotting was conducted to assess the pCRKL IC50 in SUP-B15 P (parental) and IR (imatinib-resistant) cells. These cells were exposed to increasing concentrations of imatinib (ranging from 0.25 µM to 100 µM) for a 2-hour incubation at 37°C with 5% CO_2. SUP-B15 IR cells underwent overnight washout as described in '2.7.3. Cell washout protocol for TKI resistant cells of Chapter 2: Methods and Materials'. Subsequently, densitometry analysis of both pCRKL and CRKL protein levels was carried out using Image Studio Lite software, and corresponding graphs were generated. The concentration of imatinib required to inhibit pCRKL by 50% within this 2-hour timeframe (IC50) was calculated using Microsoft Excel. The presented Western blots represent data collected from three independent experiments (n=1-3), with a red triangle indicating the approximate IC50 concentration.

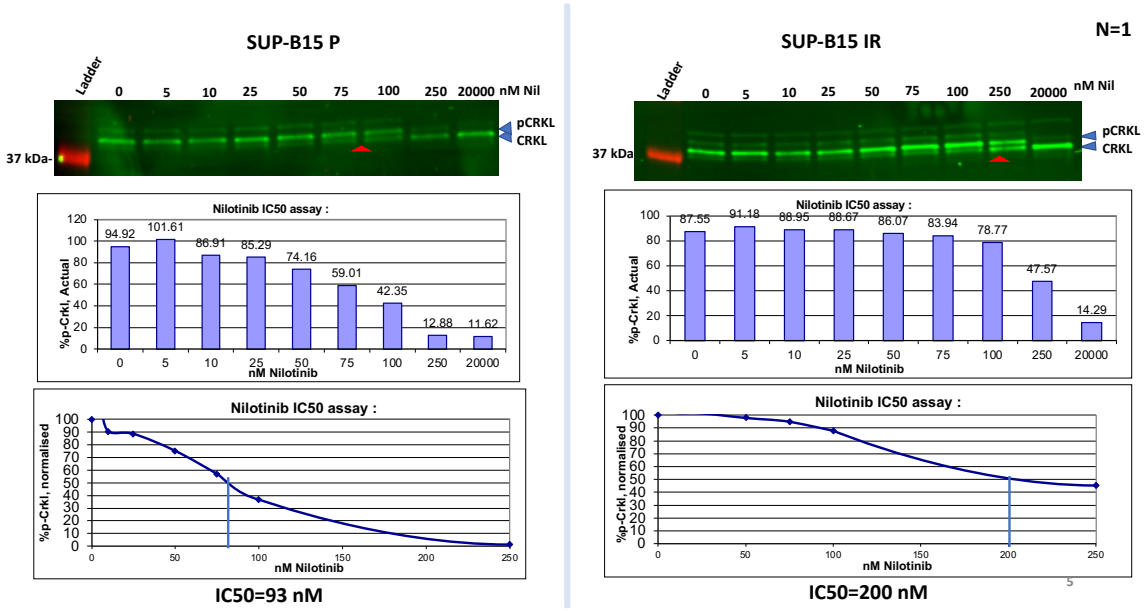

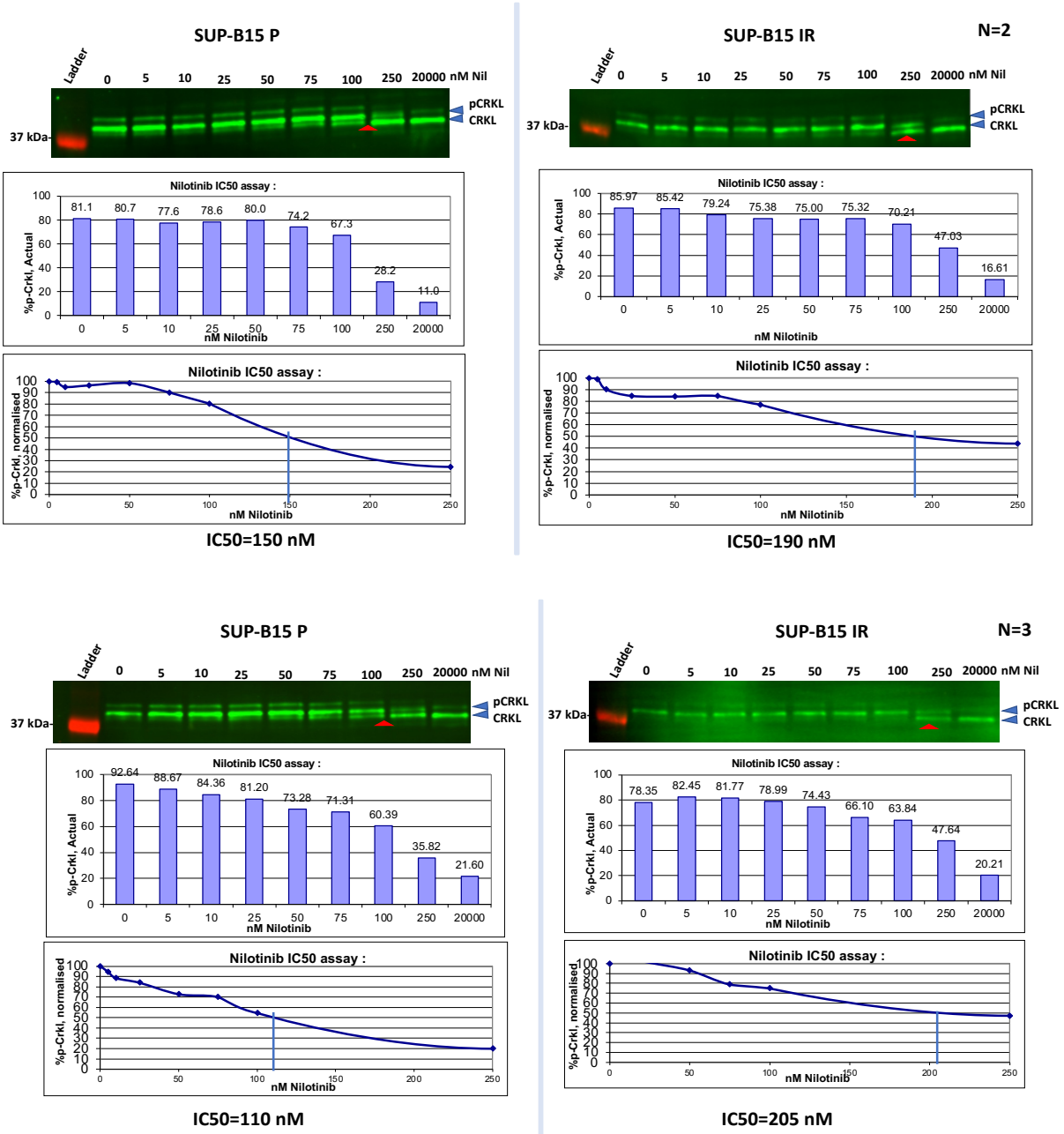

2. SUP-B15 IR cells have higher nilotinib pCRKL IC50 compared to SUP-B15 P cells.

To investigate the differential sensitivity to nilotinib, Western immunoblotting was conducted to assess the pCRKL IC50 in SUP-B15 P (parental) and IR (imatinib-resistant) cells. These cells were exposed to increasing concentrations of nilotinib, ranging from 5 nM to 20,000 nM, for a 2-hour incubation at 37°C with 5% CO_2. SUP-SUP-B15 IR cells underwent overnight washout as described in '2.7.3. Cell washout protocol for TKI resistant cells of Chapter 2: Methods and Materials'. Subsequently,

densitometry analysis of both pCRKL and CRKL protein levels was performed using Image Studio Lite software, and corresponding graphs were generated. The concentration of nilotinib required to inhibit pCRKL by 50% within this 2-hour timeframe (IC50) was calculated using Microsoft Excel. The presented Western blots represent data collected from three independent experiments (n=1-3), with a red triangle indicating the approximate IC50 concentration.

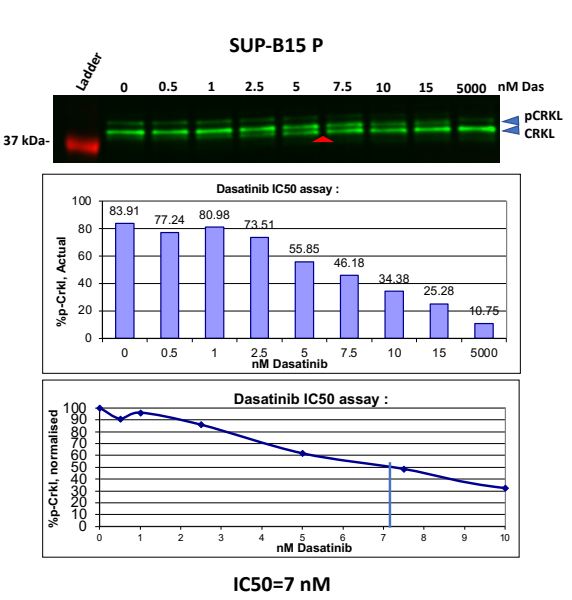

IC50=7 nM

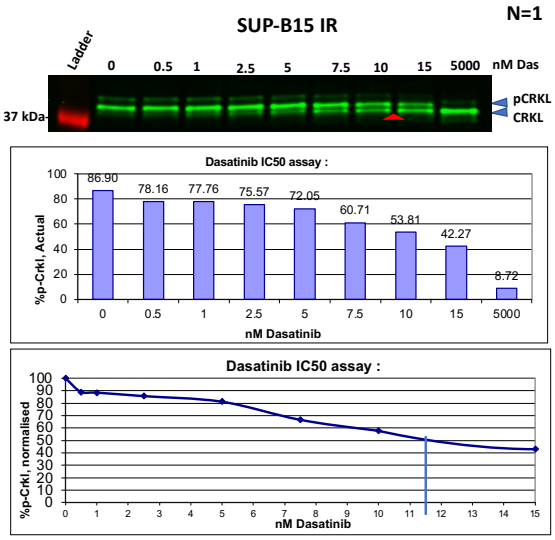

IC50=11.5 nM

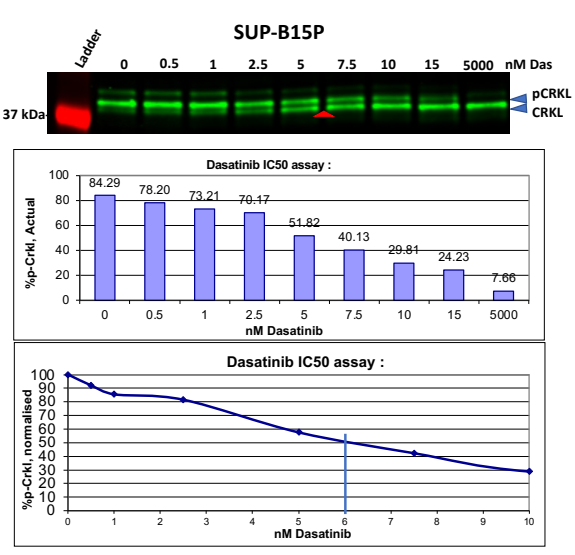

IC50=6 nM

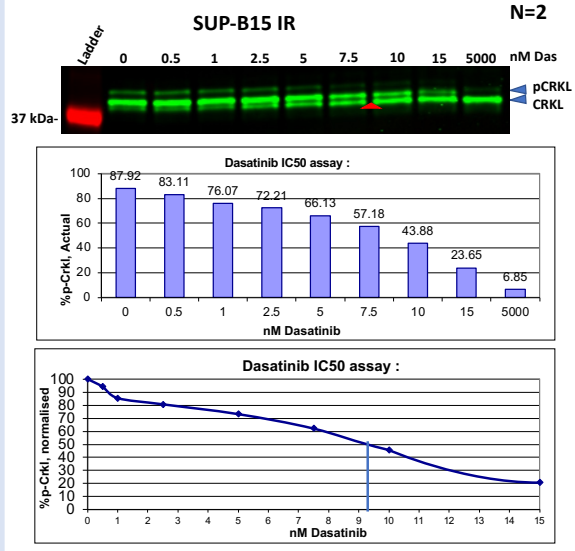

IC50=9.4 nM

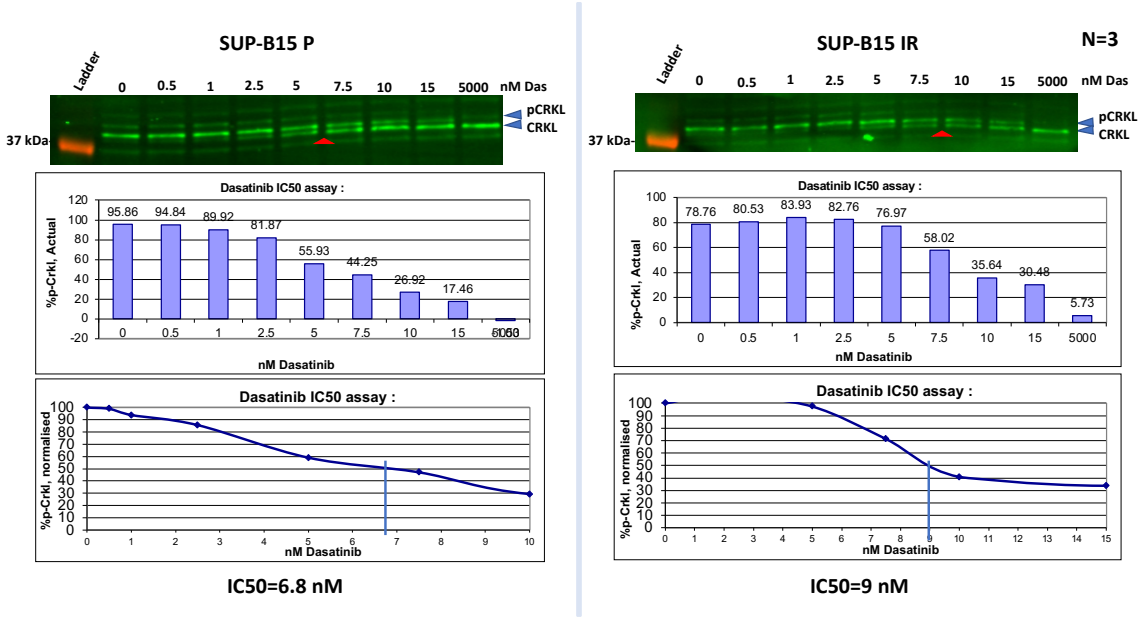

3. **SUP-B15 IR cells have higher dasatinib pCRKL IC50 compared to SUP-B15 P cells.** To investigate differences in sensitivity to dasatinib, Western immunoblotting was conducted to assess the pCRKL IC50 in SUP-B15 P (parental) and IR (imatinib-resistant) cells. These cells were exposed to increasing concentrations of dasatinib, ranging from 0.5 nM to 5000 nM, for a 2-hour incubation at 37°C with 5% CO_2. SUP-B15 IR cells underwent overnight washout as described in '2.7.3. Cell washout protocol for TKI resistant cells of Chapter 2: Methods and Materials'. Following treatment, densitometry analysis of both pCRKL and CRKL protein levels was performed using Image Studio Lite software, and corresponding graphs were generated. The concentration of dasatinib required to inhibit pCRKL by 50% within this 2-hour timeframe (IC50) was calculated using Microsoft Excel. The presented Western blots represent data collected from three independent experiments (n=1-3), with a red triangle indicating the approximate IC50 concentration.

SUP-B15 P

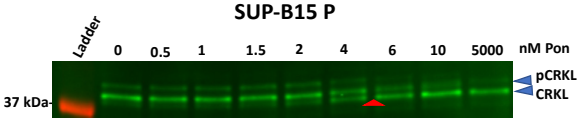

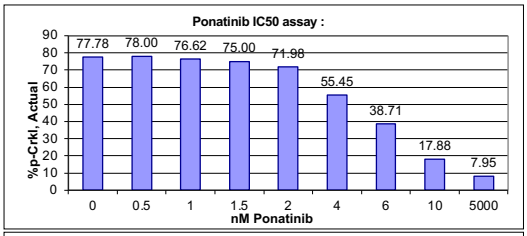

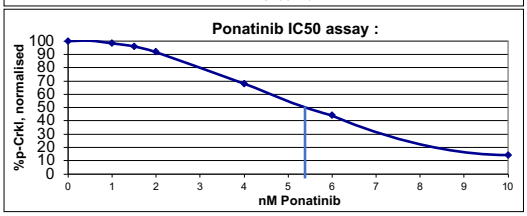

IC50=5.4 nM

SUP-B15 IR

N=1

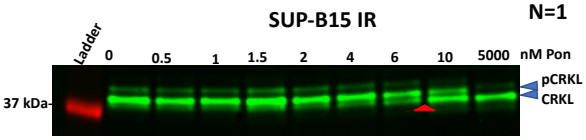

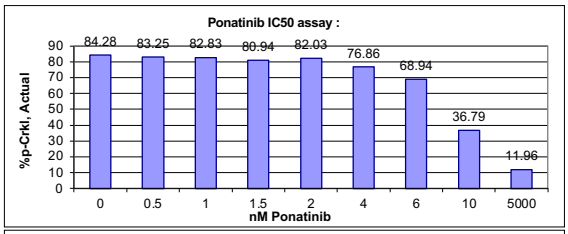

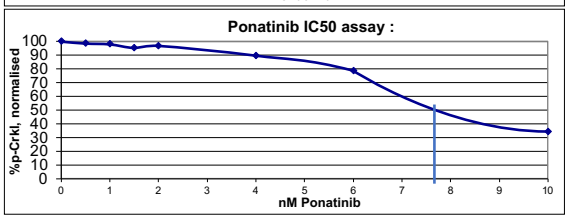

IC50=7.8 nM

SUP-B15 P

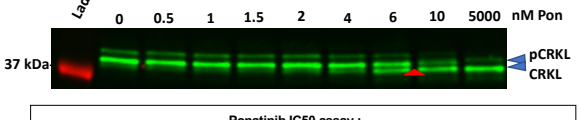

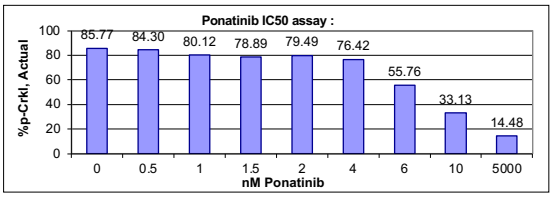

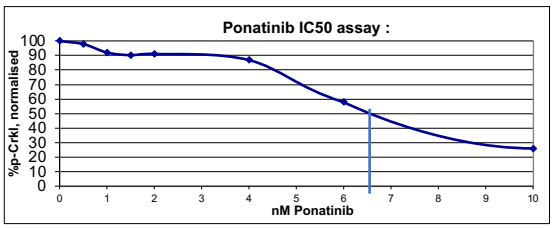

IC50=6.5 nM

SUP-B15 IR

N=2

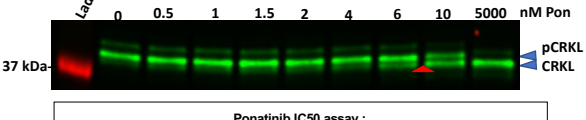

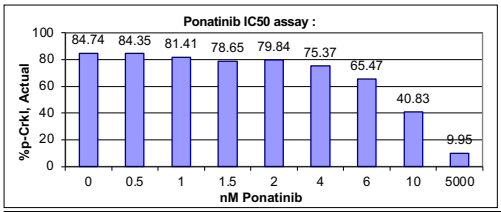

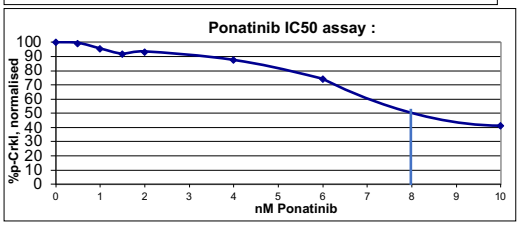

IC50=8 nM

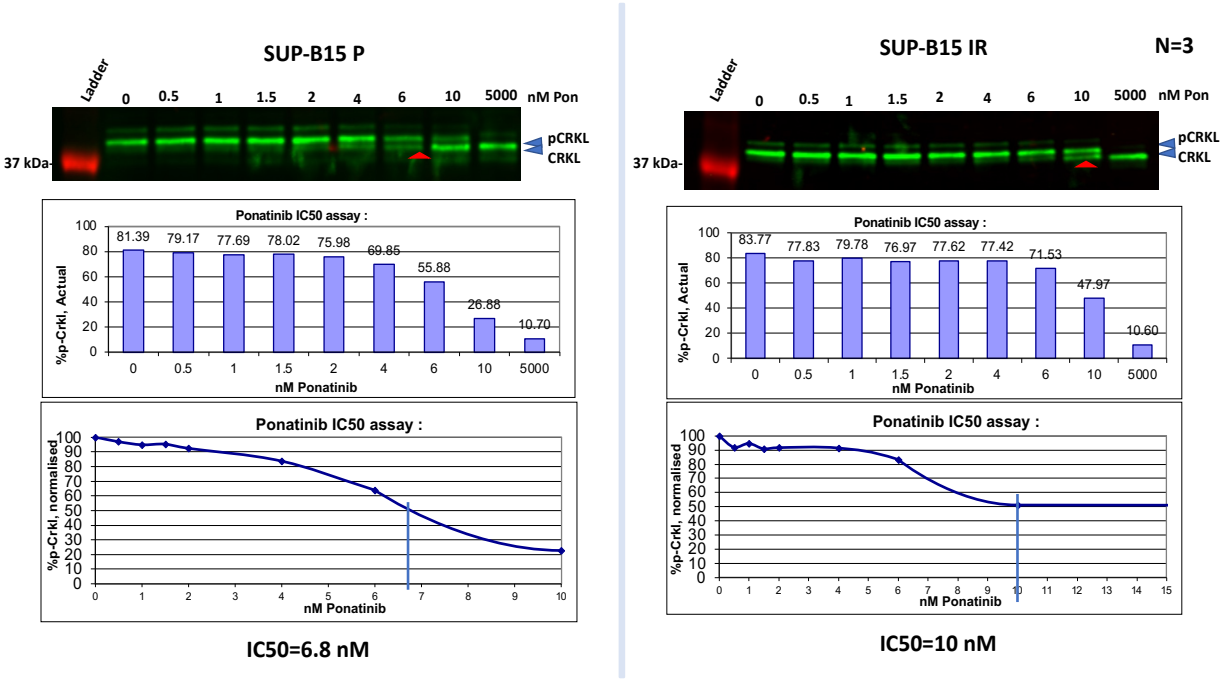

4. **SUP-B15 IR cells have higher ponatinib pCRKL IC50 compared to SUP-B15 P cells.** To investigate the differences in sensitivity to ponatinib, Western immunoblotting was conducted to assess the pCRKL IC50 in SUP-B15 P (parental) and IR (imatinib-resistant) cells. These cells were exposed to increasing concentrations of ponatinib, ranging from 0.5 nM to 5000 nM, for a 2-hour incubation at 37°C with 5% CO_2. SUP-B15 IR cells underwent overnight washout as described in '2.7.3. Cell washout protocol for TKI resistant cells of Chapter 2: Methods and Materials'. Following treatment, densitometry analysis of both pCRKL and CRKL protein levels was performed using Image-Studio Lite software, and corresponding graphs were generated. The concentration of ponatinib required to inhibit pCRKL by 50% within this 2-hour timeframe (IC50) was calculated using Microsoft Excel. The Western blots displayed represent data from three independent experiments (n=1-3), with a red triangle indicating the approximate IC50 concentration.

APPENDIX 3

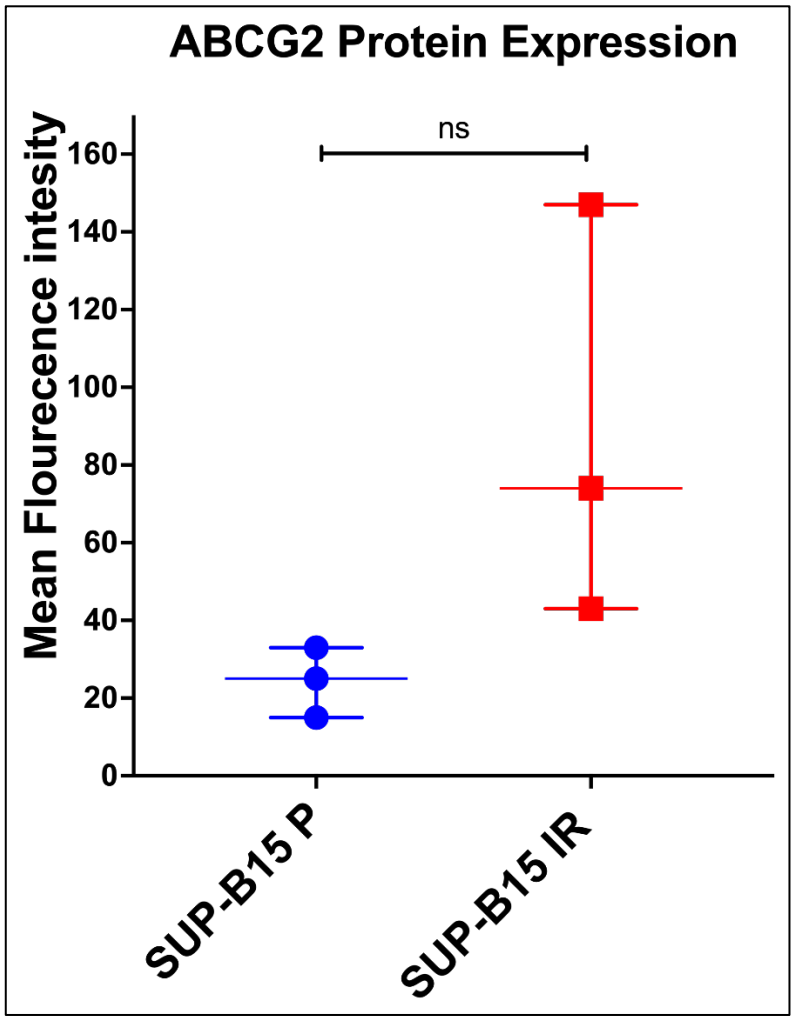

SUP-B15 IR cells exhibit similar ABCG2 protein expression levels. To assess the expression of the ABCG2 protein, phospho-flow analysis was conducted on SUP-B15 cells. Specifically, in cultures containing 5 μM imatinib, SUP-B15 IR (imatinib-resistant) cells were examined for potential differences in ABCG2 transporter protein expression when compared to SUP-B15 P (parental) cells. Statistical analysis was performed by using Unpaired t-test with Welch's correction. ABCG2 protein levels are quantified as the mean fluorescence intensity detected by the ABCG2 antibody. The data presented in this analysis were collected from three independent experiments (n=3).

APPENDIX 4

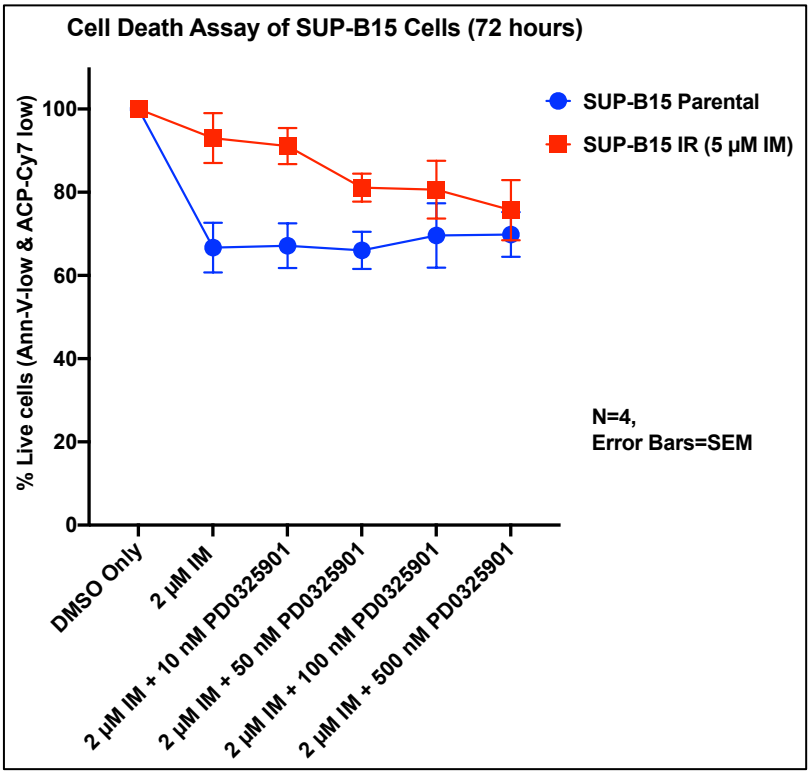

The effect of imatinib and MEK inhibitor combination treatment on SUP-B15 cells.

To evaluate the impact of combination treatment with 2 µM imatinib and increasing concentrations of the MEK inhibitor PD0325901, a cell death assay was conducted on SUP-B15 cells. The cells were treated for 72 hours, and viability was assessed by measuring Annexin-V-PE and Fixable Viability Stain 780 using flow cytometry. SUP-B15 IR cells underwent overnight washout procedure as described in '2.7.3. Cell washout protocol for TKI resistant cells of Chapter 2: Methods and Materials'. The Y-axis in the graph represents Annexin-V-PE low and Fixable Viability Stain low values, expressed as a percentage of viable cells. The data presented in this analysis were obtained from three independent experiments (n=3), and error bars indicate the standard deviation (SD) based on these three independent experiments.

CHAPTER 4: Cell line modelling confirms the role of Phosphotyrosine phosphatase domain PTPN11 mutations in the development of TKI resistance and overexpression of BCL-XL and MCL-1

Chapter 4 Summary

Chapter 3 provides insights into the mechanisms driving TKI resistance in SUPB15 IR cells, emphasizing the roles of p-BCR::ABL1(Y177), sustained activation of pERK1/2, and the upregulation of anti-apoptotic proteins BCL-XL and MCL-1. While the study suggests the potential of the MEK inhibitor in targeting the RAS/ERK pathway to combat this resistance, it's essential to acknowledge certain limitations within these findings. Notably, the removal of imatinib from resistant cells may have rendered them more susceptible to MEK inhibitor treatment. Additionally, the higher toxicities associated with MEK inhibitors necessitate exploration of alternative, more precisely targeted treatment strategies. Furthermore, the exact mechanisms underlying the overexpression of pERK1/2, MCL-1, and BCL-XL in SUP-B15 IR cells remain elusive, highlighting the need for further investigation in this area.

RNAseq analysis conducted in Chapter 4 identified two mutations within the phosphotyrosine phosphatase (PTP) domain of the PTPN11 gene (p.A461T and p.P491H) in SUPB-15 IR cells, which are absent in their parental counterparts. Notably, p.A461T mutation is commonly associated with developmental disorders, while p.P491H is prevalent in haematological malignancies, including acute lymphoblastic leukaemia and juvenile myelomonocytic leukaemia [1-4]. In Chapter 4, these mutations were meticulously modelled in multiple cell lines to investigate their potential involvement in the development of both BCR::ABL1-dependent and -independent mechanisms of resistance across various cell models.

Introduction

Tyrosine Kinase Inhibitors (TKIs) have significantly improved the outcomes of patients with Ph+ leukaemias. However, the development of TKI resistance poses a substantial challenge, particularly for those without ABL1 kinase domain mutations. Instead, many of these patients acquire non-BCR::ABL1 mutations in genes such as IKAROS Family Zinc Finger 1 (*IKZF1*), Additional Sex Combs Like 1 (*ASXL1*), runt-related transcription factor 1(*RUNX1*), Tumour Protein P53 (*TP53*), cyclin-dependent kinase inhibitor 2A/B (*CDKN2A/B*), Paired Box 5 (*PAX5*), and B-Cell Translocation Gene 1 (*BTG1*). These mutations are associated with poor prognosis [5, 6]. Advances in next-generation sequencing now allow for more sensitive detection of clinically relevant somatic mutations, offering the potential for a precision medicine approach to enhance response rates in Ph+ leukaemia [7].

Activating lesions of Rat Sarcoma (RAS)-Extracellular Signal-Regulated Kinase (ERK) pathway genes (*NRAS, KRAS, PTPN11, NF1*) and *BRAF* functionally mimic pre-BCR signalling by activating oncogenic RAS/ERK pathway leading to tumour progression in B-cell malignancies [8]. Specifically, mutations in Phospho-Tyrosine Phosphatase Nonreceptor type-11 (*PTPN11*) have been well-documented in various forms of leukaemia [9]. In patients with Ph+ leukaemia, including Chronic Myeloid Leukaemia (CML) and Ph+ Acute Lymphoblastic Leukaemia (ALL), PTPN11 mutations are associated with poor prognosis [10, 11].

PTPN11 encodes Src homology phosphatase-2 (SHP-2), a phosphotyrosine phosphatase with N-SH2 and C-SH2 domains and a phosphotyrosine phosphatase (PTP) domain at the C-terminus [12]. SHP-2 functions downstream of receptor tyrosine kinases, acting as a

positive regulator of the RAS/ERK pathway in response to growth factors [13, 14]. This allosteric enzyme can toggle between its N-SH2 and PTP domains, playing a crucial role in BCR::ABL1-induced myeloid and lymphoid leukaemia [15][16].

Interestingly, germline mutations in PTPN11 result in developmental disorders, including Noonan syndrome (NS) and Noonan syndrome with multiple lentigines (NSML) or LEOPARD syndrome, with up to 90% of NSML cases linked to PTPN11 mutations [17, 18][19]. Children with Noonan syndrome carrying PTPN11 mutations have an increased risk of developing various leukaemia, such as Juvenile Myelomonocytic Leukaemia (JMML), acute myeloid leukaemia, chronic myelomonocytic leukaemia, myelodysplastic syndrome, and B-ALL [20-22]. A smaller percentage of Noonan syndrome patients have also been reported to develop CML, and Hodgkin's Lymphoma [23-28].

Notably, most cancer and Noonan syndrome-associated PTPN11 mutations are somatic gain-of-function mutations, such as E76K and D61Y, located at the interface of N-SH2 and the PTP domain, rendering SHP-2 constitutively active and in the open conformation [29]. Conversely, loss-of-function mutations, including A461T, T468M and G503R/A, primarily found within the PTP domain, affect SHP-2's catalytic activity and are prevalent in NSML and JMML patients [30, 31]. Despite studies indicating that PTPN11 mutations are linked to a poor clinical prognosis and therapy resistance, the role of PTP domain PTPN11 mutations in driving resistance in Ph+ ALL remains insufficiently understood.

This study seeks to answer the question of whether PTP domain PTPN11 mutations contribute to TKI resistance in Ph+ ALL. Notably, developing SHP-2 inhibitors to target activating mutations has been challenging due to the high homology with SHP-1, which

plays a significant role in imatinib resistance in CML cell lines [32]. Therefore, cancers with PTP domain PTPN11 mutations currently lack targeted therapies, primarily due to the difficulty in directly targeting PTPN11 and limited understanding of the pathogenesis involving PTPN11 mutations [33].

In this chapter, I employ RNAseq analysis to compare mutations between SUP-B15 parental and imatinib-resistant SUP-B15 (SUP-B15 IR) cells. RNAseq analysis identified two PTP domain PTPN11 mutations (p.A461T VAF% and p.P491H VAF%) in SUP-B15 IR cells. I investigated the transformative potential of these mutations in murine pro-B (BaF3) cells and their role in TKI resistance when overexpressed in BaF3 cells transduced with BCR::ABL1 p190. Furthermore, I confirmed my findings by knocking down the PTPN11 gene in SUP-B15 IR cells, which fully restored imatinib sensitivity. Overexpression of PTPN11 mutations led to increased expression of anti-apoptotic proteins MCL-1 and BCL-XL, providing a survival advantage to BaF3 cells without IL-3 supplementation. Knocking down PTPN11 in SUP-B15 IR cells not only reduced pERK1/2 but also diminished MCL-1 and BCL-XL expression. Finally, I explored the therapeutic potential of targeting the SHP-2 pathway in SUP-B15 IR cells. This study underscores the critical role of SHP-2 in maintaining TKI sensitivity in BCR::ABL1-positive leukaemia and highlights the challenges when SHP-2 is mutated in Ph+ ALL cells.

Results

RNAseq identified two PTPN11 mutations in imatinib resistant SUP-B15 cells

To investigate the mechanisms of resistance involved in SUP-B15 IR cells, I utilized our standard ALL pipeline established for detecting variants (SNVs and INDELs) and gene fusions by mRNA sequence analysis in patients [34] and performed mRNA sequencing in SUP-B15 cells. Briefly, total RNA was extracted from SUP-B15 cells and converted to strand-specific Illumina compatible sequencing libraries. Library pool was sequenced by using Illumina Nextseq. The reads were then mapped to the GRCh37 human reference genome. Please, refer to **2.13 Transcriptomic Sequencing (mRNA-seq)** in Chapter 2 for more details.

RNA-seq analysis of SUP-B15 IR cells revealed the presence of two mutations in the PTPN11 gene (p.A461T and p.P491H) with variant allele frequencies (VAF) of 63.7% and 40.2%, respectively, which were absent in the parental cell line (**Figure 4.1A**). The identified PTPN11 mutations from the RNA-seq analysis were further validated through Sanger sequencing (**Appendix 1 A-D**). For more details on the RNAseq analysis please refer to "Chapter 2: Materials and Methods in section **2.13 Transcriptomic Sequencing (mRNA-seq)**". While these mutations exhibit sub-clonal characteristics with VAFs less than 100%, further investigation into the PTPN11 gene was conducted by PCR amplification from SUP-B15 IR cells, followed by insertion into a vector and subsequent Sanger sequencing. Notably, this analysis revealed that both mutations were co-located on the same allele (detailed in **Appendix1 E-G**). These mutations were confirmed as somatic variants in the COSMIC database and were found to be located within the PTP domain (**Figure 4.1B**). Importantly, these mutations have been previously described as gain-of-function mutations, with p.A461T associated with a loss of catalytic activity [4].

SHP-2 protein, encoded by PTPN11, exhibited a moderate reduction in expression in the resistant SUP-B15 cells (p = 0.0014) (**Figure 4.1E and F**). It's worth highlighting that gene ontology analysis revealed a pattern of positive regulation of the ERK1/2 cascade in SUP-B15 IR cells, providing additional support for the hypothesis that the RAS/ERK pathway may play a role in the mechanisms of resistance (**Figure 4.1C**). The RNAseq analysis was conducted on SUP-B15 IR cells 72 hours after imatinib washout. Consequently, the observed enrichment of pERK1/2, as depicted in continuous imatinib culture **(Figure 3.7 of Chapter 3)**, may not have been fully captured.

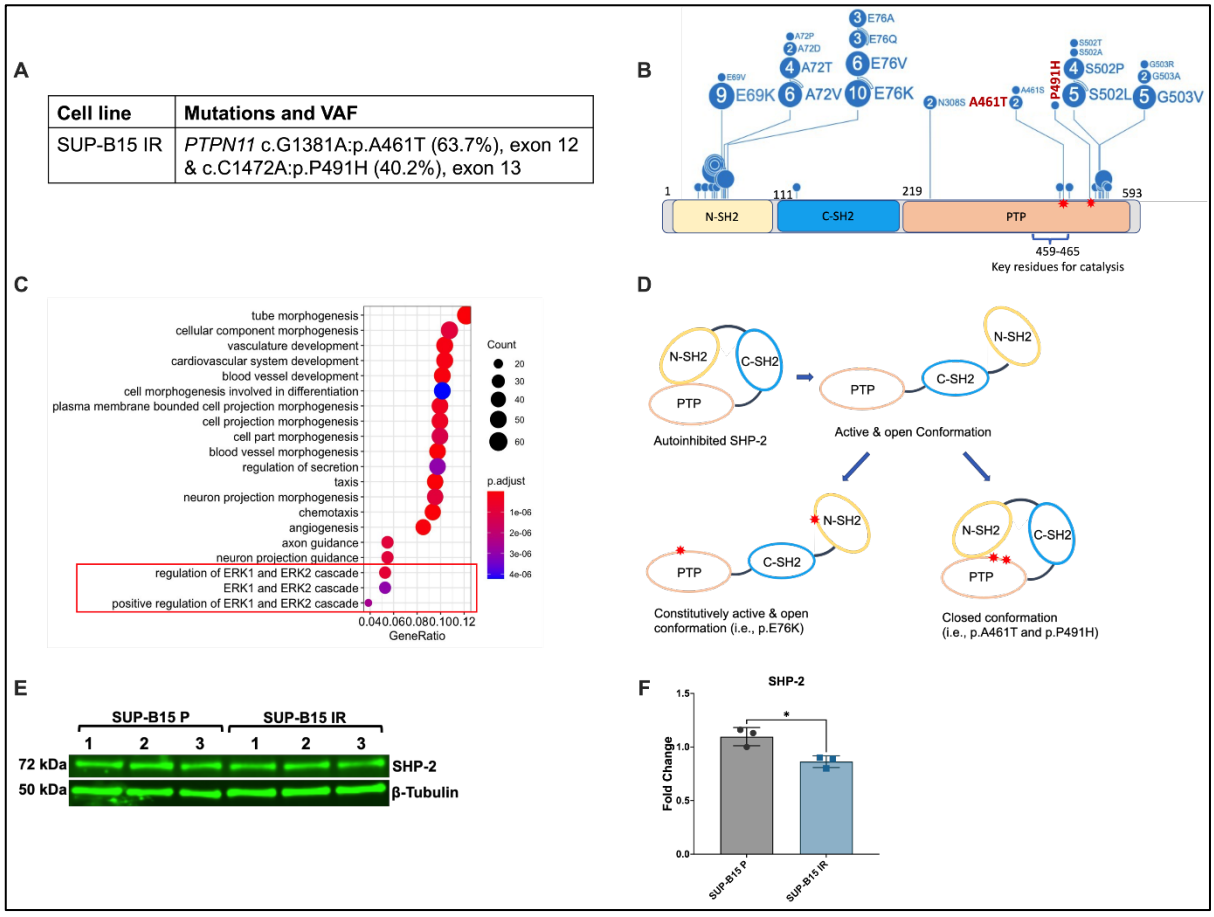

Figure 4.1: **SUP-B15 IR cells have two *PTPN11* mutations**. (A) Mutations specific to SUP-B15 IR cells, absent in SUP-B15 P cells, are depicted along with their respective locations and variant allele frequencies (VAFs). (B) A schematic representation of the

SHP-2 protein is provided, highlighting its N- and C-terminal SH2 domains, phosphotyrosine phosphatase (PTP) domain, and common PTPN11 mutations found in paediatric cancers, as obtained from St. Jude Cloud. Notably, PTPN11 p.A461T and p.P491H mutations, identified in RNAseq analysis of SUP-B15 IR cells, are highlighted in red. Three independent replicates (n=3) were used. (C) Visual representation of gene ontology (GO) analysis of RNAseq data. Enriched GO categories associated with the gene expression profile of SUP-B15 IR cells are highlighted with biological pathways and molecular functions significantly linked to these cells. (D) A schematic diagram showcases the SHP-2 protein in various conformations, including the autoinhibited closed state, active and open states. Depending on mutation status, the protein can assume either a constitutively active and open or closed conformation. (E, F) Western blot analysis and densitometry assessment of SHP-2 expression in SUP-B15 IR cells continually cultured in 5 μM imatinib compared to the parental control. Samples from three independent experiments (n=3) are indicated as numbers 1-3. Statistical analysis was conducted using an unpaired t-test. Error bars represent standard deviation (SD) derived from three independent experiments. '*' signifies $p \leq 0.05$.

PTPN11 mutations identified in TKI resistant SUP-B15 cells provided survival advantage to BaF3 cells in the absence of IL-3 via anti-apoptotic pathway activation

To test any transformative potential of either of mutations *PTPN11* p.A461T, p.P491H or *PTPN11* compound p.A461T + p.P491H mutations, I introduced the empty pLVX-EF1α-IRES-ZsGreen1 mammalian expression vector and pLVX containing *PTPN11* wild type, *PTPN11* with p.A461T, p.P491H, compound p.A461T + p.P491H and p.E76K mutants into BaF3 cells. I included *PTPN11* p.E76K mutation because it is the most common gain of

function *PTPN11* mutation reported in leukaemia including JMML and this mutation renders SHP-2 into a constitutively active open conformation [4, 35, 36]. Studies have shown that both *PTPN11* p.A461T and p.P491H mutations individually do not affect the conformation of SHP-2 protein [4]. Successful transduction of PTPN11 mutants were confirmed by measuring GFP by flow cytometry and SHP-2 protein expression by Western blot (**Appendix 2A**). Overexpression of wild type or *PTPN11* p.A461T, p.P491H or p.E76K mutants individually did not provide any survival advantage to BaF3 cells without IL-3 (**Figure 4.2A**). To the contrary, *PTPN11* compound p.A461T + p.P491H mutations, provided survival advantage to BaF3 cells ($p<0.0001$) when IL-3 was removed from the culture for 72 hours (**Figure 4.2A**). In the absence of IL-3, none of the PTPN11 mutations exhibited a comparable transformative potential compared to BaF3 BCR::ABL1 p190 cells [37] (**Figure 4.2A**). This means that the PTPN11 mutations, when introduced into BaF3 cells, did not possess the capability to eliminate the requirement for IL-3 to drive cell growth in these cells. Transformative potential is defined as the capacity of a genetic mutation to either independently induce or significantly contribute to the process of cellular transformation. BaF3 *BCR::ABL1* p190 is a known reference point for assessing the transformative potential of genetic alterations. BaF3 *BCR::ABL1* p190 was included as a positive control because it is IL-3 independent. To minimize the potential impact of off-target effects and ensure the robustness of my findings, I independently generated BaF3 cells with PTPN11 mutants through two separate lentiviral transduction experiments. This approach was adopted to enhance the reliability and reproducibility of the observed phenotypes associated with PTPN11 mutations.

Compelling evidence that BaF3 cells transduced with PTPN11 mutations may have anti-apoptotic pathway activation was tested by measuring anti-apoptotic proteins BCL-XL, MCL-1 and BCL-2 by Western blot. While overexpression of PTPN11 mutants including p.E76K did not affect the expression of pERK1/2, the expression of anti-apoptotic protein MCL-1 was higher in BaF3 cells transduced with p.A461T + p.P491H (p=0.022) and p.E76K (p=0.008) (**Figure 4.2B-E**). Expression of anti-apoptotic protein BCL-XL was also increased in response to PTPN11 p.A461T + p.P491H (p=0.036) and p.E76K (p=0.0014) in BaF3 cells (**Figure 4.2B and F**). There was no difference in BCL-2 expression in BaF3 cells in response overexpression of either p.A461T or p.P491H or compound p.A461T + p.P491H and p.E76K PTPN11 mutant (**Appendix 2**). The results are consistent with BCL-XL and MCL-1 overexpression in SUP-B15 IR cells with PTP domain PTPN11 mutations.

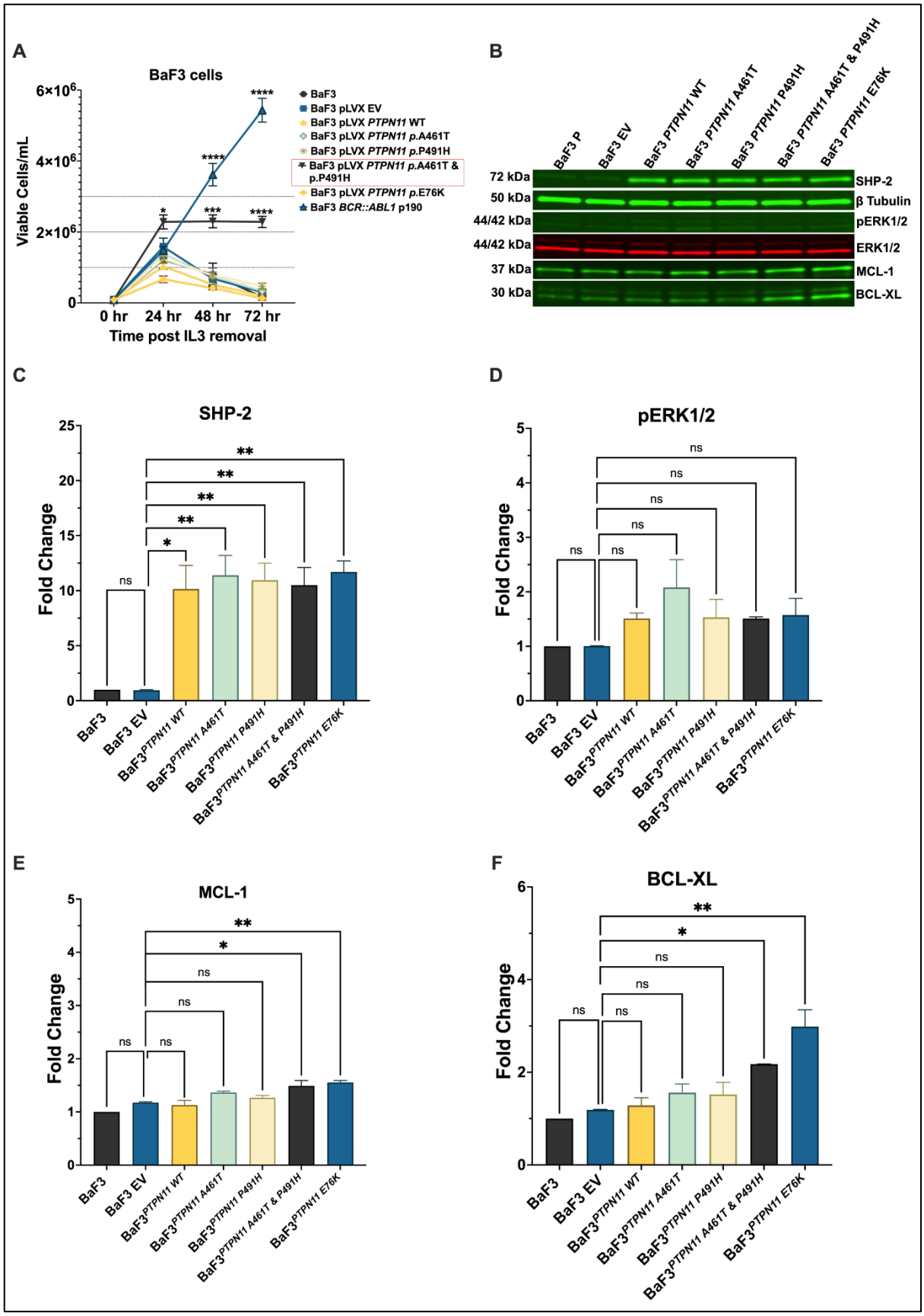

Figure 4.2: Mutations found in SUP-B15 IR cells provided survival advantage to

BaF3 cells without IL-3. (A) BaF3 cells transduced with pLVX+ PTPN11 constructs, including empty vector, wild type, A461T, P491H, A461T and P491H, and E76K mutants, were subjected to a trypan blue exclusion viability assay. Cell viability was monitored for up to 72 hours following IL-3 withdrawal. (B-F) Western blot analysis of SHP-2, pERK1/2, MCL-1, and BCL-XL expression in BaF3 cells transduced with various PTPN11 constructs. Data presented are derived from at least two independent experiments (n=2). Statistical analysis was conducted using One-Way ANOVA. Error bars represent the standard deviation (SD) based on at least two independent experiments. 'Ns' signifies p>0.05, *, **, *** and **** represent p≤0.05, p≤0.01, p≤0.001 and p≤0.0001, respectively.

PTPN11 mutations identified in TKI resistant SUP-B15 cells led to the development of imatinib resistance in BaF3 *BCR::ABL1* p190 cells

To independently validate the effects of *PTPN11* p.A461T and p.P491H mutations on TKI resistance, I introduced the empty pLVX-EF1α-IRES-ZsGreen1 mammalian expression vector and pLVX containing *PTPN11* wild type, *PTPN11* with p.A461T, p.P491H, compound p.A461T + p.P491H or p.E76K mutants into BaF3 *BCR::ABL1* p190 cells. I again included the gain of function *PTPN11* mutation, p.E76K, into this study as a positive control. Successful transduction of PTPN11 mutants were confirmed by measuring GFP by flow cytometry (**Appendix 2B**) and by measuring SHP-2 protein overexpression by Western blot (**Figure 4.3A and B**). Phospho-BCR::ABL1(Y177) was not affected by SHP2 overexpression in BaF3 *BCR::ABL1* p190 cells (**Figure 4.3C**).

Cell death assay showed that *PTPN11* p.A461T and compound p.A461T + p.P491H mutations led to higher LD50s for imatinib (1.98±0.33 μM, p<0.0001 and 3.43±0.11 μM, p<0.0001 respectively vs 0.61±0.52 μM for empty vector) when overexpressed in BaF3

BCR::ABL1 p190 cells (**Figure 4.3D and E**). Overexpression of either wild type PTPN11 (0.23±0.04 μM vs 0.61±0.52 μM for empty vector control, p=0.268) or p.P491H (0.13±0.07 μM vs 0.61±0.52 μM for empty vector control, p=0.117) mutation or p.E76K (0.22±0.08 μM vs 0.61±0.52 μM, p=0.251) mutation did not induced imatinib resistance in BaF3 *BCR::ABL1* p190 cells (**Figure 4.3D and E**). Results suggest that mutations that reduces catalytic activity of SHP-2 protein (such as p.A461T) may be responsible for the development of imatinib resistance not the mutations that increases SHP-2 activity such as p.E76K in BaF3 *BCR::ABL1* p190 cells. I tested whether BaF3 *BCR::ABL1* p190 cells transduced *PTPN11* p.A461T and compound p.A461T + p.P491H mutations were sensitive to higher generation TKIs. I excluded p.P491H and p.E76K mutants, as they are already sensitive to imatinib. While BaF3 *BCR::ABL1* p190 cells transduced with *PTPN11* p.A461T mutation alone only showed reduced sensitivity to asciminib, an allosteric inhibitor of BCR::ABL1, the *PTPN11* compound p.A461T + p.P491H mutations had reduced sensitivity to all TKIs tested including nilotinib, dasatinib, ponatinib and asciminib (**Figure 4.3F**)**.** Asciminib resistance in BaF3 *BCR::ABL1* p190 cells transduced with *PTPN11* p.A461T mutation support the argument that p.A461T mutant may be responsible for BCR::ABL1 dependent mechanism of resistance. Sensitivity to higher generation TKIs seen in imatinib resistant p.A461T mutant further support this hypothesis. Taken together, these results are consistent with the hypothesis that the *PTPN11* compound p.A461T + p.P491H mutations drive BCR::ABL1 independent TKI resistance and additionally possible BCR::ABL1 dependent mechanism seen in p.A461T mutant BaF3 *BCR::ABL1* p190 cells.

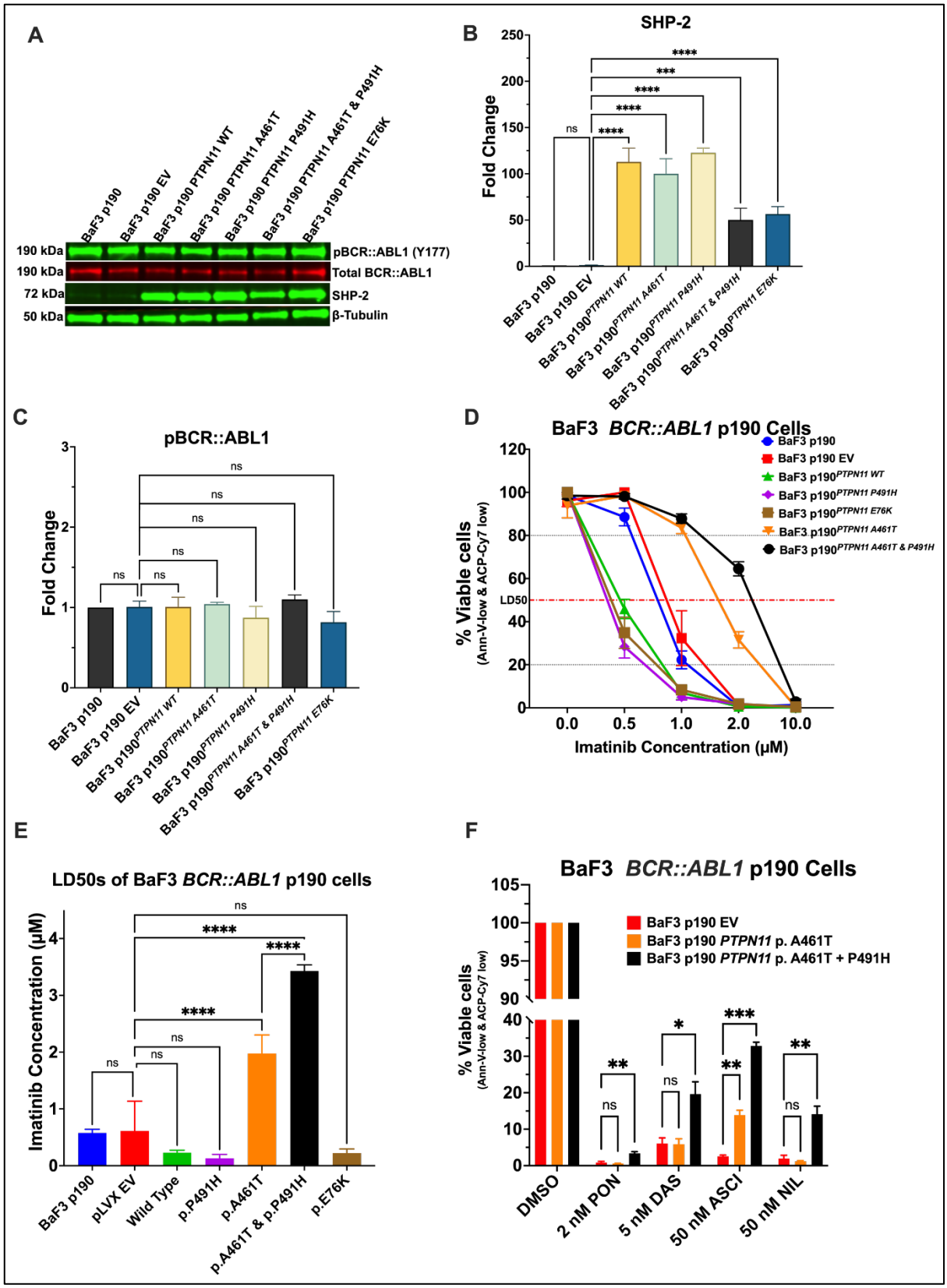

Figure 4.3: ***PTPN11*** **p.A461T + p.P491H mutations led to TKI resistance in BaF3** ***BCR::ABL1*** **p190 cells.** (A-C) Western blot assessment of SHP-2 and pBCR::ABL1 (Y177)

expression in BaF3 BCR::ABL1 p190 cells transduced with pLVX constructs containing PTPN11 wild type, PTPN11 with p.A461T, p.P491H, p.A461T + p.P491H, or p.E76K mutants. (D) Cell death assay of BaF3 BCR::ABL1 p190 cells transduced with pLVX+ PTPN11 constructs, including empty vector, p.A461T, p.P491H, p.A461T + p.P491H, and p.E76K mutants. Cells were treated with increasing concentrations of imatinib for 72 hours, and viability was determined by measuring Annexin-V-PE and Fixable Viability Stain 780 using flow cytometry. The Y-axis represents Annexin-V-PE low and Fixable Viability Stain low, expressed as the percentage of viable cells. (E) LD50 values of PTPN11-transduced cells following 72-hour imatinib treatment. Statistical analysis was performed using Ordinary one-way ANOVA. (F) Cell death assay of BaF3 BCR::ABL1 p190 cells transduced with pLVX+ PTPN11 constructs, including empty vector, p.A461T, and p.A461T + p.P491H mutants. Cells were treated with 2 nM ponatinib, 5 nM dasatinib, 50 nM asciminib, and 50 nM nilotinib for 72 hours, and viability was assessed using Annexin-V-PE and Fixable Viability Stain 780 via flow cytometry. Data presented are from three independent experiments (n=3). Statistical analysis was performed by using One-Way ANOVA. Error bars represent standard deviation (SD) of three independent experiments. Ns, *, **, *** and **** represent $p>0.05$, $p\leq0.05$, $p\leq0.01$, $p\leq0.001$ and $p\leq0.0001$ respectively.

PTPN11 mutations identified in TKI resistant SUP-B15 cells led to higher imatinib IC50 in BaF3 *BCR::ABL1* p190 cells

To test my hypothesis from imatinib LD50 data that p.A461T mutant may be responsible for BCR::ABL1 dependent mechanism of resistance in BaF3 *BCR::ABL1* p190 cells, I assessed imatinib pCRKL IC50 for BaF3 *BCR::ABL1* p190 cells. BaF3 *BCR::ABL1* p190 cells transduced with *PTPN11* p.A461T and compound p.A461T + p.P491H mutations led to

higher IC50s for imatinib (2.37±0.4 μM, p<0.0001 and 2.5±0.1 μM, p<0.0001 respectively vs 1.03±0.15 μM for empty vector) (**Figure 4.4A-F and Appendix 3**). The effects of *PTPN11* p.P491H was similar to that of wild type on imatinib IC50 values (1.5±0.1 μM vs 1.3±0.1 μM, p=0.56 for wild type) and also had similar sensitivity to imatinib treatments when overexpressed in BaF3 *BCR::ABL1* p190 cells (LD50s 0.23±0.04 μM vs 0.13±0.07 μM imatinib respectively, p=0.999) (**Figure 4.4A-F, Appendix 3 and Figure 4.3E**). The results confirms that the PTPN11 p.A461T mutant was responsible for BCR::ABL1 dependent mechanisms of resistance in BaF3 *BCR::ABL1* p190 cells. Interestingly, PTPN11 p.E76K mutant, unable to induce imatinib resistance when overexpressed in BaF3 *BCR::ABL1* p190 cells also had higher IC50 for imatinib (3.03±0.21 μM, p<0.0001 vs 1.03±0.15 μM for empty vector) (**Figure 4.4A, E, F, Appendix 3 and Figure 4.3E**). The possible explanation for this observation is that activating mutant p.E76K may directly aid activation of CRKL leading to BCR::ABL1 independent higher pCRKL because studies have shown that SHP-2 forms a complex with CRKL in a multiprotein domain in propagating signal transduction [38].

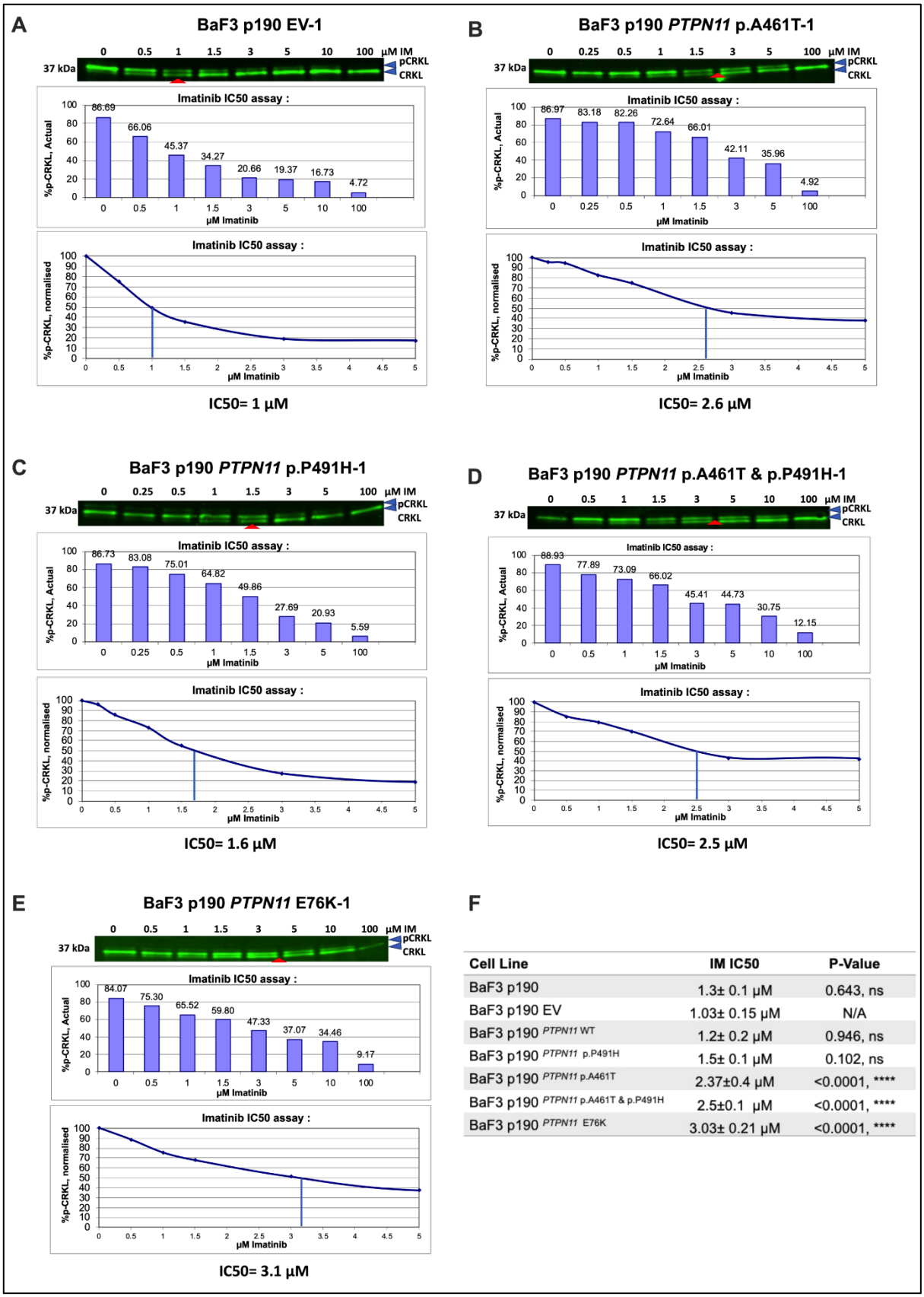

Cell Line	IM IC50	P-Value
BaF3 p190	1.3± 0.1 µM	0.643, ns
BaF3 p190 EV	1.03± 0.15 µM	N/A
BaF3 p190 *PTPN11* WT	1.2± 0.2 µM	0.946, ns
BaF3 p190 *PTPN11* p.P491H	1.5± 0.1 µM	0.102, ns
BaF3 p190 *PTPN11* p.A461T	2.37±0.4 µM	<0.0001, ****
BaF3 p190 *PTPN11* p.A461T & p.P491H	2.5±0.1 µM	<0.0001, ****
BaF3 p190 *PTPN11* E76K	3.03± 0.21 µM	<0.0001, ****

Figure 4.4: BaF3 *BCR::ABL1* p190 cells transduced with *PTPN11* p.A461T, compound p.A461T + p.P491H and p.E76K mutations had higher IC50s for

imatinib. (A-E) Western immunoblotting of pCRKL IC50 for BaF3 *BCR::ABL1* p190 cells transduced with *PTPN11* with pLVX and pLVX containing *PTPN11* wild type, *PTPN11* with p.A461T, p.P491H, p.A461T + p.P491H and p.E76K mutants exposed to increasing concentrations (0 to 100 μM) of imatinib for 2 hours at 37°C/5% CO2. The densitometry analysis of pCRKL and CRKL was performed in Image Studio Lite, and the concentration of imatinib required to inhibit pCRKL by 50% in 2 hours (IC50) was calculated and graphs were generated in Microsoft excel. Western blots shown represents three independent experiments and red triangle indicate approximate IC50 concentration. (F) Data represents mean IC50s from three independent experiments (n=3). Statistical analysis was performed by using unpaired t-test. *, ** and *** represent p≤0.05, p≤0.01, and p≤0.001 respectively.

Knockdown of *PTPN11* in SUP-B15 IR cells with shRNA reduced pERK1/2, BCL-XL and restored imatinib sensitivity

Because *PTPN11* mutations were able to induce resistance in BaF3 *BCR::ABL1* p190 cells, I investigated whether targeting the mutated SHP-2 protein could be a strategic method for restoring sensitivity to TKIs. I therefore knocked down *PTPN11* with shRNA in SUP-B15 sensitive and IM resistant cells. Successful lentiviral delivery of at least three different shRNAs specific for *PTPN11* led to significant reduction in SHP-2 protein expression in both SUP-B15 IR ($p<0.0001$) and parental ($p=0.0001$) cells (**Figure 4.5A and B**). While there was no difference in total BCR::ABL1 expression between wild type and PTPN11 knockdown SUP-B15 parental and IR cells, there was an increase in pBCR::ABL1 (Y177) ($p=0.0401$) and pBCR::ABL1 (Y245) ($p=0.0157$) only in SUP-B15 IR cells, but not in parental cells (**Figure 4.5A, C-E**). SUP-B15 IR cells were incubated in 75 hours in TKI free media to allow restoration of BCR::ABL1 activity, therefore there was

no difference in pBCR::ABL1 (Y177 and Y245) between SUP-B15 P shControl and SUP-B15 IR shControl (**Figure 4.5A and D**). Interestingly, knockdown of PTPN11 only reduced pERK1/2 (p=0.0018) and BCL-XL (p=0.0013) expression, without affecting MCL-1 (p=0.07) and BCL-2 (0.96) expression in SUP-B15 IR cells **(Figure 4.5A, F-I**). Of note, pERK1/2 and BCL-XL were found to be overexpressed in SUP-B15 IR cells as possible mechanisms of resistance in those cells as described in chapter 3.

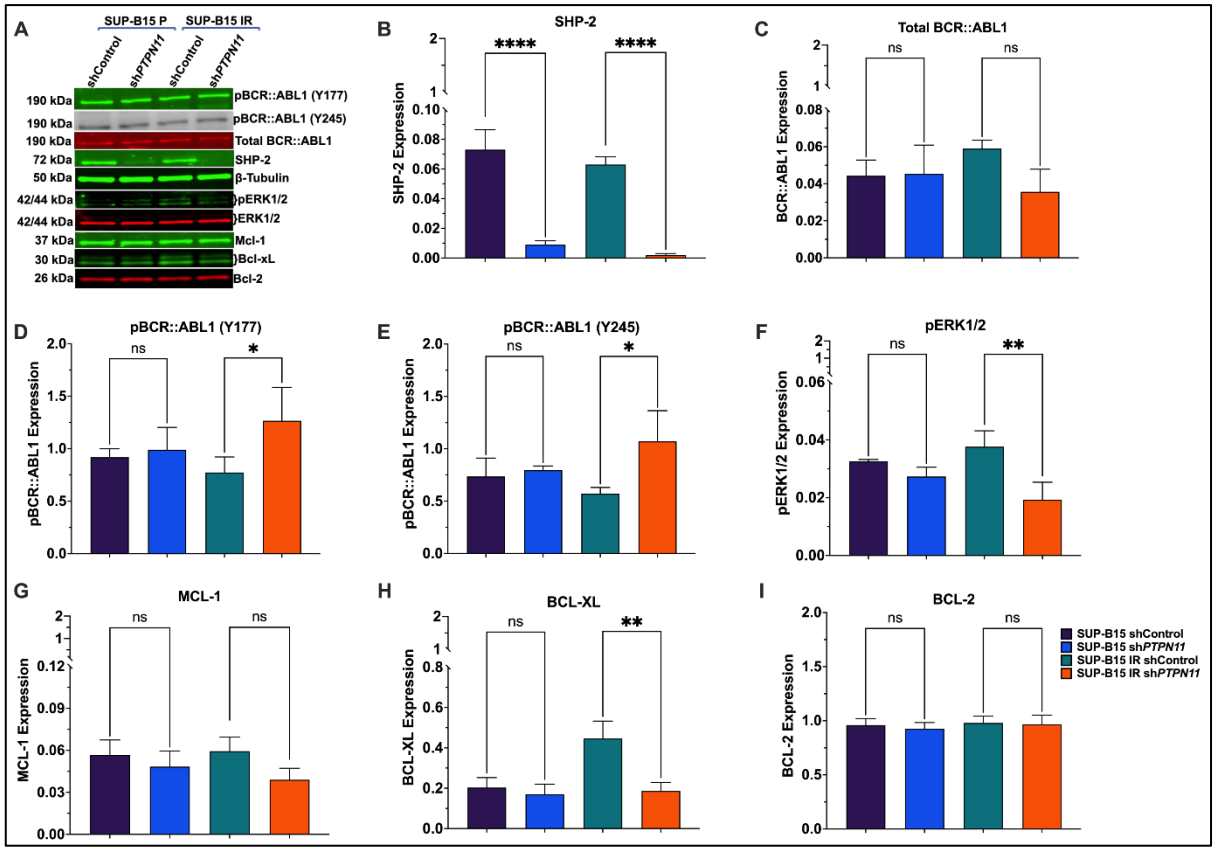

Figure 4.5: Knockdown of *PTPN11* with shRNA reduced pERK1/2, BCL-XL and restored imatinib sensitivity in SUP-B15 IR cells. (A) Western blot analysis of PTPN11 knockdown in SUP-B15 cells using shRNAs, including controls and at least 3 different shRNAs specific for PTPN11 in both SUP-B15 parental and IR cells. Expression levels of SHP-2, pBCR::ABL1 (Y177), pBCR::ABL1 (Y245), pERK1/2, MCL-1, BCL-XL, and BCL-2 were assessed in response to knockdown. (B-H) Quantitative densitometry analysis of SHP-2, pBCR::ABL1 (Y177), pBCR::ABL1 (Y245), pERK1/2, MCL-1, BCL-XL, and BCL-2 in

SUP-B15 parental and IR cells transduced with control and PTPN11-specific shRNAs. Data presented are derived from three independent experiments (n=3). Statistical analysis was conducted using One-Way ANOVA. Error bars represent the standard deviation (SD) based on three independent experiments (n=3). Ns, *, **, *** and **** represent $p>0.05$, $p\leq0.05$, $p\leq0.01$, $p\leq0.001$ and $p\leq0.0001$ respectively.

Confirming the results from cell line modelling that PTP domain PTPN11 mutations are responsible for imatinib resistance in SUP-B15 IR cells, shRNA knockdown of *PTPN11* restored full sensitivity to imatinib treatment (LD50s 26.05±10.67 μM vs 5.84±2.11 μM in *PTPN11* knockdown, p=0.0036) (**Figure 4.6A and B**). However, no significant change in sensitivity to imatinib (LD50s, 4.72±0.89 μM vs 5.27±0.53 μM respectively, p=0.998) was observed in SUP-B15 parental cells with PTPN11 knockdown (**Figure 4.6A and B**). Consistent with the results presented in chapter 3, PTPN11 knockdown supported the notion that overexpression of pERK1/2 and BCL-XL are the key players in the development of imatinib resistance in SUP-B15 IR cells because knockdown of PTPN11 decreased these two critical proteins and restored full sensitivity to imatinib. Reduction of pERK1/2 and restoration of imatinib sensitivity after PTPN11 knockdown in SUP-B15 IR cells are consistent with my finding of higher sensitivity to MEK inhibitor as demonstrated in chapter 3.

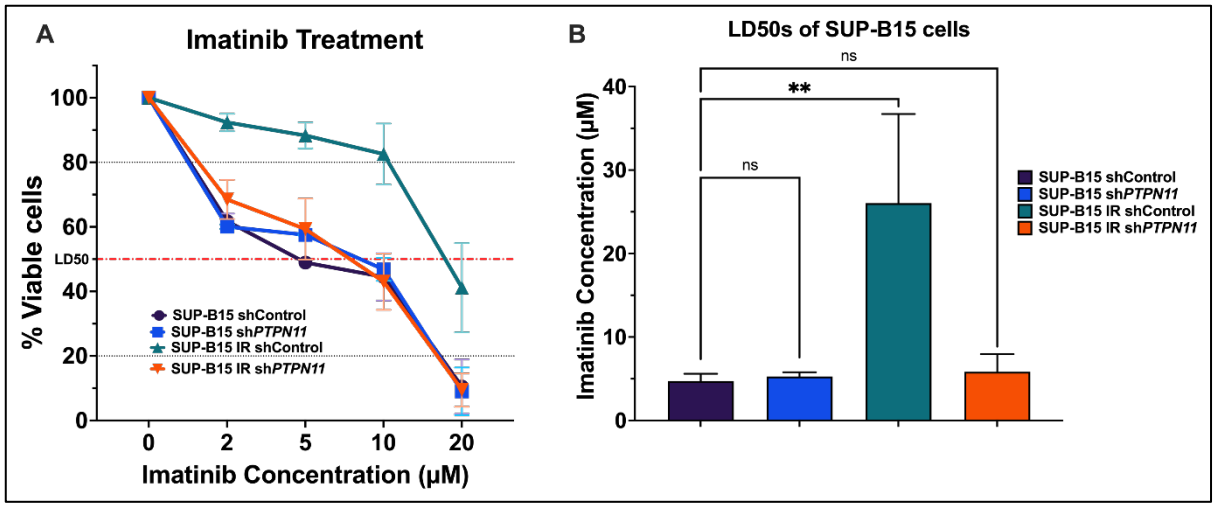

Figure 4.6: Inhibition of *PTPN11* with shRNA full imatinib sensitivity in SUP-B15 IR cells. (A) Cell death assay of SUP-B15 cells transduced with control and *PTPN11* specific shRNAs treated with increasing concentrations of imatinib for 72 hours and their viability was measured by measuring Annexin-V-PE and Fixable Viability Stain 780 in flow-cytometer. Y-axis represents Annexin-V-PE low and Fixable Viability Stain low expressed as percentage of viable cells. The concentration of imatinib required to induce apoptosis in 50% of cells (Lethal dose, LD50) was calculated by using GraphPad Prism 9. Data presented are from three independent experiments (n=3). Statistical analysis was performed by using One-Way ANOVA. Error bars represent standard deviation (SD) of three independent experiments. Ns, *, **, *** and **** represent $p>0.05$, $p\leq0.05$, $p\leq0.01$, $p\leq0.001$ and $p\leq0.0001$ respectively.

Knockdown of *PTPN11* in SUP-B15 IR cells with shRNA also restored imatinib IC50

After confirming that shRNA knockdown of *PTPN11* restores imatinib resistance in SUP-B15 IR cells by lowering proteins expression involved in BCR::ABL1 independent mechanisms of resistance, I wanted to test whether this knockdown restores the pCRKL IC50s of imatinib. Interestingly, shRNA knockdown of PTPN11 in SUP-B15 IR cells

restored pCRKL IC50s of imatinib (1.63±0.12 μM vs 1.23±0.06 μM, p=0.0278), without affecting imatinib IC50s (1.33±0.06 μM vs 1.13±0.15 μM, p=0.483) in SUP-B15 parental cells (**Figure 4.7A-E and Appendix 3**). Notably, there was a moderate increase in BCR::ABL1 activity in response to PTPN11 knockdown in SUP-B15 IR cells indicating their involvement in BCR::ABL1 activation and inhibition process. Reducing SHP-2 (by PTPN11 knockdown) probably reduced the involvement of mutated SHP-2 in BCR::ABL1 activation leading to better response to imatinib treatment (lower IC50). Taking together the data from BaF3 *BCR::ABL1* p190 cells transduced with PTPN11 mutations and the results from shRNA knockdown of PTPN11 confirmed that the mechanism of resistance was likely mediated by *PTPN11* mutations in SUP-B15 IR cells (**Figure 4.7A-E and Appendix 3**).

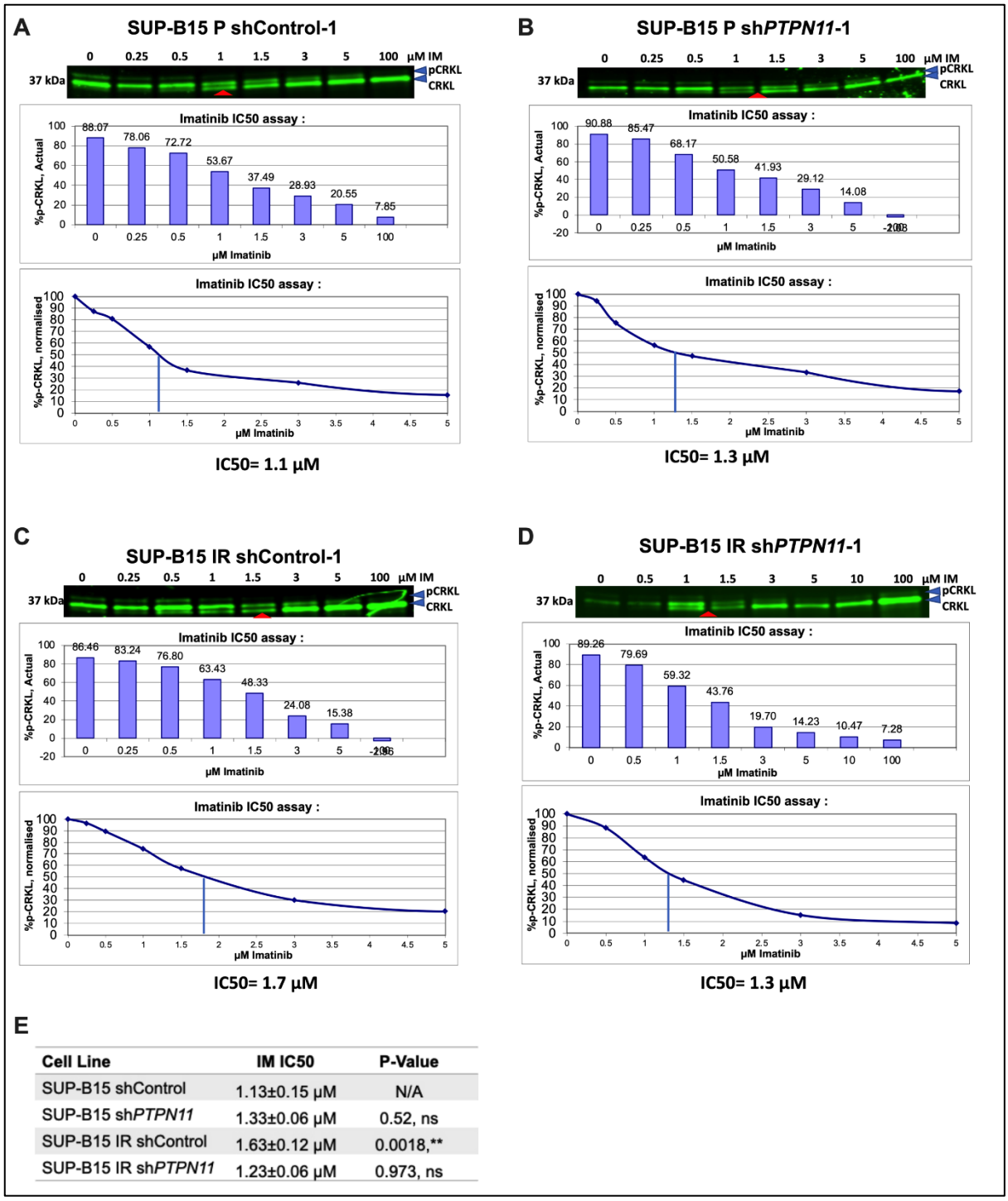

E

Cell Line	IM IC50	P-Value
SUP-B15 shControl	1.13±0.15 µM	N/A
SUP-B15 sh*PTPN11*	1.33±0.06 µM	0.52, ns
SUP-B15 IR shControl	1.63±0.12 µM	0.0018,**
SUP-B15 IR sh*PTPN11*	1.23±0.06 µM	0.973, ns

Figure 4.7: Knockdown of *PTPN11* with shRNA restores imatinib IC50 in SUP-B15 IR cells. (A-D) Western immunoblotting of pCRKL IC50 for SUP-B15 parental and IR cells transduced with shRNA specific for PTPN11. SUP-B15 IR cells underwent overnight washout procedure as described in '2.7.3. Cell washout protocol for TKI resistant cells of Chapter 2: Methods and Materials'. Cells were exposed to increasing concentrations (0 to

100 μM) of imatinib for 2 hours at 37°C/5% CO_2. Densitometry analysis of pCRKL and CRKL was performed using Image Studio Lite, and the resulting graphs display the concentration of imatinib required to inhibit pCRKL by 50% in 2 hours (IC50), calculated in Microsoft Excel. Western blots shown represent data from three independent experiments (n=3), with the red triangle indicating the approximate IC50 concentration. (E) This panel displays the mean IC50 values obtained from three independent experiments. Statistical analysis was conducted using an unpaired t-test. *, ** and *** represents $p \leq 0.05$, $p \leq 0.01$, and $p \leq 0.001$ respectively.

SUP-B15 IR cells showed reduced sensitivity to SHP-2 inhibition with TNO155

Because of the presence of *PTPN11* p.P491H mutation, I hypothesized that the *PTPN11* compound p.A461T + p.P491H mutations may not have completely lost its catalytic activity or may have gained additional function despite having known loss of function mutation p.A461T. Therefore, I tested the sensitivity of SUP-B15 cells to TNO155, a selective allosteric inhibitor of SHP-2 [39]. I used TNO155, because it stabilizes SHP-2 in an auto-inhibited confirmation reducing its catalytic activity [40]. TNO155 is under clinical trial for the treatment of advanced solid tumours [41]. Both SUP-B15 P and SUP-B15 IR cells had reduced sensitivity to TNO155 with LD50s greater than maximum concentration (5 μM) used (**Figure 4.8**). However, the effects of TNO155 on SUP-15 IR cells was lower compared to SUP-B15 parental cells for concentrations at and above 100 nM (**Figure 4.8**). The results suggest that phenotype seen in SUP-B15 IR cells may not be due to increase in catalytic activity of SHP-2 protein, rather it is probably due to gain of additional functions. This explanation is supported by the shRNA knockdown of PTPN11, where reduction in SHP-2 protein reversed signalling responsible for resistance and

restored sensitivity to imatinib removing the additional function brought about by mutated SHP-2 protein.

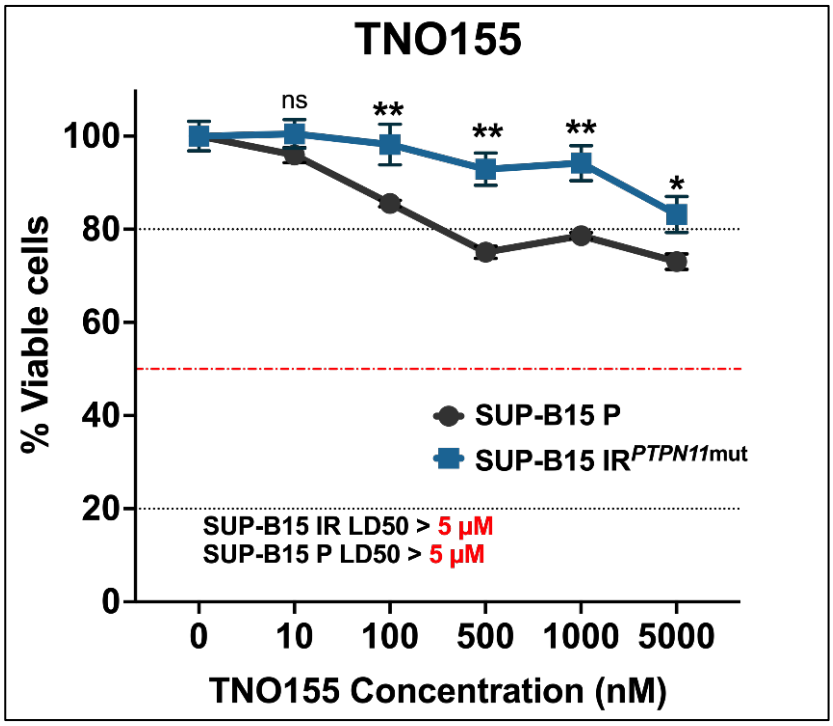

Figure 4.8: SUP-B15 IR cells were less sensitive to SHP-2 inhibitor than parental cells. SUP-B15 P and IR cells were subjected to treatment with increasing concentrations of the SHP-2 inhibitor, TNO155, for a duration of 72 hours. SUP-B15 IR cells underwent overnight washout procedure as described in '2.7.3. Cell washout protocol for TKI resistant cells of Chapter 2: Methods and Materials'. Viability was assessed by measuring Annexin-V-PE and Fixable Viability Stain 780 using flow cytometry. The Y-axis represents Annexin-V-PE low and Fixable Viability Stain low, expressed as a percentage of viable cells. Data presented are derived from three independent experiments (n=3).

Discussion

This study is, to my knowledge, the first study showing the effects of PTP domain *PTPN11* mutations in the context of BCR::ABL1. My results showed that in Ph positive cells (BaF3 *BCR::ABL1* p190 cells), PTPN11 mutations that do not alter the catalytic site such as p.P491H [42] and p.E76K did not reduce sensitivity to imatinib compared to wildtype whether the mutation led to open (p.E76K) or closed (p.P491H) conformation. However, mutations that reduces the catalytic activity of SHP-2 protein such as p.A461T [4] lead to reduced sensitivity to imatinib compared to wild type.

The analysis of RNA-seq data from SUP-B15 IR cells unveiled the presence of two mutations within the PTPN11 gene, namely p.A461T and p.P491H, exhibiting variant allele frequencies (VAF) of 63.7% and 40.2%, respectively. These mutations were conspicuously absent in the parental cell line. Since the variant allele frequencies (VAFs) of these mutations do not approach 100%, they exhibit sub-clonal characteristics. Notably, p.A461T seems to have occurred early (higher VAF) and may have played a crucial role in the observed phenotype. While it's possible that individual sub-clones with these mutations exist in the culture, the cloning experiment revealed a unique scenario: both mutations were identified within a single allele. This suggests the presence of a sub-clone harbouring mutations with these characteristics.

The SHP-2 protein has N-SH2, PTP and C-SH2 domains, and the N-SH2 domain is connected to the PTP domain by flexible polypeptide linkers leading to auto-inhibition of SHP-2 caused by blocking of the catalytic site [12]. Binding of SHP-2 to phosphorylated tyrosine residues in the target protein is mediated via the N-SH2 domain which leads to the conformational change that exposes the catalytic site to the substrates [43-46]. The

PTP domain of SHP-2 has a phosphate binding site, the cysteine residue at 459 position, responsible for the catalytic activity of SHP-2 [47]. Residues 459-465, including p.A461T are key residues for catalysis [48]. The p.P491H is a non-contributor to either N-SH2/PTP interaction or the catalytic function of SHP-2 [42]. Interestingly mutations in p.P491 position are frequently found in JMML and ALL patients and are associated with poor outcome [1-3]. Prior studies have postulated that *PTPN11* mutations at the p.P491 position might occur as a late event in ALL patients providing proliferative advantage in a leukaemia subclone [1-3]. The p.A461T mutation is common in Noonan syndrome with multiple lentigines and has been shown to reduce phosphatase activity of SHP-2 protein by 930-fold compared to wild type because this mutation alters active site pocket and destabilizes the first transition state of the substrate during the catalysis process [4]. The X-ray crystallography has been done previously to show SHP-2 protein with p.A461T mutation remains in the autoinhibited closed conformation, similar to that of wild type [4]. However, the effects of the combination of p.A461T and p.P491H mutations has never been previously investigated.

In Ph positive cells (BaF3 *BCR::ABL1* p190 cells), it was intriguing to see imatinib resistance with PTPN11 p.A461T mutant and reduced sensitivity to nilotinib, dasatinib ponatinib and asciminib with the compound p.A461T + p.P491H mutations. The increased pCRKL IC50s for imatinib with these mutations further supported the resistance mechanisms in BaF3 *BCR::ABL1* p190 cells. Overexpression of wild type PTPN11 or p.P491H mutant in BaF3 *BCR::ABL1* p190 cells neither developed imatinib resistance nor increased imatinib IC50. However, the overexpression of p.E76K did not induce imatinib resistance despite having higher imatinib IC50 in BaF3 *BCR::ABL1* p190 cells. The results also suggest that p.P491H mutant does not influence imatinib IC50, but

potentially supports p.A461T mutant to induce multi TKI resistance in BaF3 *BCR::ABL1* p190 cells. In the case of the p.E76K mutant, the possible explanation for this observation is that this mutation results in a constitutively active SHP-2 protein which form a complex with CRKL protein and may influence its activation without input from BCR::ABL1 activation, the interesting phenomenon that needs further investigation. Studies have shown that CRKL forms a complex with SHP-2 in response to IL-2 stimulation [38] and also physically associates with SHP-2 when phosphorylated in Epo stimulated cells to regulate the activation of RAS/ERK pathway [49]. Therefore, the mutated SHP-2 may also directly interact with CRKL to influence its phosphorylation status in BaF3 *BCR::ABL1* p190 cells.

Despite the fundamental differences between BaF3 BCR::ABL1 p190 cells and SUP-B15 cells in terms of cell type, both cell lines demonstrated strikingly similar phenotypic responses when subjected to PTPN11 mutations. Mirroring the observations made in SUP-B15 IR cells, the BaF3 BCR::ABL1 p190 cells exhibited elevated IC50 values and a notable resistance to imatinib upon the expression of PTPN11 mutations identical to those identified in SUP-B15 IR cells. Remarkably, the genetic silencing of PTPN11 in SUP-B15 IR cells not only reinstated imatinib's effectiveness, as evidenced by a reduction in IC50 values, but also rendered these cells responsive to imatinib treatment once more.

In Ph negative cells (BaF3 cells), wild type or p.A461T or p.P491H or p.E76K mutant could not provide any survival advantage to BaF3 cells in the absence of IL-3. The compound p.A461T + p.P491H mutant likely have additional function that provided them with a survival advantage. Unable to drive IL-3 independent proliferation similar to that by BaF3 cells transduced with BCR::ABL1, support the argument that survival advantage may be

driven by prevention of apoptosis, not proliferation [50-52]. Notably, none of those PTPN11 mutations activated RAS/ERK pathway as in most cases PTPN11 does not initiate RAS/ERK signalling rather it modulates the feed-back regulation of this pathway [53, 54]. Apoptotic pathway activation hypothesis was supported by overexpression of anti-apoptotic proteins BCL-XL and MCL-1 in BaF3 cells with compound p.A461T + p.P491H PTPN11 mutations. Results are consistent with previous work by Thomas et al. who showed that overexpression of BCL-XL was sufficient to inhibit apoptosis in BaF3 cells [55]. Though BaF3 and SUP-B15 cells are very different, higher BCL-XL was also observed in imatinib resistant SUP-B15 cells with compound p.A461T + p.P491H PTPN11 mutations, which was reduced upon PTPN11 knockdown. In contrast to my finding on *PTPN11* p.E76K mutant, Loh *et al.* showed enhanced survival of BaF3 p.E76K SHP-2 cells after 8 days of IL-3 removal and reported growth factor independent proliferation after prolonged culture [56]. Since I only investigated 72 hours post IL-3 withdrawal, I did not see any increased survival or proliferative ability within that timeframe. I was unable to culture BaF3 cells beyond 72 hours due to significant decline in cell viability. However, consistent with what I found, a more recent study reported that survival and proliferation was observed in virally transduced HCD-57 cells with SHP-2 E76K mutant when erythropoietin was withdrawn but not in BaF3 cells with SHP-2 E76K mutant when IL-3 was withdrawn [57].

The absence of ERK signalling upregulation by the compound PTPN11 mutant in BaF3 cells compared to SUP-B15 IR cells suggests a potentially different mechanism in the SUP-B15 IR context. This variation likely stems from the unique cellular environment, the presence of other genetic alterations, differences in signalling networks between the two cell types due to their BCR::ABL1 status.

In the context of PTNP11 p.A461T mutation in BaF3 BCR::ABL1 p190 cells, it's interesting to note that this mutation doesn't seem to have an effect on ERK signalling or the expression of anti-apoptotic proteins. However, despite these observations, it still induces resistance to tyrosine kinase inhibitors (TKIs). The BaF3 BCR::ABL1 p190 cells with the p.A461T mutation likely directly affect the effectiveness of imatinib to inhibit BCR::ABL1, as suggested by higher IC50s, leading to imatinib resistance. This suggests that this specific mutation may interfere with imatinib's ability to target and inhibit BCR::ABL1, providing a potential mechanistic explanation for the observed TKI resistance in these cells. The impact of PTPN11 p.A461T + p.P491H mutations on ERK signalling in BaF3 BCR::ABL1 p190 cells was found to be minimal. Sustained ERK activation was observed exclusively in SUP-B15 IR cells that were continuously cultured in the presence of 5 μM imatinib. Interestingly, this effect was not observed when imatinib was removed overnight, followed by a subsequent 4-hour treatment with 5 μM imatinib (please refer to Figure 3.6 of Chapter 3). These findings suggest that the re-activation of ERK signalling in SUP-B15 IR cells is a long-term consequence of imatinib exposure, potentially explaining the absence of ERK activation in BaF3 BCR::ABL1 p190 cells, despite the presence of PTPN11 mutations.

Moreover, it's crucial to recognize that the employment of shRNA in the experiments introduces a potential limitation. While shRNA is designed to target PTPN11 expression, it doesn't discriminate between mutant and wild-type alleles. Consequently, interpreting the data becomes intricate due to the ambiguity surrounding which allele predominantly contributes to the observed effects. It's essential to keep this limitation in mind when assessing this study's outcomes. Nevertheless, it's worth noting that the complete loss of

SHP-2 protein signifies the comprehensive inhibition of the PTPN11 gene in SUP-B15 IR cells.

In conclusion, I independently validated the role of PTP domain *PTPN11* mutations in the development of TKI resistance. To my knowledge, this is the first study to show PTP domain PTPN11 mutations responsible for TKI resistance in BCR::ABL1 positive cells. I have shown that knockdown of PTPN11 reduces pERK1/2 and restores imatinib sensitivity in SUP-B15 IR cells supporting my finding in chapter 3 that RAS/ERK pathway played role in mechanism of resistance in those cells. However, directly targeting SHP-2 activity was not effective in overcoming resistance indicating the mechanisms of resistance do not rely on SHP-2 catalytic activity. This hypothesis is being further tested by measuring the catalytic activity of SHP-2 protein with PTP domain mutations. In the next chapter, I will investigate alternative targets such as anti-apoptotic proteins including inhibitors of BCL-XL, MCL-1 and BCL-2 and test whether inhibiting one or more of these proteins can overcome resistance in SUP-B15 IR cells.

References:

1. Tartaglia, M., et al., *Diversity and functional consequences of germline and somatic PTPN11 mutations in human disease.* Am J Hum Genet, 2006. **78**(2): p. 279-90.
2. Tartaglia, M., et al., *Genetic evidence for lineage-related and differentiation stage–related contribution of somatic PTPN11 mutations to leukemogenesis in childhood acute leukemia.* Blood, 2004. **104**(2): p. 307-313.
3. Tartaglia, M., et al., *Somatic PTPN11 mutations in childhood acute myeloid leukaemia.* British journal of haematology, 2005. **129**(3): p. 333-339.
4. Yu, Z.-H., et al., *Molecular basis of gain-of-function LEOPARD syndrome-associated SHP2 mutations.* Biochemistry, 2014. **53**(25): p. 4136-4151.
5. Branford, S., et al., *Laying the foundation for genomically-based risk assessment in chronic myeloid leukemia.* Leukemia, 2019. **33**(8): p. 1835-1850.
6. Komorowski, L., et al., *Philadelphia Chromosome-Positive Leukemia in the Lymphoid Lineage—Similarities and Differences with the Myeloid Lineage and Specific Vulnerabilities.* International Journal of Molecular Sciences, 2020. **21**(16): p. 5776.
7. Soverini, S., R. Bassan, and T. Lion, *Treatment and monitoring of Philadelphia chromosome-positive leukemia patients: recent advances and remaining challenges.* Journal of Hematology & Oncology, 2019. **12**(1): p. 39.
8. Chan, L.N., et al., *Signaling input from divergent pathways subverts malignant B-cell transformation.* bioRxiv, 2020: p. 2020.03.12.989749.
9. Pandey, G., et al., *RMC-4550, an Allosteric Inhibitor of SHP2, Displays Therapeutic Efficacy in Pre-Clinical Models of Myeloproliferative Neoplasms.* Blood, 2019. **134**: p. 4198.
10. Branford, S., et al., *Laying the foundation for genomically-based risk assessment in chronic myeloid leukemia.* Leukemia, 2019. **33**(8): p. 1835-1850.
11. Boni, C. and C. Sorio, *Current Views on the Interplay between Tyrosine Kinases and Phosphatases in Chronic Myeloid Leukemia.* Cancers (Basel), 2021. **13**(10).
12. Song, Y., et al., *Crystallographic landscape of SHP2 provides molecular insights for SHP2 targeted drug discovery.* Medicinal Research Reviews, 2022. **42**(5): p. 1781-1821.
13. Tonks, N.K., *Protein tyrosine phosphatases: from genes, to function, to disease.* Nature reviews Molecular cell biology, 2006. **7**(11): p. 833-846.
14. Pandey, R., M. Saxena, and R. Kapur, *Role of SHP2 in hematopoiesis and leukemogenesis.* Current opinion in hematology, 2017. **24**(4): p. 307.
15. Chan, R.J. and G.-S. Feng, *PTPN11 is the first identified proto-oncogene that encodes a tyrosine phosphatase.* Blood, 2007. **109**(3): p. 862-867.
16. Gu, S., et al., *SHP2 is required for BCR-ABL1-induced hematologic neoplasia.* Leukemia, 2018. **32**(1): p. 203-213.
17. Kratz, C.P., et al., *The mutational spectrum of PTPN11 in juvenile myelomonocytic leukemia and Noonan syndrome/myeloproliferative disease.* Blood, 2005. **106**(6): p. 2183-2185.
18. Tartaglia, M., et al., *PTPN11 mutations in Noonan syndrome: molecular spectrum, genotype-phenotype correlation, and phenotypic heterogeneity.* The American Journal of Human Genetics, 2002. **70**(6): p. 1555-1563.
19. Gelb, B.D. and M. Tartaglia, *Noonan syndrome with multiple lentigines.* 2022.
20. Jongmans, M.C., et al., *Cancer risk in patients with Noonan syndrome carrying a PTPN11 mutation.* European Journal of Human Genetics, 2011. **19**(8): p. 870-874.

21. Molteni, C.G., et al., *PTPN11 mutations in childhood acute lymphoblastic leukemia occur as a secondary event associated with high hyperdiploidy.* Leukemia, 2010. **24**(1): p. 232-235.
22. Chan, G., D. Kalaitzidis, and B.G. Neel, *The tyrosine phosphatase Shp2 (PTPN11) in cancer.* Cancer and Metastasis Reviews, 2008. **27**(2): p. 179-192.
23. Chantrain, C.F., et al., *Therapy-related acute myeloid leukemia in a child with Noonan syndrome and clonal duplication of the germline PTPN11 mutation.* Pediatric blood & cancer, 2007. **48**(1): p. 101-104.
24. Karow, A., et al., *Clonal duplication of a germline PTPN11 mutation due to acquired uniparental disomy in acute lymphoblastic leukemia blasts from a patient with Noonan syndrome.* Leukemia, 2007. **21**(6): p. 1303-1305.
25. La Starza, R., et al., *A new NDE1/PDGFRB fusion transcript underlying chronic myelomonocytic leukaemia in Noonan Syndrome.* Leukemia, 2007. **21**(4): p. 830-833.
26. Lo, F.-S., et al., *Hodgkin's lymphoma in a patient with Noonan syndrome with germ-line PTPN11 mutations.* International journal of hematology, 2008. **88**(3): p. 287-290.
27. Matsubara, K., et al., *Acute myeloid leukemia in an adult Noonan syndrome patient with PTPN11 mutation.* American journal of hematology, 2005. **79**(2): p. 171-172.
28. Roti, G., et al., *Acute lymphoblastic leukaemia in Noonan syndrome.* British journal of haematology, 2006. **133**(4): p. 448-450.
29. Stasik, S., et al., *Impact of PTPN11 mutations on clinical outcome analyzed in 1529 patients with acute myeloid leukemia.* Blood Adv, 2021. **5**(17): p. 3279-3289.
30. Fobare, S., et al., *Molecular, clinical, and prognostic implications of PTPN11 mutations in acute myeloid leukemia.* Blood Adv, 2022. **6**(5): p. 1371-1380.
31. Bentires-Alj, M., et al., *Activating mutations of the noonan syndrome-associated SHP2/PTPN11 gene in human solid tumors and adult acute myelogenous leukemia.* Cancer research, 2004. **64**(24): p. 8816-8820.
32. Esposito, N., et al., *SHP-1 expression accounts for resistance to imatinib treatment in Philadelphia chromosome–positive cells derived from patients with chronic myeloid leukemia.* Blood, 2011. **118**(13): p. 3634-3644.
33. Pádua, R.A.P., et al., *Mechanism of activating mutations and allosteric drug inhibition of the phosphatase SHP2.* Nature Communications, 2018. **9**(1): p. 4507.
34. Mäkinen, V.P., et al., *Multi-Cohort Transcriptomic Subtyping of B-Cell Acute Lymphoblastic Leukemia.* Int J Mol Sci, 2022. **23**(9).
35. Zheng, H., et al., *Gain-of-function mutations in the gene encoding the tyrosine phosphatase SHP2 induce hydrocephalus in a catalytically dependent manner.* Sci Signal, 2018. **11**(522).
36. Takada, M., et al., *Activating Mutations in PTPN11 and KRAS in Canine Histiocytic Sarcomas.* Genes, 2019. **10**(7).
37. Li, S., et al., *The P190, P210, and P230 Forms of the BCR/ABL Oncogene Induce a Similar Chronic Myeloid Leukemia–like Syndrome in Mice but Have Different Lymphoid Leukemogenic Activity.* Journal of Experimental Medicine, 1999. **189**(9): p. 1399-1412.
38. Gesbert, F., C. Guenzi, and J. Bertoglio, *A New Tyrosine-phosphorylated 97-kDa Adaptor Protein Mediates Interleukin-2-induced Association of SHP-2 with p85-Phosphatidylinositol 3-Kinase in Human T Lymphocytes*.* Journal of Biological Chemistry, 1998. **273**(29): p. 18273-18281.

39. Brana, I., et al., *Initial results from a dose finding study of TNO155, a SHP2 inhibitor, in adults with advanced solid tumors.* Journal of Clinical Oncology, 2021. **39**(15_suppl): p. 3005-3005.
40. Chen, Y.-N.P., et al., *Allosteric inhibition of SHP2 phosphatase inhibits cancers driven by receptor tyrosine kinases.* Nature, 2016. **535**(7610): p. 148-152.
41. Brana, I., et al., *Initial results from a dose finding study of TNO155, a SHP2 inhibitor, in adults with advanced solid tumors.* J Clin Oncol, 2021. **39**(suppl 15): p. 3005.
42. Tartaglia, M., et al., *Diversity and Functional Consequences of Germline and Somatic PTPN11 Mutations in Human Disease.* The American Journal of Human Genetics, 2006. **78**(2): p. 279-290.
43. Hof, P., et al., *Crystal structure of the tyrosine phosphatase SHP-2.* Cell, 1998. **92**(4): p. 441-450.
44. Eck, M.J., et al., *Spatial constraints on the recognition of phosphoproteins by the tandem SH2 domains of the phosphatase SH-PTP2.* Nature, 1996. **379**(6562): p. 277-280.
45. Koch, C.A., et al., *SH2 and SH3 domains: elements that control interactions of cytoplasmic signaling proteins.* Science, 1991. **252**(5006): p. 668-674.
46. Shen, D., et al., *Therapeutic potential of targeting SHP2 in human developmental disorders and cancers.* European Journal of Medicinal Chemistry, 2020. **190**: p. 112117.
47. Yu, B., et al., *Targeting protein tyrosine phosphatase SHP2 for the treatment of PTPN11-associated malignancies.* Molecular cancer therapeutics, 2013. **12**(9): p. 1738-1748.
48. Athota, J.P., et al., *Molecular and clinical studies in 107 Noonan syndrome affected individuals with PTPN11 mutations.* BMC Medical Genetics, 2020. **21**(1): p. 50.
49. Arai, A., et al., *CrkL is recruited through its SH2 domain to the erythropoietin receptor and plays a role in Lyn-mediated receptor signaling.* J Biol Chem, 2001. **276**(35): p. 33282-90.
50. Daley, G.Q. and D. Baltimore, *Transformation of an interleukin 3-dependent hematopoietic cell line by the chronic myelogenous leukemia-specific P210bcr/abl protein.* Proceedings of the National Academy of Sciences, 1988. **85**(23): p. 9312-9316.
51. Bai, R.-Y., et al., *Nucleophosmin-anaplastic lymphoma kinase of large-cell anaplastic lymphoma is a constitutively active tyrosine kinase that utilizes phospholipase C-γ to mediate its mitogenicity.* Molecular and cellular biology, 1998. **18**(12): p. 6951-6961.
52. Hayakawa, F., et al., *Tandem-duplicated Flt3 constitutively activates STAT5 and MAP kinase and introduces autonomous cell growth in IL-3-dependent cell lines.* Oncogene, 2000. **19**(5): p. 624-631.
53. Grossmann, K.S., et al., *Chapter 2 - The Tyrosine Phosphatase Shp2 in Development and Cancer*, in *Advances in Cancer Research*, G.F. Vande Woude and G. Klein, Editors. 2010, Academic Press. p. 53-89.
54. Dance, M., et al., *The molecular functions of Shp2 in the Ras/Mitogen-activated protein kinase (ERK1/2) pathway.* Cellular Signalling, 2008. **20**(3): p. 453-459.
55. Thomas, J., Y. Leverrier, and J. Marvel, *Bcl-X is the major pleiotropic anti-apoptotic gene activated by retroviral insertion mutagenesis in an IL-3 dependent bone marrow derived cell line.* Oncogene, 1998. **16**(11): p. 1399-1408.
56. Loh, M.L., et al., *Mutations in PTPN11 implicate the SHP-2 phosphatase in leukemogenesis.* Blood, 2004. **103**(6): p. 2325-2331.

57. Zhao, Y., et al., *Leukemogenic SHP2 mutations lead to erythropoietin independency of HCD-57 cells: a novel model for preclinical research of SHP2-mutant JMML.* Experimental Hematology & Oncology, 2023. **12**(1): p. 20.

APPENDIX 1

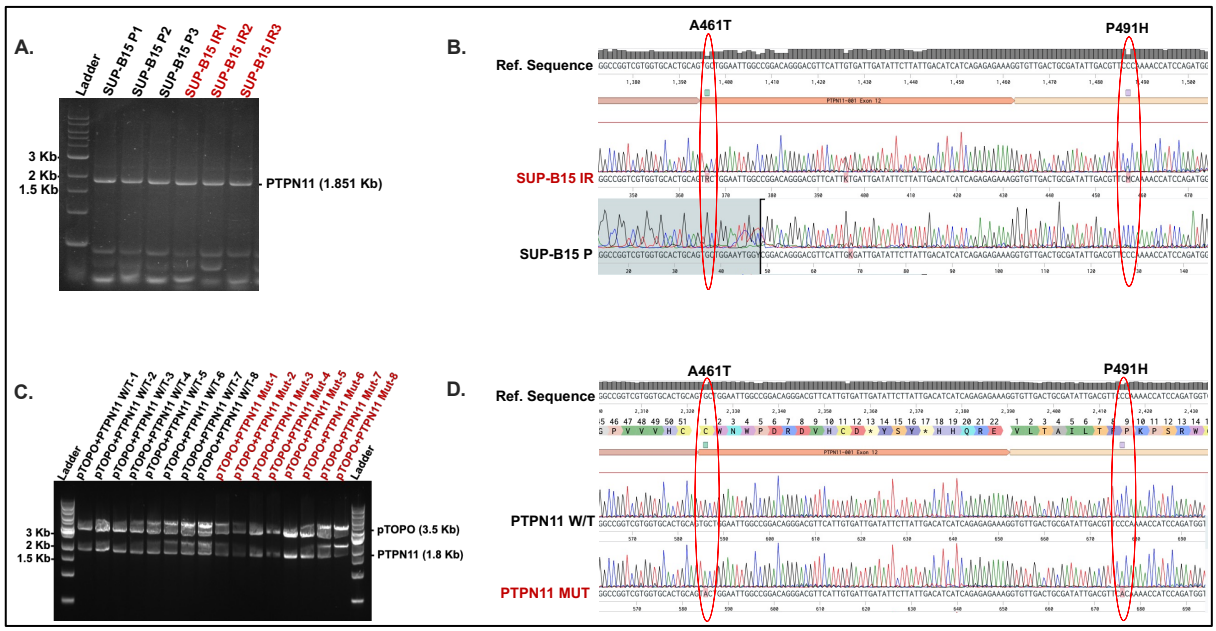

E.

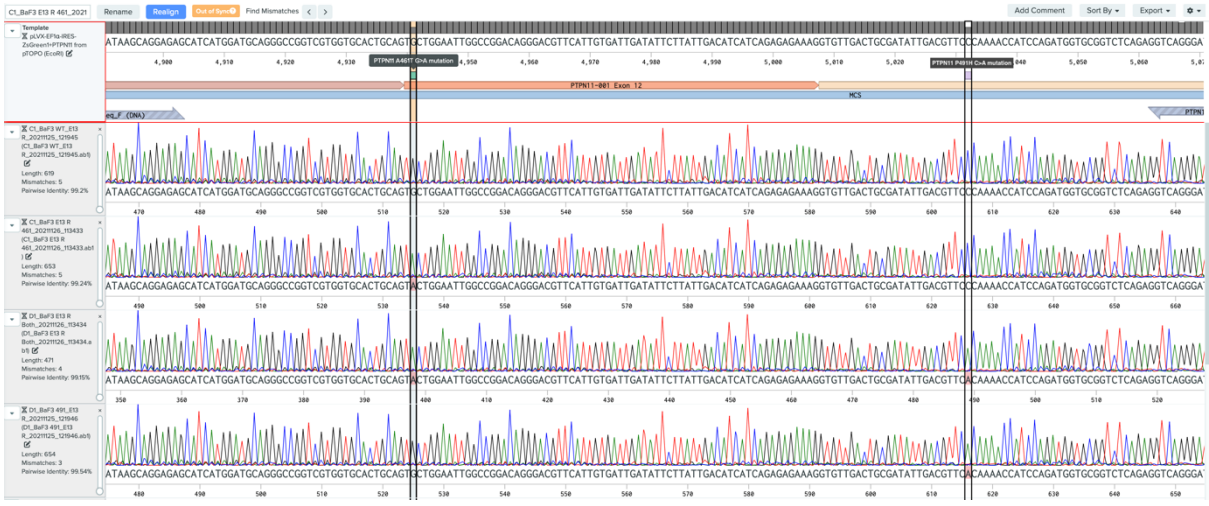

F.

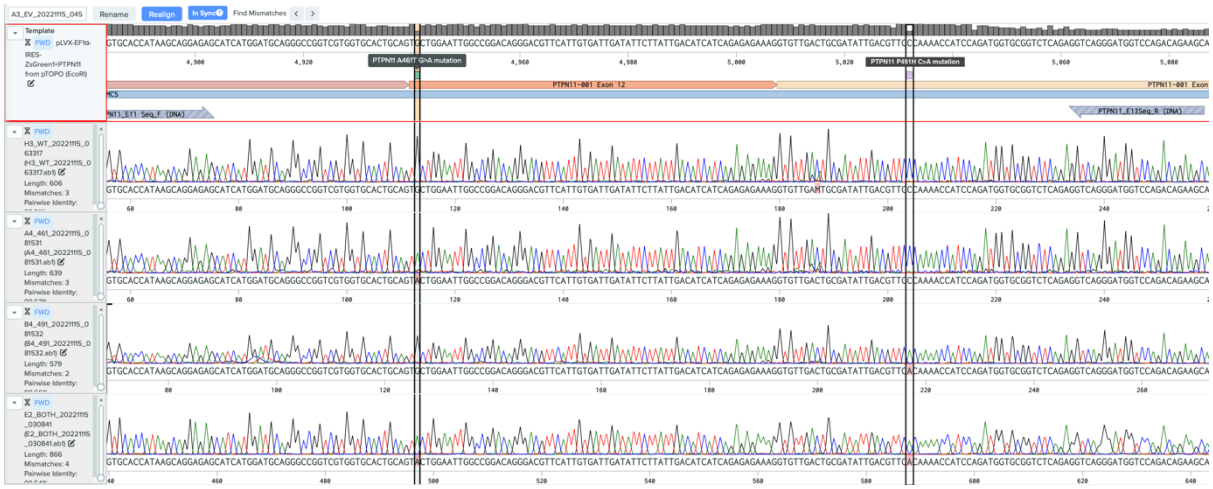

G.

Figure 1. Molecular cloning and analysis of PTPN11 gene mutations in BaF3 and BaF3 *BCR::ABL1* p190 cells.

(A) PCR amplification of PTPN11 cDNA from SUP-B15 parental (P) and SUP-B15 imatinib resistant (IR) cells. Agarose gel electrophoresis shows the PTPN11 PCR products amplified from cDNA derived from mRNA using the SuperScript II RT-PCR protocol. Primers used: PTPN11_PCR_F: 5' GAGGGCGGGAGGAACATGACATC 3' and PTPN11_PCR_R: 5' GGGAGAGGGTGAAAGTCCACATC 3'.

(B) Sanger sequencing analysis of PTPN11 cDNA from SUP-B15 P and IR$^{PTPN11\text{mut}}$ cells. Sequences were aligned to the PTPN11 reference sequence using Benchling.

(C) Screening of 5-DHα E. coli containing pTOPO vector with PTPN11 insert. Agarose gel electrophoresis shows EcoRI restriction digest products from pTOPO+PTPN11 WT and plasmids with PTPN11 mutations extracted using the miniprep protocol.

(D) Sanger sequencing analysis of pTOPO+PTPN11 WT and mutated plasmids extracted from miniprep confirms PTPN11 (p.A461T and p.P491H compound) mutations in pTOPO+PTPN11 Mut plasmid. Sequences were aligned to the PTPN11 reference sequence using Benchling.

(E) Sanger sequencing confirms PTPN11 (p.A461T, p.P491H, and both p.A461T/p.P491H) mutations in BaF3 cells. Sequences from top to bottom represent the PTPN11 reference sequence, wild type human PTPN11, PTPN11 p.A461T, p.A461T + p.P491H sequences transduced into BaF3 cells.

(F) Sanger sequencing confirms PTPN11 (p.A461T, p.P491H, and both p.A461T/p.P491H) mutations in BaF3 *BCR::ABL1* p190 cells. Sequences from top to bottom represent the PTPN11 reference sequence, wild type human PTPN11, PTPN11 p.A461T, p.P491H, and p.A461T + p.P491H sequences transduced into BaF3 *BCR::ABL1* p190 cells.

(G) The PTPN11 cDNA with p.E76K mutation was purchased from Integrated DNA Technologies Pte. Ltd. (Coralville, USA) as a gBlocks Gene Fragments 1751-2000 bp and it was directly ligated into pLVX-EF1α-IRES-ZsGreen1 vector then transduced into BaF3 and BaF3 BCR::ABL1 p190 cells. Sanger sequencing confirms PTPN11 p.E76K mutation in BaF3 and BaF3 BCR::ABL1 p190 cells. Sequences from top to bottom represent the PTPN11 reference sequence (with p.E76K, G>A) mutation, PTPN11 p.E76K, PTPN11 wild

type sequences transduced into BaF3 BCR::ABL1 p190 cells and followed by PTPN11 reference sequence (with p.E76K, G>A) mutation, PTPN11 p.E76K, PTPN11 wild type sequences transduced into BaF3 cells.

APPENDIX 2

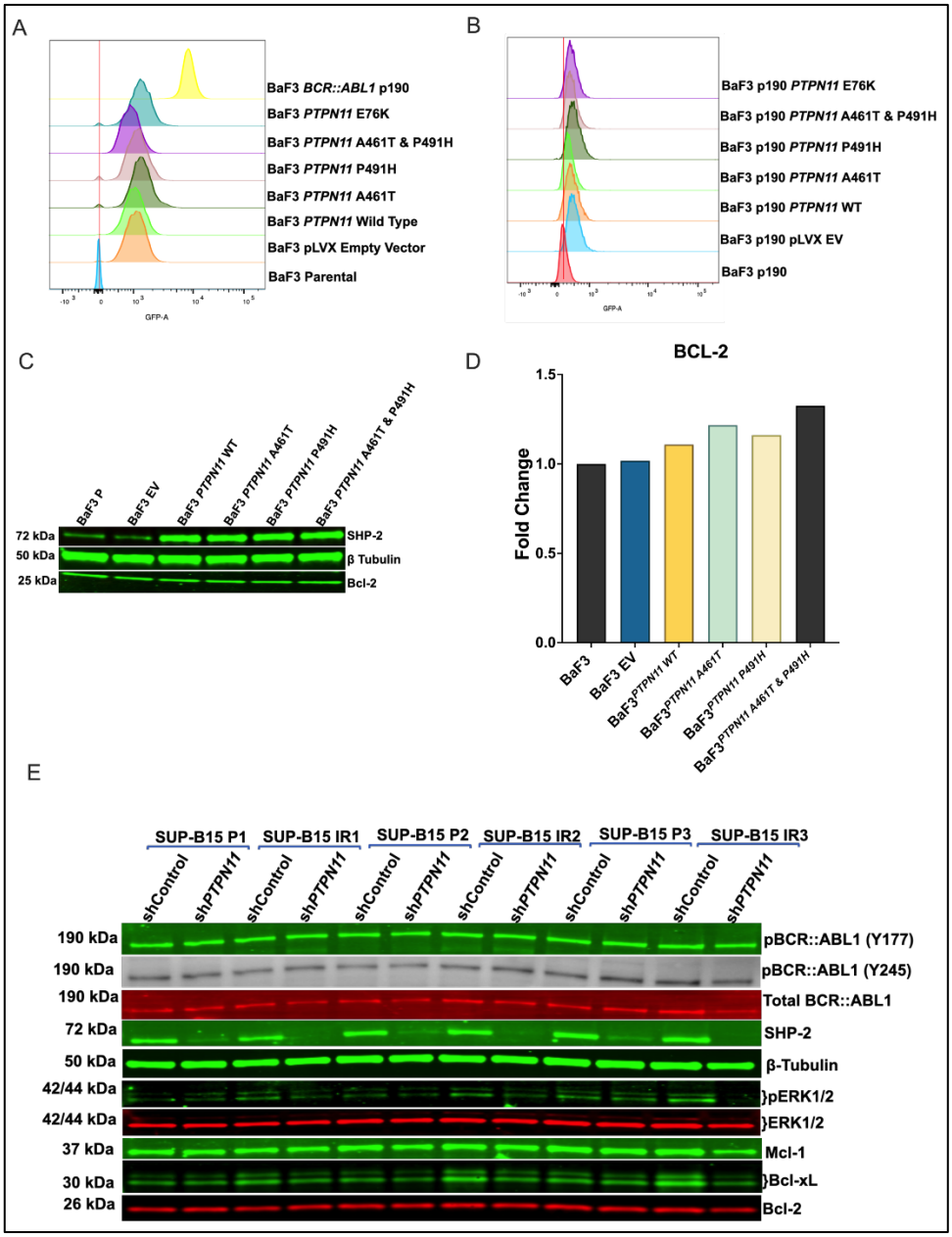

2. Successful transduction of pLVX-EF1α-IRES-ZsGreen1 mammalian expression vector with *PTPN11* mutants into BaF3 and BaF3 *BCR::ABL1* p190 cells. (A and B)

BaF3 and BaF3 BCR::ABL1 p190 cells were transduced with pLVX and pLVX containing PTPN11 wild type, PTPN11 with p.A461T, p.P491H, p.A461T + p.P491H, or p.E76K mutants. Green fluorescent protein (GFP) expression was observed. (C and D) Western blot and densitometry analysis of SHP-2 and BCL-2 in BaF3 cells transduced with pLVX and pLVX containing PTPN11 wild type, PTPN11 with p.A461T, p.P491H, and p.A461T + p.P491H mutants. Results are from a single replicate. (E) Western blot analysis of PTPN11 knockdown in SUP-B15 cells using shRNAs for controls and shRNAs specific for PTPN11 in both SUP-B15 parental and IR cells. Expression of SHP-2, pBCR::ABL1 (Y177), pBCR::ABL1 (Y245), pERK1/2, MCL-1, BCLXL, and BCL-2 were assessed in response to knockdown. Numbers (1-3) at the end of samples represent independent biological replicate numbers.

APPENDIX 3

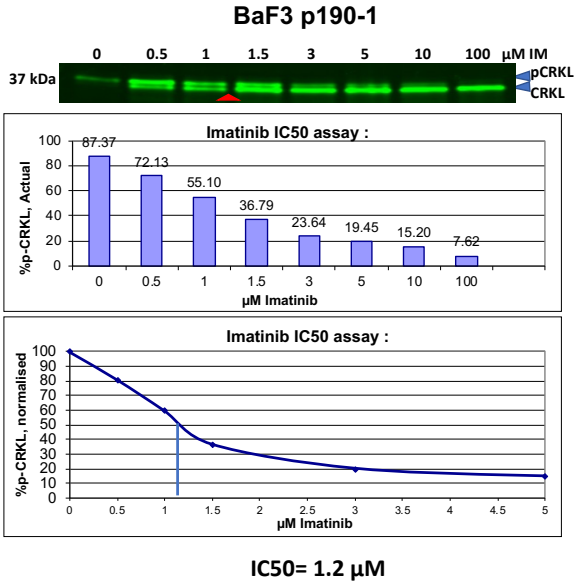

IC50= 1.2 µM

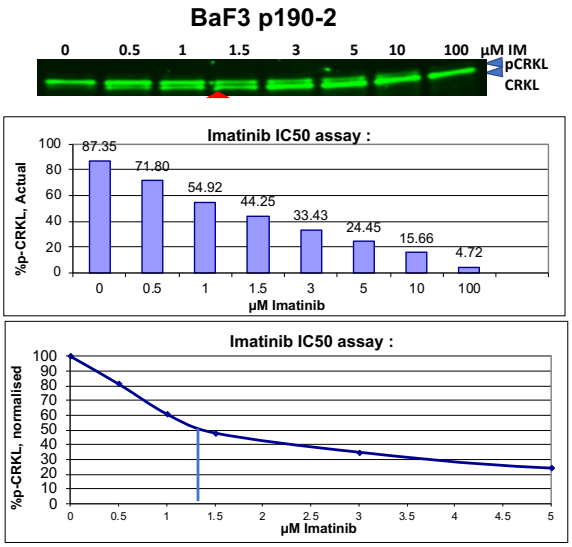

IC50=1.4 µM

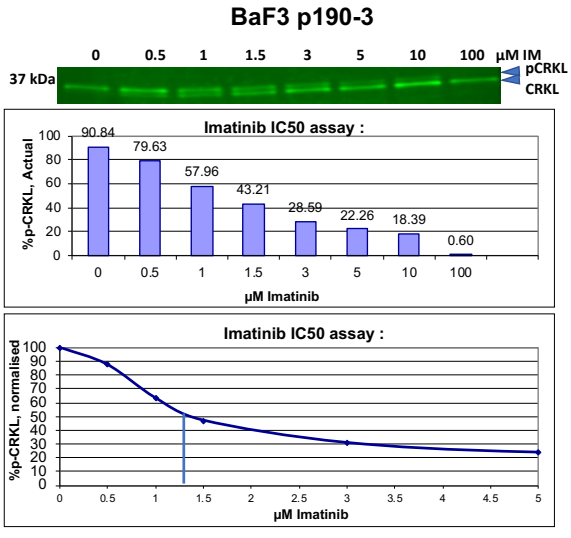

IC50= 1.3 µM

1. Imatinib pCRKL IC50 assays of BaF3 *BCR::ABL1* p190 cells. Western immunoblotting of pCRKL IC50 for BaF3 BCR::ABL1 p190 cells exposed to increasing concentrations (0, 0.25, 0.5, 1, 1.5, 3, 5, and 100 µM) of imatinib for 2 hours at 37°C/5% CO_2. The densitometry analysis of pCRKL and CRKL was performed in Image Studio Lite, and the graphs were created and the concentration of imatinib required to inhibit pCRKL by 50% in 2 hours (IC50) was calculated in Microsoft excel. Western blots shown are three independent experiments (n=3) and red triangle indicates approximate IC50 concentration.

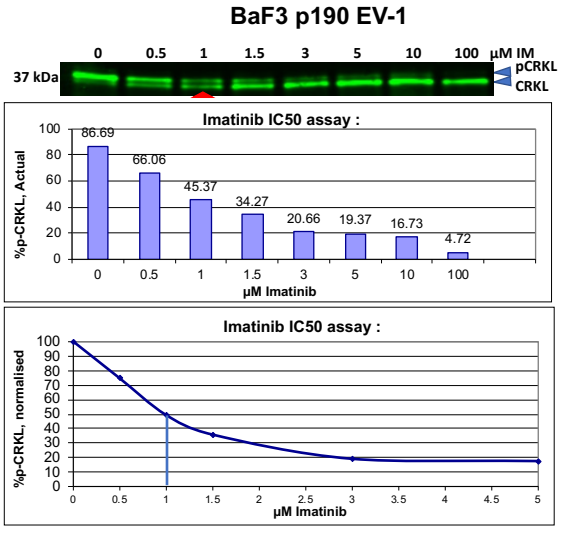

IC50= 1 µM

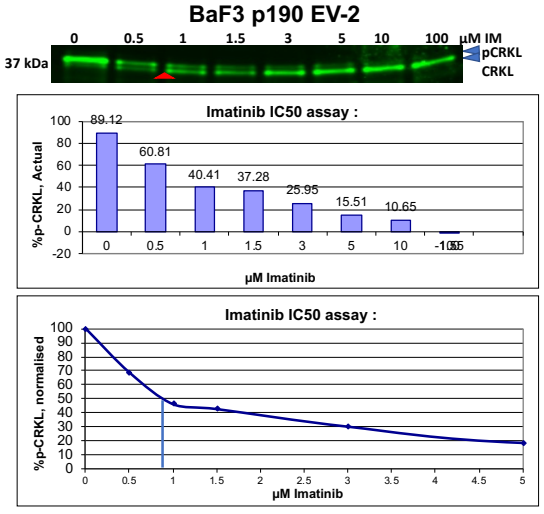

IC50=0.9 µM

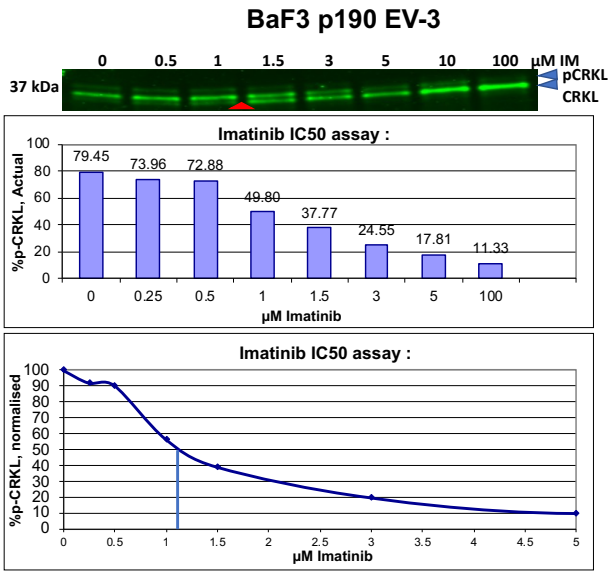

IC50= 1.2 µM

2. Imatinib pCRKL IC50 assays of BaF3 *BCR::ABL1* p190 pLVX Empty Vector cells. Western immunoblotting of pCRKL IC50 for BaF3 BCR::ABL1 p190 cells exposed to increasing concentrations (0, 0.25, 0.5, 1, 1.5, 3, 5, and 100 µM) of imatinib for 2 hours at 37°C/5% CO_2. The densitometry analysis of pCRKL and CRKL was performed in Image Studio Lite, and the graphs were created and the concentration of imatinib required to inhibit pCRKL by 50% in 2 hours (IC50) was calculated in Microsoft excel. Western blots shown are three independent experiments (n=3) and red triangle indicates approximate IC50 concentration.

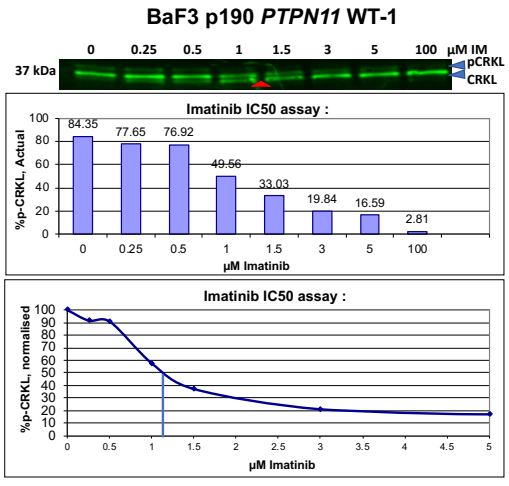

IC50= 1.2 µM

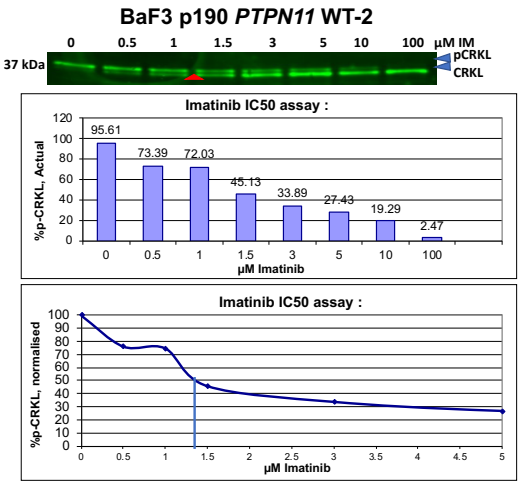

IC50= 1.4 µM

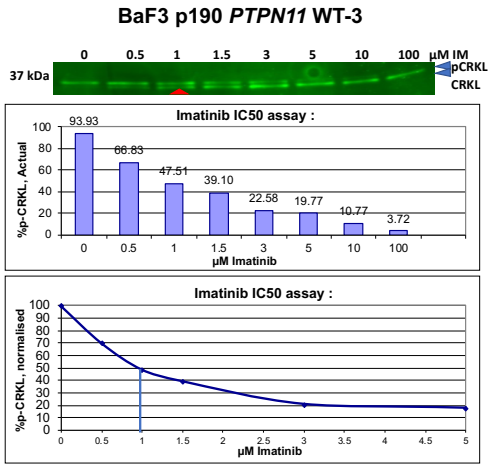

IC50= 1 µM

3. Imatinib pCRKL IC50 assays of BaF3 *BCR::ABL1* p190 pLVX PTPN11 Wild Type cells. Western immunoblotting of pCRKL IC50 for BaF3 BCR::ABL1 p190 cells exposed to increasing concentrations (0, 0.25, 0.5, 1, 1.5, 3, 5, and 100 µM) of imatinib for 2 hours at 37°C/5% CO_2. The densitometry analysis of pCRKL and CRKL was performed in Image Studio Lite, and the graphs were created and the concentration of imatinib required to inhibit pCRKL by 50% in 2 hours (IC50) was calculated in Microsoft excel. Western blots shown are three independent experiments (n=3) and red triangle indicates approximate IC50 concentration.

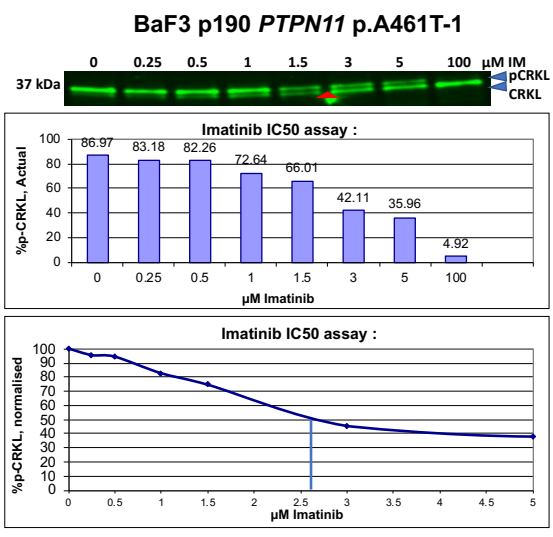

IC50= 2.6 µM

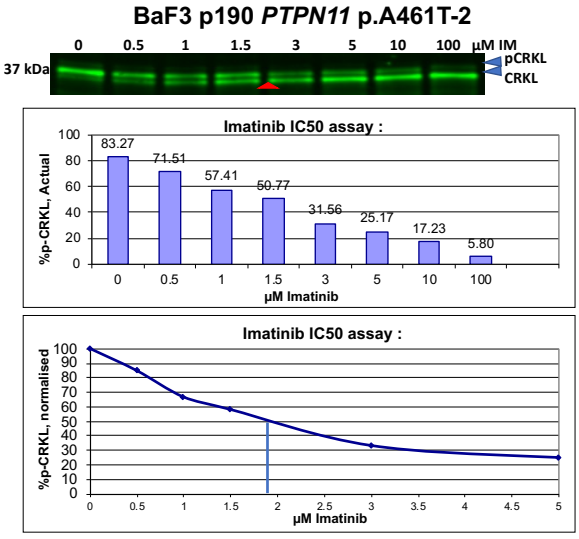

IC50= 1.9 µM

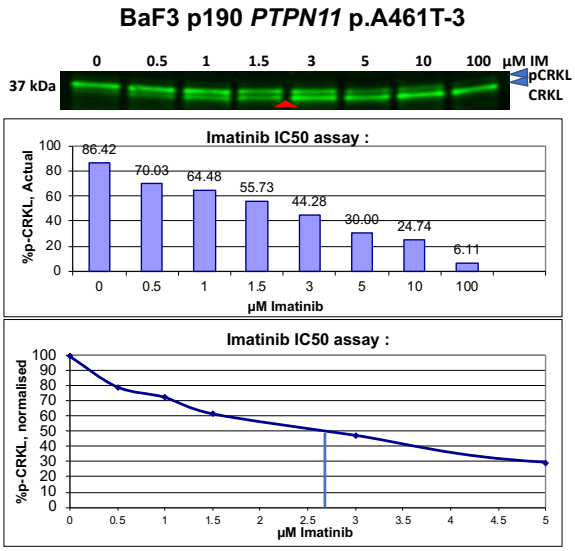

IC50= 2.6 µM

4. Imatinib pCRKL IC50 assays of BaF3 *BCR::ABL1* p190 *PTPN11* p.A461T cells. Western immunoblotting of pCRKL IC50 for BaF3 BCR::ABL1 p190 cells exposed to increasing concentrations (0, 0.25, 0.5, 1, 1.5, 3, 5, and 100 µM) of imatinib for 2 hours at 37°C/5% CO_2. The densitometry analysis of pCRKL and CRKL was performed in Image Studio Lite, and the graphs were created and the concentration of imatinib required to inhibit pCRKL by 50% in 2 hours (IC50) was calculated in Microsoft excel. Western blots shown are three independent experiments (n=3) and red triangle indicates approximate IC50 concentration.

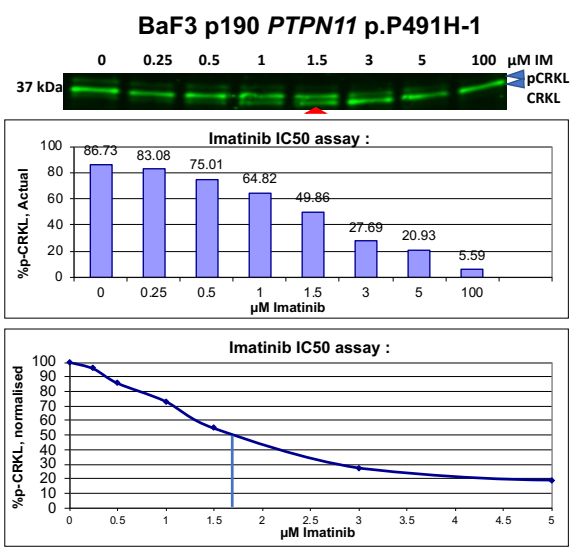

IC50= 1.6 µM

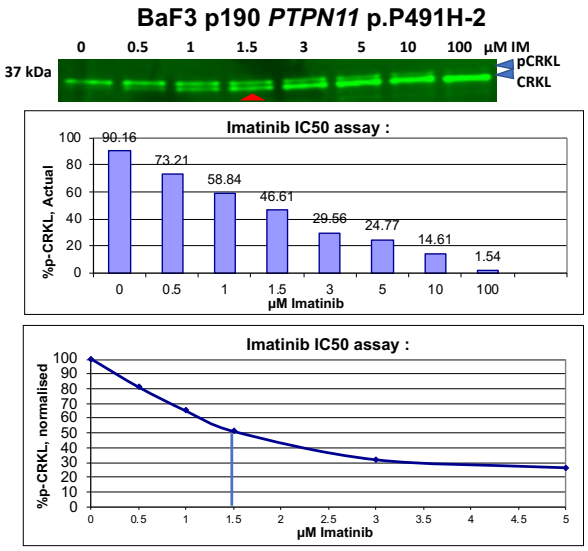

IC50= 1.5 µM

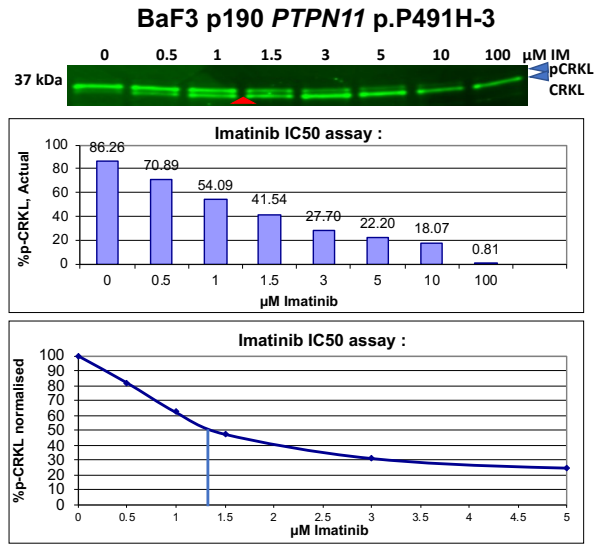

IC50= 1.4 µM

5. Imatinib pCRKL IC50 assays of BaF3 *BCR::ABL1* p190 *PTPN11* p.P491H cells. Western immunoblotting of pCRKL IC50 for BaF3 BCR::ABL1 p190 cells exposed to increasing concentrations (0, 0.25, 0.5, 1, 1.5, 3, 5, and 100 µM) of imatinib for 2 hours at 37°C/5% CO_2. The densitometry analysis of pCRKL and CRKL was performed in Image Studio Lite, and the graphs were created and the concentration of imatinib required to inhibit pCRKL by 50% in 2 hours (IC50) was calculated in Microsoft excel. Western

blots shown are three independent experiments (n=3) and red triangle indicates approximate IC50 concentration.

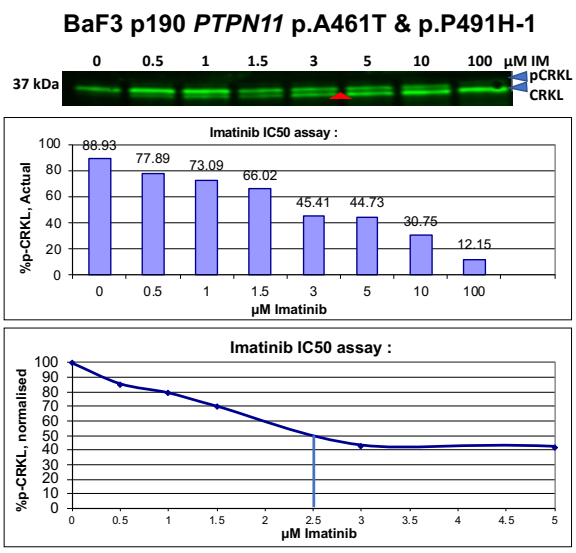

IC50= 2.5 µM

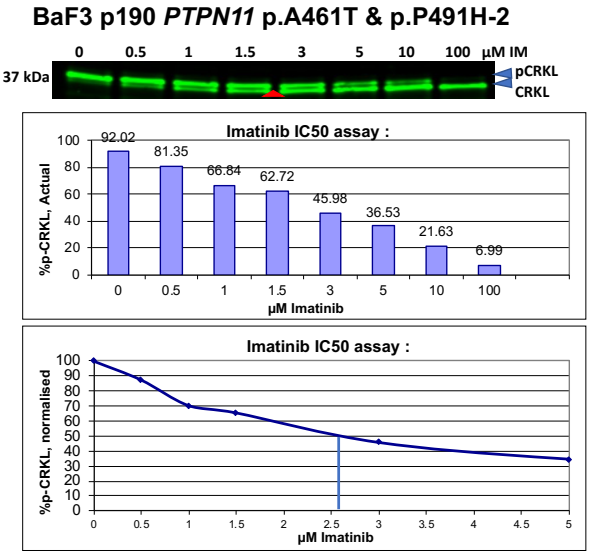

IC50= 2.6 µM

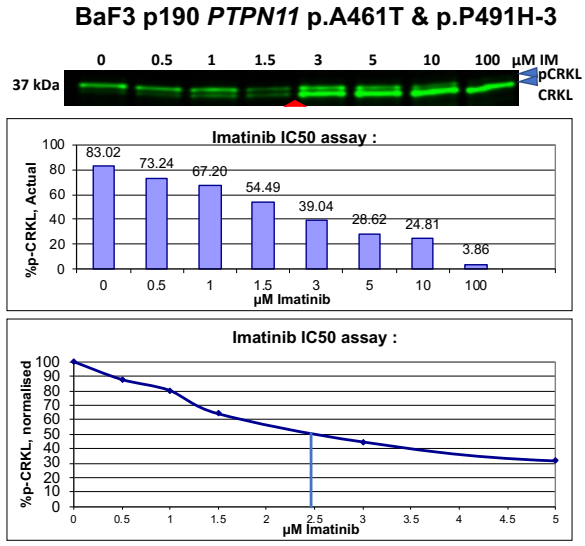

IC50= 2.4 µM

6. Imatinib pCRKL IC50 assays of BaF3 *BCR::ABL1* p190 *PTPN11* p.A461T & p.P491H cells. Western immunoblotting of pCRKL IC50 for BaF3 BCR::ABL1 p190 cells exposed to increasing concentrations (0, 0.25, 0.5, 1, 1.5, 3, 5, and 100 µM) of imatinib for 2 hours at 37°C/5% CO_2. The densitometry analysis of pCRKL and CRKL was performed in Image Studio Lite, and the graphs were created and the concentration of imatinib

required to inhibit pCRKL by 50% in 2 hours (IC50) was calculated in Microsoft excel. Western blots shown are three independent experiments (n=3) and red triangle indicates approximate IC50 concentration.

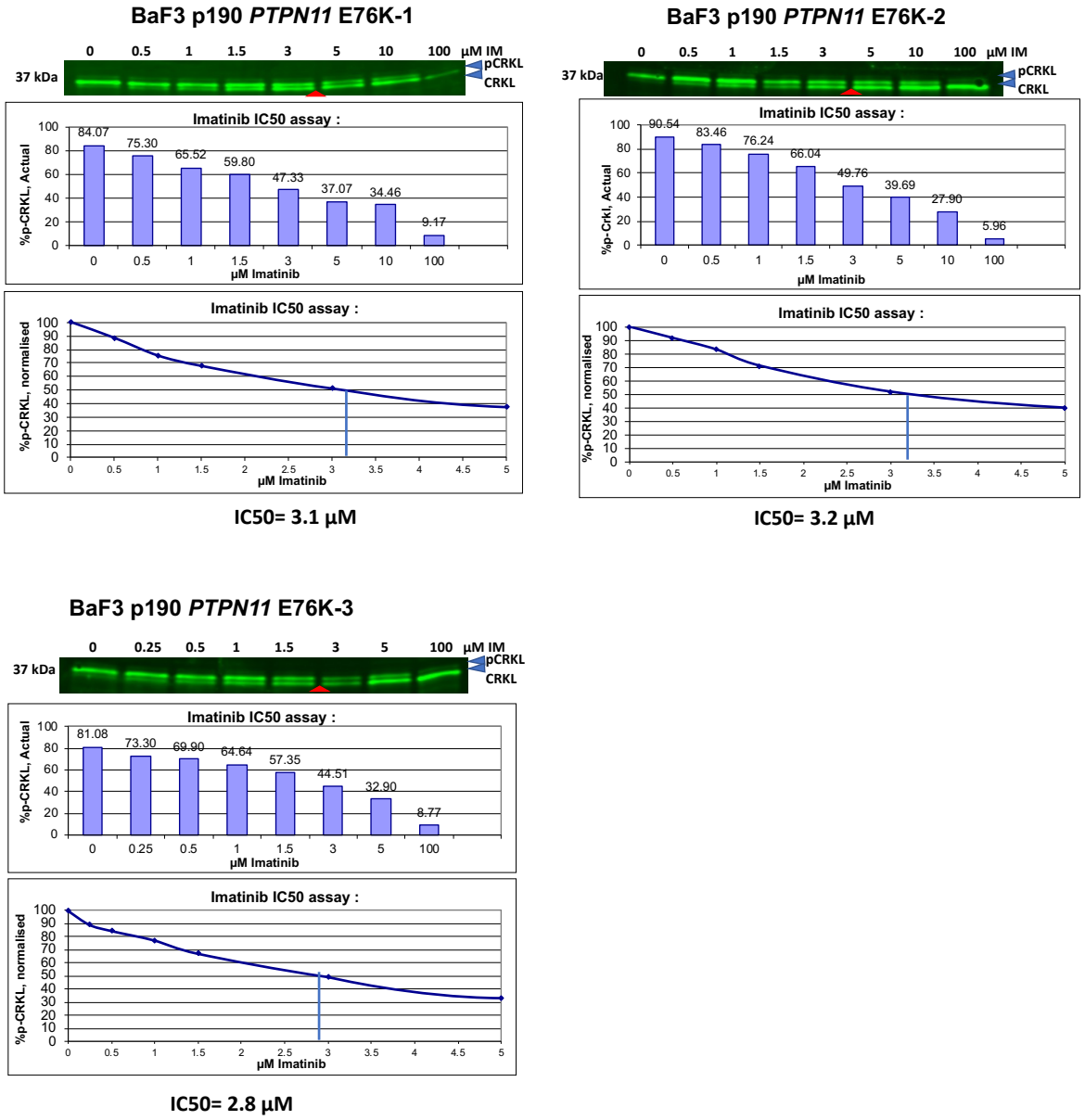

7. Imatinib pCRKL IC50 assays of BaF3 *BCR::ABL1* p190 *PTPN11* p.E76K cells. Western immunoblotting of pCRKL IC50 for BaF3 BCR::ABL1 p190 cells exposed to increasing concentrations (0, 0.25, 0.5, 1, 1.5, 3, 5, and 100 µM) of imatinib for 2 hours at 37°C/5% CO_2. The densitometry analysis of pCRKL and CRKL was performed in Image

Studio Lite, and the graphs were created and the concentration of imatinib required to inhibit pCRKL by 50% in 2 hours (IC50) was calculated in Microsoft excel. Western blots shown are three independent experiments (n=3) and red triangle indicates approximate IC50 concentration.

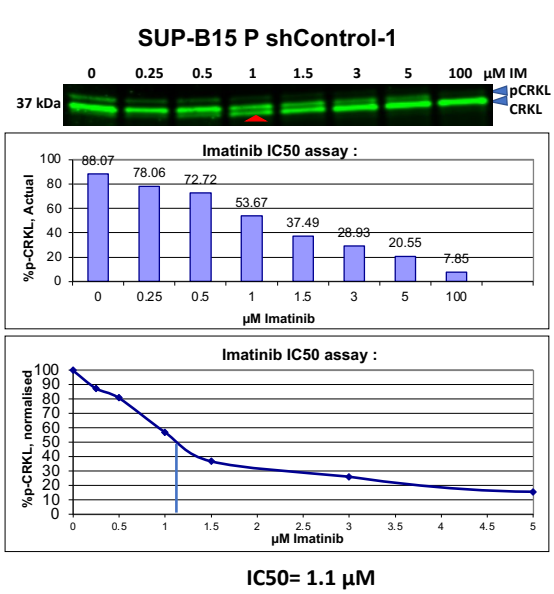

IC50= 1.1 µM

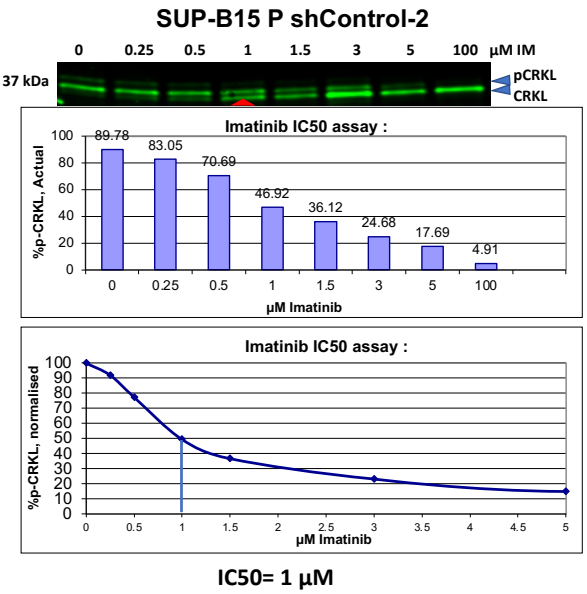

IC50= 1 µM

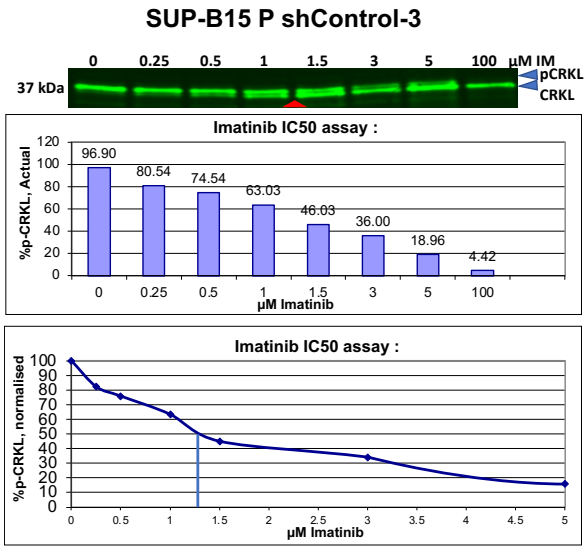

IC50= 1.3 µM

8. Western immunoblotting of pCRKL IC50 for SUP-B15 parental cells transduced with control shRNA, exposed to increasing concentrations (0, 0.25, 0.5, 1, 1.5, 3, 5, and 100 µM) of imatinib for 2 hours at 37°C/5% CO_2. The densitometry analysis of pCRKL and

CRKL was performed in Image Studio Lite, and the graphs were created and the concentration of imatinib required to inhibit pCRKL by 50% in 2 hours (IC50) was calculated in Microsoft excel. Western blots shown are three independent experiments (n=3) and red triangle indicates approximate IC50 concentration.

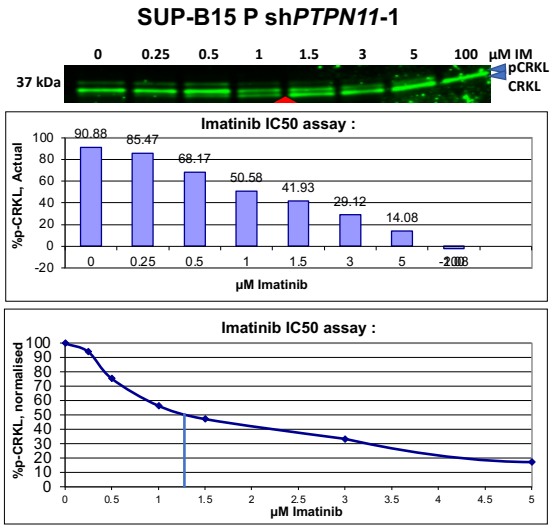

IC50= 1.3 µM

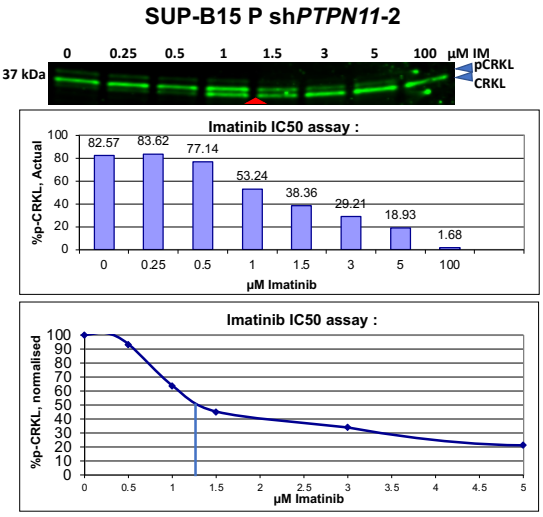

IC50= 1.3 µM

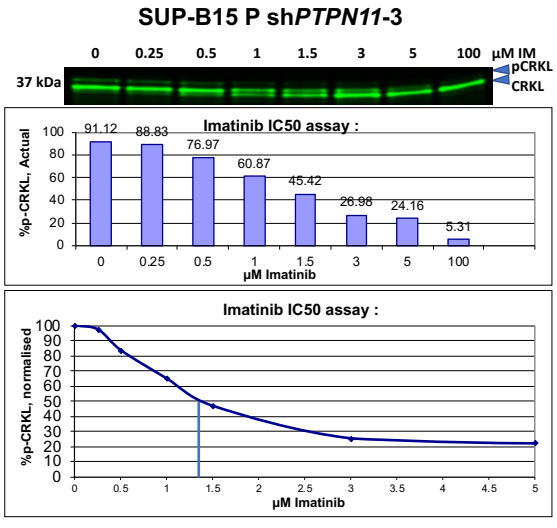

IC50= 1.4 µM

9. Western immunoblotting of pCRKL IC50 for SUP-B15 parental cells transduced with shRNA specific for *PTPN11*, exposed to increasing concentrations (0, 0.25, 0.5, 1, 1.5, 3, 5, and 100 µM) of imatinib for 2 hours at 37°C/5% CO2. The densitometry analysis

of pCRKL and CRKL was performed in Image Studio Lite, and the graphs were created and the concentration of imatinib required to inhibit pCRKL by 50% in 2 hours (IC50) was calculated in Microsoft excel. Western blots shown are three independent experiments (n=3) and red triangle indicates approximate IC50 concentration.

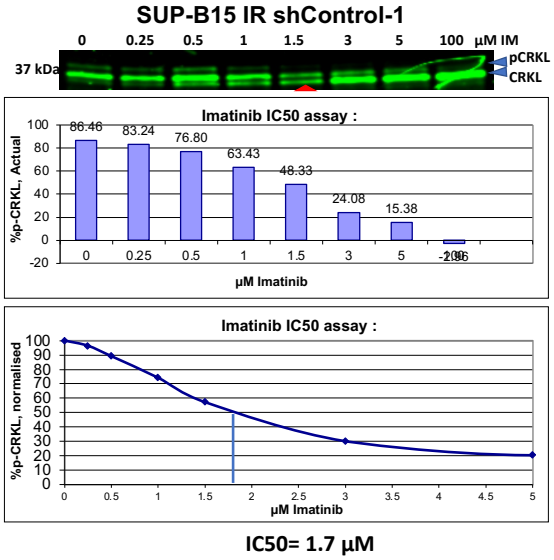

IC50= 1.7 µM

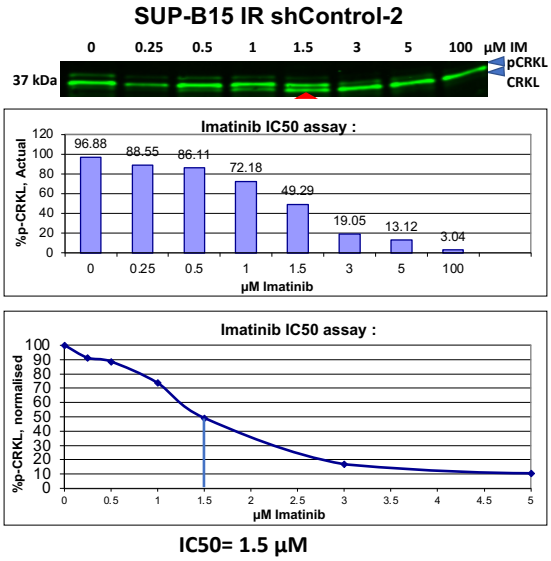

IC50= 1.5 µM

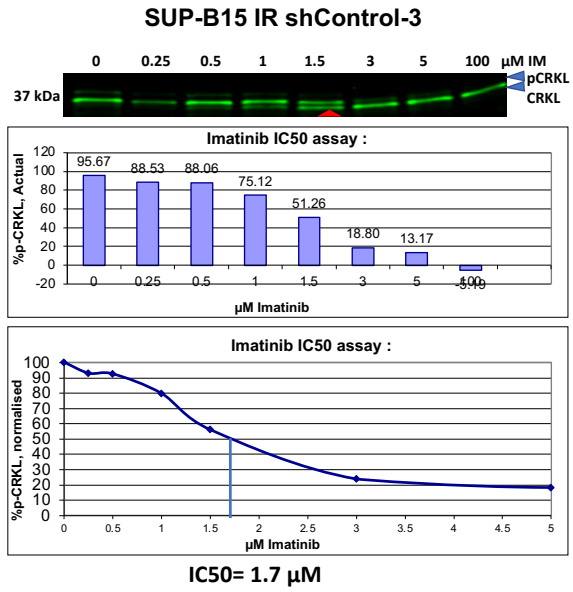

IC50= 1.7 µM

10. Western immunoblotting of pCRKL IC50 for SUP-B15 IR cells transduced with control shRNA, exposed to increasing concentrations (0, 0.25, 0.5, 1, 1.5, 3, 5, and 100 µM) of imatinib for 2 hours at 37°C/5% CO_2. The densitometry analysis of pCRKL and CRKL

was performed in Image Studio Lite, and the graphs were created and the concentration of imatinib required to inhibit pCRKL by 50% in 2 hours (IC50) was calculated in Microsoft excel. Western blots shown are three independent experiments (n=3) and red triangle indicates approximate IC50 concentration.

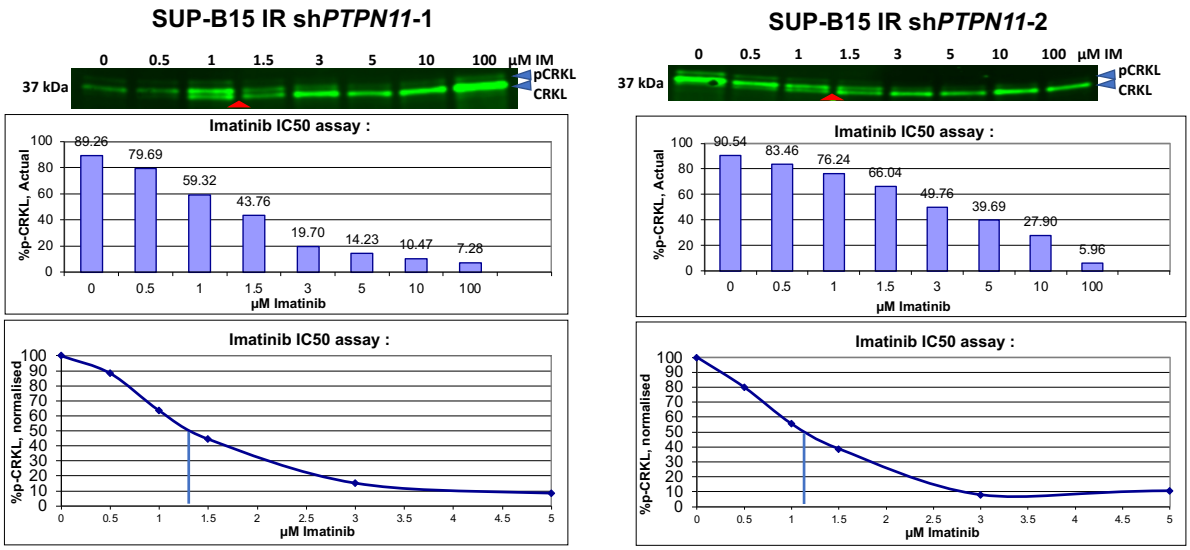

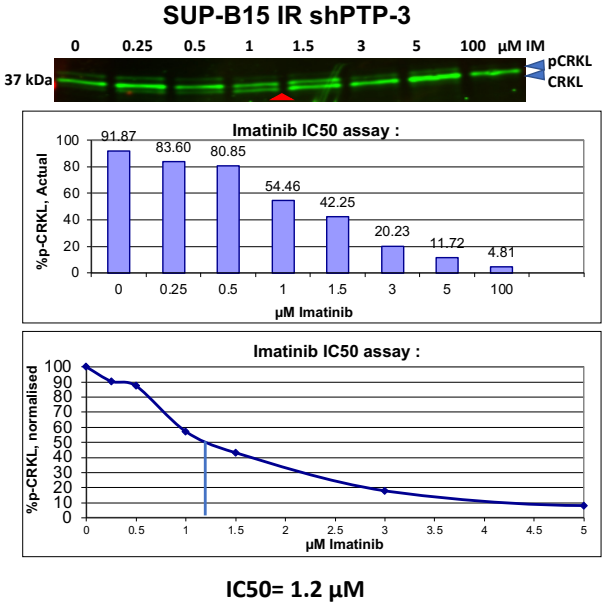

11. Western immunoblotting of pCRKL IC50 for SUP-B15 IR cells transduced with shRNAs specific for *PTPN11* and exposed to increasing concentrations (0, 0.25, 0.5, 1,

1.5, 3, 5, and 100 μM) of imatinib for 2 hours at 37°C/5% CO_2. The densitometry analysis of pCRKL and CRKL was performed in Image Studio Lite, and the graphs were created and the concentration of imatinib required to inhibit pCRKL by 50% in 2 hours (IC50) was calculated in Microsoft excel. Western blots 1-3 shown are three independent experiments (n=3) and red triangle indicates approximate IC50 concentration.

CHAPTER 5: PTPN11 Mutations Induce Resistance to Venetoclax which can be overcome by Combination Therapy of Venetoclax with Tyrosine Kinase Inhibitors

Chapter 5 Summary

Chapter 3 delved into the elucidation of resistance mechanisms in imatinib-resistant SUP-B15 cells, which included a focus on the identification and characterization of imatinib resistant SUP-B15 cells with phosphotyrosine phosphatase non-receptor type-11 (PTPN11) mutations. Chapter 4 serves as a continuation of this investigation, providing further validation of the role played by PTPN11 mutations in the development of resistance to tyrosine kinase inhibitors (TKIs). Together, these chapters shed light on a previously unrecognized resistance mechanism, distinct from BCR::ABL1 mutations, in Philadelphia chromosome-positive acute lymphoblastic leukemia (Ph+ ALL). This discovery underscores the complexity of treating Ph+ ALL and highlights the need for innovative therapeutic strategies. As demonstrated in the preceding chapters, the presence of mutations in cancer-related genes, beyond those in the BCR::ABL1 gene, presents a substantial clinical challenge in the context of Ph+ leukemia, including Ph+ ALL. A noteworthy fact is that TKI resistance accounts for approximately one-fourth of hematological relapses in Ph+ ALL, and the 5-year survival rate remains less than 50% [1]. Consequently, there is an urgent demand for the development of novel treatment approaches to enhance patient outcomes.

Chapter 5 presents an exploration of novel therapeutic strategies using the Ph+ ALL SUP-B15 cell line harboring dual PTP domain PTPN11 mutations (p.A461T and p.P491H). This investigation assesses the in-vitro effectiveness of anti-apoptotic protein inhibitors, both as monotherapy and in combination with TKIs, to address the complex challenge posed by PTPN11-driven resistance. Within this chapter, it is demonstrated that SUP-B15 IR cells exhibit resistance to venetoclax or the MCL-1 inhibitor (S63845) when administered as individual agents. However, these cells display sensitivity to higher concentrations of

the BCL-XL inhibitor (A-1155463). Intriguingly, synergistic effects emerge when simultaneously inhibiting BCL-XL/BCL-2 and MCL-1 using their specific inhibitors, effectively surmounting resistance driven by PTPN11 mutations. Moreover, this chapter reveals the restoration of inhibition through MCL-1 blockade when TKIs are employed, thus highlighting the cooperative interplay between PTPN11 mutation-induced BCL-XL expression and pBCR::ABL1 (Y177)-mediated MCL-1 expression as pivotal in overcoming resistance in SUP-B15 cells. In conclusion, a combination of TKIs and venetoclax emerges as a promising salvage option for addressing PTPN11-driven resistance in Ph+ ALL.

Introduction

The treatment of Ph+ ALL has been significantly improved, firstly with the addition of Tyrosine Kinase Inhibitors (TKIs) to intensive chemotherapy, and secondly with the development of more potent second and third generation TKIs [2]. However, non-BCR::ABL1 mutational resistance poses a treatment challenge despite having more potent TKIs. For instance, about a quarter of Ph+ ALL patients fail to maintain remission due the development of TKI resistance and approximately 30% of poor responder patients develop TKI resistance without any kinase domain mutations [3-5]. The mechanism of resistance in those patients is poorly understood. Mutations in cancer associated genes such as phosphotyrosine phosphatase non-receptor type-11 (*PTPN11*) are prevalent in haematological malignancies and have been shown to confer resistance to targeted therapy including in Chronic Myeloid Leukaemia (CML) and Ph+ ALL [6-8]. Src homology phosphatase 2 (SHP-2) is encoded by *PTPN11* gene, and it is essential for full and sustained activation of the RAS/ERK pathway. SHP-2 is also needed for BCR::ABL1 induced myeloid and lymphoid leukaemias [9, 10]. Moreover, PTPN11 mutations have been described as being involved in venetoclax resistance with anti-

apoptotic protein MCL-1 overexpression in Acute Myeloid Leukaemia (AML) [11]. Therefore, they may be implicated in venetoclax resistance also in Ph+ ALL because venetoclax is an emerging therapy for the treatment of Ph+ ALL [12]. PTPN11 mutations account for more than 35% of juvenile myelomonocytic leukaemia, 10% myelodysplastic syndromes, 5% acute myeloid leukaemia and 7% B-cell ALL [13]. Since there are no targeted treatment against PTPN11 mutations for the treatment of any haematological malignancies including Ph+ ALL, safer and targeted treatment approaches are urgently needed.

The B-cell lymphoma-2 family proteins play critical roles in controlling mitochondrial-mediated intrinsic apoptosis [14] and maintaining leukaemic cell viability [15, 16]. Intrinsic mitochondrial apoptosis is controlled by pro- apoptotic proteins such as BCL-2-interacting mediator of cell death (BIM), truncated form of BH3-interacting domain death agonist (tBID), p53-upregulated modulator of apoptosis (PUMA) etc. and anti-apoptotic proteins B-cell lymphoma 2 (BCL-2), B-cell lymphoma-extra-large (BCL-XL), Myeloid cell leukemia 1 (MCL-1), B-cell lymphoma-w (BCL-W) and A BCL-2-related protein A1/BCL-2-related isolated from foetal liver-11 (A1/BFL-1) (**Figure 5.1**) [16]. Change in the balance towards pro- versus anti-apoptotic proteins lead to activation of effector proteins BCL-2 antagonist/killer (BAK) and BCL-2-associated X protein (BAX) which form multimeric pores in the outer mitochondrial membrane leading to the release of cytochrome c into the cytoplasm and induction of apoptosis (**Figure 5.1B**) [16, 17]. The pro-apoptotic proteins are also known as BH3-only proteins that exclusively share the BH3 domain [18]. In BCR::ABL1 positive cells, the balance of BCL-2 family proteins shifts in favour of cell survival [19]. Deregulation of BCL-2 family proteins have been implicated in TKI resistance in Ph+ leukaemia [20, 21]. In primary Ph+ B-ALL cells, BCL-2 has been

demonstrated as a key survival factor and its inhibition has been show to induce more potent cell killing than inhibition of BCR::ABL1 [22]. This study recommends further investigation into BCL-2 as an attractive anti-leukaemic target in Ph+ ALL as a single agent. Additionally, dependence of Ph+ ALL on BCL-2 has been previously demonstrated by RNA interference which led to strong induction of apoptosis [23]. Similarly, MCL-1 is another anti-apoptotic protein that is frequently overexpressed in cancer cells and is associated with tumorigenesis, drug resistance and poor prognosis [24].

A number of BH3-only mimetics that resembles BH3-only pro-apoptotic proteins such as BIM binds to the hydrophobic groove of the anti-apoptotic BCL-2 family proteins (such as BCL-2 and MCL-1) and inhibits their functional activity [25]. These mimetics have been developed to directly target anti-apoptotic proteins [25]. One example is venetoclax, a specific inhibitor of BCL-2 approved by the FDA for the treatment of chronic lymphocytic leukemia and acute myeloid leukemia [26]. Venetoclax is an emerging therapy for the treatment of haematological malignancies [27]. Venetoclax has shown promising *in-vitro* therapeutic activity in Ph+ ALL [23, 28, 29] and pre-clinical activity against TKI resistant CML cells [30]. Similarly, a variety of MCL-1 inhibitors such as A1210477, AMG17620, VU661013 and AZD5591 [31] and BCL-XL inhibitors A-1155463 and A-1331852 [32] have been developed and are undergoing pre-clinical investigation. MCL-1 inhibitors, S64315 and S63845 are similar compounds being widely used in scientific research [33]. S64315 is currently being evaluated in Phase 1 clinical trial to determine the maximum tolerated dose [24] and S63845 is currently under pre-clinical studies [34]. The BH3-Only mimetics have been investigated as a potential treatment option for treatment resistant Ph+ ALL cells [23, 29, 35, 36]. Inhibitors of BCL-2 and MCL-

1 have been shown to synergize *in-vitro* and *in-vivo* potent activity against high-risk B-ALL patient derived xenografts [37].

In this study, I investigated venetoclax and MCL-1 inhibitor (S63845) as potential treatment options and showed that imatinib resistant SUP-B15 cells were resistant to either BCL-2 or MCL-1 inhibition alone and were sensitive to BCL-XL inhibition at very high concentrations (>5 μM). This line includes compound *PTPN11* mutations (p.A461T and p.P491H, VAF 63.7% and 40.2% respectively, hereafter SUP-B15 $IR^{PTPN11mut}$). I also included SUP-B15 cells with BCR::ABL1 independent TKIs resistance driven by *KRAS* (G12S, VAF 37%) (SUP-B15 $DR^{KRASmut}$) and *NRAS* (G12S, VAF 100%) (SUP-B15 $PR^{NRASmut}$) mutations as a positive control for RAS/ERK pathway mutations. These cells lines were generated by incremental dose escalation of dasatinib and ponatinib to 200 nM concentration respectively. As demonstrated in chapter 3 and 4, the PTPN11 mutant cells had overexpression of anti-apoptotic proteins BCL-XL and MCL-1. This chapter describes the involvement of anti-apoptotic proteins BCL-XL and MCL-1 in both venetoclax and TKIs resistance. This study demonstrates that PTPN11 knockdown decreases BCL-XL protein expression and increases venetoclax sensitivity and provides a rationale for dual targeting BCL-XL and MCL-1 or BCL-2 and MCL-1 for overcoming resistance. In SUP-B15 cells with PTPN11 mutations, MCL-1 expression could be blocked by blocking BCR::ABL1 activation. Therefore, imatinib or asciminib were used in combination with venetoclax which synergistically overcame resistance in SUP-B15 cells with PTP domain *PTPN11* mutations. TKI and venetoclax combination treatment could be a promising targeted salvage option for Ph+ ALL patients with PTP domain *PTPN11* mutations.

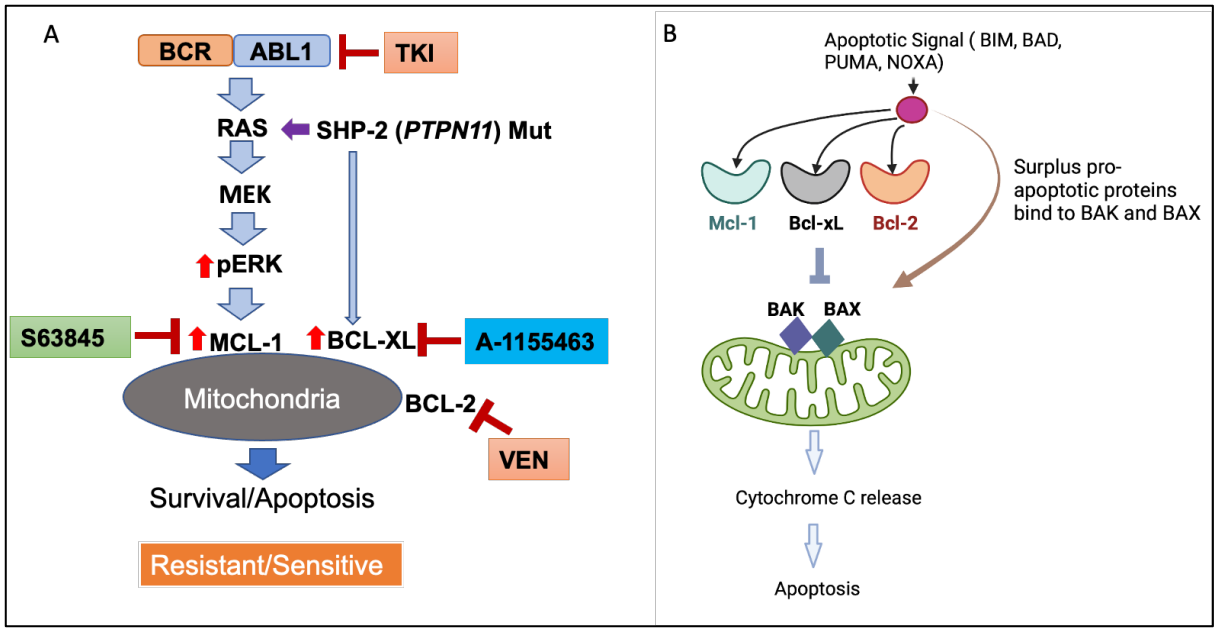

Figure 5.1: Mechanisms of Resistance and Mitochondrial Apoptosis Pathway in SUP-B15 Cells with PTPN11 Mutations and Inhibitor Strategies. (A) This schematic illustrates the resistance mechanisms present in SUP-B15 cells carrying PTPN11 mutations and their response to different inhibitors: Tyrosine Kinase Inhibitor (TKI), S63845, A-1155463, and venetoclax (VEN). The respective targets of these inhibitors are BCR::ABL1, MCL-1, BCL-XL, and BCL-2. BCR::ABL1 activation leads to MCL-1 overexpression, partially mediated via the RAS/ERK axis, while mutated SHP-2 protein induces BCL-XL overexpression. Elevated levels of MCL-1 and BCL-XL contribute to resistance to TKIs. This elevated expression of anti-apoptotic proteins also contributes to resistance against venetoclax. However, the resistance barrier can be effectively surmounted through the simultaneous inhibition of any two out of the three anti-apoptotic proteins: MCL-1, BCL-XL, and BCL-2. (B) This schematic depicts the intrinsic mitochondrial apoptosis pathway. In response to various stress stimuli, including drug treatments or pro-apoptotic proteins (such as BIM, BAD, PUMA, etc.), apoptotic signals are generated. These pro-apoptotic proteins bind to anti-apoptotic proteins like BCL-XL, MCL-1, and BCL-2, preventing apoptosis. However, with increased stimulus, excess pro-

apoptotic proteins become available to bind and activate effector proteins, BCL-2 antagonist/killer (BAK) and BCL-2-associated X protein (BAX), located on the mitochondrial membrane. Activated BAK and BAX form multimeric pores on the outer mitochondrial membrane, leading to the release of cytochrome c into the cytoplasm and the induction of apoptosis.

Results

TKI resistant SUP-B15 cells with PTPN11 mutations were resistant to MCL-1 inhibitor and venetoclax treatment

Previous studies have shown that anti-apoptotic protein MCL-1 is critical for the survival of Ph+ ALL cells and overexpression of anti-apoptotic proteins BCL-XL, MCL-1 and BCL-2 are implicated in TKI resistance [20, 21, 38]. Therefore, overexpression of MCL-1 and BCL-XL in SUP-B15 IR$^{PTPN11\text{mut}}$ cells shown in previous chapters led to the hypothesis that inhibition of these anti-apoptotic proteins could overcome resistance in those cells. I tested the sensitivity of SUP-B15 IR$^{PTPN11\text{mut}}$ cells to a BCL-XL inhibitor (A-1155463), a selective MCL-1 inhibitor (S63845), venetoclax (ABT-199) and inhibitor of BCL-2/BCL-XL, navitoclax (ABT-263). While SUP-B15 IR$^{PTPN11\text{mut}}$ cells demonstrated moderate sensitivity to the BCL-XL inhibitor at concentrations up to 500 nM, neither SUP-B15 P nor SUP-B15 IR$^{PTPN11\text{mut}}$ cells exhibited sensitivity to the BCL-XL inhibitor at higher concentrations (LD50s > 5 μM, the maximum concentration used) (**Figure 5.2A**). Intriguingly, SUP-B15 IR$^{PTPN11\text{mut}}$ cells displayed resistance to venetoclax at all concentrations tested ($p \leq 0.01$), with an LD50 > 50 nM, compared to 2.1±0.33 nM in the parental cell line (**Figure 5.2B**). Additionally, SUP-B15 IR$^{PTPN11\text{mut}}$ cells exhibited resistance ($p \leq 0.01$) to S63845, a specific MCL-1 inhibitor, at all concentrations tested, with an LD50 of 386±17.2 nM, compared to 46.3±7 nM in the parental cell line ($p < 0.0001$)

(**Figure 5.2C**). These results are consistent with the hypothesis that loss of one anti-apoptotic protein may be compensated by overexpression of another to maintain ratio of pro vs anti-apoptotic proteins below threshold required for the initiation of mitochondrial apoptosis. Interestingly, SUP-B15 IR$^{PTPN11\text{mut}}$ cells also showed reduced sensitivity navitoclax, an inhibitor with BCL-2 and BCL-XL dual target, at concentrations greater than 10 nM ($p \leq 0.01$) with an LD50 > 50 nM vs 22.6±7.9 nM for parental (**Figure 5.2D**). This was likely mediated via MCL-1 overexpression because reduced sensitivity to navitoclax has been reported in AML cells with higher MCL-1 expression [39].

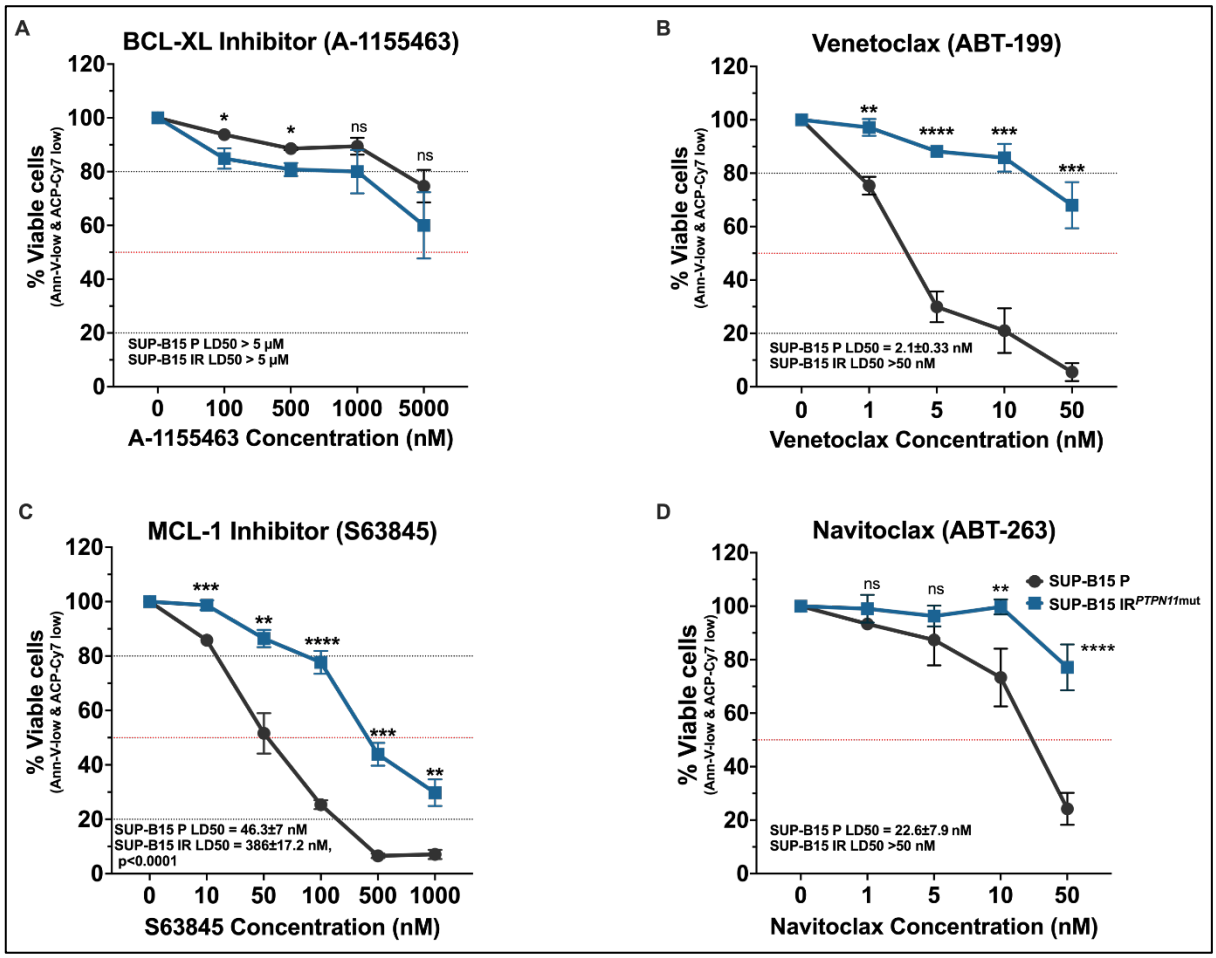

Figure 5.2: SUP-B15 cells with PTPN11 mutations are resistant to inhibitors of MCL-1 and BCL-2. (A-D) Cell death assay of SUP-B15 cells in response to increasing concentrations of a BCL-XL inhibitor (A-1155463), MCL-1 inhibitor (S63845), venetoclax (ABT-199), and navitoclax (ABT-263) for 72 hours. SUP-B15 IR$^{PTPN11\text{mut}}$ cells underwent

overnight washout procedure as described in '2.7.3. Cell washout protocol for TKI resistant cells of Chapter 2: Methods and Materials'. Viability was assessed by measuring Annexin-V-PE and Fixable Viability Stain 780 using flow cytometry. The Y-axis represents Annexin-V-PE low and Fixable Viability Stain low, expressed as a percentage of viable cells. The lethal dose (LD50) indicates the concentration of BH3-Only mimetics required to induce apoptosis in 50% of cells. Data presented are derived from three independent experiments (n=3). Statistical analysis was performed using One-Way ANOVA. Ns, *, **, *** and **** represent $p>0.05$, $p\leq0.05$, $p\leq0.01$, $p\leq0.001$ and $p\leq0.0001$ respectively.

SUP-B15 cells with RAS pathway (NRAS and KRAS) mutations have BCR::ABL1 independent mechanisms of resistance and are resistant to all TKIs tested

To gain insights into the underlying mechanisms of venetoclax resistance in SUP-B15 IR$^{PTPN11\text{mut}}$ cells, I examined two sub-lines of SUP-B15 cells that were exposed to incremental dose escalation of dasatinib and ponatinib up to 200 nM. These sub-lines developed KRAS (G12S, VAF 37%) mutations and NRAS (G12S, VAF 100%) mutations respectively (**Figure 5.3A**). Notably, these cells exhibited sustained activation of the RAS/ERK pathway in the presence of tyrosine kinase inhibitors (TKIs), as indicated by increased levels of pERK1/2 (**see Appendix 1**).

As anticipated, both the SUP-B15 DR$^{KRAS\text{mut}}$ and SUP-B15 PR$^{NRAS\text{mut}}$ cell lines demonstrated substantial resistance to a range of TKIs, including imatinib, nilotinib, dasatinib, ponatinib, and the allosteric BCR::ABL1 inhibitor, asciminib (LD50s > maximum concentrations used) (**Figure 5.3D-I**). Western blot analysis revealed that these cells effectively inhibited pBCR::ABL1 (Y177) when treated with imatinib at a

concentration of 5 µM, which is typically effective in parental cells. However, this inhibition had minimal to no effect on cell viability in SUP-B15 DR^{KRASmut} and SUP-B15 PR^{NRASmut} cells (**Figure 5.4B, C, and D**).

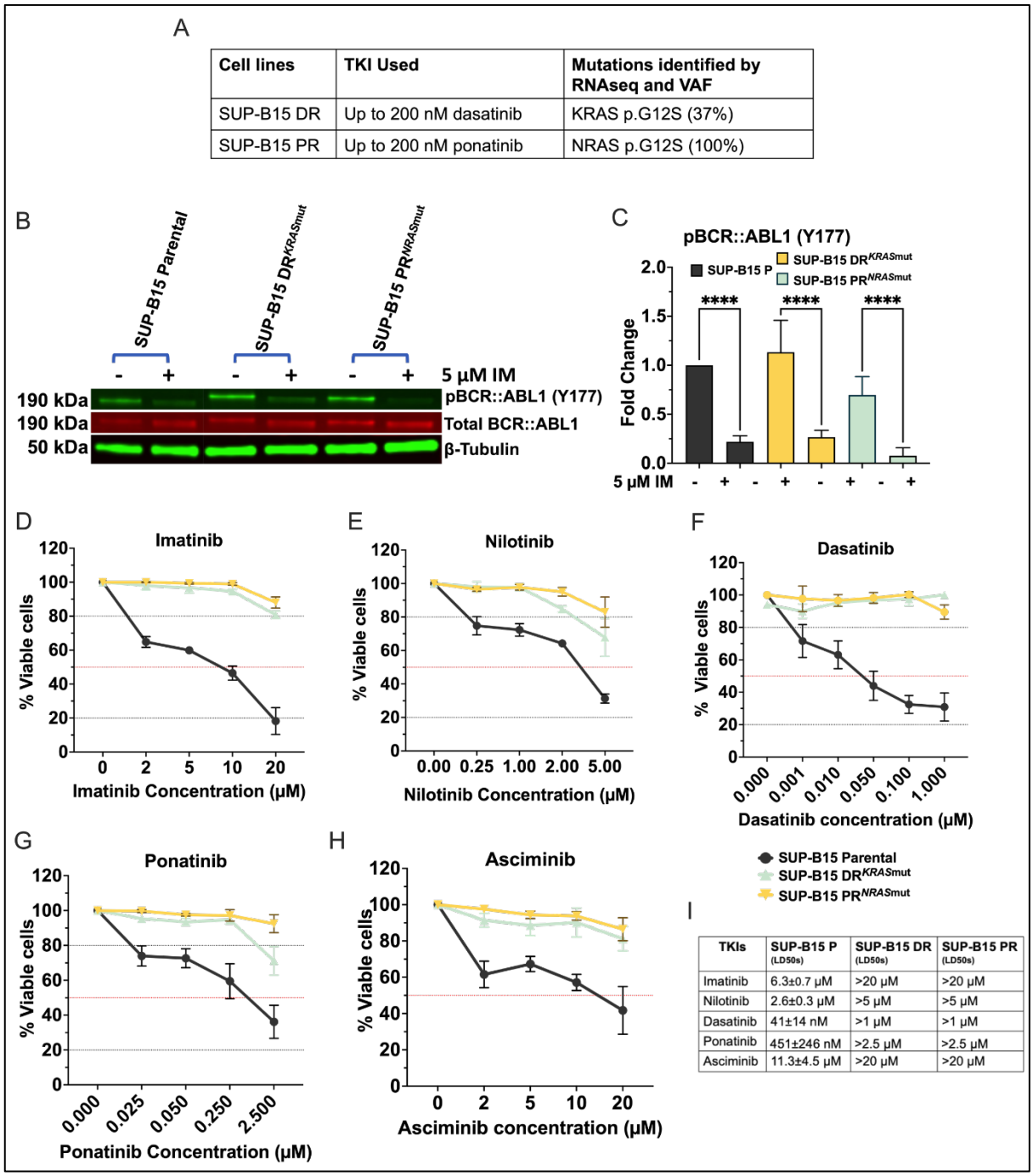

Cell lines	TKI Used	Mutations identified by RNAseq and VAF
SUP-B15 DR	Up to 200 nM dasatinib	KRAS p.G12S (37%)
SUP-B15 PR	Up to 200 nM ponatinib	NRAS p.G12S (100%)

TKIs	SUP-B15 P (LD50s)	SUP-B15 DR (LD50s)	SUP-B15 PR (LD50s)
Imatinib	6.3±0.7 µM	>20 µM	>20 µM
Nilotinib	2.6±0.3 µM	>5 µM	>5 µM
Dasatinib	41±14 nM	>1 µM	>1 µM
Ponatinib	451±246 nM	>2.5 µM	>2.5 µM
Asciminib	11.3±4.5 µM	>20 µM	>20 µM

Figure 5.3: SUP-B15 DR^{KRASmut} and SUP-B15 PR^{NRASmut} cells were resistant to, first, second and third generation TKIs as well as to asciminib. (A) Identification of KRAS and NRAS mutations through RNAseq analysis in dasatinib-resistant (to 200 nM) and

ponatinib-resistant (to 200 nM) SUP-B15 cells, respectively, along with variant allele frequency (%VAF) for these mutations. (B and C) Western immunoblotting and densitometry analysis of pBCR::ABL1 in response to 5 μM imatinib treatment, a concentration at which both SUP-B15 DR$^{KRAS\text{mut}}$ and SUP-B15 PR$^{NRAS\text{mut}}$ cell lines exhibit overt resistance. Data represent results from three independent experiments (n=3). Statistical analysis was conducted using One-Way ANOVA, and error bars depict standard deviation (SD) of three independent experiments (n=3). Ns, *, **, *** and **** represent $p>0.05$, $p\leq0.05$, $p\leq0.01$, $p\leq0.001$ and $p\leq0.0001$ respectively. (D-H) Viability assay of SUP-B15 DR$^{KRAS\text{mut}}$ and PR$^{NRAS\text{mut}}$ cells treated with increasing concentrations of imatinib, nilotinib, dasatinib, ponatinib, and asciminib for 72 hours. TKI resistant SUP-B15 cells underwent overnight washout procedure as described in '2.7.3. Cell washout protocol for TKI resistant cells of Chapter 2: Methods and Materials'. Viability is represented as Annexin-V-PE low and Fixable Viability Stain low, expressed as a percentage of viable cells normalized to the no treatment/DMSO-only control. (I) Lethal dose (LD50s) for SUP-B15 P, DR$^{KRAS\text{mut}}$ and PR$^{NRAS\text{mut}}$ cells treated with increasing concentrations of imatinib, nilotinib, dasatinib, ponatinib, and asciminib for 72 hours. Viability is represented as Annexin-V-PE low and Fixable Viability Stain low, expressed as a percentage of viable cells normalized to the no treatment/DMSO-only control.

Dynamics of anti-apoptotic protein expression and venetoclax sensitivity in RAS pathway driven TKI resistance

To assess whether the most prevalent RAS pathway mutations play a role in inducing venetoclax resistance, I conducted experiments to evaluate the sensitivity of SUP-B15 DR$^{KRAS\text{mut}}$ and PR$^{NRAS\text{mut}}$ cell lines to venetoclax treatment. Intriguingly, despite the presence of RAS pathway mutations, both SUP-B15 DR$^{KRAS\text{mut}}$ and SUP-B15 PR$^{NRAS\text{mut}}$ cell

lines exhibited sensitivity to venetoclax treatment, with LD50 values of 8.58±2.26 nM and 6.06±1.01 nM, respectively, as compared to 2.15±0.33 nM for the parental control ($p>0.9$) (**Figure 5.4A**).

To delve deeper into this intriguing finding, I conducted a comparative analysis of the expression levels of anti-apoptotic proteins in these cells, contrasting them with imatinib-resistant SUP-B15 IR$^{PTPN11\text{mut}}$ cells bearing PTPN11 mutations. Consistent with the hypothesis that venetoclax resistance in SUP-B15 IR$^{PTPN11\text{mut}}$ cells stems from the overexpression of BCL-XL and MCL-1, both SUP-B15 DR$^{KRAS\text{mut}}$ and SUP-B15 PR$^{NRAS\text{mut}}$ cell lines did not exhibit significantly elevated levels of BCL-XL ($p= 0.083$ and 0.220, respectively) and MCL-1 ($p=0.16$ and 0.39, respectively) expression (**Figure 5.4B, D-F**).

Interestingly, despite demonstrating higher BCL-2 expression ($p=0.019$), SUP-B15 PR$^{NRAS\text{mut}}$ cells did not exhibit altered sensitivity to venetoclax (**Figure 5.4B and E**), suggesting that resistance driven by BCL-2 overexpression could potentially be fully overcome by a BCL-2 inhibitor. Additionally, it's worth noting that SUP-B15 IR$^{PTPN11\text{mut}}$ cells displayed elevated pBCR::ABL1(Y177) levels, consistent with their higher MCL-1 expression (**Figure 5.4B and C**).

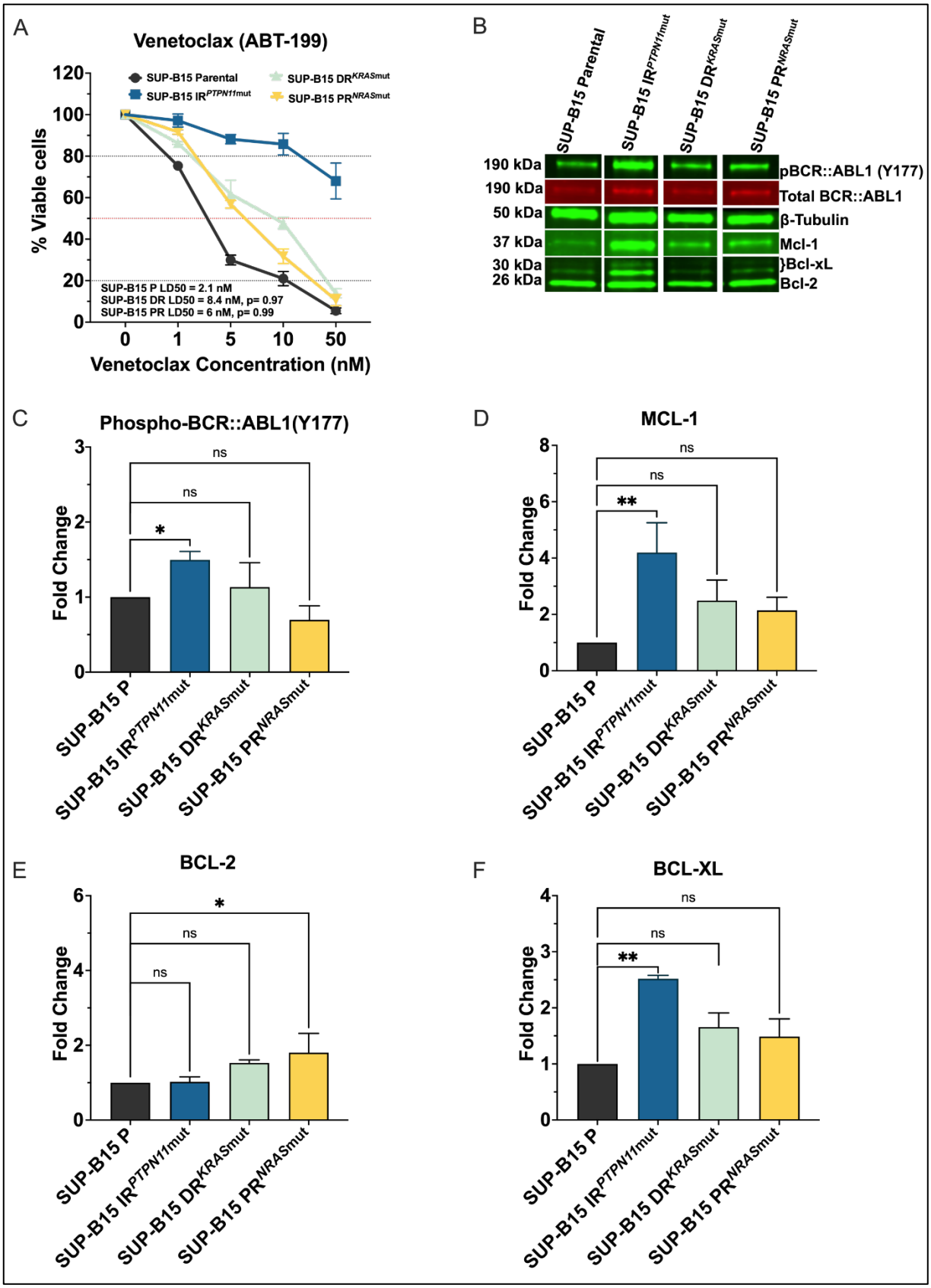

Figure 5.4: Venetoclax resistance correlates with the level of anti-apoptotic protein expression. (A) Cell death assay of SUP-B15 IR^{PTPN11mut}, SUP-B15 DR^{KRASmut} and SUP-B15

PR^{NRASmut} cells in response to increasing concentration of venetoclax for 72 hours. SUP-B15 IR cells underwent overnight washout procedure as described in '**2.7.3. Cell washout protocol for TKI resistant cells** of Chapter 2: Methods and Materials'. Viability was assessed by measuring Annexin-V-PE and Fixable Viability Stain 780 using flow cytometry. The Y-axis represents Annexin-V-PE low and Fixable Viability Stain low, expressed as a percentage of viable cells. Calculation of the lethal dose (LD50) of venetoclax required to induce apoptosis in 50% of SUP-B15 cells was performed using GraphPad Prism 9. (B-F) Western blot and densitometry analysis of anti-apoptotic proteins MCL-1, BCL-XL and BCL-2 in SUP-B15 parental, SUP-B15 IR^{PTPN11mut}, SUP-B15 DR^{KRASmut} and SUP-B15 PR^{NRASmut} cell lines (see **Appendix 2** for full size blot). Data are derived from three independent experiments (n=3). Statistical analysis was conducted using One-way ANOVA. Error bars represent standard deviation (SD) of three independent experiments. Ns, *, **, *** and **** represent $p>0.05$, $p\leq0.05$, $p\leq0.01$, $p\leq0.001$ and $p\leq0.0001$ respectively.

Genetic knockdown of PTPN11 in SUP-B15 IR^{PTPN11mut} cells increases venetoclax sensitivity

To substantiate the role of PTPN11 mutations in the emergence of venetoclax resistance, I conducted RNA interference experiments to effectively knock down the PTPN11 gene within SUP-B15 IR^{PTPN11mut} cells. This was achieved using 3-5 distinct shRNAs that specifically targeted PTPN11. In alignment with the findings presented in **Figure 4.5** of Chapter 4, wherein a reduction in BCL-XL and MCL-1 expression was observed following PTPN11 knockdown in SUP-B15 IR^{PTPN11mut} cells, the outcome of this intervention was a notable increase in venetoclax sensitivity (LD50 reduced to 7.1±0.7 nM from >50 nM) (**Figure 5.5A and B**). PTPN11 knockdown in SUP-B15 IR^{PTPN11mut} cells significantly

increased sensitivity (p≤0.01) to all concentrations of venetoclax compared to the non-knockdown counterpart.

Crucially, the sensitivity of venetoclax remained unaltered upon PTPN11 knockdown in SUP-B15 parental cells (5.3±1.4 nM vs 3.2±0.8 nM, for shControl and sh*PTPN11* respectively, p =0.091) (**Figure 5.5A and B**). This observation strongly suggests that the mutated SHP-2 protein played a pivotal role in driving the development of venetoclax resistance in SUP-B15 IR^{PTPN11mut} cells.

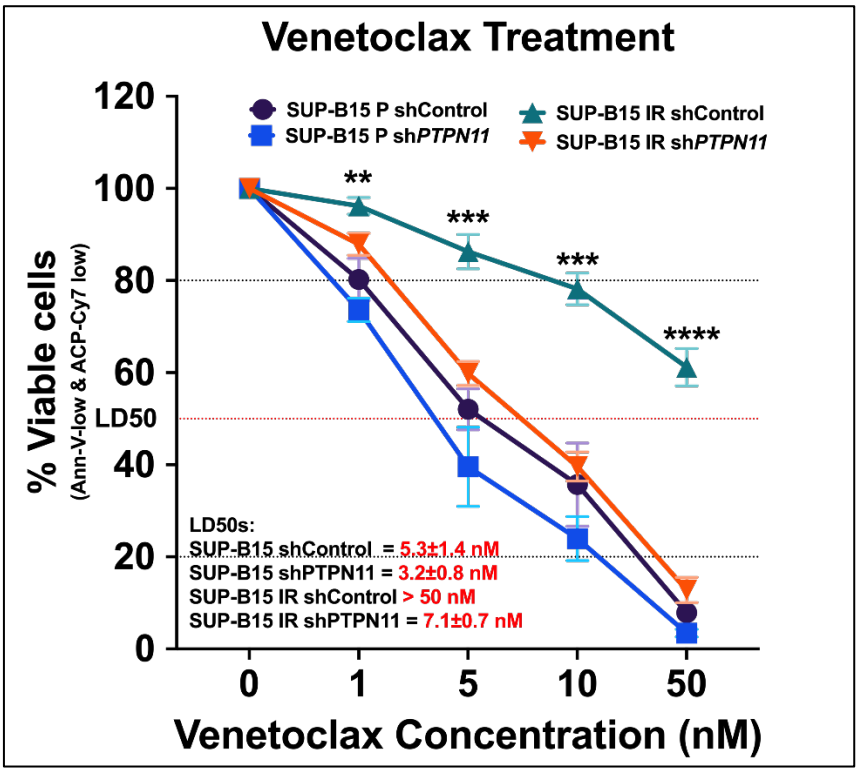

Figure 5.5: Inhibition of PTPN11 with shRNA restored venetoclax sensitivity in SUP-B15 cells with *PTPN11* mutations. (A and B) Cell death assay of SUP-B15 cells transduced with control and PTPN11-specific 3-5 shRNAs, followed by treatment with increasing concentrations of venetoclax for 72 hours. Viability was assessed by measuring Annexin-V-PE and Fixable Viability Stain 780 using flow cytometry. The Y-axis represents Annexin-V-PE low and Fixable Viability Stain low, expressed as a percentage

of viable cells. Calculation of the lethal dose (LD50) of venetoclax required to induce apoptosis in 50% of cells was performed using GraphPad Prism 9. Data are derived from three independent experiments (n=3). Statistical analysis was conducted using unpaired t-test. Error bars on the graph represent the standard deviation (SD) of three independent experiments between SUP-B15 IR^{PTPN11mut} transduce with shControl and sh*PTPN11*. Ns, *, **, *** and **** represent p>0.05, p≤0.05, p≤0.01, p≤0.001 and p≤0.0001 respectively.

Co-inhibition of MCL-1 and BCL-XL synergistically overcomes resistance in SUP-B15 IR^{PTPN11mut} cells

Building upon the insights gained from the PTPN11 knockdown experiment, which effectively reduced BCL-XL and MCL-1 expression while restoring venetoclax sensitivity, I formulated a hypothesis suggesting that simultaneous inhibition of both BCL-XL and MCL-1 might be imperative to overcome resistance in SUP-B15 IR^{PTPN11mut} cells. Consistent with the findings from the PTPN11 knockdown data, the concurrent inhibition of BCL-XL and MCL-1 using A-1155463 and S63845 exhibited synergistic effectiveness in inducing cell death within SUP-B15 IR^{PTPN11mut} cells, surpassing its impact on parental cells (CI = 0.025 for 50 nM A-1155463 and 50 nM S63845) (**Figure 5.6**).

To assess the degree of interaction between these drugs, I employed Calculsyn software (Biosoft, UK) to calculate the combination index (CI). The CI serves as a measure of drug interaction, with values indicating additive effects (CI = 1), synergistic effects (CI < 1), or antagonistic effects (CI > 1) [40]. While BCL-XL inhibition alone had minimal effects on both parental and resistant cells, the resistant cells exhibited increased sensitivity to the combined inhibition of BCL-XL and MCL-1 (**Figure 5.6**).

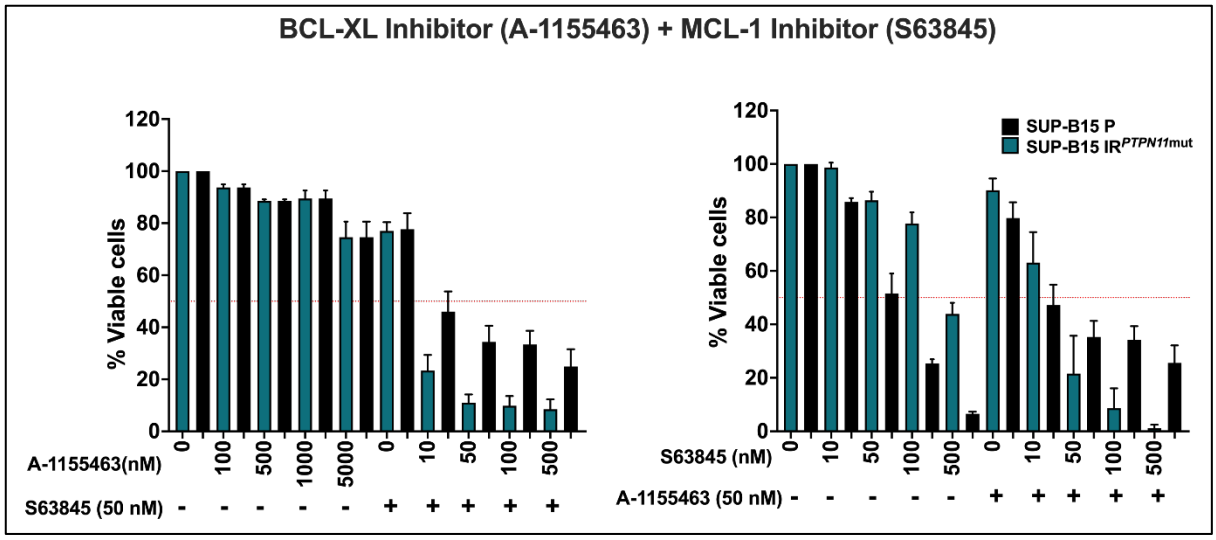

Figure 5.6: Co-inhibition of BCL-XL and MCL-1 synergistically overcame resistance in SUP-B15 IR^{PTPN11mut} cells. Cell death assays were conducted on SUP-B15 cells, with treatments involving either 50 nM of the MCL-1 inhibitor (S63845) and increasing concentrations of the BCL-XL inhibitor (A-1155463), or 50 nM of the BCL-XL inhibitor (A-1155463) and increasing concentrations of the MCL-1 inhibitor (S63845). SUP-B15 IR^{PTPN11mut} cells underwent overnight washout procedure as described in '2.7.3. Cell washout protocol for TKI resistant cells of Chapter 2: Methods and Materials'. The experiments were carried out over a 72-hour duration, and viability was assessed by measuring Annexin-V-PE and Fixable Viability Stain 780 using flow cytometry. The Y-axis represents Annexin-V-PE low and Fixable Viability Stain low, expressed as a percentage of viable cells. Data are derived from three independent experiments (n=3). Error bars indicate the standard deviation (SD) of three independent experiments.

Venetoclax in combination with either MCL-1 or BCL-XL inhibitors synergistically overcomes resistance in SUP-B15 IR^{PTPN11mut} cells

Furthermore, I conducted experiments to assess the sensitivity of SUP-B15 IR^{PTPN11mut} cells to the co-inhibition of either BCL-2 and MCL-1 or BCL-XL. The combination

treatments, involving venetoclax and S63845 (an MCL1 inhibitor) (CI= 0.053 for 5 nM VEN and 50 nM S63845) (**Figure 5.7A**), as well as venetoclax and A-1155463 (a BCL-XL inhibitor) (CI=0.046 for 5 nM VEN and 50 nM A-1155463) (**Figure 5.7B**), exhibited a synergistic capacity to overcome resistance in SUP-B15 IR$^{PTPN11\text{mut}}$ cells.

These results strongly suggest that the inhibition of any two out of the three major anti-apoptotic proteins, namely BCL-2, BCL-XL, and MCL-1, is adequate to overcome resistance in SUP-B15 IR$^{PTPN11\text{mut}}$ cells.

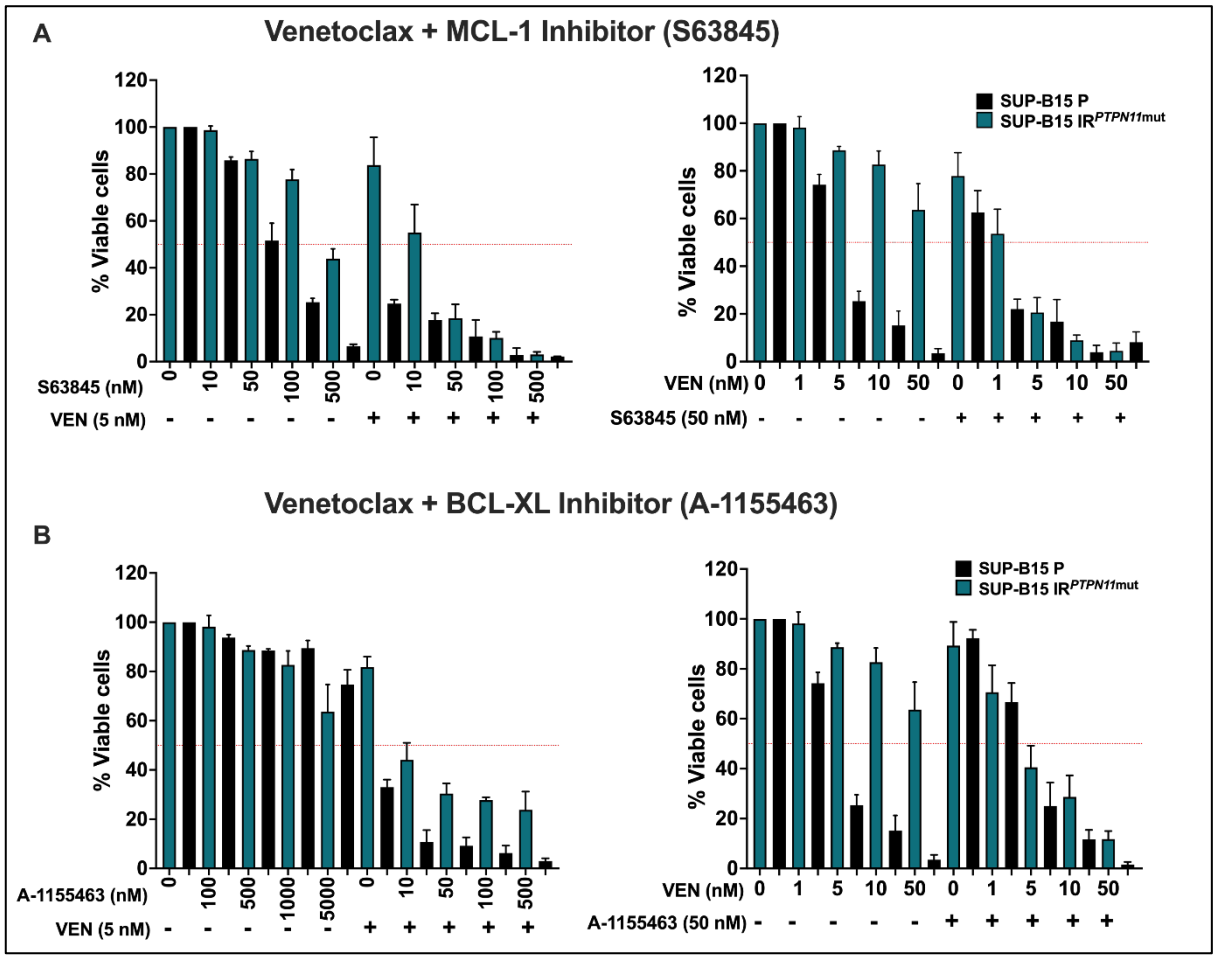

Figure 5.7: Co-inhibition of BCL-2 and MCL-1 or BCL-XL synergistically overcame resistance in SUP-B15 IR$^{PTPN11\text{mut}}$ cells. (A) Cell death assays were performed on SUP-B15 IR$^{PTPN11\text{mut}}$ cells, with treatments consisting of 5 nM venetoclax and increasing concentrations of the MCL-1 inhibitor (S63845), as well as 50 nM S63845 and increasing

concentrations of venetoclax. SUP-B15 IR^{PTPN11mut} cells underwent overnight washout procedure as described in '2.7.3. Cell washout protocol for TKI resistant cells of Chapter 2: Methods and Materials'. These experiments were conducted over a 72-hour period, and viability was assessed by measuring Annexin-V-PE and Fixable Viability Stain 780 using flow cytometry. (B) Cell death assays were conducted on SUP-B15 IR^{PTPN11mut} cells, with treatments comprising 5 nM venetoclax and increasing concentrations of the BCL-XL inhibitor (A-1155463), as well as 50 nM A-1155463 and increasing concentrations of venetoclax. SUP-B15 IR^{PTPN11mut} cells underwent overnight washout procedure as described in '2.7.3. Cell washout protocol for TKI resistant cells of Chapter 2: Methods and Materials'. The experiments were carried out over a 72-hour duration, and viability was determined by measuring Annexin-V-PE and Fixable Viability Stain 780 using flow cytometry. The Y-axis represents Annexin-V-PE low and Fixable Viability Stain low, expressed as a percentage of viable cells. Data are derived from three independent experiments (n=3). Error bars indicate the standard deviation (SD) of three independent experiments.

Imatinib or asciminib in combination with venetoclax also overcomes resistance in SUP-B15 IR^{PTPN11mut} cells

In my study, the administration of Imatinib demonstrated a notable reduction in MCL-1 expression within SUP-B15 IR^{PTPN11mut} cells, a finding prominently illustrated in **'Figure 3.8** of Chapter 3.' Armed with this insight, I strategically employed Imatinib to indirectly modulate MCL-1 expression. My subsequent investigation entailed the evaluation of the combined impact of Imatinib and Venetoclax on inducing cell death in SUP-B15 IR^{PTPN11mut} cells.

Remarkably, my results revealed a synergistic effect when Imatinib and Venetoclax were employed in tandem, effectively overcoming resistance in SUP-B15 IR$^{PTPN11\text{mut}}$ cells. This synergy was particularly striking with a combination index (CI) of 0.049, observed at concentrations of 2 µM Imatinib and 5 nM Venetoclax (**Figure 5.8A**).

Furthermore, to substantiate the specificity of this effect to BCR::ABL1, I conducted additional experiments using Asciminib, an allosteric inhibitor of BCR::ABL1, in lieu of Imatinib. Encouragingly, I observed a similar synergistic outcome with Asciminib and Venetoclax, attaining a CI of 0.032 at concentrations of 2 µM Asciminib and 5 nM Venetoclax (**Figure 5.8B**). This finding strongly suggests that the observed effect was indeed BCR::ABL1-specific, effectively excluding the possibility of off-target effects attributed to Imatinib [41].

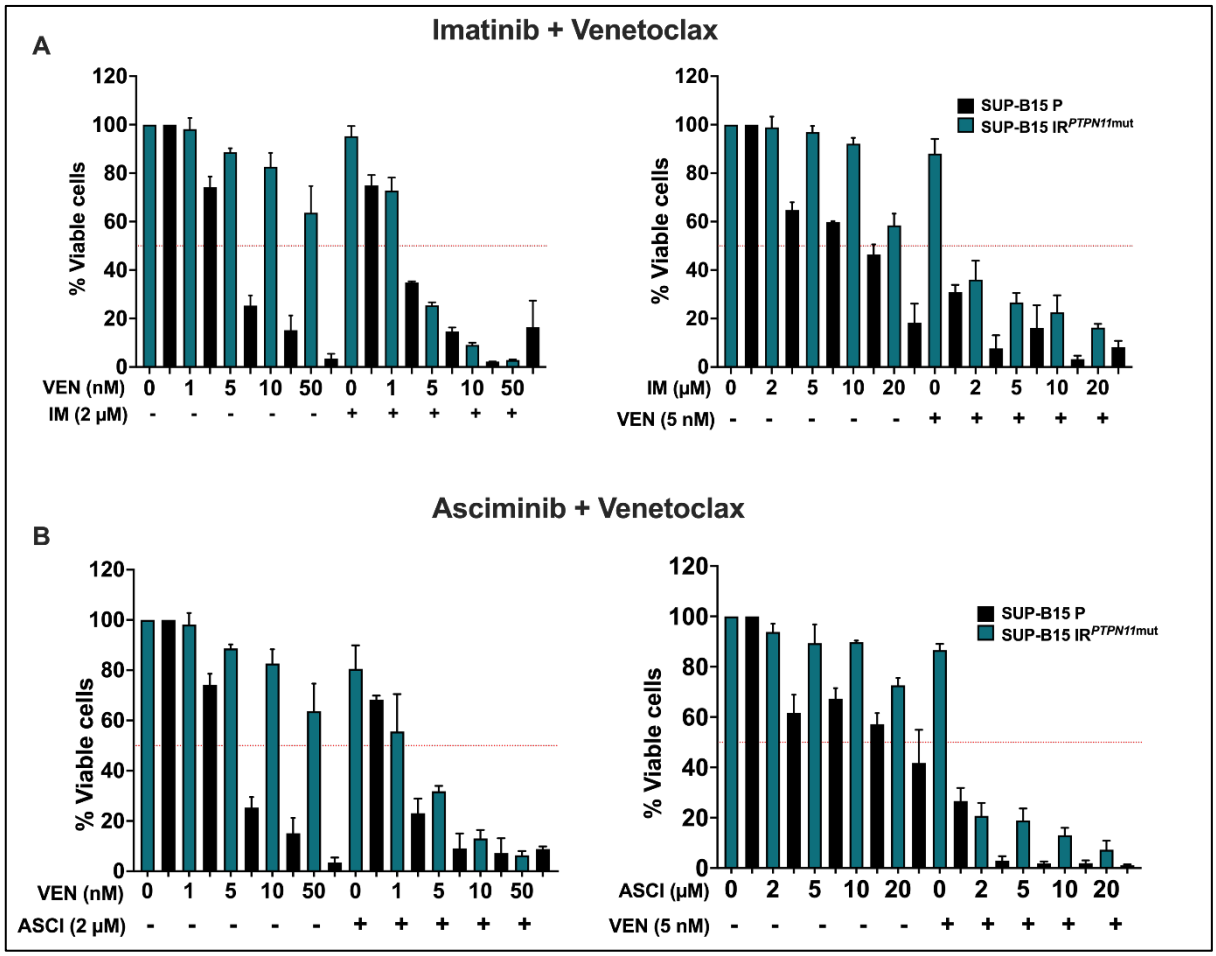

Figure 5.8: Combined inhibition of pBCR::ABL1 and BCL-2 also synergistically induced cell death in SUP-B15 IR^{PTPN11mut} cells. (A-D) Cell death assays were conducted on SUP-B15 cells over a 72-hour period in response to treatments combining venetoclax with either imatinib or asciminib. SUP-B15 IR^{PTPN11mut} cells underwent overnight washout procedure as described in '2.7.3. Cell washout protocol for TKI resistant cells of Chapter 2: Methods and Materials'. The viability was assessed by measuring Annexin-V-PE and Fixable Viability Stain 780 using flow cytometry. The Y-axis represents Annexin-V-PE low and Fixable Viability Stain low, expressed as a percentage of viable cells. Data are derived from three independent experiments (n=3). Error bars indicate the standard deviation (SD) of three independent experiments.

I also investigated the combination of imatinib with other inhibitors targeting anti-apoptotic proteins, namely S63845 (an MCL-1 inhibitor) and A-1155463 (a BCL-XL inhibitor). When imatinib (2 μM) was paired with a lower concentration (10 nM) of S63845, the combination exhibited antagonistic behaviour (CI=2.18) (**Figure 5.9A**). However, the synergy between imatinib and S63845 became evident at and above 50 nM of S63845, with a calculated CI of 0.62 for 2 μM imatinib and 50 nM S63845. It's worth noting that the CI score for this combination was notably higher when compared to the imatinib and venetoclax combination at the same concentrations (CI=0.049) (**Figure 5.9A**).

A-1155463 also showed synergy with imatinib but yielded higher synergy scores (CI > 0.5) for all concentrations, indicating a weaker synergy between these two combinations (**Figure 5.9B**). The limited synergy observed between imatinib, and the MCL-1 inhibitor may be attributed to their singular focus on targeting a single anti-apoptotic protein. In

contrast, the suboptimal synergy between imatinib and BCL-XL likely arose from dose-related factors. Interestingly, enhanced synergy was observed at higher imatinib concentrations, suggesting that increased imatinib levels may lead to more effective control of MCL-1.

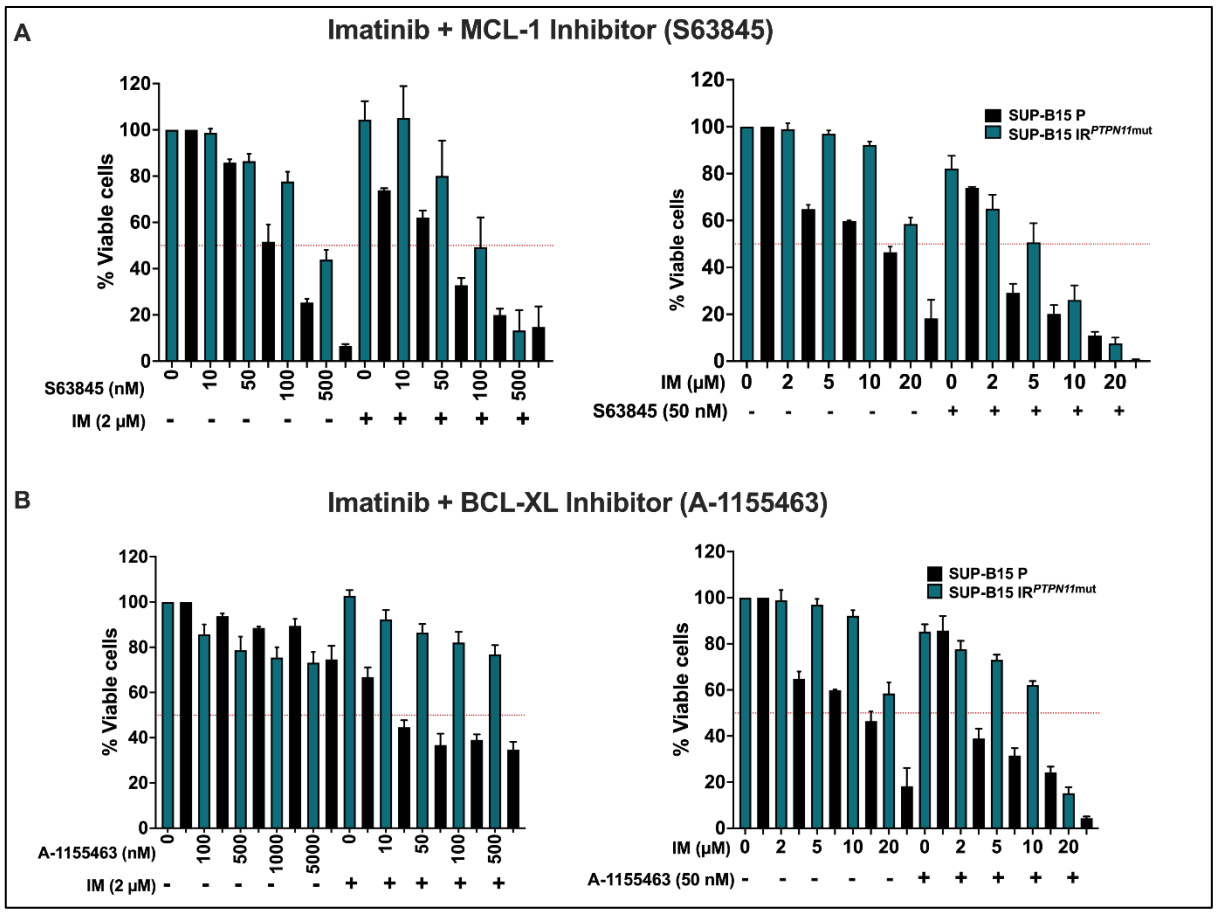

Figure 5.9: Combination treatment of imatinib and either MCL-1 inhibitor (S63845) and BCL-XL inhibitor (A-1155463) were less effective in inducing cell death in SUP-B15 IR^{PTPN11mut} cells. (A -D) Cell death assays were conducted on SUP-B15 cells over a 72-hour period in response to treatments combining venetoclax and imatinib or asciminib. SUP-B15 IR^{PTPN11mut} cells underwent overnight washout procedure as described in '2.7.3. Cell washout protocol for TKI resistant cells of Chapter 2: Methods and Materials'. Viability was assessed by measuring Annexin-V-PE and Fixable Viability Stain 780 using flow cytometry. The Y-axis represents Annexin-V-PE low and Fixable

Viability Stain low, expressed as a percentage of viable cells. Data are derived from three independent experiments (n=3). Error bars indicate the standard deviation (SD) of three independent experiments.

Imatinib and venetoclax combination reduced MCL-1 expression and increased cleaved-PARP in SUP-B15 IR^{PTPN11mut} cells

To validate the impact of the imatinib and venetoclax combination on the expression of anti-apoptotic proteins, I conducted a Western blot analysis using a treatment regimen consisting of 5 μM imatinib and 50 nM venetoclax for a 4-hour duration. SUP-B15 IR^{PTPN11mut} cells underwent overnight washout procedure as described in '2.7.3. Cell washout protocol for TKI resistant cells of Chapter 2: Methods and Materials'. Prior to any treatment, SUP-B15 IR^{PTPN11mut} cells exhibited similar levels of pBCR::ABL1(Y177) (p=0.413) and BCL-2 (p=0.994) expression when compared to untreated parental control cells. However, they displayed elevated levels of pERK1/2 (p=0.0018), MCL-1 (p<0.0001), and BCL-XL (p=0.001) compared to the parental control (**Figure 5.10A-F**).

Upon treatment with imatinib (5 μM), there was a reduction in pBCR::ABL1 (Y177) (p=0.0004), pERK1/2 (p<0.0001), and MCL-1 (p<0.0001) in SUP-B15 IR^{PTPN11mut} cells (**Figure 5.10A-F**). However, this treatment did not have a significant impact on BCL-XL (p>0.99) and BCL-2 (p=0.999) expression (**Figure 5.10A-F**). These results suggest that BCL-XL may potentially contribute to imatinib resistance in SUP-B15 IR^{PTPN11mut} cells when treated as a monotherapy.

Venetoclax (5 nM) treatment, on the other hand, did not significantly alter the expression levels of pBCR::ABL1(Y177) (p=0.998), pERK1/2 (p=0.788), MCL-1 (p=0.957), BCL-XL

(p=0.912), or BCL-2 (p>0.999) (**Figure 5.10A-F**). Notably, while imatinib alone did not induce the production of cleaved-poly(ADP-ribose) polymerase (Cleaved-PARP), an apoptotic marker [42], in parental control cells within the 4-hour timeframe (p>0.999), the treatment with venetoclax led to a rapid increase in cleaved-PARP (p=0.009) (**Figure 5.10A and G**) in parental control (p>0.999) in 4-hour suggesting imatinib may take longer than 4 hours to induce cleaved-PARP. The treatment with venetoclax resulted in rapid increase in cleaved-PARP (p=0.009) (**Figure 5.10A and G**). These results provide evidence that venetoclax is effective in triggering rapid apoptosis in those cells within 4 hours (**Figure 5.10A and G**). Consistent with the venetoclax resistance seen in SUP-B15 IR$^{PTPN11\text{mut}}$ cells, cleaved-PARP expression was similar (p=0.145) in venetoclax treated cells to that of untreated cells (**Figure 5.10A and G**). These findings suggest that venetoclax is effective in inducing rapid apoptosis in these cells within the 4-hour window (**Figure 5.10A and G**). However, consistent with the observed venetoclax resistance in SUP-B15 IR$^{PTPN11\text{mut}}$ cells, the expression of cleaved-PARP remained similar (p=0.145) in venetoclax-treated cells when compared to untreated cells (**Figure 5.10A and G**).

The combination treatment of imatinib (5 μM) and venetoclax (5 nM) not only resulted in a reduction of pBCR::ABL1(Y177) (p=0.0003), pERK1/2 (p<0.0001), and MCL-1 (p<0.0001) but also effectively inhibited BCL-2. This combination treatment led to a significant increase in cleaved-PARP (p<0.0001) within 4 hours compared to untreated controls (**Figure 5.10A-G**). Therefore, it is likely that the combination treatment reduced MCL-1 expression to synergize with BCL-2 inhibition, ultimately inducing apoptosis in SUP-B15 IR$^{PTPN11\text{mut}}$ cells.

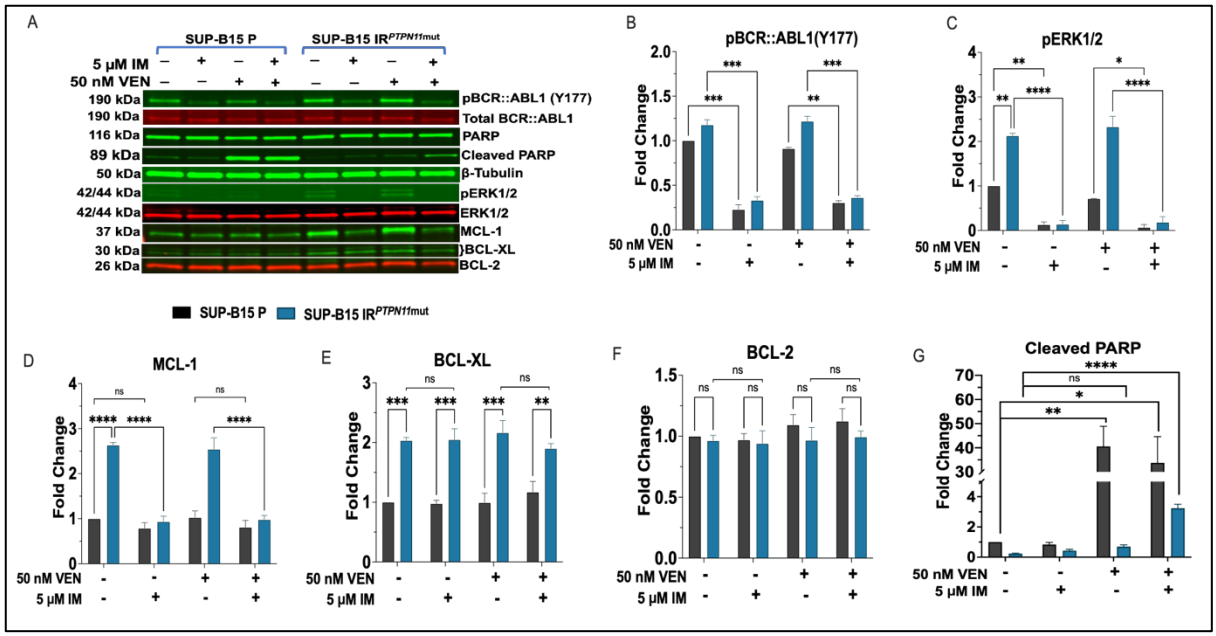

Figure 5.10: Imatinib reduced MCL-1 to induce synergistic cell killing with venetoclax in SUP-B15 IR cells. (A-G) Western immunoblotting was performed following treatment with imatinib (5 μM), venetoclax (50 nM), and their combination in SUP-B15 IR$^{PTPN11\text{mut}}$ cells. SUP-B15 IR cells underwent overnight washout procedure as described in '2.7.3. Cell washout protocol for TKI resistant cells of Chapter 2: Methods and Materials'. Densitometry analysis of key proteins, including pBCR::ABL1(Y177), pERK1/2, MCL-1, BCL-XL, BCL-2, and cleaved-PARP, in response to these treatments is presented. Data represent results from three independent experiments (n=3). Statistical analysis was conducted using Two-way ANOVA, except for cleaved PARP, where One-way ANOVA was used. Error bars indicate the standard deviation (SD) of three independent experiments. Ns, *, **, ***, **** represent $p>0.05$, $p\leq0.05$, $p\leq0.01$, $p\leq0.001$, and $p\leq0.0001$ respectively.

Discussion

This study addresses the formidable challenge of TKI resistance in Ph+ ALL patients, which is closely associated with poor overall survival rates [4, 43]. Non-BCR::ABL1 mutational resistance mechanisms, such as upregulation of anti-apoptotic pathways and cancer-associated gene mutations, present treatment challenges that remain unaddressed by current regimens. Notably, PTPN11 mutations have been linked to poor prognosis and therapy resistance in various haematological malignancies [13, 20, 44]. In this study, I delved into the resistance dynamics of TKI-resistant Ph+ ALL cells carrying PTP domain PTPN11 mutations, which also exhibited resistance to venetoclax and MCL-1 inhibitors. To tackle this resistance, I explored combination therapies involving TKIs and inhibitors targeting anti-apoptotic proteins, with a particular focus on MCL-1 and BCL-2, offering a promising avenue for treatment in Ph+ ALL patients carrying PTPN11 mutations.

In addition to my primary findings, I expanded my investigation to examine RAS/ERK pathway mutations and their role in venetoclax resistance. Using two distinct SUP-B15 cell lines harbouring BCR::ABL1-independent TKI resistance driven by KRAS and NRAS mutations, I discovered that these cells remained sensitive to venetoclax treatment. Unlike PTP domain PTPN11 mutations, KRAS and NRAS mutations were associated with the overexpression of a single anti-apoptotic protein, which likely underlies their sensitivity to venetoclax. The critical role of overexpressed anti-apoptotic proteins BCL-XL and MCL-1 in conferring venetoclax resistance in PTPN11-mutated SUP-B15 cells was further elucidated. Knockdown of PTPN11 not only restored venetoclax sensitivity but also led to a reduction in BCL-XL expression. However, targeting a single anti-apoptotic protein alone was insufficient to overcome resistance in these cells, highlighting the need

for a more comprehensive approach. Combining inhibitors targeting any two of the three major anti-apoptotic proteins: MCL-1, BCL-2, and BCL-XL proved to be the key to synergistic cell death.

My findings align with previous research indicating that overexpression of BCL-XL and MCL-1 is a common cause of venetoclax resistance. My findings are consistent with the report that overexpression of BCL-XL and MCL-1 are the most common cause of venetoclax resistance [45]. Venetoclax resistance is chiefly driven by the sequestration of BIM, preventing it from activating BAK and BAX to initiate mitochondrial apoptosis due to the binding of other anti-apoptotic proteins such as BCL-XL and MCL-1 [46, 47]. Similar observations have been made in AML cell lines [7], where prolonged exposure to venetoclax resulted in increased BCL-XL and MCL-1 expression, leading to resistance. However, this resistance was effectively countered by targeting BCL-XL and MCL-1 with specific inhibitors [48, 49]. Additionally, AML cells with PTPN11 p.A72D mutations have been found to confer venetoclax resistance by inducing sustained expression of MCL-1 and BCL-XL [50]. Combination strategies involving BCL-2 inhibition by venetoclax and MCL-1 inhibition with an MCL-1 inhibitor (AZD5991) have shown promise in reducing MCL-1 levels in these cells.

The concept of co-targeting anti-apoptotic proteins, either alone or in combination with tyrosine kinase inhibition, presents an exciting avenue for anti-leukemic therapy [29]. For instance, Moujalled et al. demonstrated synergistic cell killing by co-targeting BCL-2 and MCL-1 in high-risk B-ALL cells [37]. This combination displayed superior efficacy compared to standard chemotherapy and TKIs in primary samples from both Ph+ ALL and Ph-like ALL adult patients. In Ph+ ALL, the combined inhibition of BCL-2 and MCL-1

proved to be as effective as, or even more potent than, combinations involving dasatinib and venetoclax or dasatinib alongside an MCL-1 inhibitor [37]. I also showed synergistic cell death in SUP-B15 cells carrying PTPN11 mutations when venetoclax is combined with either an MCL-1 or BCL-XL inhibitor. Similar synergy was also observed in T-cell ALL cells with a combination of venetoclax and an MCL-1 inhibitor (S63845) [52]. In Ph+ ALL cells, combining dasatinib (which inhibits ABL/LYN and reduces MCL-1 expression) with venetoclax led to enhanced apoptosis [29]. Importantly, the combination of TKIs and venetoclax has shown promise in eradicating chronic myeloid leukemia stem cells, aided by the concurrent inhibition of MCL-1 and BCL-XL by TKIs [53].

While my above findings provide valuable insights, further exploration is warranted in alternative systems, including other cell lines harbouring PTP domain PTPN11 mutations, and in in vivo studies to assess the efficacy and potential clinical relevance of these combination treatment strategies. It's important to note that simultaneous use of MCL-1 and BCL-XL inhibitors in patients may carry an increased risk of on-target toxicities [51].

In conclusion, PTP domain PTPN11 mutations drive venetoclax and MCL-1 inhibitor resistance, accompanied by overexpression of BCL-XL and MCL-1 in Ph+ ALL cells. Venetoclax sensitivity can be restored through PTPN11 knockdown or the co-inhibition of BCL-2 and MCL-1. My study underscores the potential of combined inhibition of pBCR::ABL1 with imatinib and BCL-2 with venetoclax as a precision medicine approach for treating Ph+ ALL patients carrying PTPN11 mutations. Given that both imatinib and venetoclax are FDA-approved drugs with high specificity, this combination therapy offers a promising treatment option for this specific subset of patients.

References

1. Fielding, A.K., *Curing Ph+ ALL: assessing the relative contributions of chemotherapy, TKIs, and allogeneic stem cell transplant.* Hematology Am Soc Hematol Educ Program, 2019. **2019**(1): p. 24-29.
2. Samra, B., et al., *Evolving therapy of adult acute lymphoblastic leukemia: state-of-the-art treatment and future directions.* Journal of hematology & oncology, 2020. **13**(1): p. 1-17.
3. Mian, A.A., et al., *Oncogene-independent resistance in Philadelphia chromosome - positive (Ph(+)) acute lymphoblastic leukemia (ALL) is mediated by activation of AKT/mTOR pathway.* Neoplasia, 2021. **23**(9): p. 1016-1027.
4. Short, N.J., H. Kantarjian, and E. Jabbour, *SOHO State of the Art Updates & Next Questions: Intensive and Non–Intensive Approaches for Adults With Philadelphia Chromosome-Positive Acute Lymphoblastic Leukemia.* Clinical Lymphoma Myeloma and Leukemia, 2022. **22**(2): p. 61-66.
5. Ribera, J.-M. and S. Chiaretti, *Modern Management Options for Ph+ ALL.* Cancers, 2022. **14**(19): p. 4554.
6. Prahallad, A., et al., *PTPN11 Is a Central Node in Intrinsic and Acquired Resistance to Targeted Cancer Drugs.* Cell Rep, 2015. **12**(12): p. 1978-85.
7. Stevens, B.M., et al., *PTPN11 Mutations Confer Unique Metabolic Properties and Increase Resistance to Venetoclax and Azacitidine in Acute Myelogenous Leukemia.* Blood, 2018. **132**(Supplement 1): p. 909-909.
8. Swoboda, D.M., et al., *PTPN11 Mutations Are Associated with Poor Outcomes across Myeloid Malignancies.* Blood, 2020. **136**: p. 8-9.
9. Gu, S., et al., *SHP2 is required for BCR-ABL1-induced hematologic neoplasia.* Leukemia, 2018. **32**(1): p. 203-213.
10. Saxton, T.M., et al., *Abnormal mesoderm patterning in mouse embryos mutant for the SH2 tyrosine phosphatase Shp-2.* The EMBO journal, 1997. **16**(9): p. 2352-2364.
11. Zhang, Q., et al., *Activation of RAS/MAPK pathway confers MCL-1 mediated acquired resistance to BCL-2 inhibitor venetoclax in acute myeloid leukemia.* Signal Transduction and Targeted Therapy, 2022. **7**(1): p. 51.
12. Wang, H., et al., *Venetoclax-ponatinib for T315I/compound-mutated Ph+ acute lymphoblastic leukemia.* Blood Cancer J, 2022. **12**(1): p. 20.
13. Kanumuri, R., et al., *Targeting SHP2 phosphatase in hematological malignancies.* Expert Opinion on Therapeutic Targets, 2022. **26**(4): p. 319-332.
14. Kale, J., E.J. Osterlund, and D.W. Andrews, *BCL-2 family proteins: changing partners in the dance towards death.* Cell Death & Differentiation, 2018. **25**(1): p. 65-80.
15. Lagadinou, E.D., et al., *BCL-2 inhibition targets oxidative phosphorylation and selectively eradicates quiescent human leukemia stem cells.* Cell Stem Cell, 2013. **12**(3): p. 329-41.
16. Carter, B.Z., et al., *Combined targeting of BCL-2 and BCR-ABL tyrosine kinase eradicates chronic myeloid leukemia stem cells.* Sci Transl Med, 2016. **8**(355): p. 355ra117.
17. Santucci, R., et al., *Cytochrome c: An extreme multifunctional protein with a key role in cell fate.* International journal of biological macromolecules, 2019. **136**: p. 1237-1246.
18. Hartman, M.L. and M. Czyz, *BCL-w: apoptotic and non-apoptotic role in health and disease.* Cell Death & Disease, 2020. **11**(4): p. 260.

19. Brown, L.M., et al., *Dysregulation of BCL-2 family proteins by leukemia fusion genes.* J Biol Chem, 2017. **292**(35): p. 14325-14333.
20. Poudel, G., et al., *Mechanisms of Resistance and Implications for Treatment Strategies in Chronic Myeloid Leukaemia.* Cancers, 2022. **14**(14): p. 3300.
21. Hata, A.N., J.A. Engelman, and A.C. Faber, *The BCL2 Family: Key Mediators of the Apoptotic Response to Targeted Anticancer Therapeutics.* Cancer Discovery, 2015. **5**(5): p. 475-487.
22. Massimino, M., et al., *Targeting BCL-2 as a therapeutic strategy for primary p210BCR-ABL1-positive B-ALL Cells.* in vivo, 2020. **34**(2): p. 511-516.
23. Scherr, M., et al., *Differential expression of miR-17□ 92 identifies BCL2 as a therapeutic target in BCR-ABL-positive B-lineage acute lymphoblastic leukemia.* Leukemia, 2014. **28**(3): p. 554-565.
24. Wang, H., et al., *Targeting MCL-1 in cancer: current status and perspectives.* Journal of Hematology & Oncology, 2021. **14**(1): p. 67.
25. Shahar, N. and S. Larisch, *Inhibiting the inhibitors: Targeting anti-apoptotic proteins in cancer and therapy resistance.* Drug Resistance Updates, 2020. **52**: p. 100712.
26. Scheffold, A., B.M.C. Jebaraj, and S. Stilgenbauer, *Venetoclax: Targeting BCL2 in Hematological Cancers.* Recent Results Cancer Res, 2018. **212**: p. 215-242.
27. Li, Q., et al., *Efficacy and Safety of Bcl-2 Inhibitor Venetoclax in Hematological Malignancy: A Systematic Review and Meta-Analysis of Clinical Trials.* Front Pharmacol, 2019. **10**: p. 697.
28. Scherr, M., et al., *Optimized induction of mitochondrial apoptosis for chemotherapy-free treatment of BCR-ABL+ acute lymphoblastic leukemia.* Leukemia, 2019. **33**(6): p. 1313-1323.
29. Leonard, J.T., et al., *Targeting BCL-2 and ABL/LYN in Philadelphia chromosome–positive acute lymphoblastic leukemia.* Science translational medicine, 2016. **8**(354): p. 354ra114-354ra114.
30. Maiti, A., et al., *Venetoclax and BCR-ABL Tyrosine Kinase Inhibitor Combinations: Outcome in Patients with Philadelphia Chromosome-Positive Advanced Myeloid Leukemias.* Acta Haematol, 2020. **143**(6): p. 567-573.
31. Fletcher, S., *MCL-1 inhibitors–where are we now (2019)?* Expert opinion on therapeutic patents, 2019. **29**(11): p. 909-919.
32. Wang, L., et al., *Discovery of A-1331852, a First-in-Class, Potent, and Orally-Bioavailable BCL-XL Inhibitor.* ACS Medicinal Chemistry Letters, 2020. **11**(10): p. 1829-1836.
33. Szlávik, Z., et al., *Structure-guided discovery of a selective Mcl-1 inhibitor with cellular activity.* Journal of Medicinal Chemistry, 2019. **62**(15): p. 6913-6924.
34. Algarín, E.M., et al., *Preclinical evaluation of the simultaneous inhibition of MCL-1 and BCL-2 with the combination of S63845 and venetoclax in multiple myeloma.* Haematologica, 2020. **105**(3): p. e116-e120.
35. Korfi, K., et al., *BIM mediates synergistic killing of B-cell acute lymphoblastic leukemia cells by BCL-2 and MEK inhibitors.* Cell death & disease, 2016. **7**(4): p. e2177-e2177.
36. Jones, L., et al., *A review of new agents evaluated against pediatric acute lymphoblastic leukemia by the Pediatric Preclinical Testing Program.* Leukemia, 2016. **30**(11): p. 2133-2141.
37. Moujalled, D.M., et al., *Cotargeting BCL-2 and MCL-1 in high-risk B-ALL.* Blood Advances, 2020. **4**(12): p. 2762-2767.

38. Koss, B., et al., *Requirement for antiapoptotic MCL-1 in the survival of BCR-ABL B-lineage acute lymphoblastic leukemia.* Blood, The Journal of the American Society of Hematology, 2013. **122**(9): p. 1587-1598.
39. Budhraja, A., et al., *Modulation of Navitoclax Sensitivity by Dihydroartemisinin-Mediated MCL-1 Repression in BCR-ABL(+) B-Lineage Acute Lymphoblastic Leukemia.* Clin Cancer Res, 2017. **23**(24): p. 7558-7568.
40. Bijnsdorp, I.V., E. Giovannetti, and G.J. Peters, *Analysis of drug interactions.* Methods Mol Biol, 2011. **731**: p. 421-34.
41. Hughes, T.P., et al., *Asciminib in Chronic Myeloid Leukemia after ABL Kinase Inhibitor Failure.* N Engl J Med, 2019. **381**(24): p. 2315-2326.
42. Boulares, A.H., et al., *Role of poly (ADP-ribose) polymerase (PARP) cleavage in apoptosis: caspase 3-resistant PARP mutant increases rates of apoptosis in transfected cells.* Journal of Biological Chemistry, 1999. **274**(33): p. 22932-22940.
43. Liu, S. and R. Kurzrock, *Toxicity of targeted therapy: Implications for response and impact of genetic polymorphisms.* Cancer treatment reviews, 2014. **40**(7): p. 883-891.
44. Fobare, S., et al., *Molecular, clinical, and prognostic implications of PTPN11 mutations in acute myeloid leukemia.* Blood Adv, 2022. **6**(5): p. 1371-1380.
45. Ong, F., K. Kim, and M.Y. Konopleva, *Venetoclax resistance: mechanistic insights and future strategies.* Cancer Drug Resistance, 2022. **5**(2): p. 380.
46. Ma, J., et al., *Inhibition of Bcl-2 Synergistically Enhances the Antileukemic Activity of Midostaurin and Gilteritinib in Preclinical Models of FLT3-Mutated Acute Myeloid LeukemiaJoint FLT3 and BCL-2 Inhibition in FLT3-Mutated AML.* Clinical Cancer Research, 2019. **25**(22): p. 6815-6826.
47. Niu, X., et al., *Binding of released Bim to Mcl-1 is a mechanism of intrinsic resistance to ABT-199 which can be overcome by combination with daunorubicin or cytarabine in AML cells.* Clinical Cancer Research, 2016. **22**(17): p. 4440-4451.
48. Lin, K.H., et al., *Targeting MCL-1/BCL-XL forestalls the acquisition of resistance to ABT-199 in acute myeloid leukemia.* Scientific reports, 2016. **6**(1): p. 1-10.
49. Zhang, Q., et al., *Activation of RAS/MAPK pathway confers MCL-1 mediated acquired resistance to BCL-2 inhibitor venetoclax in acute myeloid leukemia.* Signal transduction and targeted therapy, 2022. **7**(1): p. 1-13.
50. Zhang, H., et al., *Integrated analysis of patient samples identifies biomarkers for venetoclax efficacy and combination strategies in acute myeloid leukemia.* Nature Cancer, 2020. **1**(8): p. 826-839.
51. Fairlie, W.D. and E.F. Lee, *Targeting the BCL-2-regulated apoptotic pathway for the treatment of solid cancers.* Biochemical Society Transactions, 2021. **49**(5): p. 2397-2410.
52. Li, Z., S. He, and A.T. Look, *The MCL1-specific inhibitor S63845 acts synergistically with venetoclax/ABT-199 to induce apoptosis in T-cell acute lymphoblastic leukemia cells.* Leukemia, 2019. **33**(1): p. 262-266.
53. Carter, B.Z., et al., *Combined targeting of BCL-2 and BCR-ABL tyrosine kinase eradicates chronic myeloid leukemia stem cells.* Science translational medicine, 2016. **8**(355): p. 355ra117-355ra117.

APPENDIX 1

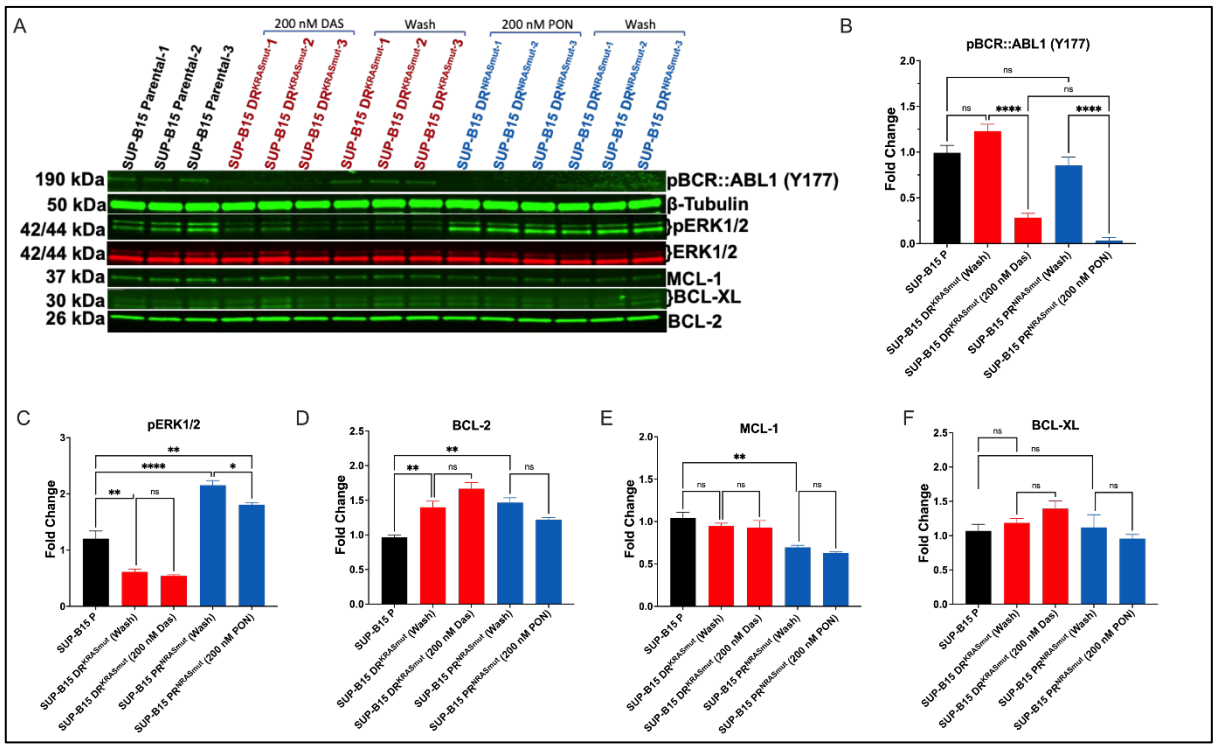

1. **SUP-B15 DR^{KRASmut} and SUP-B15 PR^{NRASmut} cells had BCR::ABL1 independent sustained RAS/ERK pathway activation.** (A-E) Western blot and densitometry analysis of pBCR::ABL1 (Y177), pERK1/2, BCL-2, MCL-1 and BCL-XL of SUP-B15 DR^{KRASmut} and SUP-B15 PR^{NRASmut} cells when they are in 200 nM dasatinib and 200 nM ponatinib culture respectively and TKI was out overnight. Sample 1-3 represents three independent samples. Statistical analysis was performed by using One Way ANNOVA. Error bars represent standard deviation (SD) of three independent experiments. Ns, *, **, ***, **** represents $p>0.05$, $p\leq0.05$, $p\leq0.01$, $p\leq0.001$ and $p\leq0.0001$ respectively.

2: Full three biological replicates for cropped Western blot used in Figure 5.4B

N-1

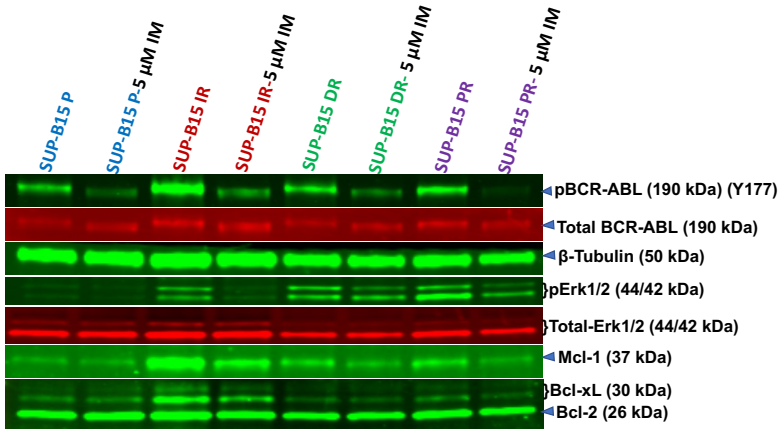

N-2

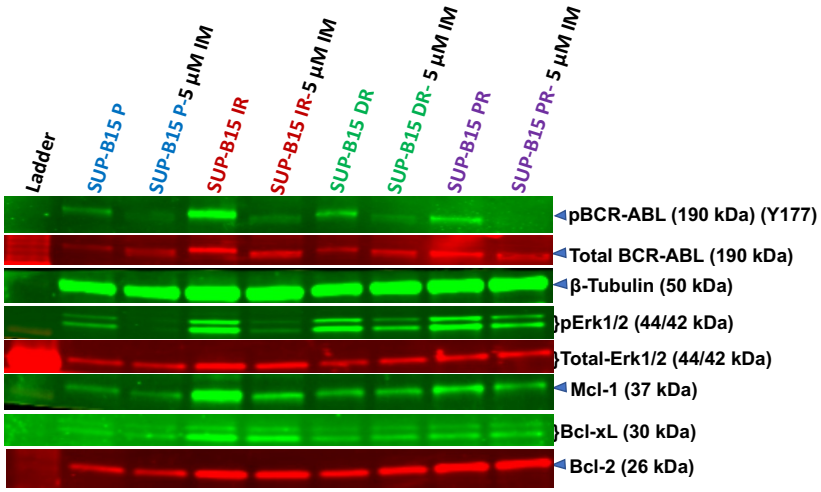

N-3

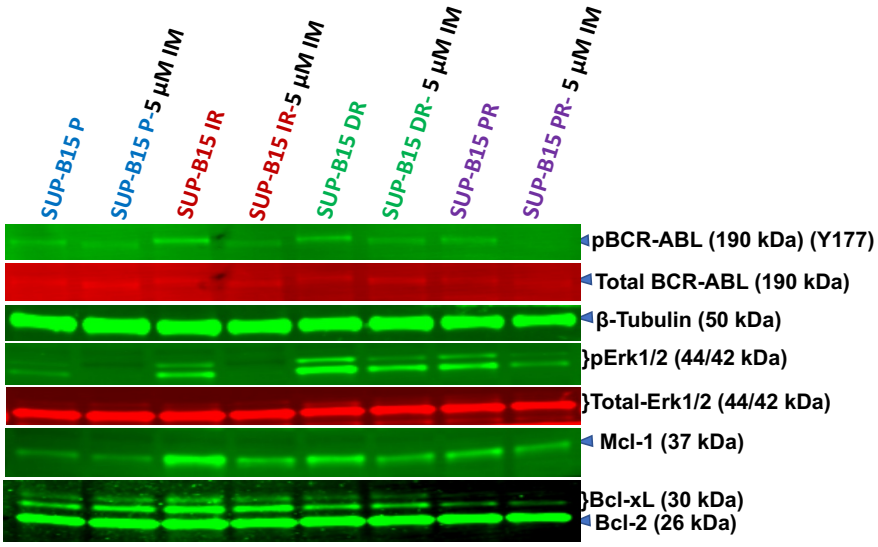

CHAPTER 6: Concluding Remarks and Future Directions

Despite the significant survival benefit of using Tyrosine Kinase Inhibitors (TKIs) in Ph+ leukaemia, TKI resistance remains a major issue (1). A considerable proportion of patients fail TKI treatment and relapse without evidence of BCR::ABL1 kinase domain mutations. Alternative mechanisms involved in the activation of alternative survival pathways, anti-apoptotic pathways, or acquire mutations in cancer-associated genes, are all likely mechanisms of for BCR::ABL1-independent resistance. (2, 3). However, the exact mechanisms remain poorly understood, necessitating further investigation to develop better targeted treatment strategies. Mutations in cancer-associated genes such as *ASXL1*, *RUNX1*, and *PTPN11* are frequently observed in Ph+ leukaemia patients associated with a poor prognosis, but their role in TKI resistance is not well defined (4, 5). *PTPN11* mutations, common in haematological malignancies including Juvenile myelomonocytic leukemia (JMML), acute myeloid leukaemia (AML), chronic myelomonocytic leukaemia, myelodysplastic syndrome, and B-ALL, confer therapy resistance (6). Mutations in *PTPN11* may also be implicated in TKI resistance in the Ph+ leukaemia setting, as well as resistance to emerging therapies such as venetoclax (6). Unfortunately, no targeted treatment options are currently available in the clinic against *PTPN11* mutations (7).

In this study, I conducted an investigation to examine the impact of non-BCR::ABL1 mutations, specifically focusing on PTPN11 mutations, on the development of resistance in Ph+ ALL cell models. My findings demonstrate that PTPN11 Phosphotyrosine phosphatase (PTP) mutations play a role in activating both the RAS/ERK and anti-apoptotic pathways, thereby contributing to resistance. The study further explored potential treatment strategies, including the use of MEK inhibitors to target the RAS/ERK pathway and inhibitors that target the anti-apoptotic pathways, such as venetoclax and

inhibitors of MCL-1 and BCL-XL. Additionally, the combination of venetoclax and TKI was investigated as an effective treatment option for specifically targeting Ph+ ALL cells with PTPN11 PTP mutations. These findings underscore the potential of targeted treatment approaches to overcome resistance mechanisms in Ph+ ALL.

Chapter 3 of this study provides evidence of a novel mechanism of TKI resistance mediated by PTPN11 mutations in multi-TKI-resistant Ph+ ALL cell lines. The mutations led to the re-activation of pBCR(Y177), a part of the BCR::ABL1 protein, which sustained the expression of pERK1/2. Despite inhibition of pABL1(Y245), a TKI target, with imatinib, PTPN11 mutations dysregulated the phosphorylation sites of BCR::ABL1 to escape complete suppression by TKIs. Previous studies have shown that SHP-2, encoded by PTPN11, is required for the pathogenesis of BCR::ABL1+ myeloid and lymphoid malignancies and activates the pBCR(Y177)/pERK1/2 axis in BCR::ABL1+ cells (8). Chapter 3 confirms that PTPN11 mutations affect pBCR(Y177)/pERK1/2 signalling and that targeting pBCR(Y177)/pMEK1/2 with a MEK inhibitor can overcome resistance driven by PTPN11 mutations. However, in the context of addressing TKI resistance in Ph+ leukemias, it's crucial to recognize the limitations of this study. SUP-B15 IR cells rely on imatinib for their long-term optimal growth, and during MEK inhibitor treatment, imatinib was withdrawn from the culture medium. The increased susceptibility of SUP-B15 IR cells to MEK inhibition could potentially be attributed to the absence of imatinib, as evidenced by the negligible impact of MEK inhibitor treatment on cell viability when combined with imatinib. Therefore, while these results are promising, the context of imatinib dependency must be considered when interpreting the findings. Furthermore, drug transporters that are most widely implicated in TKI resistance have been investigated in this study. Therefore, a more comprehensive analysis of drug transporters

could shed light on their role in the mechanisms of TKI resistance and further enhance our understanding.

In Chapter 4, I solidify the pivotal role of PTP domain PTPN11 mutations in driving TKI resistance and affirm the survival advantage they confer. Genetic silencing of the PTPN11 gene effectively restores imatinib sensitivity in Ph+ ALL cells bearing PTP domain PTPN11 mutations. This study provides compelling validation for the involvement of PTP domain PTPN11 mutations in TKI resistance development, marking the first evidence of their influence in BCR::ABL1 positive cells. Through targeted knockdown experiments on PTPN11, I observed reduced pERK1/2 levels and the resumption of imatinib sensitivity in SUP-B15 IR cells, underscoring the significance of the RAS/ERK pathway in the resistance mechanism. Notably, direct targeting of SHP-2 activity did not fully overcome resistance, suggesting that the resistance mechanisms extend beyond SHP-2's catalytic function. Further research is underway to assess SHP-2 protein's catalytic activity with PTP domain mutations, delving into this hypothesis in depth.

In BaF3 BCR::ABL1 p190 cells bearing the PTPN11 p.A461T mutation, there is no discernible impact on ERK signalling or anti-apoptotic protein expression. Surprisingly, this mutation still confers resistance to TKIs, likely by reducing imatinib's efficacy against BCR::ABL1, as evidenced by elevated IC50 values. This implies that the p.A461T mutation may disrupt imatinib's ability to target BCR::ABL1, offering a potential explanation for TKI resistance. As for PTPN11 p.A461T + p.P491H mutations, their effect on ERK signalling in BaF3 BCR::ABL1 p190 cells is minimal. Sustained ERK activation is exclusive to SUP-B15 IR cells continuously exposed to 5 μM imatinib. Importantly, this effect dissipates when imatinib is removed overnight, followed by a 4-hour treatment with 5

μM imatinib. These findings suggest that extended imatinib exposure triggers ERK re-activation in SUP-B15 IR cells, potentially clarifying the absence of ERK activation in BaF3 BCR::ABL1 p190 cells carrying PTPN11 mutations. Further investigation into this observation may shed light on the additional mechanisms involved.

In Chapter 5, I demonstrated that Ph+ ALL cell lines with PTPN11 mutations exhibited BCR::ABL1-independent overexpression of BCL-XL and BCR::ABL1-dependent overexpression of MCL-1, leading to resistance to venetoclax treatment (9), a BCL-2 inhibitor. Overexpression of BCL-XL and MCL-1 are common mechanisms of venetoclax resistance, but co-targeting these anti-apoptotic proteins with their specific inhibitors overcame resistance in cells with PTPN11 mutations. In addition, blockade of BCR::ABL1 activation resulted in MCL-1 inhibition, leading to venetoclax sensitivity in these cells. These findings highlight the role of PTPN11 mutations in the development of TKI and venetoclax resistance in Ph+ ALL cells. Both TKIs and venetoclax are FDA-approved therapies and highly specific to their targets. While Chapter 5 offers valuable insights into the resistance mechanisms associated with PTPN11 mutations in Ph+ ALL, it is important to acknowledge few limitations. Firstly, the study's limited clinical data underscores the need for robust clinical validation to confirm the relevance of PTPN11 mutations in TKI and venetoclax resistance among actual patient populations. Secondly, the focus on single-agent studies may oversimplify the intricate interplay of drugs and resistance mechanisms commonly encountered in clinical practice. To address these limitations comprehensively, future research should incorporate patient-derived samples, encompass diverse PTPN11 mutations, and consider combination therapies to better reflect the clinical landscape of Ph+ ALL.

My study revealed a novel mechanism of TKI and venetoclax resistance mediated by PTP domain PTPN11 mutations and provides a strong rationale for using BCL-XL and MCL-1 overexpression as biomarkers to identify patients who may benefit from dual targeting of BCR::ABL1 and BCL-2 to overcome resistance. Moreover, I have discovered a novel non-BCR::ABL1 mutational mechanism of resistance in BCR::ABL1-positive cells. This resistance is mediated through PTPN11 mutations and the activation of pBCR::ABL1 (Y177), leading to sustained activation of pERK1/2.

Nonetheless, it's important to acknowledge certain limitations in drawing conclusions and charting future directions. Firstly, the conclusions derived here are primarily based on cell line experiments. Expanding this research to encompass more extensive models, such as primary cells and in-vivo studies, holds the potential to significantly amplify the impact of the findings from this study. Additionally, delving into the effects of PTPN11 mutations on SHP-2 catalytic activity through activity assays could provide valuable insights. Furthermore, while to my knowledge the dual mutations (p.A461T and p.P491H) in PTPN11 presented in this thesis have not been reported in patients to date, it is noteworthy that these mutations individually occur frequently in leukemia and Noonan syndrome patients. This study, nonetheless, advances our understanding of TKI resistance mechanisms mediated by PTPN11 mutations and provides potential strategies to overcome such resistance.

These findings suggest a promising precision medicine approach for Ph+ ALL patients with PTPN11 mutations and warrant further testing and validation in other Ph+ leukemias, including AML and JMML, and solid tumours with PTPN11 mutations. Animal models should be used to assess whether the in-vitro results are supported by in-vivo

studies. Additionally, this knowledge can inform the understanding of PTPN11 mutations and potentially be applied to other malignancies such as JMML and AML where effective treatment options are limited. The results underscore the importance of a precision medicine approach for cancer patients, where individualized targeted treatment based on biomarkers can improve outcomes and minimize toxicity.

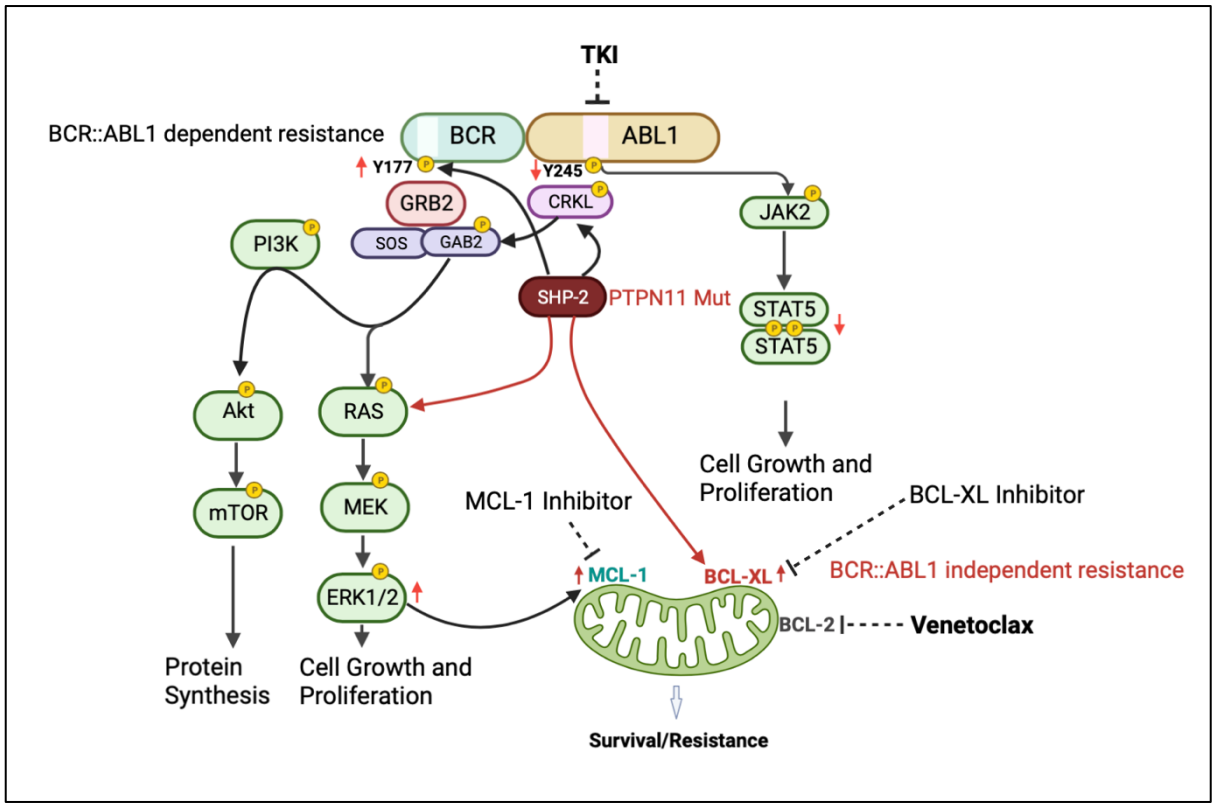

Summary Figure: Schematic of resistance mechanisms in Ph+ ALL cells with PTPN11 mutations. In this schematic, longer black arrows represent the BCR::ABL1-dependent pathway, while longer red arrows indicate BCR::ABL1-independent mechanisms of resistance. The small red up or down arrows denote the overexpression and downregulation of respective proteins, respectively. The small, encircled "p" represents phosphorylation. Dotted lines indicate the inhibition of proteins by their inhibitors. Mutated SHP-2 (PTPN11 mut) plays a crucial role in mediating both BCR::ABL1-dependent and independent mechanisms of resistance to tyrosine kinase inhibitors (TKIs) as well as resistance to venetoclax. Figure created in BioRender.com.

References:

1. Samra, B., et al., *Evolving therapy of adult acute lymphoblastic leukemia: state-of-the-art treatment and future directions.* Journal of Hematology & Oncology, 2020. **13**(1): p. 70.
2. Poudel, G., et al., *Mechanisms of Resistance and Implications for Treatment Strategies in Chronic Myeloid Leukaemia.* Cancers, 2022. **14**(14): p. 3300.
3. Braun, T.P., C.A. Eide, and B.J. Druker, *Response and Resistance to BCR-ABL1-Targeted Therapies.* Cancer Cell, 2020. **37**(4): p. 530-542.
4. Soverini, S., R. Bassan, and T. Lion, *Treatment and monitoring of Philadelphia chromosome-positive leukemia patients: recent advances and remaining challenges.* Journal of Hematology & Oncology, 2019. **12**(1): p. 39.
5. Fedullo, A.L., et al., *Prognostic implications of additional genomic lesions in adult Philadelphia chromosome-positive acute lymphoblastic leukemia.* Haematologica, 2019. **104**(2): p. 312-318.
6. Kanumuri, R., et al., *Targeting SHP2 phosphatase in hematological malignancies.* Expert Opinion on Therapeutic Targets, 2022. **26**(4): p. 319-332.
7. Fobare, S., et al., *Molecular, clinical, and prognostic implications of PTPN11 mutations in acute myeloid leukemia.* Blood Adv, 2022. **6**(5): p. 1371-1380.
8. Gu, S., et al., *SHP2 is required for BCR-ABL1-induced hematologic neoplasia.* Leukemia, 2018. **32**(1): p. 203-213.
9. Xu, Y. and H. Ye, *Progress in understanding the mechanisms of resistance to BCL-2 inhibitors.* Experimental Hematology & Oncology, 2022. **11**(1): p. 31.